antibiotics

Special Issue Reprint

Antibiofilm Activity against Multidrug-Resistant Pathogens

Edited by
Verica Aleksic Sabo and Petar Knezevic

mdpi.com/journal/antibiotics

MDPI

Antibiofilm Activity against Multidrug-Resistant Pathogens

Antibiofilm Activity against Multidrug-Resistant Pathogens

Guest Editors

Verica Aleksic Sabo
Petar Knezevic

MDPI

Basel • Beijing • Wuhan • Barcelona • Belgrade • Novi Sad • Cluj • Manchester

Guest Editors

Verica Aleksic Sabo
Department of Biology
and Ecology
University of Novi Sad
Novi Sad
Serbia

Petar Knezevic
Department of Biology
and Ecology
University of Novi Sad
Novi Sad
Serbia

Editorial Office
MDPI AG
Grosspeteranlage 5
4052 Basel, Switzerland

This is a reprint of the Special Issue, published open access by the journal *Antibiotics* (ISSN 2079-6382), freely accessible at: https://www.mdpi.com/journal/antibiotics/special_issues/N9ZY9N778C.

For citation purposes, cite each article independently as indicated on the article page online and as indicated below:

Lastname, A.A.; Lastname, B.B. Article Title. *Journal Name* **Year**, *Volume Number*, Page Range.

ISBN 978-3-7258-8903-7 (Hbk)
ISBN 978-3-7258-8904-4 (PDF)
https://doi.org/10.3390/books978-3-7258-8904-4

© 2026 by the authors. Articles in this reprint are Open Access and distributed under the Creative Commons Attribution (CC BY) license. The reprint as a whole is distributed by MDPI under the terms and conditions of the Creative Commons Attribution-NonCommercial-NoDerivs (CC BY-NC-ND) license (https://creativecommons.org/licenses/by-nc-nd/4.0/).

Contents

About the Editors . . . . . **vii**

Preface . . . . . **ix**

Ting Qin, Kai Chen, Bingwen Xi, Liangkun Pan, Jun Xie, Liushen Lu and Kai Liu
In Vitro Antibiofilm Activity of Resveratrol against *Aeromonas hydrophila*
Reprinted from: *Antibiotics* **2023**, *12*, 686, https://doi.org/10.3390/antibiotics12040686 . . . . . **1**

Jeonghoon Lee, Hyunchan Song and Kiyoung Kim
Inhibition of *Candida albicans* Biofilm Formation and Attenuation of Its Virulence by *Liriope muscari*
Reprinted from: *Antibiotics* **2024**, *13*, 434, https://doi.org/10.3390/antibiotics13050434 . . . . . **17**

Peihui Zou, Jia Liu, Peng Li and Qingxian Luan
Antifungal Activity, Synergism with Fluconazole or Amphotericin B and Potential Mechanism of Direct Current against *Candida albicans* Biofilms and Persisters
Reprinted from: *Antibiotics* **2024**, *13*, 521, https://doi.org/10.3390/antibiotics13060521 . . . . . **30**

Isidora Nikolic, Verica Aleksic Sabo, Damir Gavric and Petar Knezevic
Anti-*Staphylococcus aureus* Activity of Volatile Phytochemicals and Their Combinations with Conventional Antibiotics Against Methicillin-Susceptible *S. aureus* (MSSA) and Methicillin-Resistant *S. aureus* (MRSA) Strains
Reprinted from: *Antibiotics* **2024**, *13*, 1030, https://doi.org/10.3390/antibiotics13111030 . . . . . **47**

Virág D. Ángyán, Viktória L. Balázs, Marianna Kocsis, Béla Kocsis, Györgyi Horváth, Ágnes Farkas and Lilla Nagy-Radványi
Synergistic Antibiofilm Effects of Chestnut and Linden Honey with Lavender Essential Oil Against Multidrug-Resistant Otitis Media Pathogens
Reprinted from: *Antibiotics* **2025**, *14*, 146, https://doi.org/10.3390/antibiotics14020146 . . . . . **67**

Amit Rimon, Jonathan Belin, Ortal Yerushalmy, Yonatan Eavri, Anatoly Shapochnikov, Shunit Coppenhagen-Glazer, et al.
Pulsed Blue Light and Phage Therapy: A Novel Synergistic Bactericide
Reprinted from: *Antibiotics* **2025**, *14*, 481, https://doi.org/10.3390/antibiotics14050481 . . . . . **87**

Yunah Oh and Tae-Jong Kim
Temperature Adaptive Biofilm Formation in *Yersinia enterocolitica* in Response to pYV Plasmid and Calcium
Reprinted from: *Antibiotics* **2025**, *14*, 857, https://doi.org/10.3390/antibiotics14090857 . . . . . **102**

Minji Kim, Jesmina Khatun, Fazlurrahman Khan and Young-Mog Kim
Lactic Acid Bacteria as Natural Antimicrobials: Biofilm Control in Food and Food Industry
Reprinted from: *Antibiotics* **2026**, *15*, 248, https://doi.org/10.3390/antibiotics15030248 . . . . . **117**

Manal Dahdah, Yasmine Ettouil, Hawraa Issa, Latifa Koussih, Mikhlid H. Almutairi, Mahmoud Rouabhia and Abdelhabib Semlali
Evaluation of the Antifungal Activity of the Polyphenol Formulation *Viroelixir* Against *Candida albicans*
Reprinted from: *Antibiotics* **2026**, *15*, 420, https://doi.org/10.3390/antibiotics15040420 . . . . . **143**

About the Editors

Verica Aleksic Sabo

Verica Aleksić Sabo is an Assistant Professor at the Faculty of Sciences, University of Novi Sad, Serbia, and is currently engaged in research activities in the field of microbiology and antimicrobial resistance. Her research interests include microbial biofilms, multidrug-resistant pathogens, antimicrobial agents, natural products, and alternative strategies for infection control. Her scientific work focuses on the characterization of biofilm-associated microbial traits and evaluation of novel antibiofilm approaches, including phytochemicals, essential oils, and combined antimicrobial therapies. She has participated in national and international research projects and has been involved in the development of innovative plant-based antibiofilm solutions supported through proof-of-concept and technology-transfer initiatives. She has authored numerous scientific publications and contributed as a reviewer and editor for international scientific journals. Her research activities aim to advance the understanding and development of effective strategies to combat antimicrobial resistance and biofilm-associated infections.

Petar Knezevic

Petar Knežević is a Full Professor at the Faculty of Sciences, University of Novi Sad, Serbia. He completed postdoctoral research at the Laboratory of Gene Technology, KU Leuven, Belgium. His research interests include antimicrobial resistance, bacteriophages, phage therapy, microbial pathogenesis, biofilm control, and the development of alternative antimicrobial strategies. His scientific work focuses on the isolation and characterization of bacteriophages, phage-based antimicrobial approaches, phage-antibiotic interactions, and the evaluation of novel agents against multidrug-resistant bacterial pathogens. He has coordinated and participated in national and international research projects, including projects focused on bacteriophage-based therapies, biofilm eradication strategies, and novel antimicrobial agents. He is a member of the International Committee on Taxonomy of Viruses and Chair of the study group for the order *Tubulavirales*. He has served as Guest Associate Editor for international scientific journals and has published extensively in the fields of microbiology, antimicrobial resistance, and phage therapy. His research has contributed to advancing innovative approaches for the prevention and treatment of infections caused by multidrug-resistant microorganisms.

Preface

The increasing prevalence of antimicrobial resistance represents one of the most critical challenges in modern medicine and public health. Among the factors contributing to treatment failure, microbial biofilms play a central role due to their complex structure, enhanced tolerance to antimicrobial agents, and ability to support persistent infections. This Reprint aims to provide an overview of current research efforts focused on understanding biofilm-associated microbial behavior and developing effective strategies for biofilm control and eradication.

This Reprint brings together contributions addressing different aspects of antibiofilm research, including investigations of biofilm formation mechanisms, evaluation of novel antimicrobial compounds, natural products, alternative therapeutic approaches, and synergistic strategies against resistant microorganisms. The collected studies reflect the multidisciplinary nature of biofilm research, combining microbiological, pharmacological, and translational perspectives.

We hope that this Reprint will serve as a valuable resource for researchers, healthcare professionals, and scientists involved in antimicrobial discovery, infection management, and the development of innovative approaches to overcome biofilm-related infections. We would like to sincerely thank all authors and reviewers whose valuable contributions made this collection possible.

Verica Aleksic Sabo and Petar Knezevic
Guest Editors

antibiotics

MDPI

Article

In Vitro Antibiofilm Activity of Resveratrol against *Aeromonas hydrophila*

Ting Qin [1], Kai Chen [1], Bingwen Xi [1,2,*], Liangkun Pan [1], Jun Xie [1,2], Liushen Lu [1] and Kai Liu [1,2]

[1] Key Laboratory of Aquatic Animal Nutrition and Health, Freshwater Fisheries Research Center, Chinese Academy of Fishery Science, Wuxi 214081, China
[2] Wuxi Fisheries College, Nanjing Agricultural University, Wuxi 214081, China
* Correspondence: xibw@ffrc.cn

Abstract: *Aeromonas hydrophila* is a Gram-negative bacterium that widely exists in various aquatic environments and causes septicemia in fish and humans. Resveratrol, a natural polyterpenoid product, has potential chemo-preventive and antibacterial properties. In this study, we investigated the effect of resveratrol on *A. hydrophila* biofilm formation and motility. The results demonstrated that resveratrol, at sub-MIC levels, can significantly inhibit the biofilm formation of *A. hydrophila*, and the biofilm was decreased with increasing concentrations. The motility assay showed that resveratrol could diminish the swimming and swarming motility of *A. hydrophila*. Transcriptome analyses (RNA-seq) showed that *A. hydrophila* treated with 50 and 100 μg/mL resveratrol, respectively, presented 230 and 308 differentially expressed genes (DEGs), including 90 or 130 upregulated genes and 130 or 178 downregulated genes. Among them, genes related to flagellar, type IV pilus and chemotaxis were significantly repressed. In addition, mRNA of virulence factors OmpA, extracellular proteases, lipases and T6SS were dramatically suppressed. Further analysis revealed that the major DEGs involved in flagellar assembly and bacterial chemotaxis pathways could be regulated by cyclic-di-guanosine monophosphate (c-di-GMP)- and LysR-Type transcriptional regulator (LTTR)-dependent quorum sensing (QS) systems. Overall, our results indicate that resveratrol can inhibit *A. hydrophila* biofilm formation by disturbing motility and QS systems, and can be used as a promising candidate drug against motile Aeromonad septicemia.

Keywords: resveratrol; *Aeromonas hydrophila*; biofilm formation; motility; RNA-seq; quorum sensing

1. Introduction

Aeromonas hydrophila is a typically zoonotic pathogen with a worldwide distribution in aquatic environment, and has different pathogenic potential between aquatic animals and mammals [1,2]. It can not only cause motile aeromonad septicemia in fish, leading to severe economic losses in aquaculture, but also cause various diseases in humans, such as gastroenteritis, skin infections, meningitis, and necrotizing fasciitis [3,4]. Traditionally, antibiotics are widely used to treat *A. hydrophila* infections. However, the wide and frequent use of antibiotics in fish farming has led to the emergence of antibiotic resistance in pathogens and treatment fail ure [5,6]. This phenomenon threatens the healthy development of aquaculture and safety of aquatic products. Therefore, novel strategies are required to combat drug resistant *A. hydrophila*.

A. hydrophila possesses a variety of virulence factors, among which biofilm has been well characterized and considered one of the most critical virulence factors for establishing infections [7–9]. Biofilms are sessile microbial communities that attach to surfaces using a self-produced extracellular polymeric matrix [10]. The bacteria in biofilms become much more resistant to antibiotic treatments and host defense compared to their free-floating state [11]. Biofilm formation greatly enhances the survival of pathogens in hosts, and results in the persistence of bacterial infections. The beginning of biofilm formation is the

attachment of planktonic cells to a surface [12], which makes motility the most important factor in the early phase of biofilm formation [13,14]. Moreover, biofilm formation is also coordinated by the quorum sensing (QS) system in pathogens [15,16]. Once the biofilm structure is disrupted, the antibiotic restores its efficacy and the host resolves the bacterial infections. Therefore, the antibiofilm strategy has been considered as a promising approach to overcome the bacterial infections [17].

Resveratrol (3,5,4′-Trihydroxystilbene) is a small natural plant polyphenol belonging to the stilbene family. The stilbene structure consists of precisely two aromatic rings and phenolic hydroxyl groups with double bonds (C6-C2-C6 carbon skeleton) [18]. Resveratrol is present in various plants, such as grapes, berries, peanuts, and is also found in high concentrations of red wine. It exists both in a *cis*- and *trans*-isomer, with the *trans*-isomer being the predominant form in plants and the most studied due to its greater availability and higher stability [18]. Resveratrol exhibits antioxidant, anti-inflammatory, immunomodulatory, cardioprotective, and neuroprotective effects, as well as potential therapeutic effects on diabetes, cancer, and Parkinson's disease [18–20]. In addition, resveratrol has antibacterial, anti-viral, and antifungal activity [21]. As a natural product, resveratrol was demonstrated to be an effective antibiofilm and anti-QS agent for several bacterial pathogens [22–25]. The antibiofilm effect of resveratrol (0.02 mg/mL) on *Escherichia coli* is mediated by repressing the expression of genes related to curli production, motility, and AI-2 QS system [10]. In methicillin-resistant *Staphylococcus aureus* (MRSA), 150 μg/mL resveratrol inhibited biofilm formation by disturbing the expression of genes associated with QS, surface and capsular polysaccharides [24]. As for *Fusobacterium nucleatum*, resveratrol attenuated the biofilm formation by decreasing the expression of genes involved in QS and virulence [22]. Resveratrol may inhibit bacterial biofilm formation by disturbing the QS system. Furthermore, resveratrol ($\geq$100 μg/mL) had no antibiofilm activity on *S. aureus* ATCC6538 [26,27]. The molecular mechanism of the antibiofilm effect of resveratrol may be different among various bacteria.

Our previous study showed that resveratrol, at sub-minimum inhibitory concentration (MIC), significantly inhibited *A. hydrophila* biofilm formation and hemolytic activity, and reduced the mortality of crucian carp challenged with *A. hydrophila* [28]. However, the action mechanism responsible for the antibiofilm activity of resveratrol is complex and has not been completely elucidated. In the present study, we investigated the biofilm inhibitory activity of resveratrol against *A. hydrophila*, mainly focusing on the biofilm formation, biofilm structure, and motility. Furthermore, RNA-seq was also performed to screen genes closely associated with resveratrol treatment and attempt to explore its possible mechanisms through functionally annotated and pathway-enriched analysis.

2. Results

2.1. Effects of Resveratrol on Biofilm Formation

Crystal violet staining results showed that 100 μg/mL resveratrol significantly inhibited biofilm formation compared to the control group, while 50 μg/mL resveratrol did not dramatically change the biofilm formed by *A. hydrophila* NJ-35 (Figure 1A). With increasing concentrations of resveratrol, the amount of biofilm reduced to 90.27 $\pm$ 0.11% and 49.34 $\pm$ 0.10% at 50 and 100 μg/mL resveratrol, respectively. In addition, both 50 and 100 μg/mL resveratrol decreased the exopolysaccharides (EPS) production (Figure 1B), and 100 μg/mL resveratrol noticeably repressed the total biofilm protein production of *A. hydrophila* NJ-35 (Figure 1C). The above three experimental results showed a similar trend; that is, the indicators of biofilm formation sequentially decreased following the increasing concentrations of resveratrol.

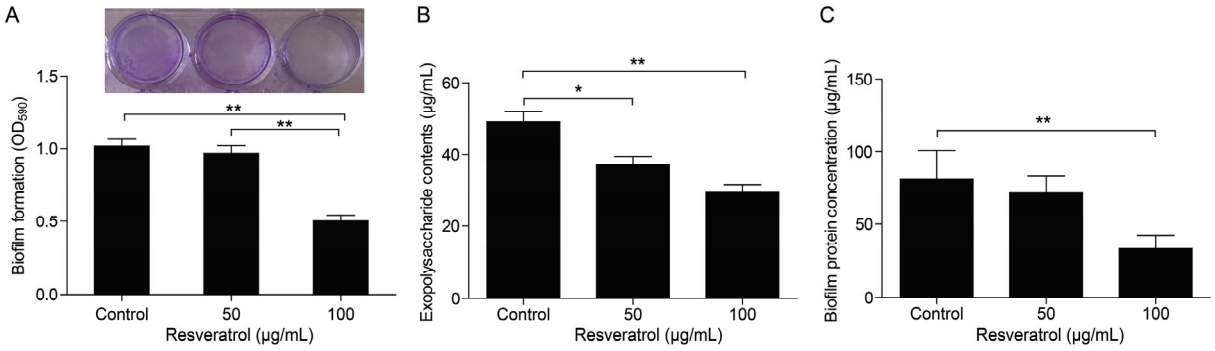

Figure 1. Inhibitory effects of resveratrol on biofilm formation of *A. hydrophila* NJ-35. (**A**) Crystal violet staining assay. (**B**) Exopolysaccharide production of formed biofilm. (**C**) The total protein of biofilm. The data were presented as the mean ± SD (n = 3) of three independent experiments. * $p < 0.05$, ** $p < 0.01$.

2.2. Effects of Resveratrol on Biofilm Structure

Microscopic observations matched the quantitative biofilm data well (Figure 2). In the absence of resveratrol, the biofilm formed by *A. hydrophila* NJ-35 had a uniform distribution with a dense coverage of the coverslip. When treated with resveratrol, the biofilm formed by *A. hydrophila* NJ-35 was sparser than that in the control group, and the biofilm structure became looser as the concentration of resveratrol increased.

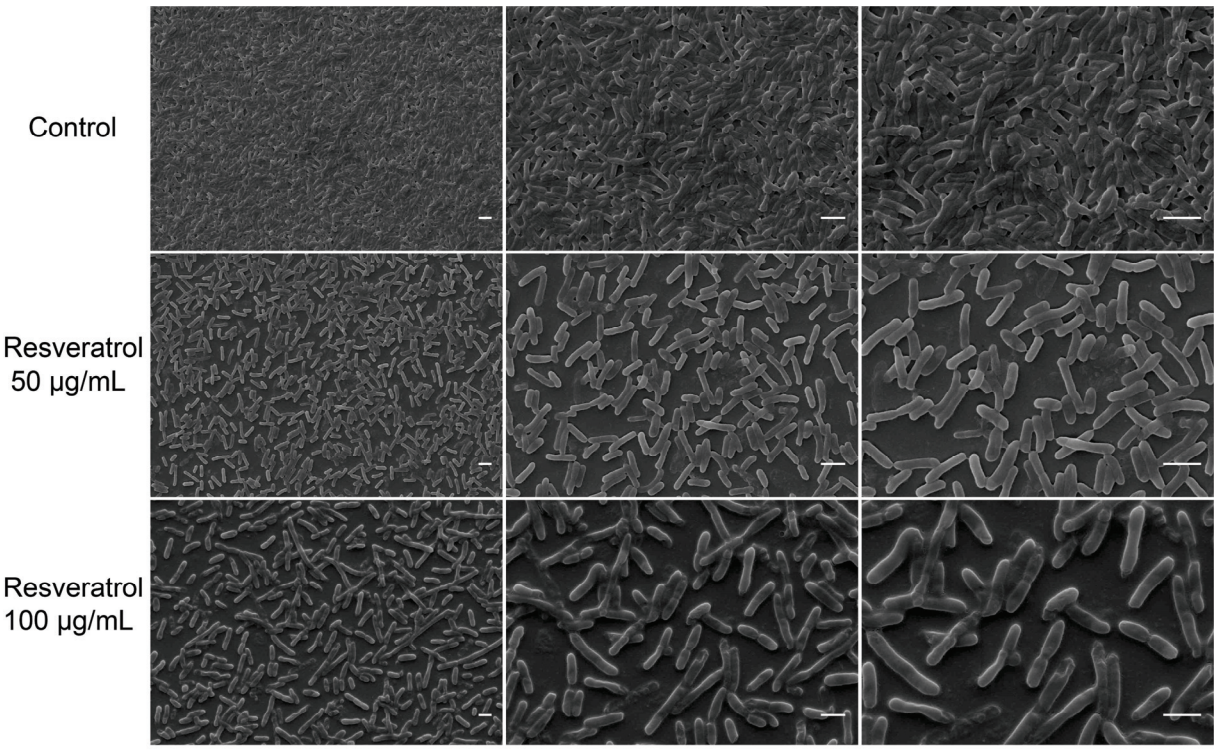

Figure 2. Scanning electron micrographs (SEM) of biofilm formed by *A. hydrophila* with different concentrations of resveratrol. Bars, 2 μm at magnification 2000 (**left**), 4000 (**medial**), and 6000 (**right**).

2.3. Effects of Resveratrol on Motility

The effects of resveratrol on the swimming and swarming motilities of *A. hydrophila* NJ-35 were also examined. As shown in Figure 3, resveratrol at 50 μg/mL did not affect the swimming motility, whereas resveratrol at 100 μg/mL significantly reduced the swimming motility of *A. hydrophila* NJ-35 ($p < 0.05$). In contrast, both 50 and 100 μg/mL resveratrol noticeably decreased the swarming motility of *A. hydrophila* NJ-35 in a dose-dependent

manner ($p < 0.05$). These results suggested that the inhibition of biofilm formation by resveratrol at 50 μg/mL was more closely related to swarming rather than swimming, while resveratrol at 100 μg/mL was involved in both swimming and swarming motilities.

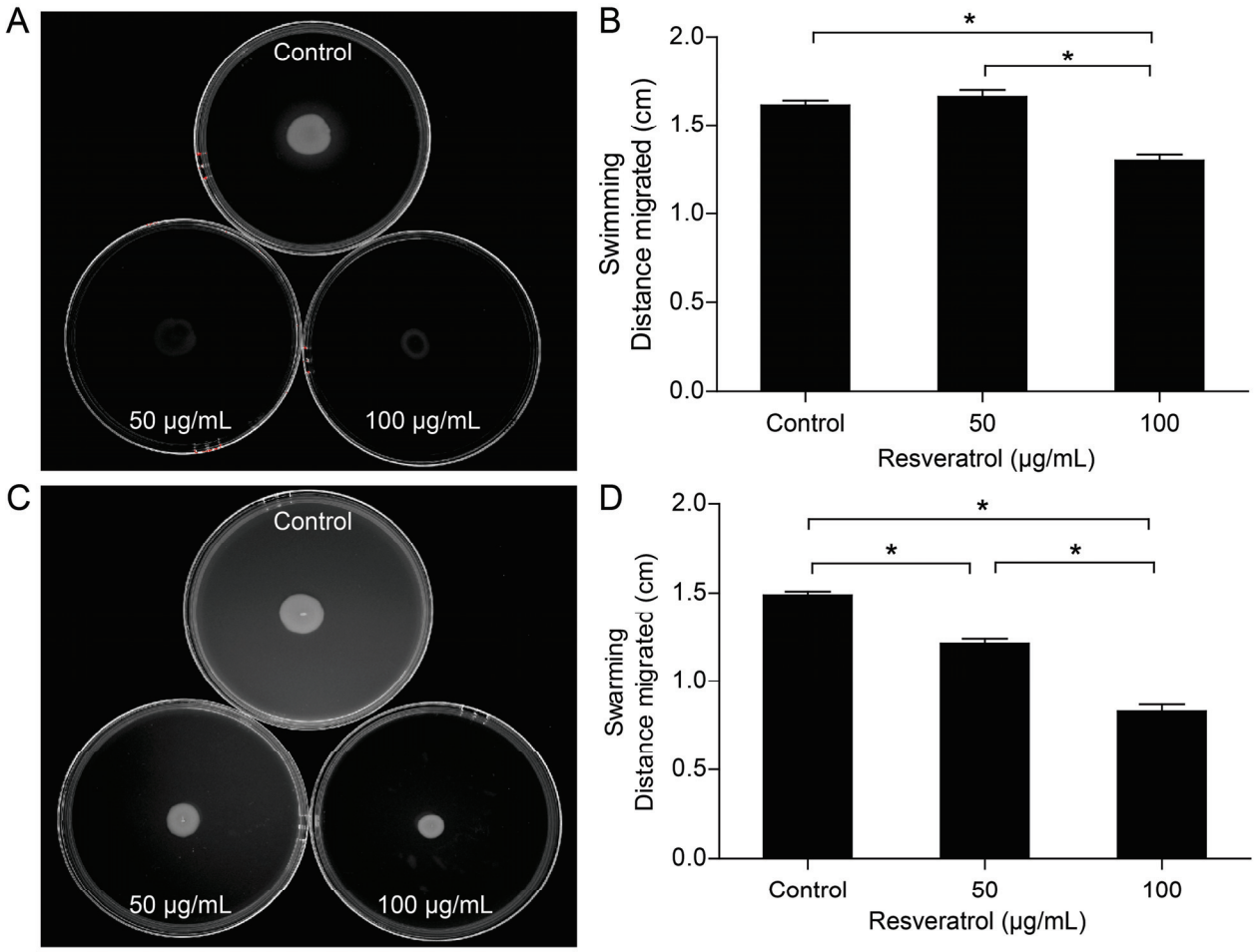

Figure 3. Effects of resveratrol on the swimming and swarming motility of *A. hydrophila*. The abilities of swimming (**A**,**B**) and swarming (**C**,**D**) motility were assessed by examining the migration of bacteria through the agar, from the center toward the periphery of the plate. The results were reproduced in three independent experiments, and the error bars represent SDs. * $p < 0.05$.

2.4. Cytotoxicity of Resveratrol on J774A.1, with or without A. hydrophila NJ-35 Infection

The cytotoxic effect of resveratrol, at sub-MIC concentrations on J774A.1 cells, was detected by LDH activity. As shown in Figure 4, the cytotoxicity of 1% DMSO on J774A.1 cells was less than 1%, and there was no significant difference in cytotoxicity between the 50 μg/mL resveratrol and 1% DMSO. However, the cytotoxicity of resveratrol on J774A.1 cells remarkably increased when co-cultured with 100 μg/mL resveratrol. To directly examine the antibacterial activity, J774A.1 cells were exposed to *A. hydrophila* NJ-35, treated with or without resveratrol. Compared to the drug-free group (only *A. hydrophila* NJ-35 infection), 50 μg/mL resveratrol significantly decreased the LDH release of J774A.1 cells, but no significant difference was observed between the 100 μg/mL resveratrol and drug-free groups. The results indicate that resveratrol within 50 μg/mL is not cytotoxic to J774A.1 cells and has a good protective effect on the J774A.1 cells infected by *A. hydrophila* NJ-35.

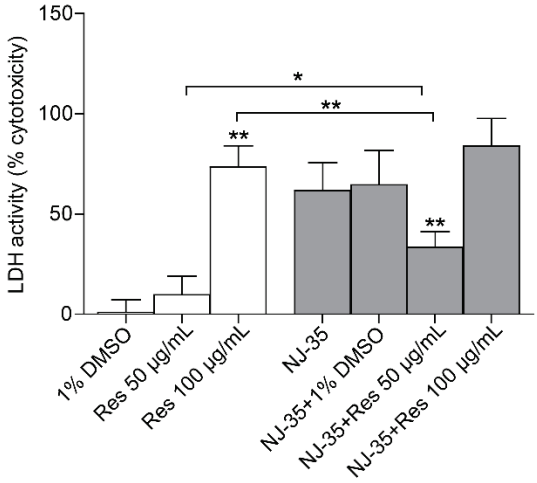

Figure 4. LDH release of J774A.1 cells with or without *A. hydrophila* NJ-35 treatment, and the indicated concentrations of resveratrol. The data were presented as the mean ± SD (n = 6). * $p < 0.05$, ** $p < 0.01$.

2.5. Transcriptome Analysis of A. hydrophila NJ-35 Treated with Resveratrol

As demonstrated above, *A. hydrophila* NJ-35 showed reduced biofilm formation and motility in a dose-dependent manner when treated with resveratrol. In order to determine the molecular mechanism of these changes, RNA-seq was performed on *A. hydrophila* NJ-35 with 0, 50 and 100 μg/mL resveratrol (coded as Res 0, Res 50 and Res 100 groups). The differentially expressed genes (DEGs) were analyzed to infer the candidate genes related to biofilm and motility affected by resveratrol treatment, and to reveal the possible function of these differential genes and related molecular mechanisms.

2.5.1. Screening and Functional Enrichment Analysis

Using the criteria of fold-change ≥ 2 and *p*-value < 0.05, we identified 230 (90 up- and 140 downregulated) and 308 DEGs (130 up- and 178 downregulated) in the presence of 50 and 100 μg/mL resveratrol compared to cultures grown without resveratrol, respectively, of which 120 DEGs were common in both datasets (Figure 5A). After comparing Res 100 and Res 50 groups, 242 DEGs (130 up- and 109 downregulated) were detected, of which 17 DEGs also occurred in Res 50 vs. Res 0, but not in Res 100 vs. Res 0; and 109 DEGs appeared in Res 100 vs. Res 0, but not in Res 50 vs. Res 0 (Figure 5B).

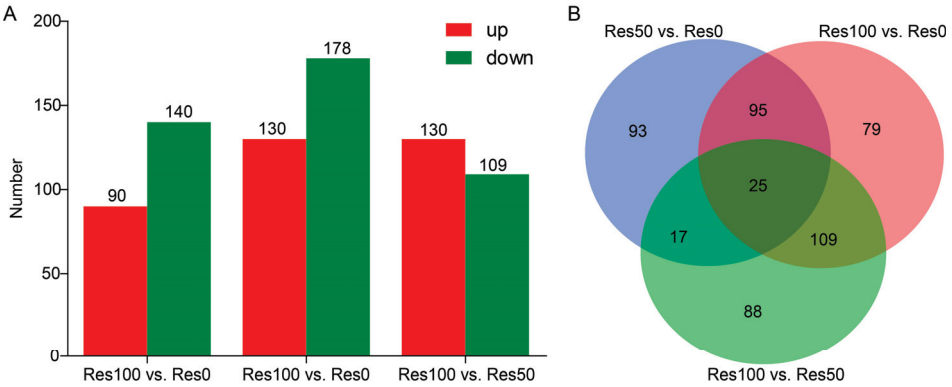

Figure 5. Differentially expressed gene (DEG) analysis. (**A**) Number of upregulated and downregulated DEGs between resveratrol-treated and control groups. (**B**) Venn analysis between resveratrol-treated and control groups.

To gain insight into the functions of the DEGs that were altered by resveratrol treatment, all of the DEGs were mapped to terms in the GO and KEGG databases. GO analysis showed that among the up- and down-regulated genes of *A. hydrophila* NJ-35 in Res

50 and Res 100 groups, "metabolic process", and "cellular process" in biological process, "cell", "cell part", and "membrane" in the cellular component, "catalytic activity", "binding", and "transporter activity" in molecular function were the major enriched groups (Figure 6). In addition, we noted that the number of downregulated genes distributed in the biological process of "response to stimulus" and "locomotion" was much higher than the number of upregulated genes. The top 5 KEGG pathways were as follows: "phenylalanine metabolism", "tyrosine metabolism", and "bacterial chemotaxis" in both Res 50 and Res 100 groups, "phenylalanine, tyrosine and tryptophan biosynthesis" and "histidine metabolism" in Res 50 group, "plant–pathogen interaction" and "selenocompound metabolism" in Res 100 group (Figure 7). It can be found that "bacterial chemotaxis" was the key enrichment pathway of the DEGs in both Res 50 and Res 100 groups, which indicated that the treatment of resveratrol had a significant impact on the motility of *A. hydrophila* NJ-35.

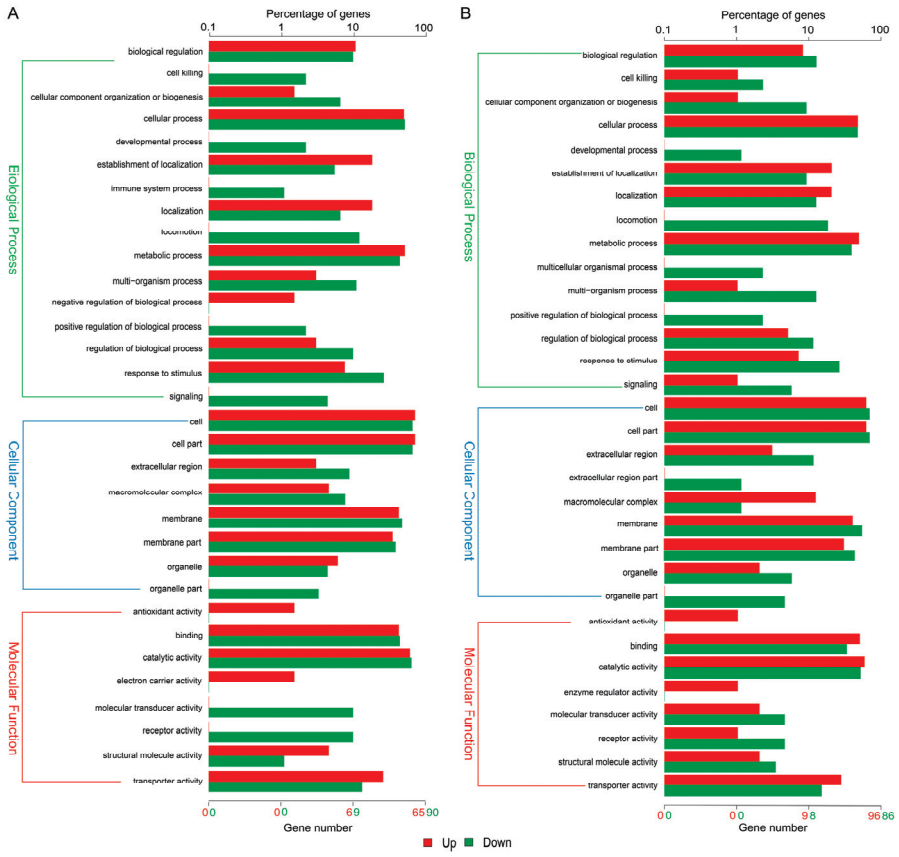

Figure 6. GO functional annotation for DEGs. (**A**) Res 50 vs. Res 0 groups. (**B**) Res 100 vs. Res 0 groups.

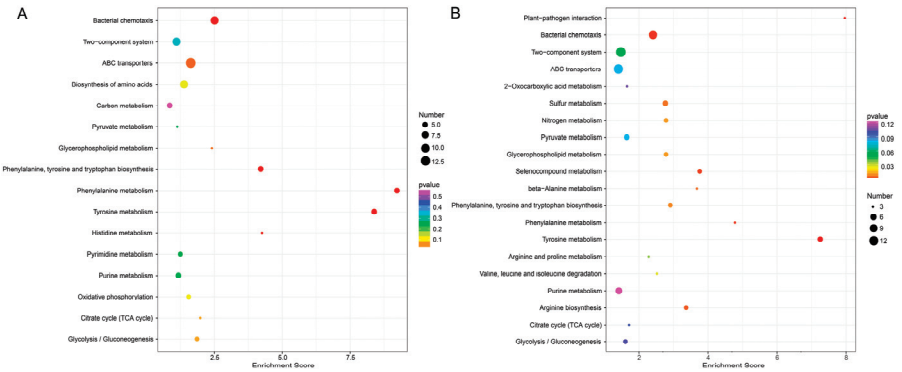

Figure 7. Top 20 DEGs of KEGG pathway enrichment. (**A**) Res 50 vs. Res 0 groups. (**B**) Res 100 vs. Res 0 groups.

2.5.2. Analysis of DEGs Related to Biofilm Formation and Motility

In this study, we focused our analysis on the major genes which were related to biofilm formation and motility. The KEGG classifications associated with "cell motility" and "cellular community prokaryotes" can be found in both Res 50 and Res 100 groups, which contained 12 and 2 DEGs in the Res 50 group, 13 and 5 DEGs in the Res 100 group, respectively (Figure S1). Notably, most of them were downregulated after resveratrol treatment. Not surprisingly, the expressions of the DEGs in "bacterial chemotaxis (ko02030)" and "flagellar assembly (ko02040)" pathways were almost repressed in resveratrol-treated groups. Interestingly, two genes associated with type IV pilus were downregulated, while the other two genes, encoding Flp family proteins, were upregulated. In addition, two GGDEF-domain-containing proteins (encoded by *U876_RS00255* and *U876_RS04630*), that are required for the production of the second messenger cyclic-di-guanosine monophosphate (c-di-GMP) and a helix-turn-helix transcriptional regulator (encoded by *U876_RS01620*) belonging to LysR-Type transcriptional regulators (LTTRs), were decreased. Besides the genes mentioned above, resveratrol also inhibited the expression of other virulence factors, including OmpA, T6SS, lipase and extracellular proteases (protease, elastase and collagenase) (Table 1).

Table 1. A list of some of the important differentially expressed genes between the resveratrol-treated and untreated *A. hydrophila* NJ-35, including genes related to motility, biofilm formation and other virulence factors.

Gene ID	**log2 Fold-Change**		**Description**
	Res 50/Res 0	**Res 100/Res 0**	
Motility			
U876_RS13815	−1.55	−3.00	Flagellin
U876_RS13830	-	−3.12	Flagellin
U876_RS13835	-	−2.50	Flagellin-like protein
U876_RS15700	−1.80	-	Flagellar biosynthesis protein FlhB
U876_RS05370	−1.39	-	Type IV pilus biogenesis protein PilO
U876_RS15085	1.89	-	Flp pilus assembly protein CpaB
U876_RS15095	2.30	2.04	Flp family type IVb pilin
U876_RS19675	−1.45	−2.03	type IV pilin
Chemotaxis			
U876_RS17720	−2.20	−3.57	Chemotaxis protein CheA
U876_RS17730	−2.77	−2.89	Chemotaxis protein CheW
U876_RS17740	−1.96	−3.06	Protein-glutamate O-methyltransferase CheR
U876_RS21115	−3.57	−4.71	Chemotaxis protein
c-di-GMP			
U876_RS00255	-	−1.81	GGDEF-domain-containing protein
U876_RS04630	−4.55	−5.06	GGDEF-domain-containing protein
Extracellular Proteases			
U876_RS04035	−1.86	−2.85	Protease
U876_RS18875	−2.76	−4.74	Elastase
U876_RS20565	−2.94	−3.58	Collagenase

Table 1. *Cont.*

Gene ID	log2 Fold-Change		Description
	Res 50/Res 0	**Res 100/Res 0**	
Lipase			
U876_RS20585	−1.66	−2.34	Lipase
U876_RS20590	−1.68	−1.93	Lipase chaperone
T6SS			
U876_RS21275	−1.47	-	Type II/IV secretion system protein
U876_RS13095	−1.72	-	Type VI secretion system baseplate subunit TssK
U876_RS13100	−1.73	-	Type VI secretion system lipoprotein TssJ
U876_RS13105	−1.69	-	Type VI secretion system-associated FHA domain protein TagH
U876_RS13110	−1.34	-	Type VI secretion system baseplate subunit TssG
U876_RS13155	-	−1.81	Type VI secretion system tip protein VgrG
Small drug resistance			
U876_RS03760	−3.43	-	SMR family multidrug efflux pump
U876_RS03765	−2.91	−2.21	SMR family multidrug efflux pump
Others			
U876_RS01620	−1.93	−3.42	Helix-turn-helix transcriptional regulator
U876_RS08385	-	−2.26	OmpA family protein

2.6. Validation of Differentially Expressed Genes by qRT-PCR

A total of five genes were randomly selected to be measured the relative mRNA transcript levels using real-time quantitative PCR. As shown in the Figure 8, the qRT-PCR results showed similar expression tendency as the RNA-seq data, despite some quantitative differences at the expression level. The result suggested that the transcription abundance of DEGs in transcriptome analysis was highly reliable.

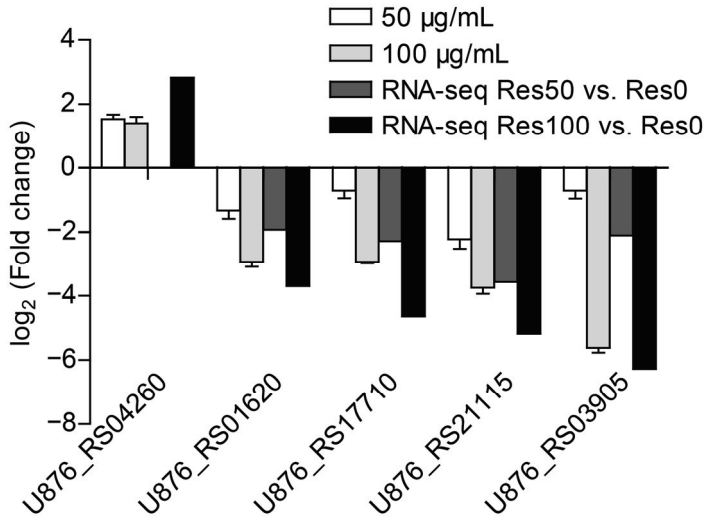

Figure 8. Validation of four different randomly selected genes by qRT-PCR.

3. Discussion

A. hydrophila, one of the most common bacterial pathogens in aquaculture environments, has been reported to be resistant to a number of antibiotics [29,30]. The role of biofilm formation in *A. hydrophila* pathogenesis is well established, as it provides the bacterium with enhanced tolerance to antimicrobial agents and host defenses [8,9,31].

Therefore, inhibiting biofilm formation is of great significance to combat the infection of *A. hydrophila*. Antibiotic therapy typically alleviates the symptoms caused by planktonic bacteria, but fails to kill bacteria in biofilms [32]. During aggravation of bacterial resistance, plant-derived compounds have attracted much attention because of their safety, availability and low toxicity. Resveratrol is a natural plant polyphenol that occurs in various plants, and has been demonstrated to have antibiofilm effects on many Gram-negative and Gram-positive bacterial pathogens [33]. In the present study, resveratrol, at the sub-inhibitory concentrations, can significantly inhibit the biofilm formation of *A. hydrophila* NJ-35 in a dose-dependent manner, which was consistent with our previous findings [28]. Thus, we further investigated the action mechanism of resveratrol on *A. hydrophila* biofilms.

Bacterial adhesion and colonization play an important role in the process of biofilm formation [34]. With the formation of biofilm, bacterial pathogenicity enhances significantly. In our study, the biofilms formed by *A. hydrophila* NJ-35 on the slides were destroyed by resveratrol; meanwhile, as the resveratrol concentration increased, the biofilms decreased gradually and became sparsely distributed on the slides, which had a similar trend to the results obtained by crystal violet staining, EPS production and the total biofilm protein.Therefore, we speculated that resveratrol decreased the adhesion of *A. hydrophila* NJ-35, thus inhibiting biofilm formation. This finding was also confirmed in *S. aureus* and avian pathogenic *E. coli* [24,35].

Motility has a positive influence on the development of biofilm formation, as it facilitates pathogens to colonize, adhere and invade the host cells [36,37]. *Aeromonas* species possess polar flagella for swimming motility and lateral flagella for swarming motility over surfaces [38]. The main antibiofilm activities of resveratrol comprised the inhibition of QS and motility [21]. Our study showed that resveratrol diminished the swimming and swarming motility of *A. hydrophila* NJ-35 in a dose-dependent manner. Particularly, resveratrol dramatically repressed swarming motility even at 50 μg/mL. In EHEC, *trans*-resveratrol inhibited both swimming and swarming motility, and suppressed the expression of several key motility and flagellar genes, including *flhD*, *fimA*, *fimH*, and *motB* [10]. Additionally, reduced swarming ability has also been reported for *Proteus mirabilis* and *V. vulnificus* [39,40]. Given the above, resveratrol might impel the biofilm formation of *A. hydrophila* NJ-35 via disrupting its adhesion and inhibiting swimming and swarming motility.

We further explored the molecular mechanism of these changes through transcriptome analyses (Figure 9). With the increasing concentration of resveratrol, numbers of DEGs in the Res 50 and Res 100 groups increased. As was expected, a large number of DEGs were significantly enriched in biofilm- and motility-related pathways, especially in flagellar and type IV pilus assembly, as well as in bacterial chemotaxis. It has been reported that flagellar motility and chemotaxis exert profound influences on bacterial behaviors, including swarming, biofilm formation and auto-aggregation; the type IV pilus plays an important role in structural biofilm development, including initial formation and dispersal [41,42]. Thus, Resveratrol indeed regulated the biofilm formation and motility of *A. hydrophila* at the transcriptional level.

It is known that the GGDEF-domain-containing proteins contribute to the synthesis of the intracellular signaling molecule c-di-GMP. The latter coordinates the bacterial lifestyle transition from motility to sessility and vice versa [43]. Generally, low c-di-GMP levels are conducive to bacterial motility, such as swimming, twitching and swarming, and inconducive to biofilm formation. In contrast, high c-di-GMP levels promote biofilm formation and restrict bacterial motility [43,44]. Kozlova et al. [45] have demonstrated that c-di-GMP overproduction in *A. hydrophila* SSU dramatically increased the transcripts of *luxS*, *litR*, *vpsT*, *fleQ*, and *fleN*, thus enhancing biofilm formation, but reducing motility, which was consistent with that of the Δ*luxS*. Unlike Δ*luxS*, overproduction of c-di-GMP in Δ*ahyRI* resulted in a slight increase in biofilm formation with no effect on motility, due to the high level of c-di-GMP upregulating the transcriptional level of *vpsR* and downregulating the levels of *vpsT* and *fleN*. On the contrary, Δ*qseB* exhibited a significant reduction in biofilm formation with no effect on swimming motility when c-di-GMP was overproduced,

which was correlated with altered levels of *fleN* and *vpsT* [46]. In addition, resveratrol has been demonstrated to repress the expression of *ahyR* and *ahyI*, as well as T6SS [15,47]. Thus, we indicated that resveratrol may inhibit *A. hydrophila* biofilm formation though AhyRI QS system in a c-di-GMP manner. However, further studies are necessary to demonstrate this.

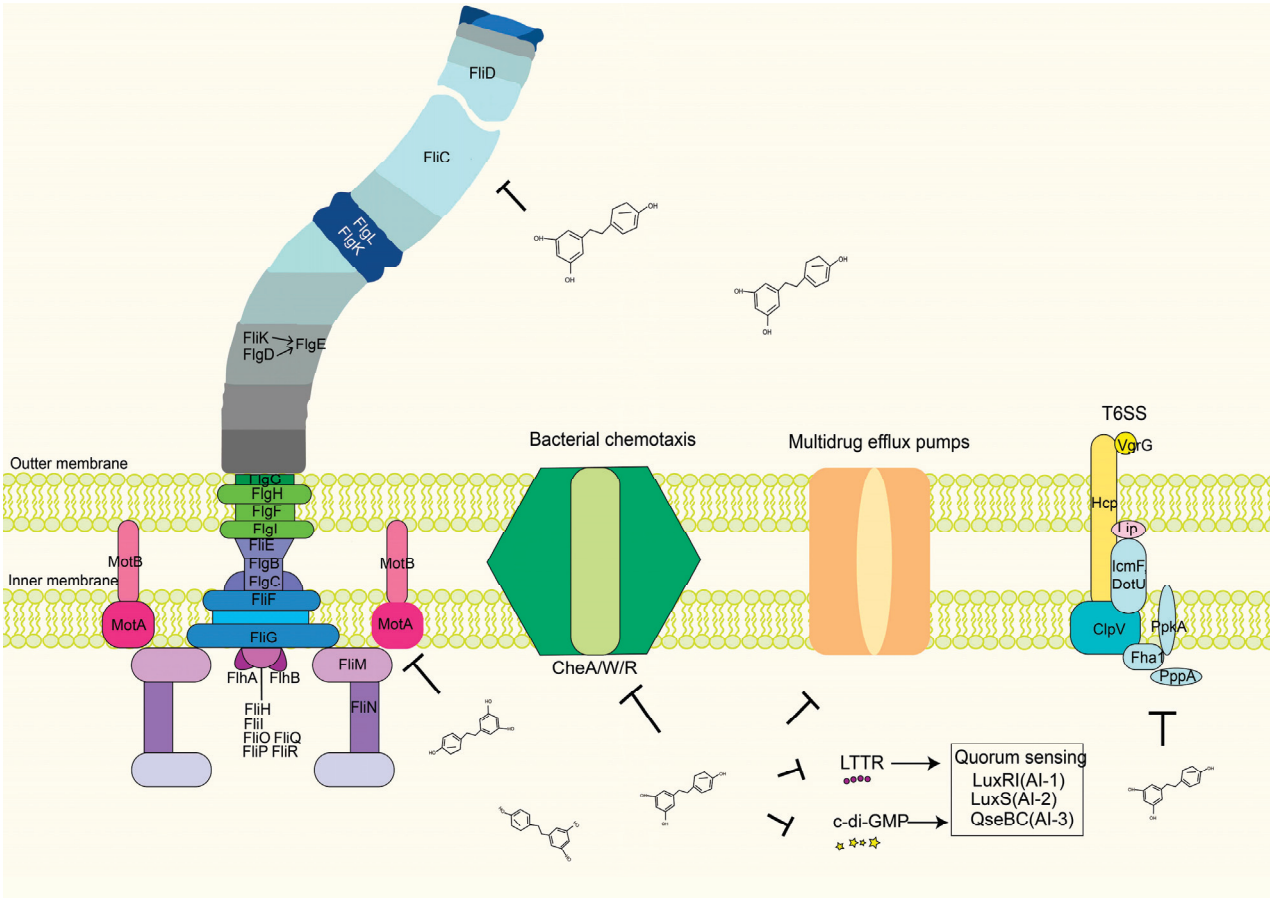

Figure 9. Schematic diagram of the inhibitory effects of resveratrol on *A. hydrophila*. "⊤" denotes inhibition.

The LTTRs are the largest family of diverse and well-characterized global transcriptional regulators of prokaryotes [48]. This family of proteins is involved in the regulation of various processes, including multidrug resistance, virulence, QS, motility and biofilm formation [49–51]. An in-frame deletion of *Bcal3178* (a LysR-type regulator) caused a significant downregulation of biofilm formation and protease production, which are controlled by QS systems in *Burkholderia cenocepacia* [50]. Four putative LTTR family proteins (A0KIU1, A0KJ82, A0KPK0, and A0KQ63) were decreased in *A. hydrophila* following antibiotic treatment, and the deletion of A0KQ63 exhibited multidrug resistance properties [52]. In this study, U876_RS01620 encoding a LTTR was downregulated after adding resveratrol in *A. hydrophila*, while the expression of the two other genes encoding the SMR family of multidrug efflux pumps were repressed. One possible explanation is that the protein encoded by *U876_RS01620* may not affect the above two genes, and resveratrol may activate other pathways to regulate SMR family proteins. In this regard, it may be of interest to evaluate whether resveratrol regulates drug resistance of *A. hydrophila* through the LTTR and whether the LTTR is mediated by the c-di-GMP.

The pathogenesis of *A. hydrophila* is multifactorial, and characterized by the involvement of a number of virulence factors, such as adhesins, outer membrane proteins, hemolysins, protease, and secretion system [53,54]. Our study showed that resveratrol dramatically decreased the gene expression of OmpA, lipase, protease, elastase, collagenase, and T6SS. In addition, resveratrol has been demonstrated to affect the QS-related gene

expression, weaken the hemolytic activity in vitro, and attenuate the in vivo virulence of *A. hydrophila* in the crucian carp infection, supporting the protective role of resveratrol against fish disease [28,47]. Following these results, we speculated that the natural compound resveratrol might inhibit *A. hydrophila* biofilm formation by disturbing the c-di-GMP- and LTTR-dependent QS systems, which could regulate adhesion, motility and virulence. Further study needs to be performed.

4. Materials and Methods

4.1. Bacterial Strains and Growth Conditions

A. hydrophila NJ-35 (CGMCC No.8319) was cultured in Luria broth (LB) or on LB agar at 28 °C [55]. Resveratrol (99%, Aladdin, Shanghai, China) was dissolved in dimethyl sulfoxide (DMSO) as a 10 mg/mL stock solution, and diluted to the required working concentrations depending on the assay type.

4.2. Crystal Violet Biofilm Assay

An assay of static biofilm formation was performed in 96-well polystyrene plates, as previously reported [56]. An overnight culture of *A. hydrophila* NJ-35 was collected and normalized to 1×10^7 CFU/mL, then diluted 1:100 in a fresh LB medium. In our earlier studies, the MIC of resveratrol against *A. hydrophila* NJ-35 was recorded as 1024 μg/mL, whereas the resveratrol concentration below 64 μg/mL did not affect the growth of *A. hydrophila* NJ-35 [28]. Resveratrol was added for experimental cultures at final concentrations of 50 and 100 μg/mL, respectively. DMSO (0.1%, *v*/*v*) was added as the control group. Two hundred microliters of the above dilutions were dispensed to the wells of microtiter plates and incubated at 28 °C for 48 h without agitation. Following incubation, cell growth was measured at 600 nm. Then, the suspended culture was poured out and the wells were washed three times with sterile phosphate-buffered saline (PBS). The adherent cells were fixed with 200 μL methanol for 15 min and dried at room temperature. Subsequently, each well was stained with 200 μL of 1% (wt/vol) crystal violet solution for 15 min and washed with PBS to remove the unbound dye. The formed biofilm was dissolved in absolute ethanol, and the absorbance was measured at 590 nm using a spectrophotometer (MultiskanGO, Thermo Scientific, Vantaa, Finland). The results were normalized to reduce the differences caused by bacterial growth rates according to the method of Niu and Gilbert [57].

4.3. Exopolysaccharides Assay

A. hydrophila NJ-35 was cultured with or without resveratrol in 6-well plates, at 28 °C for 48 h. The formed biofilms were washed three times with PBS, then resuspended in 0.85% NaCl containing 0.22% formaldehyde. After centrifugation, the supernatants were collected and the EPS were determined by the phenol-sulfuric acid method [58].

4.4. Total Biofilm Protein Assay

The biofilms formed in 6-well plates were resuspended in 1 mL PBS. After ultrasonication, the total biofilm protein concentrations were detected using the Modified Bradford Protein Assay Kit (Sangon Biotech, Shanghai, China).

4.5. Scanning Electron Microscopy

The inhibitory effect of resveratrol on the biofilm formation of *A. hydrophila* NJ-35 was observed using SEM. Overnight bacterial culture was normalized to 1×10^7 CFU/mL and diluted 1:100 in LB medium with 50 and 100 μg/mL resveratrol, respectively, and 0.1% (*v*/*v*) DMSO was added as a control. Pre-sterilized coverslips (Φ = 14 mm) were placed into 12-well plates, then 1 mL bacterial dilution was dispensed to each well and incubated at 28 °C for 48 h. The slides were rinsed well with PBS and fixed with 2.5% glutaraldehyde for 4 h. The samples were dehydrated with a series of gradient acetone (10, 30, 50, 70, 90, and 100%, *v*/*v*) for 15 min, and dehydrated in 100% acetone twice. Finally, the sample

was observed under a scanning electron microscope (S-4800, Hitachi, Tokyo, Japan). Nine random positions in three independent experiments were chosen for microscopic analysis.

4.6. Lactate Dehydrogenase Assay

J774A.1 murine macrophages were cultured in DMEM medium with high glucose (HyClone, Beijing, China) containing 10% fetal bovine serum (FBS, Every green, Hangzhou, China) at 37 °C with 5% CO_2. Cells (1×10^5 cells/well) were cultured in 96-well plates for 24 h, then washed three times with PBS. Cells were divided into two groups: resveratrol treatment group and *A. hydrophila* NJ-35 + resveratrol treatment group. DMEM medium and 1% DMSO served as negative control and solvent control, respectively. For infection, bacteria grown to logarithmic phase were collected, washed and seeded with or without resveratrol into each well at the multiplicity of infection (MOI) of 1:1. After 3 h of incubation, the supernatant was harvested and the LDH activity was measured by the LDH Cytotoxicity Assay Kit (Invitrogen, Carlsbad, CA, USA).

4.7. Swimming and Swarming Motility

An LB medium with 0.3% agar for swimming motility and 0.5% agar for swarming motility were prepared, as described previously. Resveratrol was added to the LB agar to final concentrations of 50 or 100 μg/mL. Additionally, DMSO (0.1%) was added as a control. Overnight bacterial culture was normalized to 1×10^7 CFU/mL with the LB medium. Then, 5 μL culture was spotted into the middle of the plate and incubated at 28 °C for 24 h. Motility was assessed by measuring the migration diameter of bacteria from the inoculation point to the periphery of the plate.

4.8. Transcriptome Analysis

A. hydrophila NJ-35 was inoculated into 100 mL LB medium, supplemented with 50 and 100 μg/mL resveratrol at an initial OD_{600} of 0.05, and cultured at 28 °C until the OD_{600} reached 0.8. Bacteria treated with 0.1% DMSO were set as a control group. Cells were collected and washed with PBS for RNA-seq using Illumina HiSeq^{TM} 2500 at Shanghai OE Biotech Co., Ltd. (Shanghai, China) Three parallel samples for each group were pooled as biological replicates for transcriptome analyses. Reads were aligned to the reference genome NZ_CP006870.1 [55] using Rockhooper2 [59]. Gene transcript expression levels were calculated by RPKM [60]. Differential expression analysis was conducted using DESeq [61], then the DEGs picked out, such that p-value < 0.05 and difference of multiples >2. GO and KEGG enrichment analyses of DEGs were performed by hypergeometric distribution tests to determine the biological functions or pathways that are mainly affected by differential genes.

4.9. Real-Time Quantitative PCR (qRT-PCR) Verification

Total RNA was extracted from bacteria with RNAiso Plus (TaKaRa, Tokyo, Japan), according to the manufacturer's instructions, and quantified to 40 ng/μL with a Nanodrop 2000 (Thermo Fisher Scientific, Wilmington, MA, USA). Two microliters of diluted RNA were directly used for qRT-PCR with One Step SYBR® PrimeScript® Plus RT-PCR Kit (TaKaRa, Dalian, China). The primers were listed in Table 2. The expression levels of the tested genes were analyzed with *rpoB* as the reference gene. Fold-change was calculated using the $2^{-\Delta\Delta Ct}$ method [62].

Table 2. Primers used in qRT-PCR.

Gene ID	Description	Primer	Sequence (5′ to 3′)	Reference
U876_RS04260	Universal stress protein	F	CCACAAGGCTGAACTCAA	This study
		R	CAGGTCGGCTTTCTCTTC	
U876_RS17710	Response regulator	F	CGGTTATGAGGTGATGGAG	This study
		R	TTCCTGCTTCTTGCTGTC	
U876_RS21115	Chemotaxis protein	F	TGCTGTACGCCTTCTAATG	This study
		R	CATGCTGTAGTGCTGACC	
U876_RS03905	Competence protein ComEA	F	ATGAACTACAAGACCCTGAC	This study
		R	GATCCACGGTAGTGAACTT	
U876_RS01620	Helix-turn-helix transcriptional regulator	F	GCGATCTGGTCAACTACTA	This study
		R	GCGGTTCTTCACATTCAAT	
ropB	Housekeeping gene, RNA polymerase beta subunit	F	ACCGACGAAGTGGACTATCT	[53]
		R	CGGCGTTCATAAAGGTGGAT	

4.10. Statistical Analysis

All experiments were repeated independently three times. The data were expressed as the mean ± SD. A one-way analysis of variance (ANOVA) was conducted to identify the significant differences, followed by Bonferroni's post-test (IBM SPSS Statistics, version 19.0, Armonk, NY, USA). A p-value of <0.05 or <0.01 was considered statistically significant.

5. Conclusions

Our study highlights that resveratrol at sub-MIC has an inhibitory effect on the biofilm formation and motility of *A. hydrophila*. Transcriptome analysis found that resveratrol significantly repressed bacterial chemotaxis and flagellar assembly pathways, disrupted type IV pilus synthesis, downregulated the c-di-GMP and LTTR levels, which all involved in QS systems. Thus, we concluded that resveratrol could decrease biofilm formation at concentrations without anti-*A. hydrophila* growth by inhibiting QS systems. Additionally, resveratrol also markedly suppressed the gene expression of several important virulence factors, such as OmpA, extracellular proteases, lipases, and T6SS. In conclusion, resveratrol could be considered a potential therapeutic drug by attenuating the capacity of pathogenic *A. hydrophila* to cause infection, and is unable to induce muti-drug resistance.

Supplementary Materials: The following supporting information can be downloaded at: https://www.mdpi.com/article/10.3390/antibiotics12040686/s1, Figure S1: KEGG pathway classification. (A) Res 50 vs. Res 0 groups. (B) Res 100 vs. Res 0 groups.

Author Contributions: Conceptualization, T.Q., B.X. and J.X.; methodology, T.Q.; software, T.Q. and L.L.; validation, T.Q. and K.C.; formal analysis, T.Q.; investigation, T.Q.; resources, J.X.; data curation, T.Q.; writing—original draft preparation, T.Q.; writing—review and editing, B.X. and T.Q.; visualization, T.Q. and K.L.; supervision, B.X. and L.P.; project administration, B.X.; funding acquisition, J.X. All authors have read and agreed to the published version of the manuscript.

Funding: This research was funded by the China Agriculture Research System of MOF and MARA (CARS-45).

Institutional Review Board Statement: Not applicable.

Informed Consent Statement: Not applicable.

Data Availability Statement: Data are available upon request.

Conflicts of Interest: The authors declare no conflict of interest.

References

1. Janda, J.M. Recent advances in the study of the taxonomy, pathogenicity, and infectious syndromes associated with the genus Aeromonas. *Clin. Microbiol. Rev.* **1991**, *4*, 397–410. [CrossRef] [PubMed]
2. Martins, L.M.; Marquez, R.F.; Yano, T. Incidence of toxic *Aeromonas* isolated from food and human infection. *FEMS Immunol. Med. Microbiol.* **2002**, *32*, 237–242. [CrossRef]
3. Harikrishnan, R.; Balasundaram, C. Modern trends in *Aeromonas hydrophila* disease management with fish. *Rev. Fish. Sci.* **2005**, *13*, 281–320. [CrossRef]
4. Parker, J.L.; Shaw, J.G. *Aeromonas* spp. clinical microbiology and disease. *J. Infect.* **2011**, *62*, 109–118. [CrossRef] [PubMed]
5. Defoirdt, T.; Sorgeloos, P.; Bossier, P. Alternatives to antibiotics for the control of bacterial disease in aquaculture. *Curr. Opin. Microbiol.* **2011**, *14*, 251–258. [CrossRef] [PubMed]
6. Ferri, G.; Lauteri, C.; Vergara, A. Antibiotic Resistance in the Finfish Aquaculture Industry: A Review. *Antibiotics* **2022**, *11*, 1574. [CrossRef]
7. Zhao, X.L.; Wu, G.; Chen, H.; Li, L.; Kong, X.H. Analysis of virulence and immunogenic factors in *Aeromonas hydrophila*: Towards the development of live vaccines. *J. Fish Dis.* **2020**, *43*, 747–755. [CrossRef]
8. Rasmussen-Ivey, C.R.; Figueras, M.J.; McGarey, D.; Liles, M.R. Virulence factors of *Aeromonas hydrophila*: In the wake of Reclassification. *Front. Microbiol.* **2016**, *7*, 1337. [CrossRef]
9. Lynch, M.J.; Swift, S.; Kirke, D.F.; Keevil, C.W.; Dodd, C.E.R.; Williams, P. The regulation of biofilm development by quorum sensing in *Aeromonas hydrophila*. *Environ. Microbiol.* **2002**, *4*, 18–28. [CrossRef]
10. Lee, J.H.; Cho, H.S.; Joo, S.W.; Chandra Regmi, S.; Kim, J.A.; Ryu, C.M.; Ryu, S.Y.; Cho, M.H.; Lee, J. Diverse plant extracts and trans-resveratrol inhibit biofilm formation and swarming of *Escherichia coli* O157:H7. *Biofouling* **2013**, *29*, 1189–1203. [CrossRef]
11. Cao, Y.; Naseri, M.; He, Y.; Xu, C.; Walsh, L.J.; Ziora, Z.M. Non-antibiotic antimicrobial agents to combat biofilm-forming bacteria. *J. Glob. Antimicrob. Resist.* **2020**, *21*, 445–451. [CrossRef] [PubMed]
12. Flemming, H.C.; Wingender, J. The biofilm matrix. *Nat. Rev. Microbiol.* **2010**, *8*, 623–633. [CrossRef] [PubMed]
13. Du, B.; Gu, Y.; Chen, G.; Wang, G.; Liu, L. Flagellar motility mediates early-stage biofilm formation in oligotrophic aquatic environment. *Ecotoxicol. Environ. Saf.* **2020**, *194*, 110340. [CrossRef] [PubMed]
14. Webster, S.S.; Lee, C.K.; Schmidt, W.C.; Wong, G.C.L.; O'Toole, G.A. Interaction between the type 4 pili machinery and a diguanylate cyclase fine-tune c-di-GMP levels during early biofilm formation. *Proc. Natl. Acad. Sci. USA* **2021**, *118*, e2105566118. [CrossRef]
15. Khajanchi, B.K.; Sha, J.; Kozlova, E.V.; Erova, T.E.; Suarez, G.; Sierra, J.C.; Popov, V.L.; Horneman, A.J.; Chopra, A.K. N-Acylhomoserine lactones involved in quorum sensing control the type VI secretion system, biofilm formation, protease production, and in vivo virulence in a clinical isolate of *Aeromonas hydrophila*. *Microbiology* **2009**, *155*, 3518–3531. [CrossRef]
16. Khajanchi, B.K.; Kozlova, E.V.; Sha, J.; Popov, V.L.; Chopra, A.K. The two-component QseBC signalling system regulates in vitro and in vivo virulence of *Aeromonas hydrophila*. *Microbiology* **2012**, *158*, 259–271. [CrossRef]
17. Li, X.H.; Lee, J.H. Antibiofilm agents: A new perspective for antimicrobial strategy. *J. Microbiol.* **2017**, *55*, 753–766. [CrossRef]
18. Dembic, M.; Andersen, H.S.; Bastin, J.; Doktor, T.K.; Corydon, T.J.; Sass, J.O.; Lopes, C.A.; Djouadi, F.; Andresen, B.S. Next generation sequencing of RNA reveals novel targets of resveratrol with possible implications for Canavan disease. *Mol. Genet. Metab.* **2019**, *126*, 64–76. [CrossRef]
19. Sun, J.; Zhang, M.; Chen, K.; Chen, B.; Zhao, Y.; Gong, H.; Zhao, X.; Qi, R. Suppression of TLR4 activation by resveratrol is associated with STAT3 and Akt inhibition in oxidized low-density lipoprotein-activated platelets. *Eur. J. Pharmacol.* **2018**, *836*, 1–10. [CrossRef]
20. Xu, B.P.; Yao, M.; Li, Z.J.; Tian, Z.R.; Ye, J.; Wang, Y.J.; Cui, X.J. Neurological recovery and antioxidant effects of resveratrol in rats with spinal cord injury: A meta-analysis. *Neural Regen. Res.* **2020**, *15*, 482–490. [CrossRef] [PubMed]
21. Bostanghadiri, N.; Pormohammad, A.; Chirani, A.S.; Pouriran, R.; Erfanimanesh, S.; Hashemi, A. Comprehensive review on the antimicrobial potency of the plant polyphenol Resveratrol. *Biomed. Pharmacother.* **2017**, *95*, 1588–1595. [CrossRef] [PubMed]
22. He, Z.T.; Huang, Z.W.; Zhou, W.; Tang, Z.S.; Ma, R.; Liang, J.P. Anti-biofilm Activities from Resveratrol against *Fusobacterium nucleatum*. *Front. Microbiol.* **2016**, *7*, 1065. [CrossRef] [PubMed]
23. Augustine, N.; Goel, A.K.; Sivakumar, K.C.; Kumar, R.A.; Thomas, S. Resveratrol–a potential inhibitor of biofilm formation in *Vibrio cholerae*. *Phytomedicine* **2014**, *21*, 286–289. [CrossRef]
24. Qin, N.; Tan, X.J.; Jiao, Y.M.; Liu, L.; Zhao, W.S.; Yang, S.; Jia, A.Q. RNA-Seq-based transcriptome analysis of methicillin-resistant *Staphylococcus aureus* biofilm inhibition by ursolic acid and resveratrol. *Sci. Rep.* **2014**, *4*, 5467. [CrossRef] [PubMed]
25. Santos, C.A.; Lima, E.M.F.; Franco, B.D.G.M.; Pinto, U.M. Exploring phenolic compounds as quorum sensing inhibitors in foodborne bacteria. *Front. Microbiol.* **2021**, *12*, 735931. [CrossRef]
26. Lee, K.; Lee, J.H.; Ryu, S.Y.; Cho, M.H.; Lee, J. Stilbenes reduce *Staphylococcus aureus* hemolysis, biofilm formation, and virulence. *Foodborne Pathog. Dis.* **2014**, *11*, 710–717. [CrossRef]
27. Cho, H.S.; Lee, J.H.; Cho, M.H.; Lee, J. Red wines and flavonoids diminish *Staphylococcus aureus* virulence with anti-biofilm and anti-hemolytic activities. *Biofouling* **2015**, *31*, 1–11. [CrossRef]
28. Tan, H.L.; Chen, K.; Xi, B.W.; Qin, T.; Pan, L.K.; Xie, J. Resveratrol inhibits growth, virulence and biofilm formation of *Aeromonas hydrophila*. *Acta Hydrobiol. Sin.* **2019**, *43*, 861–868. [CrossRef]

29. Hossain, S.; De Silva, B.C.J.; Dahanayake, P.S.; Heo, G.J. Characterization of Virulence Properties and Multi-Drug Resistance Profiles in Motile Aeromonas Spp. Isolated from Zebrafish (*Danio rerio*). *Lett. Appl. Microbiol.* **2018**, *67*, 598–605. [CrossRef]
30. Ranjbar, R.; Salighehzadeh, R.; Sharifiyazdi, H. Antimicrobial Resistance and Incidence of Integrons in *Aeromonas* Species Isolated from Diseased Freshwater Animals and Water Samples in Iran. *Antibiotics* **2019**, *8*, 198. [CrossRef]
31. Sun, B.; Luo, H.Z.; Jiang, H.; Wang, Z.N.; Jia, A.Q. Inhibition of Quorum Sensing and Biofilm Formation of Esculetin on *Aeromonas hydrophila*. *Front. Microbiol.* **2021**, *12*, 737626. [CrossRef] [PubMed]
32. Costerton, J.W. Bacterial biofilms: A common cause of persistent infections. *Science* **1999**, *284*, 1318–1322. [CrossRef] [PubMed]
33. Ma, D.S.L.; Tan, L.T.-H.; Chan, K.-G.; Yap, W.H.; Pusparajah, P.; Chuah, L.-H.; Ming, L.C.; Khan, T.M.; Lee, L.-H.; Goh, B.-H. Resveratrol-Potential Antibacterial Agent against Foodborne Pathogens. *Front. Pharmacol.* **2018**, *9*, 102. [CrossRef] [PubMed]
34. Mostafavi, S.K.S.; Najar-Peerayeh, S.; Mobarez, A.M.; Parizi, M.K. Characterization of uropathogenic *E. coli* O25b-B2-ST131, O15:K52:H1, and CGA: Neutrophils apoptosis, serum bactericidal assay, biofilm formation, and virulence typing. *J. Cell Physiol.* **2019**, *234*, 18272–18282. [CrossRef]
35. Ruan, X.C.; Deng, X.L.; Tan, M.; Yu, C.B.; Zhang, M.S.; Sun, Y.; Jiang, N.H. In vitro antibiofilm activity of resveratrol against avian pathogenic *Escherichia coli*. *BMC Vet. Res.* **2021**, *17*, 249. [CrossRef]
36. Kirov, S.M.; Tassell, B.C.; Semmler, A.B.; O'Donovan, L.A.; Rabaan, A.A.; Shaw, J.G. Lateral flagella and swarming motility in Aeromonas species. *J. Bacteriol.* **2002**, *184*, 547–555. [CrossRef]
37. Wood, T.K. Insights on *Escherichia coli* biofilm formation and inhibition from whole-transcriptome profiling. *Environ. Microbiol.* **2009**, *11*, 1–15. [CrossRef]
38. Kirov, S.M.; Castrisios, M.; Shaw, J.G. *Aeromonas* flagella (polar and lateral) are enterocyte adhesins that contribute to biofilm formation on surfaces. *Infect. Immun.* **2004**, *72*, 1939–1945. [CrossRef]
39. Wang, W.-B.; Lai, H.-C.; Hsueh, P.-R.; Chiou, R.Y.-Y.; Lin, S.-B.; Liaw, S.-J. Inhibition of swarming and virulence factor expression in *Proteus mirabilis* by resveratrol. *J. Med. Microbiol.* **2006**, *55*, 1313–1321. [CrossRef]
40. Kim, J.R.; Cha, M.H.; Oh, D.-R.; Oh, W.K.; Rhee, J.H.; Kim, Y.R. Resveratrol modulates RTX toxin-induced cytotoxicity through interference in adhesion and toxin production. *Eur. J. Pharmacol.* **2010**, *642*, 163–168. [CrossRef]
41. Colin, R.; Ni, B.; Laganenka, L.; Sourjik, V. Multiple functions of flagellar motility and chemotaxis in bacterial physiology. *FEMS Microbiol. Rev.* **2021**, *45*, fuab038. [CrossRef]
42. Pamp, S.J.; Tolker-Nielsen, T. Multiple roles of biosurfactants in structural biofilm development by *Pseudomonas aeruginosa*. *J. Bacteriol.* **2007**, *189*, 2531–2539. [CrossRef]
43. Romling, U.; Galperin, M.Y.; Gomelsky, M. Cyclic di-GMP: The first 25 years of a universal bacterial second messenger. *Microbiol. Mol. Biol. Rev.* **2013**, *77*, 1–52. [CrossRef]
44. Cotter, P.A.; Stibitz, S. c-di-GMP-mediated regulation of virulence and biofilm formation. *Curr. Opin. Microbiol.* **2007**, *10*, 17–23. [CrossRef] [PubMed]
45. Kozlova, E.V.; Khajanchi, B.K.; Sha, J.; Chopra, A.K. Quorum sensing and c-di-GMP dependent alterations in gene transcripts and virulence-associated phenotypes in a clinical isolate of *Aeromonas hydrophila*. *Microb. Pathog.* **2011**, *50*, 213e23. [CrossRef] [PubMed]
46. Kozlova, E.V.; Khajanchi, B.K.; Popov, V.L.; Wen, J.; Chopra, A.K. Impact of QseBC system in c-di-GMP-dependent quorum sensing regulatory network in a clinical isolate SSU of *Aeromonas hydrophila*. *Microb. Pathog.* **2012**, *53*, 115–124. [CrossRef] [PubMed]
47. Dong, J.; Zhang, L.S.; Liu, Y.T.; Zhou, S.; Yang, Y.B.; Xu, N.; Yang, Q.H.; Ai, X.H. Resveratrol influences the pathogenesis of *Aeromonas hydrophila* by inhibiting production of aerolysin and biofilm. *Food Control* **2021**, *126*, 108083. [CrossRef]
48. Maddocks, S.E.; Oyston, P.C.F. Structure and function of the LysR-type transcriptional regulator (LTTR) family proteins. *Microbiology (Reading)* **2008**, *154 Pt 12*, 3609–3623. [CrossRef] [PubMed]
49. Shaheen, A.; Tariq, A.; Shehzad, A.; Iqbal, M.; Mirza, O.; Maslov, D.A.; Rahman, M. Transcriptional regulation of drug resistance mechanisms in Salmonella: Where we stand and what we need to know. *World J. Microbiol. Biotechnol.* **2020**, *36*, 85. [CrossRef] [PubMed]
50. Wang, K.; Li, X.; Yang, C.X.; Song, S.H.; Cui, C.Y.; Zhou, X.F.; Deng, Y.Y. A LysR Family Transcriptional Regulator Modulates *Burkholderia cenocepacia* Biofilm Formation and Protease Production. *Appl. Environ. Microbiol.* **2021**, *87*, e0020221. [CrossRef]
51. Modrzejewska, M.; Kawalek, A.; Bartosik, A.A. The LysR-Type Transcriptional Regulator BsrA (PA2121) Controls Vital Metabolic Pathways in *Pseudomonas aeruginosa*. *mSystems* **2021**, *6*, e0001521. [CrossRef] [PubMed]
52. Fu, Y.Y.; Cai, Q.L.; Wang, Y.Q.; Li, W.X.; Yu, J.; Yang, G.D.; Lin, W.X.; Lin, X.M. Four LysR-type transcriptional regulator family proteins (LTTRs) involved in antibiotic resistance in *Aeromonas hydrophila*. *World J. Microbiol. Biotechnol.* **2019**, *35*, 127. [CrossRef]
53. Gao, J.W.; Xi, B.W.; Chen, K.; Song, R.; Qin, T.; Xie, J.; Pan, L.K. The stress hormone norepinephrine increases the growth and virulence of *Aeromonas hydrophila*. *Microbiologyopen* **2019**, *8*, e00664. [CrossRef] [PubMed]
54. Wang, N.N.; Wu, Y.F.; Pang, M.D.; Liu, J.; Lu, C.P.; Liu, Y.J. Protective efficacy of recombinant hemolysin co-regulated protein (Hcp) of *Aeromonas hydrophila* in common carp (*Cyprinus carpio*). *Fish Shellfish Immunol.* **2015**, *46*, 297–304. [CrossRef]
55. Pang, M.D.; Jiang, J.W.; Xie, X.; Wu, Y.F.; Dong, Y.H.; Kwok, A.H.Y.; Zhang, W.; Yao, H.C.; Lu, C.P.; Leung, F.C.; et al. Novel insights into the pathogenicity of epidemic *Aeromonas hydrophila* ST251 clones from comparative genomics. *Sci. Rep.* **2015**, *5*, 9833. [CrossRef]

56. Dong, Y.H.; Liu, J.; Pang, M.D.; Du, H.C.; Wang, N.N.; Awan, F.; Lu, C.P.; Liu, Y.J. Catecholamine-stimulated growth of *Aeromonas hydrophila* requires the TonB2 energy transduction system but is independent of the amonabactin siderophore. *Front. Cell. Infect. Microbiol.* **2016**, *6*, 183. [CrossRef]
57. Niu, C.; Gilbert, E.S. Colorimetric method for identifying plant essential oil components that affect biofilm formation and structure. *Appl. Environ. Microbiol.* **2004**, *70*, 6951–6956. [CrossRef]
58. Liu, F.; Jin, P.; Sun, Z.; Du, L.; Wang, D.; Zhao, T.; Doyle, M.P. Carvacrol oil inhibits biofilm formation and exopolysaccharide production of *Enterobacter cloacae*. *Food Control* **2021**, *119*, 107473. [CrossRef]
59. Tjaden, B. *De novo* assembly of bacterial transcriptomes from RNA-seq data. *Genome Biol.* **2015**, *16*, 1. [CrossRef]
60. Mortazavi, A.; Williams, B.A.; McCue, K.; Schaeffer, L.; Wold, B. Mapping and quantifying mammalian transcriptomes by RNA-Seq. *Nat. Methods* **2008**, *5*, 621. [CrossRef] [PubMed]
61. Anders, S. Analysing RNA-Seq data with the DESeq package. *Mol. Biol.* 2012. Available online: https://www.bioconductor.org/packages//2.7/bioc/vignettes/DESeq/inst/doc/DESeq.pdf (accessed on 19 February 2023).
62. Livak, K.J.; Schmittgen, T.D. Analysis of relative gene expression data using real-time quantitative PCR and the 2(-Delta Delta C(T)) method. *Methods* **2001**, *25*, 402–408. [CrossRef] [PubMed]

Disclaimer/Publisher's Note: The statements, opinions and data contained in all publications are solely those of the individual author(s) and contributor(s) and not of MDPI and/or the editor(s). MDPI and/or the editor(s) disclaim responsibility for any injury to people or property resulting from any ideas, methods, instructions or products referred to in the content.

antibiotics

MDPI

Article

Inhibition of *Candida albicans* Biofilm Formation and Attenuation of Its Virulence by *Liriope muscari*

Jeonghoon Lee [1,†], Hyunchan Song [2,†] and Kiyoung Kim [2,*]

[1] Department of Medical Science of Meridian, College of Korean Medicine, Graduate School, Kyung Hee University, Kyungheedae-ro 6-gil, Dongdaemun-gu, Seoul 02447, Republic of Korea; ljh@boguclinic.com
[2] Graduate School of Biotechnology, Kyung Hee University, 1732, Deogyeong-daero, Giheung-gu, Yongin-si 17104, Republic of Korea; songhchan@naver.com
* Correspondence: kiyoung@khu.ac.kr; Tel.: +82-312-012-633
† These authors contributed equally to this work.

Abstract: (1) Background: Although *Candida albicans* accounts for the majority of fungal infections, therapeutic options are limited and require alternative antifungal agents with new targets; (2) Methods: A biofilm formation assay with RPMI1640 medium was performed with *Liriope muscari* extract. A combination antifungal assay, dimorphic transition assay, and adhesion assay were performed under the biofilm formation condition to determine the anti-biofilm formation effect. qRT-PCR analysis was accomplished to confirm changes in gene expression; (3) Results: *L. muscari* extract significantly reduces biofilm formation by 51.65% at 1.56 μg/mL use and therefore increases susceptibility to miconazole. *L. muscari* extract also inhibited the dimorphic transition of Candida; nearly 50% of the transition was inhibited when 1.56 μg/mL of the extract was treated. The extract of *L. muscari* inhibited the expression of genes related to hyphal development and extracellular matrix of 34.4% and 36.0%, respectively, as well as genes within the Ras1-cAMP-PKA, Cph2-Tec1, and MAP kinase signaling pathways of 25.58%, 7.1% and 15.8%, respectively, at 1.56 μg/mL of *L. muscari* extract treatment; (4) Conclusions: *L. muscari* extract significantly reduced Candida biofilm formation, which lead to induced antifungal susceptibility to miconazole. It suggests that *L. muscari* extract is a promising anti-biofilm candidate of *Candida albicans* since the biofilm formation of *Candida albicans* is an excellent target for candidiasis regulation.

Keywords: *Candida albicans*; *Liriope muscari*; biofilm formation; antifungal agent; dimorphic transition; adherence assay

1. Introduction

Candida albicans accounts for the majority of fungal pathogens found and has a mortality rate of 40–60% [1–3]. It is typically found in the mouth, skin, and intestines. Sometimes, it can invade the human body, causing infection in the blood, bones, brain, and heart [2]. The annual expenditure for the treatment of fungal diseases was $4.5 billion in the United States alone, that for Candida infections cost the most with $1.4 billion, while that for aspergillus infections cost $1.2 billion [2–4]. Additionally, there were 3,639,037 candidiasis outpatient visits, costing $1.6 billion out of the total outpatient costs of $2.6 billion. The second-highest outpatient cost was for patients with dermatophyte infections, amounting to $802 million [4].

Recently, efforts to discover alternative methods for eradicating biofilm-related infections have increased [5]. Early antibiotics caused an increased resistance of fungi [6]. One of the new therapeutic approaches to medication for fungal infections is combinational therapies [5]. It targets several aspects of micro-organisms to control infections. Biofilm formation of pathogenic fungi is now at the center of attention due to their increasing resistance to commercially available antifungal agents and environmental conditions [7–9].

C. albicans biofilm formation involves a complex developmental process. It begins with the attachment of planktonic cells to a substrate, followed by cell proliferation, hyphal growth, and extracellular matrix production [10–12]. Eventually, mature cells disperse from the biofilm into the surrounding environment [10]. Planktonic cells are mostly vulnerable to several agents since there are no defensive barriers between the cells and the environment [13]. The biofilm formation is a critical step in pathogenesis because *C. albicans* tends to exhibit reduced sensitivity or insensitivity to antifungal agents [14,15].

Natural substances significantly contribute to the discovery and development of drugs [16,17]. More than 75% of the treatment drugs used against infectious diseases are derived from nature [18]. It has advantages over synthetic medications in cost and the number of potential candidates [19]. Also, it may lead to shortcuts to study combinational therapies [5].

The genus *Liriope* has been pharmacologically used in several Asian countries. It was historically proven to treat various diseases [20]. With the advancement of technologies, recent studies analyzed the chemicals of genus *Liriope* involved in traditional use [20,21]. *Liriope muscari*, one of the genus *Liriope* plants, has been utilized in traditional Chinese medicine for the treatment of various ailments including pharyngitis, bronchitis, pneumonia, cough, and cardiovascular disease [22]. Previous studies found that they have novel bioactive compounds including steroidal saponins, flavonoids, and sesquiterpene glucoside [20]. For example, a novel steroidal saponin DT-13 isolated from *L. muscari* reduced the adhesion of human breast cancer cells and their migration under hypoxia [23,24]. However, neither the activities of the whole extract of *L. muscari* nor the compounds in them against *C. albicans* have been studied. It means that the inhibition of attachment to the animal cells or the surrounding area, transitions from yeast to hyphae, and biofilm formation of *C. albicans* using *L. muscari* remain largely unclear. The objectives of this study were to (i) evaluate the potential inhibition by *L. muscari* on biofilm formation of *C. albicans* and (ii) improve the understanding of *L. muscari* triggering anti-biofilm mechanisms.

2. Results

2.1. Anti-biofilm effect of L. muscari

L. muscari was treated for the purpose of determining its anti-biofilm activity. *L. muscari* significantly reduced biofilm density in the strains tested (Figure 1). The IC_{50} value of *L. muscari* for inhibition of biofilm formation was nearly 1.56 μg/mL against *C. albicans* (Figure 1). With only the use of 1.56 μg/mL, 51.65 ± 7.83% of biofilm formation was inhibited.

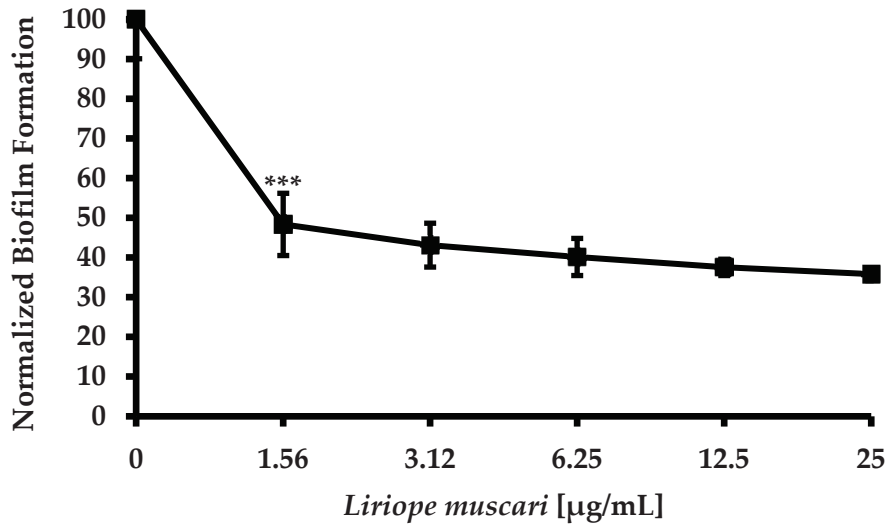

Figure 1. *L. muscari* extract inhibited biofilm formation. (***: *p*-value < 0.001).

2.2. L. muscari Extract Increased the Susceptibility of Commercial Antibiotics to C. albicans

L. muscari extract was combined with antibiotics to investigate if inhibiting biofilm formation would influence antibiotic susceptibility. After 24 h of growth, Candida cultures were treated with the indicated concentrations of miconazole (MCZ) with or without *L. muscari* (LM) extract for an additional 24 h. *L. muscari* extract increased susceptibility to antifungal agents (Figure 2). When MCZ was treated alone, 58.53 ± 2.92% of viable fungus remained. However, when *L. muscari* was treated with MCZ, a reduced amount of MCZ use for *C. albicans* control was observed, which means L. muscari-induced susceptibility of *C. albicans* on MCZ had increased.

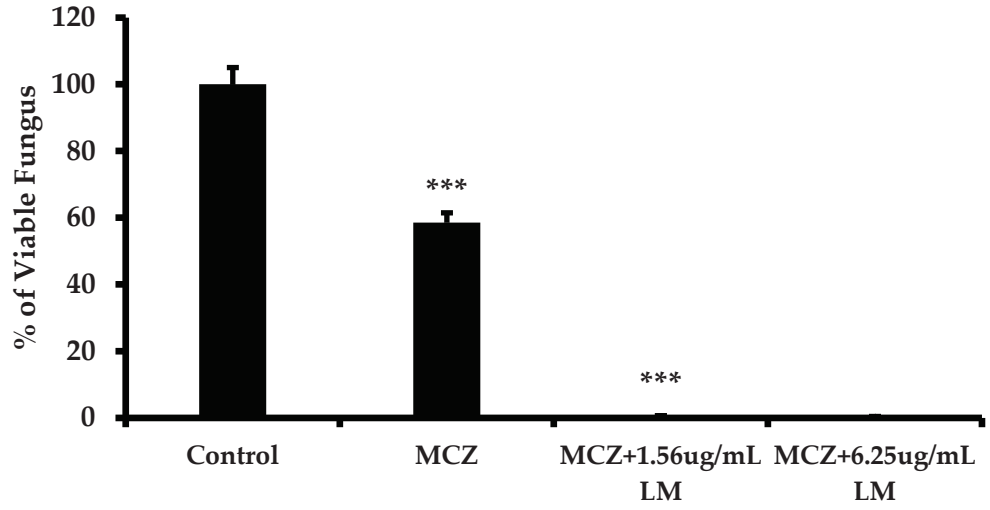

Figure 2. *L. muscari* increased the susceptibility of MCZ to *C. albicans*. Biofilms of *C. albicans* were formed after 24 h of incubation in YPD followed by 24 h of treatment with MCZ (3.125 μg/mL) alone or in combination with *L. muscari* (1.56 and 6.25 μg/mL). MCZ: Miconazole, LM: *L. muscari* extract. (***: *p*-value < 0.001).

2.3. Inhibitory Activity of L. muscari on C. albicans Dimorphic Transition from Yeast to Hyphae

Inhibition of *C. albicans* dimorphic transition by *L. muscari* was determined. Since not only can nutrient-deficient spider medium but also liquid RPMI 1640 and mammalian serum trigger the formation of hyphae, we conducted the examination using both conditions [25]. At a low concentration of 1.56 μg/mL, *L. muscari* effectively interrupted hyphal formation in RPMI 1640 or 10% FBS YPD medium to 49.3 ± 2.4% and 51.3 ± 2.5%, respectively (Figure 3a–d). Therefore, these results suggest that *L. muscari* might have the ability to impede the transition from yeast to the hyphal form of *C. albicans*.

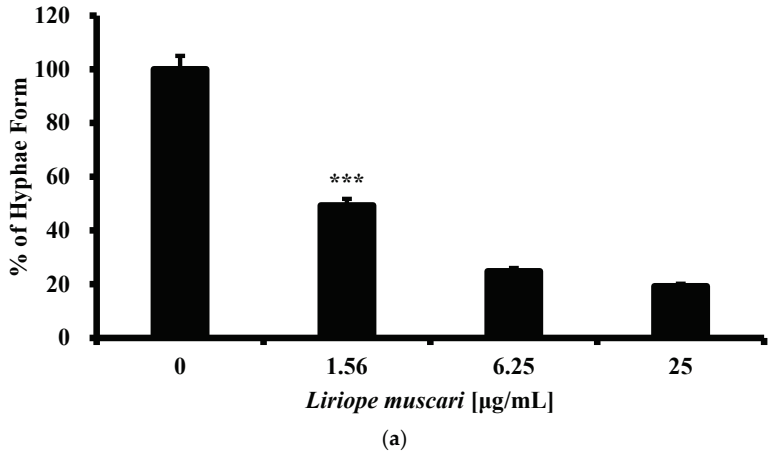

Figure 3. *Cont*.

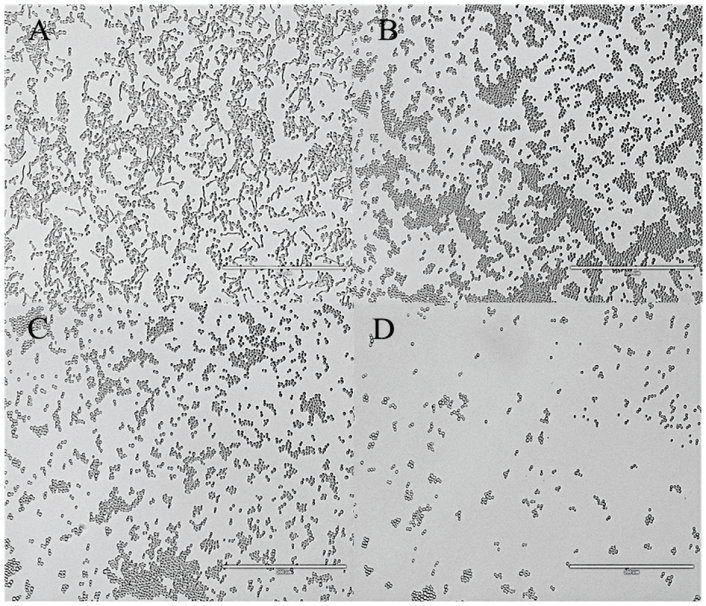

(**b**)

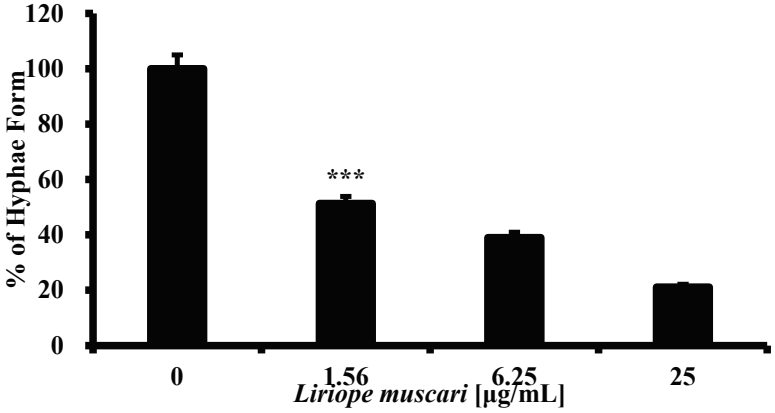

(**c**)

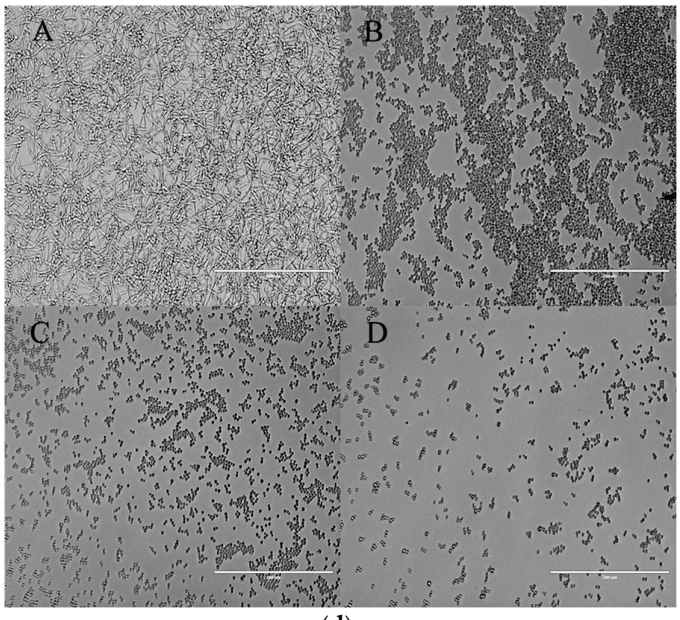

(**d**)

Figure 3. *L. muscari* inhibited the transition of *C. albicans* from yeast to hyphae. (**a**) *L. muscari* inhibited *C. albicans* filamentation induced in RPMI 1640. *C. albicans* (1×10^6 cells/mL) and *L. muscari* (1.56, 6.25,

and 25 μg/mL) were incubated at 37 °C for 4 h. (**b**) Images of *C. albicans* cells grown in RPMI 1640. *L. muscari* was added at concentrations of 1.56, 6.25, and 25 μg/mL. A: RPMI 1640 control, B: *L. muscari* 1.56 μg/mL, C: *L. muscari* 6.25 μg/mL, D: *L. muscari* 25 μg/mL. (**c**) *L. muscari* inhibited *C. albicans* filamentation induced in 10% FBS YPD medium. *C. albicans* (1×10^6 cells/mL) and *L. muscari* (1.56, 6.25, and 25 μg/mL) were incubated at 37 °C for 4 h. (**d**) Images of *C. albicans* cells incubated in 10% FBS YPD medium. *L. muscari* was added at concentrations of 1.56, 6.25, and 25 μg/mL. A: 10% FBS YPD control, B: *L. muscari* 1.56 μg/mL, C: *L. muscari* 6.25 μg/mL, D: *L. muscari* 25 μg/mL. Scale bar: 200 μm. (***: *p*-value < 0.001).

2.4. Suppression of the Gene Expression Related to Biofilm Formation Regulatory Proteins after L. muscari Treatment

To analyze the molecular background of *L. muscari*'s suppression of hyphal growth and cell attachment, qRT-PCR was conducted to determine the expression of genes involved in hyphal growth and cell attachment in *C. albicans*. The planktonic cells were included in the process to determine whether those changes were caused within the hyphal growth.

After treatment with 1.56–25 μg/mL of *L. muscari*, the expression levels of four genes (RAS1, EFG1, TEC1, and CDC35) associated with the Ras1-cAMP-Efg1 pathway [26] were significantly reduced (Figure 4a–d). Ras1p is a GTPase that acts to induce the formation of hyphae by activating both the MAPK cascade pathway and the Ras1-cAMP-Efg1 pathway [27]. Efg1p is a transcription factor of the Ras1-cAMP-Efg1 pathway, which is important in regulating the expression of certain hyphae-specific genes, including ECE1, HWP1, and ALS3 [28].

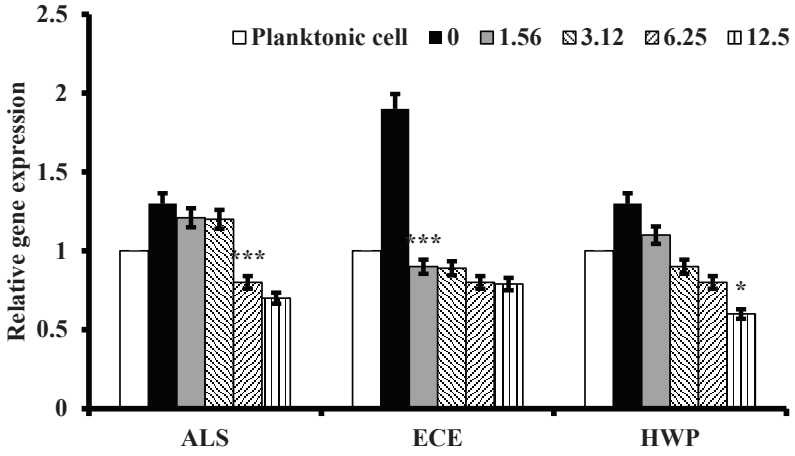

(**a**)

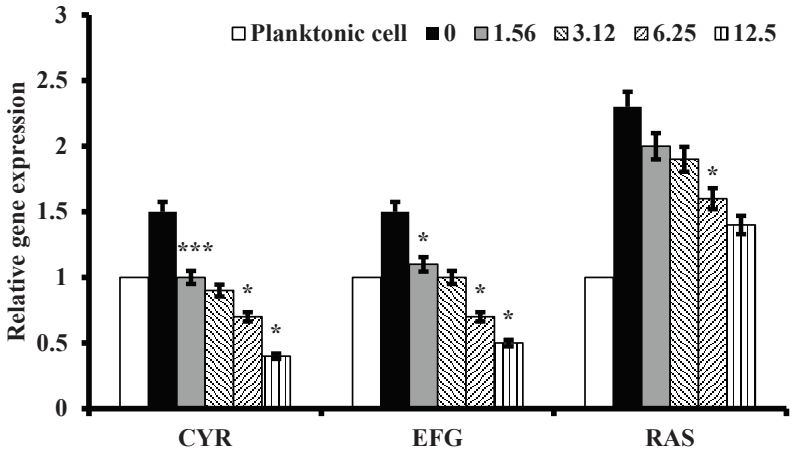

(**b**)

Figure 4. *Cont.*

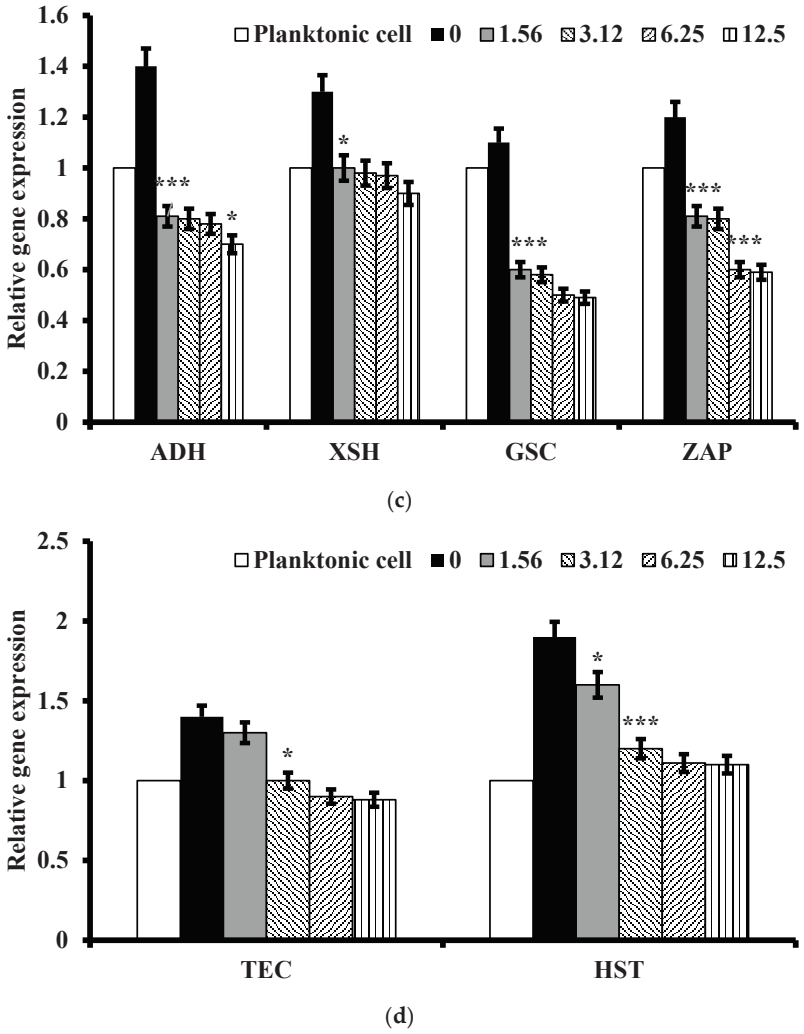

Figure 4. *L. muscari* decreased the expression of genes for hyphae-specific regulation, extracellular matrix, Ras1-cAMP-Efg1, MAP kinase, and Cph2-Tec1 in *C. albicans*. (**a**) Relative expression of genes regulating hyphae-specific genes. (**b**) Relative expression of genes regulated by the Ras1-cAMP-Efg1 pathway. (**c**) Relative expression of genes regulating extracellular matrix genes. (**d**) Relative expression of genes related to the Cph2-Tec1 pathway and the MAP kinase pathway. Total RNA was extracted from *C. albicans*, including control and biofilms treated with the indicated concentrations of *L. muscari*, synthesized cDNA, and examined by qPCR using the corresponding primers. (*: p-value <0.05, ***: p-value < 0.001).

L. muscari caused alterations in the transcription level of 12 genes involved in biofilm formation which were evaluated by qRT-PCR. The degree of gene expression for each gene was analyzed in cells treated with *L. muscari* (1.56–12.5 μg/mL) for 24 h and compared to untreated cells and planktonic cells (Figure 5). Results showed that *L. muscari* significantly repressed the expression levels of the following genes: hypha essential genes (ALS3, ECE1, and HWP1), Ras1-cAMP-Efg1 pathway (CYR1, EFG1, and RAS1), extracellular matrix (ADH5, CSH1, GSC1, and ZAP1), Cph2-Tec1 pathway (TEC1), and MAP kinase pathway (HST7). The expression of the genes related to hyphal development were decreased by 34.4%, and those of the extracellular matrix were decreased by 36.0% at 1.56 μg/mL. Also, the genes within the Ras1-cAMP-PKA, Cph2-Tec1, and MAP kinase signaling pathways were downregulated by 25.58%, 7.1%, and 15.8%, respectively, in the same concentration.

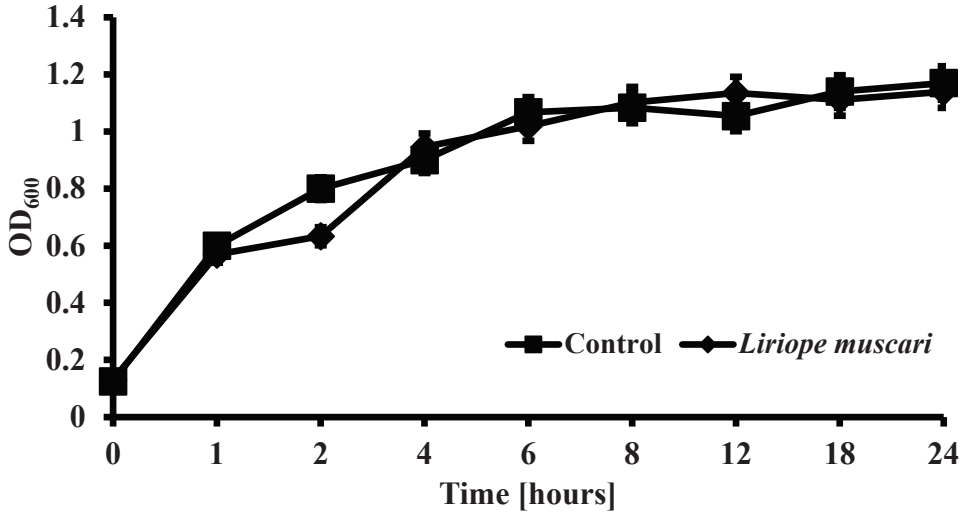

Figure 5. *L. muscari* lacks the ability to inhibit the growth of *C. albicans*.

2.5. L. muscari Had No Effect on Sum of Fungal Growth

To determine whether the inhibition of biofilm formation by *L. muscari* resulted from its antifungal activity, *C. albicans* was exposed to specified concentrations of *L. muscari* for 24 h. Surprisingly, there were no clear differences between the treatment and the control. Both groups exhibited the growth of *C. albicans* in a time-dependent manner, which means *L. muscari* only affects the biofilm formation of *C. albicans* while not affecting fungal growth (Figure 5).

3. Discussion

C. albicans is a yeast that opportunistically causes systemic infections in individuals with compromised immune systems [2]. Nosocomial *C. albicans* infections are frequently associated with their capacity to produce biofilms on mucosal surfaces and medical devices [3,29,30]. The formation of biofilms is a finely regulated process, governed by multiple interconnected signaling pathways [25], resulting in structured microbial communities attached to surfaces and enclosed in an exopolymeric extracellular matrix [3,29,31].

The formation of biofilms is a critical stage in pathogenesis, as *C. albicans* within biofilm are generally less susceptible or resistant to antifungal agents [32]. Consequently, the development of new antifungal agents with inhibitory activity on the attachment of *C. albicans* attachment, the transition of yeast-to-hyphae, and biofilm formation should be an important strategy.

In this study, *L. muscari* was examined for an inhibitor of biofilm formation by *C. albicans*. *L. muscari* also increased antifungal activity by inhibiting biofilm formation (Figure 2). Since infections caused by micro-organisms are hard to cure due to their adaptations to antibiotics and their rapid mutations [33], *L. muscari* can be useful as a great adjuvant when used with the usual antibiotics as we found in this study. Additionally, we discovered that *L. muscari* could potentially make *C. albicans* more susceptible to other chemicals by inhibiting biofilm formation. This is expected to enhance the cost-effectiveness of the currently used treatment.

L. muscari at 6.25 μg/mL inhibited the transformation of hyphal morphology in liquid RPMI 1640 and 10% FBS YPD medium (Figure 3). This indicates the potential application of *L. muscari* as an agent to counteract the virulence of *C. albicans*.

In an effort to understand the mechanisms responsible for the anti-biofilm effects of *L. muscari* on *C. albicans*, we analyzed the gene expression profiles related to cell adhesion, hyphal development, and extracellular matrix synthesis under conditions that promote biofilm formation. The major signaling pathways directing hyphal guidance and biofilm construction are the Ras1-cAMP-Efg1 and MAP kinase pathways [25,34,35]. Interestingly,

L. muscari significantly reduced the expression levels of RAS1, CYR1, and EFG1, which are part of the Ras1-cAMP-Efg1 pathway. The Ras1p GTPase activates Cyr1p adenylate cyclase to produce cAMP, leading to the activation of the Efg1p transcription factor. This factor significantly influences the regulation of several gene expressions related to hyphae, such as ALS3, HWP1, and ECE1, which are crucial for *C. albicans* adherence [36] and biofilm formation [35,37–39]. Consequently, the transcription of ALS3, HWP1, and ECE1 was also repressed.

In contrast, *L. muscari* did not alter the expression levels of HST7 and TEC1 genes. HST7 is responsible for encoding a protein kinase within the MAP kinase pathway, whereas TEC1 encodes a transcription factor that independently enhances the expression of genes specific to hyphal formation, separate from the two pathways described above [40].

While the exact components of the extracellular matrix in *C. albicans* biofilms remain not fully characterized, its known components include carbohydrates, proteins, and nucleic acids as previously described [41]. The major extracellular carbohydrate, β-1,3-glucan, produced by the enzyme β-1,3-glucan synthase (Gsc1p), led to the inclusion of the GSC1 transcript as a marker for matrix production [42]. As expected, *L. muscari* downregulated GSC1 gene expression. The protein Zap1p (zinc-responsive activator protein) in *C. albicans*, which responds to zinc levels, promotes cell dispersal by downregulating matrix production. Zap1p directly activates the expression of CSH1 and IFD6, which suppresses substrate accumulation and indirectly inhibits the expression of other alcohol dehydrogenase genes, such as ADH5, which are involved in substrate generation [43]. *L. muscari* reduced the expression of ZAP1 and CSH1 yet had no impact on ADH5 expression. It is worth noting that ZAP1is also essential for the proper morphogenesis of *C. albicans*, aligning with observations that *C. albicans* ZAP1 mutants predominantly exhibit yeast growth in biofilms [43,44]. Consistently, microscopic examination showed that *C. albicans* cells treated with *L. muscari* predominantly exhibited yeast growth after 24 h of incubation.

The identification of chemical components in *L. muscari* that possess anti-biofilm activity is a subject of our future research. Previous studies have indicated that the extract of *L. muscari*, particularly the ethanol extract, exhibits antioxidant, anticancer, and antithrombotic properties [22,45,46]. Historically, these extracts have been used as medicinal remedies in East Asia, even before the identification of their effective chemicals. With the advancements in scientific instruments, the bioactive chemical compositions of these extracts have been recently reported. For instance, DT-13 (25 (*R, S*)-ruscogenin-1-*O*-[β-d-glucopyranosyl—(1→2)] [β-d-xylopyranosyl-(1→3)]-β-d-fucopyranoside), the most extensively examined chemical in *L. muscari*, has been reported to exhibit all three aforementioned activities and is known to downregulate matrix metalloproteinases and p38 activation in cancer cells. Two other compounds, norcurlignan ((2*S*,3*R)*-methyl-7-hydroxy-2-(4-hydroxy-3-methoxy-phenyl)-3-(hydroxymethyl)-2,3-dihydrobenzofuran-5-carboxylate) and limlactone ((4R,5S)-5-(3-hydroxy-2,6-dimethylphenyl)-4-isopropyldihydrofuran-2-one) were also identified in the 80% ethanol extract of *L. muscari* and both demonstrated antioxidant activities. However, none of the of *L. muscari* have been reported to inhibit the biofilm formation of *C. albicans*. Given the increasing number of reported cases of antifungal-resistant *C. albicans*, it is worthwhile to investigate the potential anti-biofilm components of *L. muscari* [47].

These findings suggest that *L. muscari* represses the formation of *C. albicans* biofilms by influencing the yeast–hyphal transition. Consequently, *L. muscari* shows promise as a potential coating agent for prosthetic medical devices as other antifungal treatments similarly do. Additionally, preclinical in vivo animal experiments should be performed to verify the possibility that *L. muscari* can be used as an agent to increase antifungal activity. To optimize the use of *L. muscari* in clinical application, studies should also be undertaken to identify a suitable solvent substitute with adequate solvency.

4. Materials and Methods

4.1. Strains

The *C. albicans* used in this study, KCTC 7965, was obtained from the Korean Collection for Type Cultures (Korean Collection for Type Cultures, Daejeon, Republic of Korea). The strain was preserved in 20% glycerol (BD Difco, NJ, USA) at −70 °C and cultured on YPD plates [peptone 20 g/L (BD Difco, Franklin Lakes, NJ, USA), yeast extract 10 g/L (BD Difco, NJ, USA), and 2% glucose (*w/v*) (Daejung, Siheung, Republic of Korea)].

4.2. Sample Preparation

The leaves of *L. muscari* were collected in Jeju, Republic of Korea (GPS: 33.3617° N, 126.5292° E). These leaves were thoroughly rinsed with distilled water and subsequently freeze-dried in preparation for extraction. A total of 100 g of the freeze-dried leaves of *L. muscari* were subjected to extraction in 1 L of 80% ethanol for 24 h. The resulting extracts were concentrated using a rotary evaporator (EYELA, Tokyo, Japan) which was connected to a refrigerated circulating bath (Jeio Tech, Seoul, Republic of Korea). This concentrated extract was then filtered using NO.2 filter paper (WHATMAN, Buckinghamshire, UK). The filtered products were once again freeze-dried and subsequently dissolved in 99.0% DMSO (Junsei, Tokyo, Japan) to achieve a concentration of 10 mg/mL. It is important to note that for all the negative controls utilized in this study, an equivalent volume of 99.0% DMSO was used since the influence of DMSO on *C. albicans* was previously reported [48]. The final DMSO concentration for each sample was 0.25%.

4.3. Inhibition of Biofilm Formation

The formation of biofilm was detected using the crystal violet assay [49]. *C. albicans* at a concentration of 5×10^5 CFU/mL was added to the wells of a 96-well plate (SPL, Pocheon, Republic of Korea), mixed in RPMI 1640 medium (Welgene, Gyeongsan, Republic of Korea), and *L. muscari* extract, ranging from 1.56 to 25 μg/mL, was added, and the mixture was cultured at 37 °C for 24 h. The plates were then incubated at 30 °C for 24 h. Each experiment included growth control and sterilized media control wells. After three washes with 200 μL of PBS, 100 μL of 1% aqueous crystal violet solution was added and incubated for 30 min. After staining, each well was washed three times with 200 μL of PBS and immediately destained with 150 μL of 30% acetic acid (Daejung, Siheung, Republic of Korea) for 15 min. The absorbance at 595 nm was measured using a microplate reader (BioTek Instruments, Seoul, Republic of Korea). Biofilm formation was normalized to the control using the following formula: $[(1 - (OD_{595}\text{DMSO} - OD_{595}\text{ compound})/OD_{595}\text{DMSO}) \times 100\%]$ (Figure 1).

4.4. Combined Antifungal Effect of L. muscari Extract and Antifungal Agent

The combined antifungal effect of the extract and antifungal agent was measured according to previous work [50]. *C. albicans* was cultured overnight in YPD and then diluted to 1×10^6 cells/mL with fresh YPD in 96-well plates (SPL, Pocheon, Republic of Korea) prior to combinational treatment for biofilm formation. A total of 1 mL of Candida suspension was exposed to various concentrations of *L. muscari*, in combination with miconazole at a concentration of 3.125 μg/mL. The indicated concentrations of *L. muscari* and miconazole alone were also applied for comparison.

Biofilms were positioned at the bottom of the well and incubated at 30 °C for 24 h. After washing with PBS to remove planktonic cells, the cells were sonicated to break up clumps. The counts of biofilm fungal CFU were determined by plating serial dilutions on YPD agar.

4.5. Morphological Transition Using RPMI 1640 and 10% FBS YPD Liquid Medium

C. albicans was cultured overnight in a YPD medium. A concentration of 1×10^6 cells/mL with or without *L. muscari* extract was cultured in RPMI 1640 medium or 10% FBS YPD medium for 4 h at 37 °C. The inhibition of the transition from yeast to hyphal morphology

was quantified by counting the number of individual budding cells relative to the number of hyphae in the population, as previously described [51]. At least 100 cells were counted in triplicate for each well, and all analyses were repeated five times. Images of the cells were captured using a microscope.

4.6. Quantitative RT-PCR Analysis

C. albicans was cultured on YPD agar. A single colony was selected, stirred at 30 °C, and inoculated into YPD. The following day, cultures at 1×10^6 cells/mL were diluted with YPD. Aliquots of the diluted suspension were treated with *L. muscari* extract at concentrations ranging from 1.56 to 25 μg/mL and incubated at 30 °C on an orbital shaker. Total RNA extraction was performed using TRIzol reagent (Thermo Fisher Scientific, Waltham, MA, USA) according to the manufacturer's instructions. Reverse transcription was carried out with 1 μg of RNA using reverse transcriptase (NanoHelix, Daejeon, Republic of Korea) to obtain cDNA. Quantitative real-time PCR (qRT-PCR) was conducted using 2X SybrGreen qPCR Master Mix (CellSafe, Suwon, Republic of Korea). Primer sequences used for the amplification of genes including GSP1, RAS1, EFG1, TEC1, CDC35, ALS3, HWP1, and ECE1 are listed in Table 1, which were used in the previous paper [52].

Table 1. Primer list used in this paper.

Primers	Primer Sequence	Gene Function
ACT 1	F: TAGGTTTGGAAGCTGCTGG R: CCTGGGAACATGGTAGTAC	Control
ALS 3	F: GGTTATCGTCCATTTGTTG R: TTCTGTATCCAGTCCATCT	Hyphal-specific genes
CYR 1	F: GTTTCCCCCACCACTCA R: TTGCGGTAATGACACAACAG	Ras-cAMP-Efg1 pathway
ECE 1	F: ACAGTTTCCAGGACGCCAT R: ATTGTTGCTCGTGTTGCCA	Hyphal-specific genes
EFG 1	F: TTGAGATGTTGCGGCAGGAT R: ACTGGACAGACAGCAGGAC	Ras-cAMP-Efg1 pathway
GSC 1	F: CCCATTCTCTAGGCACGA R: ATCAACAACCACTTGCTTCG	Extracellular matrix
HST 7	F: GCCAGTATGGTCGGAGGAT R: ACATAGGCATCGTCTTCGTC	MAP kinases pathway
HWP 1	F: ACAGGTAGACGGTCAAGG R: GGGTAATCATCACATGGTTC	Ras-cAMP-Efg1 pathway
RAS 1	F: GAGGTGGTGGTGTTGGTA R: TCTTCTTGTCCAGCAGTATC	Cph2-Tec1 pathway
TEC 1	F: GCACTGGCTTCAAGCTCAAA R: GCTGCTGCACTCAAGTTCTG	Extracellular matrix
ZAP 1	F: ATCTGTCCAGTGTTGTTTGTA R: AGGTCTCTTTGAAAGTTGTG	Extracellular matrix
ADH 5	F: ACCTGCAAGGGCTCATTCTG R: CGGCTCTCAACTTCTCCATA	Extracellular matrix
CSH 1	F: CGTGAGGACGAGAGAGAAT R: CGAATGGACGACACAAAACA	Extracellular matrix

4.7. C. albicans Growth Test

The growth curve was obtained with some modifications [53]. Fungal cultures were set up at 1×10^6 cells/mL using fresh YPD broth. After adding *L. muscari* extract, it was cultured at 30 °C. The growth was evaluated by measuring OD_{600} with a microplate reader at intervals of 0, 1, 2, 4, 8, 12, and 24 h.

4.8. Statistical Analysis

All experiments were performed at least three times, and data were presented as the ± mean standard deviation (S.D). Statistical analysis was performed using Microsoft Excel

2021 (Microsoft, Redmond, WA, USA) and Statistical Package for the Social Sciences (SPSS) 28.0 (IBM Corp, New York, NY, USA). All graphs except microscopic images were analyzed by Microsoft Excel 2021. Statistical significance was defined at a *p*-value less than 0.05.

5. Conclusions

L. muscari should be a good candidate for anti-virulence agents against Candida infections because it inhibits biofilm formation and hyphal transition and increases antifungal susceptibility. This antifungal efficacy of *L. muscari* could suggest the direction for the development of new antifungal strategies with a lower virulence of *C. albicans*.

Author Contributions: Conceptualization, J.L. and K.K.; methodology, H.S., J.L. and K.K.; validation, H.S., J.L. and K.K.; formal analysis, H.S. and K.K.; investigation, H.S. and J.L.; resources, K.K.; data curation, K.K.; writing—original draft preparation, K.K.; writing—review and editing, K.K.; visualization, H.S.; supervision, K.K.; project administration, K.K.; funding acquisition, K.K. All authors have read and agreed to the published version of the manuscript.

Funding: This research was funded by the GRRC Program of Gyeonggi province [GRRC-KyungHee 2020(B04)], Republic of Korea. This work was supported by the National R&D Program through the National Research Foundation of Korea (NRF) funded by the Korea government (Ministry of Science and ICT) (2021R1A6A3A13046056).

Institutional Review Board Statement: Not applicable.

Informed Consent Statement: Not applicable.

Data Availability Statement: The data presented in this study are available in article.

Acknowledgments: The authors thank all the participants involved in this research.

Conflicts of Interest: The authors declare no conflicts of interest.

References

1. Atriwal, T.; Chawla, M.; Hussain, A.; Alajmi, M.F.; Abid, M. Reactive oxygen mediated apoptosis as a therapeutic approach against opportunistic *Candida albicans*. *Adv. Protein Chem. Struct. Biol.* **2021**, *155*, 25–49. [CrossRef] [PubMed]
2. Pfaller, M.A.; Diekema, D.J. Epidemiology of invasive candidiasis: A persistent public health problem. *Clin. Microbiol. Rev.* **2007**, *20*, 133–163. [CrossRef] [PubMed]
3. Chandra, J.; Kuhn, D.M.; Mukherjee, P.K.; Hoyer, L.L.; McCormick, T.; Ghannoum, M.A. Biofilm formation by the fungal pathogen *Candida albicans*: Development, architecture, and drug resistance. *J. Bacteriol.* **2001**, *183*, 5385–5394. [CrossRef] [PubMed]
4. Benedict, K.; Jackson, B.R.; Chiller, T.; Beer, K.D. Estimation of direct healthcare costs of fungal diseases in the United States. *Clin. Infect. Dis.* **2019**, *68*, 1791–1797. [CrossRef] [PubMed]
5. Koo, H.; Allan, R.N.; Howlin, R.P.; Stoodley, P.; Hall-Stoodley, L. Targeting microbial biofilms: Current and prospective therapeutic strategies. *Nat. Rev. Microbiol.* **2017**, *15*, 740–755. [CrossRef] [PubMed]
6. Woappi, Y.; Gabani, P.; Singh, A.; Singh, O.V. Antibiotrophs: The complexity of antibiotic-subsisting and antibiotic-resistant microorganisms. *Crit. Rev. Microbiol.* **2016**, *42*, 17–30. [CrossRef] [PubMed]
7. Costa-Orlandi, C.B.; Sardi, J.C.O.; Pitangui, N.S.; de Oliveira, H.C.; Scorzoni, L.; Galeane, M.C.; Medina-Alarcón, K.P.; Melo, W.C.M.A.; Marcelino, M.Y.; Braz, J.D.; et al. Fungal Biofilms and Polymicrobial Diseases. *J. Fungi* **2017**, *3*, 22. [CrossRef] [PubMed]
8. Fanning, S.; Mitchell, A.P. Fungal biofilms. *PLoS Pathog.* **2012**, *8*, e1002585. [CrossRef] [PubMed]
9. Mowat, E.; Butcher, J.; Lang, S.; Williams, C.; Ramage, G. Development of a simple model for studying the effects of antifungal agents on multicellular communities of *Aspergillus fumigatus*. *J. Med. Microbiol.* **2007**, *56*, 1205–1212. [CrossRef]
10. Blankenship, J.R.; Mitchell, A.P. How to build a biofilm: A fungal perspective. *Curr. Opin. Microbiol.* **2006**, *9*, 588–594. [CrossRef]
11. Finkel, J.S.; Mitchell, A.P. Genetic control of *Candida albicans* biofilm development. *Nat. Rev. Microbiol.* **2011**, *9*, 109–118. [CrossRef] [PubMed]
12. Lopez-Ribot, J.L. *Candida albicans* biofilms: More than filamentation. *Curr. Biol.* **2005**, *15*, 453–455. [CrossRef] [PubMed]
13. Tobudic, S.; Kratzer, C.; Lassnigg, A.; Presterl, E. Antifungal susceptibility of *Candida albicans* in biofilms. *Mycoses* **2012**, *55*, 199–204. [CrossRef] [PubMed]
14. Inigo, M.; Peman, J.; Del, P.J. Antifungal activity against Candida biofilms. *Int. J. Artif. Organs.* **2012**, *35*, 780–791. [CrossRef] [PubMed]
15. Kim, C.; Kim, J.; Kim, K.Y. Anti-Candida Potential of Sclareol in Inhibiting Growth, Biofilm Formation, and Yeast–Hyphal Transition. *J. Fungi* **2023**, *9*, 98. [CrossRef] [PubMed]
16. Hancock, R.E.W.; Sahl, H.-G. Antimicrobial and host-defense peptides as new anti-infective therapeutic strategies. *Nat. Biotechnol.* **2006**, *24*, 1551–1557. [CrossRef]

17. Fox, J.L. Antimicrobial peptides stage a comeback. *Nat. Biotechnol.* **2013**, *31*, 379–382. [CrossRef] [PubMed]
18. Nuijens, J.H.; van Berkel, P.H.; Schanbacher, F.L. Structure and biological actions of lactoferrin. *J. Mammary Gland. Biol. Neoplasia* **1996**, *1*, 285–295. [CrossRef]
19. Harvey, A.L. Natural products in drug discovery. *Drug Discov. Today* **2008**, *13*, 894–901. [CrossRef]
20. Shang, Z.P.; Wang, F.; Zhang, J.Y.; Wang, Z.J.; Lu, J.Q.; Wang, H.Y.; Li, N. The genus *Liriope*: Phytochemistry and pharmacology. *Chin. J. Nat. Med.* **2017**, *15*, 801–815. [CrossRef]
21. Li, W.J.; Cheng, X.L.; Liu, J.; Lin, R.C.; Wang, G.L.; Du, S.S.; Liu, Z.L. Phenolic compounds and antioxidant activities of *Liriope muscari*. *Molecules* **2012**, *17*, 1797–1808. [CrossRef] [PubMed]
22. Tian, Y.; Ma, S.; Lin, B.; Kou, J.; Yu, B. Anti-thrombotic activity of DT-13, a saponin isolated from the root tuber of *Liripo muscrai*. *India J. Pharmacol.* **2013**, *45*, 283–285. [CrossRef] [PubMed]
23. Ma, S.; Kou, J.; Yu, B. Safety evaluation of steroidal saponin DT-13 isolated from the tuber of *Liriope muscari* (Decne.) Baily. *Food Chem. Toxicol.* **2011**, *49*, 2243–2251. [CrossRef] [PubMed]
24. Zhang, Y.Y.; Liu, J.H.; Kou, J.P.; Yu, J.; Yu, B.Y. DT-13, a steroidal saponin from *Liriope muscari* LH Bailey, suppresses A549 cells adhesion and invasion by inhibiting MMP-2/9. *Chin. J. Nat. Med.* **2012**, *10*, 436–440. [CrossRef]
25. Biswas, S.; Van Dijck, P.; Datta, A. Environmental Sensing and Signal Transduction Pathways Regulating Morphopathogenic Determinants of *Candida albicans*. *Microbiol. Mol. Biol. Rev.* **2007**, *71*, 348–376. [CrossRef] [PubMed]
26. Jadhav, A.K.; Bhan, A.; Jangid, P.; Patil, R.; Gade, W.; Karuppayil, S.M. Modulation of Genes Involved in Yeast to Hyphal form Signal Transduction in *Candida albicans* by Indole and Isatin. *Curr. Signal Transduct. Ther.* **2017**, *12*, 116–123. [CrossRef]
27. Sun, L.; Liao, K.; Wang, D. Effects of magnolol and honokiol on adhesion, yeast-hyphal transition, and formation of biofilm by *Candida albicans*. *PLoS ONE* **2015**, *10*, e0117695. [CrossRef]
28. Wu, J.; Wu, D.; Zhao, Y.; Si, Y.; Mei, L.; Shao, J.; Wang, C. Sodium new houttuyfonate inhibits *Candida albicans* biofilm formation by inhibiting the Ras1-cAMP-Efg1 pathway revealed by RNA-seq. *Front. Microbiol.* **2020**, *11*, 2075. [CrossRef]
29. Douglas, L.J. Candida biofilms and their role in infection. *Trends Microbiol.* **2003**, *11*, 30–36. [CrossRef]
30. Hasan, F.; Xess, I.; Wang, X.; Jain, N.; Fries, B.C. Biofilm formation in clinical Candida isolates and its association with virulence. *Microbes Infect.* **2009**, *11*, 753–761. [CrossRef]
31. Donlan, R.M.; Costerton, J.W. Biofilms: Survival mechanisms of clinically relevant microorganisms. *Clin. Microbiol. Rev.* **2002**, *15*, 167–193. [CrossRef] [PubMed]
32. Viudes, A.; Peman, J.; Canton, E.; Ubeda, P.; Lopez-Ribot, J.L.; Gobernado, M. Candidemia at a tertiary-care hospital: Epidemiology, treatment, clinical outcome and risk factors for death. *Eur. J. Clin. Microbiol. Infect. Dis.* **2002**, *21*, 767–774. [CrossRef] [PubMed]
33. Woodford, N.; Ellington, M.J. The emergence of antibiotic resistance by mutation. *Clin. Microbiol. Infect.* **2007**, *13*, 5–18. [CrossRef] [PubMed]
34. Ramage, G.; VandeWalle, K.; Lopez-Ribot, J.L.; Wickes, B.L. The filamentation pathway controlled by the Efg1 regulator protein is required for normal biofilm formation and development in *Candida albicans*. *FEMS Microbiol. Lett.* **2002**, *214*, 95–100. [CrossRef] [PubMed]
35. Leberer, E.; Harcus, D.; Dignard, D.; Johnson, L.; Ushinsky, S.; Thomas, D.Y. Ras links cellular morphogenesis to virulence by regulation of the MAP kinase and cAMP signalling pathways in the pathogenic fungus *Candida albicans*. *Mol. Microbiol.* **2001**, *42*, 673–687. [CrossRef] [PubMed]
36. Tronchin, G.; Pihet, M.; Lopes-Bezerra, L.M.; Bouchara, J.-P. Adherence mechanisms in human pathogenic fungi. *Med. Mycol.* **2008**, *46*, 749–772. [CrossRef] [PubMed]
37. Staab, J.F.; Bradway, S.D.; Fidel, P.L.; Sundstrom, P. Adhesive and mammalian transglutaminase substrate properties of *Candida albicans* Hwp1. *Science* **1999**, *283*, 1535–1538. [CrossRef]
38. Nobile, C.J.; Nett, J.E.; Andes, D.R.; Mitchell, A.P. Function of *Candida albicans* adhesin hwp1 in biofilm formation. *Eukaryot. Cell* **2006**, *5*, 1604–1610. [CrossRef] [PubMed]
39. Hogan, D.A.; Sundstrom, P. The Ras/cAMP/PKA signaling pathway and virulence in *Candida albicans*. *Future Microbiol.* **2009**, *4*, 1263–1270. [CrossRef]
40. Lane, S.; Zhou, S.; Pan, T.; Dai, Q.; Liu, H. The basic helix-loop-helix transcription factor Cph2 regulates hyphal development in *Candida albicans* partly via TEC1. *Mol. Cell. Biol.* **2001**, *21*, 6418–6428. [CrossRef]
41. Al Fattani, M.A.; Douglas, L.J. Biofilm matrix of *Candida albicans* and *Candida tropicalis*: Chemical composition and role in drug resistance. *J. Med. Microbiol.* **2006**, *55*, 999–1008. [CrossRef] [PubMed]
42. Taff, H.T.; Nett, J.E.; Zarnowski, R.; Ross, K.M.; Sanchez, H.; Cain, M.T. A Candida Biofilm-Induced Pathway for Matrix Glucan Delivery: Implications for Drug Resistance. *PLoS Pathog.* **2012**, *8*, e1002848. [CrossRef] [PubMed]
43. Nobile, C.J.; Nett, J.E.; Hernday, A.D.; Homann, O.R.; Deneault, J.S.; Nantel, A. Biofilm matrix regulation by *Candida albicans* Zap1. *PLoS Biol.* **2009**, *7*, e1000133. [CrossRef] [PubMed]
44. Kim, M.J.; Kil, M.; Jung, J.H.; Kim, J. Roles of zinc-responsive transcription factor Csr1 in filamentous growth of the pathogenic yeast *Candida albicans*. *J. Microbiol. Biotechnol.* **2008**, *18*, 242–247. [PubMed]
45. Wang, Z. Antioxidant Activities of Extracts from *Ophiopogon japonicus*. *Food Ferment Ind.* **2007**, *33*, 57.
46. Li, Y.W.; Qi, J.; Zhang, Y.Y.; Huang, Z.; Kou, J.P.; Zhou, S.P.; Yu, B.Y. Novel cytotoxic steroidal glycosides from the roots of *Liriope muscari*. *Chin. J. Nat. Med.* **2015**, *13*, 461–466. [CrossRef] [PubMed]

47. Richardson, J.P. *Candida albicans*: A major fungal pathogen of humans. *Pathogens* **2022**, *11*, 459. [CrossRef] [PubMed]
48. Hazen, K.C. Influence of DMSO on antifungal activity during susceptibility testing in vitro. *Diagn. Microbiol. Infect. Dis.* **2013**, *75*, 60–63. [CrossRef]
49. Dhale, R.P.; Ghorpade, M.V.; Dharmadhikari, C.A. Comparison of various methods used to detect biofilm production of Candida species. *J. Clin. Diagn. Res.* **2014**, *8*, DC18–DC20. [CrossRef]
50. Kim, D.; Kim, K.Y. *Adenophora triphylla* var. *japonica* inhibits Candida biofilm formation, increases susceptibility to antifungal agents and reduces infection. *Int. J. Mol. Sci.* **2021**, *22*, 12523. [CrossRef]
51. Toenjes, K.A.; Munsee, S.M.; Ibrahim, A.S.; Jeffrey, R.; Edwards, J.J. Small-molecule inhibitors of the budded-to-hyphal-form transition in the pathogenic yeast *Candida albicans*. *Antimicrob. Agents Chemother.* **2005**, *49*, 963–972. [CrossRef] [PubMed]
52. Kim, D.; Kim, K.Y. *Hedera rhombea* inhibits the biofilm formation of Candida, thereby increases the susceptibility to antifungal agent, and reduces infection. *PLoS ONE* **2021**, *16*, e0258108. [CrossRef] [PubMed]
53. Kim, J.; Bao, T.H.Q.; Shin, Y.K.; Kim, K.Y. Antifungal activity of magnoflorine against *Candida strains*. *World J. Microbiol. Biotechnol.* **2018**, *34*, 167. [CrossRef]

Disclaimer/Publisher's Note: The statements, opinions and data contained in all publications are solely those of the individual author(s) and contributor(s) and not of MDPI and/or the editor(s). MDPI and/or the editor(s) disclaim responsibility for any injury to people or property resulting from any ideas, methods, instructions or products referred to in the content.

antibiotics

MDPI

Article

Antifungal Activity, Synergism with Fluconazole or Amphotericin B and Potential Mechanism of Direct Current against *Candida albicans* Biofilms and Persisters

Peihui Zou, Jia Liu, Peng Li * and Qingxian Luan *

Department of Periodontology, Peking University School and Hospital of Stomatology & National Center for Stomatology & National Clinical Research Center for Oral Diseases & National Engineering Research Center of Oral Biomaterials and Digital Medical Devices & Beijing Key Laboratory of Digital Stomatology & NHC Key Laboratory of Digital Stomatology & NMPA Key Laboratory for Dental Materials, Beijing 100081, China; zphntyc@163.com (P.Z.); dentistliujia@126.com (J.L.)

* Correspondence: lp_nathan@hotmail.com (P.L.); kqluanqx@126.com (Q.L.); Fax: +86-010-62179977 (P.L.); +86-010-62179977 (Q.L.)

Abstract: *Candida albicans*, as a notorious fungal pathogen, is associated with high morbidity and mortality worldwide due to its ability to form biofilms and persisters that can withstand currently available antifungals. Direct current (DC) has demonstrated a promising antimicrobial effect and synergistic effect with antimicrobials against various infections. Here, we first found DC exerted a killing effect on *C. albicans* planktonic and biofilm cells. Moreover, DC showed a synergistic effect with fluconazole (FLC) and amphotericin B (AMB). Notably, near-to-complete eradication of AMB-tolerant *C. albicans* biofilm persisters was achieved upon DC treatment. Next, the mechanism of action of DC was explored through mapping the genes and proteomic profiles of DC-treated *C. albicans*. The multi-omics analysis, quantitative real-time PCR and assay of reactive oxygen species (ROS) demonstrated DC exerted an antifungal effect on *C. albicans* by increasing cellular oxidative stress. As revealed by multiple analyses (e.g., protein assay based on absorbance at 280 nm and rhodamine 6G assay), DC was able to enhance membrane permeability, inhibit drug efflux and increase cellular FLC/AMB concentration of *C. albicans*, thereby mediating its synergism with the antifungals. Furthermore, DC inhibited superoxide dismutase 2 (SOD2) expression and manganese-containing SOD (Mn SOD) activity, leading to ROS production and enhanced killing of *C. albicans* biofilm persisters. The current findings demonstrate that the adjunctive use of DC in combination with antifungals is a promising strategy for effective control of *C. albicans* infections and management of antifungal resistance/tolerance in *Candida* biofilms.

Keywords: direct current; *Candida albicans*; persisters; reactive oxygen species; superoxide dismutase

1. Introduction

Candida albicans is a predominant commensal and primary pathogenic fungus responsible for various mucosal and systemic infections, particularly in immunocompromised individuals. These infections have become a significant public health concern due to their increasing prevalence, high morbidity and mortality rate [1,2]. The fungus is often prone to formation of biofilms with increased antifungal resistance on indwelling medical devices and mucosal surfaces [3,4]. Moreover, as previously described by us and other researchers, *C. albicans* biofilms can form a subpopulation of antifungal-tolerant persisters that remain viable and cannot be completely eradicated by antifungals even at lethal concentrations [3,5,6]. Notably, the persisters existing in the biofilms are capable of reviving and repopulating the biofilms once antifungal treatment stops. It is believed that the ability of *C. albicans* to form biofilms and persisters is the underlying reason for sustained and recurrent infections and therapeutic failure [1,7]. It has been demonstrated

that the currently available antifungals such as the azole antifungal fluconazole (FLC) and the polyene antifungal amphotericin B (AMB) cannot readily control the biofilms and their persisters [8,9]. Therefore, a novel effective antifungal strategy is urgently needed to tackle this challenge.

Electric current has recently drawn much attention for its ability to exert a direct killing effect and enhance the action of antimicrobials against biofilms, frequently in the form of low amplitude (1000 μA or less) direct current (DC) [10–12]. DC is a form of electric current that flows only in the same direction [13]. Our previous studies have confirmed the synergistic effect of DC with antibiotics in killing a keystone periodontal pathogen *Porphyromonas gingivalis* and subgingival plaque biofilms in vitro [14,15]. The disruption of membrane integrity as well as the generation of chlorine, hypochlorous acid, oxygen and reactive oxygen species (ROS) may play an important role in the DC-induced killing effect [14,16]. Currently, neither the antifungal effect of DC nor its synergistic effect with antifungals on *C. albicans* biofilms/persisters are well-studied, and the underlying mechanisms are largely unknown [17]. The application of DC provides a promising approach to control biofilms that display increased resistance [12,18]. Hence, the aim of this study was to investigate the DC-killing effect and coordinated action of DC with FLC and AMB on *C. albicans* biofilms and their persisters, as well as the underlying mechanisms.

2. Materials and Methods

2.1. Candida Strain, Culture, Compounds and Stimulator

A well-characterized clinical isolate used in our previous studies, *C. albicans* BF-1, was selected for this study [5,19]. For broth culture, the yeast was incubated on yeast extract peptone dextrose (YPD) media (Solario, Beijing, China). For solid culture, it was grown on Sabourauds dextrose agar (SDA, Hopebio, Qingdao, China) plate for 24 h. Fungal growth was monitored by measuring the optical density (OD_{600}) in SpectraMax Multimode Microplate Reader (Molecular Devices Ltd., San Jose, CA, USA). The suspension was adjusted to OD_{600} of about 0.08 (1×10^7 colony-forming units (CFU)/mL) and placed on 24-well plates (Corning, Corning, NY, USA) for 72 h to form biofilms. The biofilms in the bottom of each well were harvested by sonication (100 W) for 1 min and mechanical scrape with sterile pointed probe, and suspended in liquid medium.

Stock solutions of fluconazole (FLC) (Sigma-Aldrich, St. Louis, MI, USA) and polyene amphotericin B (AMB) (Sigma-Aldrich, USA) were dissolved in dimethyl sulfoxide (DMSO) (Solario, China).

The DC-stimulator apparatus (KuShi Medical Technology Co. Ltd., Shanghai, China) was described in our previous study [14]. The whole circuit maintained constant current intensity of 1000 μA by means of a DC output chip, with one 5-voltage lithium battery and two carbon electrodes inserted into the fungal solution.

2.2. Experiment Design

2.2.1. The Killing Effect of FLC/AMB on *C. albicans* in Planktonic State and Biofilm State

Various concentrations (0.25–1280 μg/mL) of FLC/AMB were used to stimulate planktonic *C. albicans* (10^7 CFU/mL, for 12 h) and the 72 hour-old *C. albicans* biofilms (for 24 h). The viable fungi were calculated by CFU counting and observed by LIVE/DEAD staining.

2.2.2. The Killing Effect of 1000 μA DC on *C. albicans* in Planktonic State and Biofilm State

Planktonic *C. albicans* (2 mL 10^7 CFU/mL) was stimulated by 1000 μA DC for 1, 6 and 12 h. *C. albicans* biofilms were stimulated by 0, 1000 μA DC for 24, 48 and 72 h. The treated *C. albicans* was analyzed by viable fungi count, cell metabolic activity assay, scanning electron microscopy (SEM) and LIVE/DEAD staining.

For examining the role of ROS in the DC-induced antifungal effect, *C. albicans* was stimulated by 1000 μA DC, Tempol (Solario, China) alone or 1000 μA DC combined with Tempol (Solario, China) for 12 h. The concentrations of Tempol used for the planktonic state

and biofilm state were 15 μM and 30 μM, respectively. Afterwards, the treated *C. albicans* was analyzed by ROS assay, CFU counting, gene expression assay, total SOD assay and fluorescence microscopy.

2.2.3. Synergistic Effect of DC with FLC/AMB on *C. albicans* in Planktonic State and Biofilm State

The *C. albicans* was stimulated by 1000 μA DC, FLC and AMB separately or 1000 μA DC combined with FLC or AMB for 6 h (in planktonic state) or 12 h (in biofilm state). The concentration of FLC/AMB for the planktonic state and biofilm state were 1 μg/mL and 8 μg/mL, respectively. Subsequently, the treated *C. albicans* was analyzed by CFU counting and LIVE/DEAD staining.

2.2.4. The Impact of DC on Membrane Permeability and Intracellular Drug Concentrations of *C. albicans*

The planktonic *C. albicans* was stimulated by 1000 μA DC for 0.5, 1, 6 and 12 h. Afterwards, the treated *C. albicans* was analyzed by A280 assay, electrical conductivity assay, transmission electron microscopy (TEM), HPLC-DAD/MS and gene expression assay. The rhodamine 6G (Rh6G) absorption and efflux assay was used to determine the transport activity after exposure to DC for different time periods.

2.2.5. The Role of SOD2-Mn SOD Pathway in the Killing Effect of DC on AMB-Tolerant Persisters of *C. albicans* Biofilms

The *C. albicans* biofilms were stimulated by 256 μg/mL AMB, MnTMPyP (10 μM) and 1000 μA DC separately or combined with MnTMPyP, or combined with both MnTMPyP and AMB for 24 h. Afterwards, the treated biofilms were subjected to the persister assay, gene expression assay, total ROS assay, mitochondrial ROS (mtROS) assay and Mn SOD activity assay.

2.3. Antimicrobial Susceptibility and MIC Testing

The minimum inhibitory concentration (MIC) of FLC and AMB against *C. albicans* was determined by broth microdilution method following M27-A3 guidelines of the Clinical and Laboratory Standards Institute [20]. Serial 2-fold dilutions of FLC and AMB (100 μL, ranging from 0 to 128 μg/mL) were made in culture media in 96-well plates (Corning, USA). The MIC was the lowest concentration that showed no visible growth. The experiment was repeated three times.

2.4. Persister Assay

The persister assay was performed as described previously [5,21]. Briefly, 72 hour-old *C. albicans* biofilms were exposed to 256 μg/mL AMB for 24 h at 37 °C. The biofilm cells were washed two times with PBS and harvested. After serial dilution, the biofilm cells were spread onto SDA plates for further counting. To confirm that the surviving colonies were persister cells, two colonies were reinoculated into fresh YPD medium and an in vitro susceptibility assay was performed to ensure that the MIC had not changed. The survival rate of persisters was calculated on the basis of viable cells out of total cells in an untreated culture.

2.5. Viable Fungi Counting

Viable fungi counting in planktonic or biofilm states was calculated by colony forming units (CFU) assay. After the treated *C. albicans* was transferred to liquid medium and serially diluted, 100 μL suspension was plated on blood agar by L-shape sterile coating bar (BIOLOGIX, Jinan, China) for further counting.

2.6. Cell Metabolic Activity Assay and Crystal Violet Staining

The cell metabolic activity of *C. albicans* biofilms was measured using an enhanced Cell Counting Kit-8 (CCK-8, Beyotime, Shanghai, China), as described by the manufacturers [22].

A volume of 100 μL of stained solution was measured in 96-well plates (Corning, USA) at 450 nm. The crystal violet staining was performed as previously described [14].

2.7. LIVE/DEAD Staining and Fluorescent Microscopy Observation

The viability of *C. albicans* was further evaluated by live/dead staining and fluorescent microscopy observation. After being stained with mixed CFSE (1 μM, live cells indicator stained green, AbMole, China) and PI solution (1 μM, dead cells indicator stained red, AbMole, China) for 20 min in the dark, the stained *C. albicans* was observed by fluorescent microscopy (Leica Microsystems, Germany), and images were obtained.

2.8. Detection of Intracellular ROS, mtROS, Total SOD Activity and Mn SOD Activity

2′,7′-Dichlorodihydrofluorescein diacetate (H2DCF-DA) (Solario, China) and MitoSOX Red (Invitrogen, Waltham, MA, USA) were used to detect total intracellular ROS and mtROS, respectively, as previously described. The ROS content in *C. albicans* was determined by fluorescence intensity. The treated *C. albicans* cells were washed and stained with DCFH-DA (10 μM) or MitoSOX Red (5 μM) for 20 min in the dark. After that, the cells were centrifuged (3000× *g*, 5 min) and washed two times with PBS. The relative fluorescence intensity (RFU) of 100 μL stained cells was detected by an Enspire microplate reader (PerkinElmer, Rodgau, Germany) at an excitation of 488 nm and an emission of 530 nm.

The total SOD activity and Mn SOD activity were evaluated by SOD assay kit and Mn-SOD Assay Kit with WST-8 (Beyotime Institute of Biotechnology, Shanghai, China) according to the manufacturer's instructions, respectively [23]. The absorbance was assessed at 450 nm using a microplate reader.

2.9. SEM Observation and TEM Observation

The samples of *C. albicans* biofilms formed on silicon wafers (Zhejiang Lijing Silicon Material Co., Quzhou, China) were washed with sterile PBS, and fixed with 2.5% (*v*/*v*) glutaraldehyde (Solario, China) for 2 h. Subsequently, the biofilms were dehydrated for 10 min using an ethanol gradient (50%, 60%, 70%, 90% and 100%). Finally, the samples were coated with gold and observed under SEM (Hitachi, Japan).

The detailed sample preparation before TEM observation was the same as in a previous study [24]. After fixation, dehydration with 30%, 50%, 70%, 90% and 100% ethanol, embedding and polymerization, the ultrathin sections (65 nm) were cut and stained. All sections were examined with transmission electron microscope JEM 1400 (JEOL Co., Tokyo, Japan).

2.10. RNA-Seq, Quantitative Proteomics Using TMT Labelling and Bioinformatics Analysis

All treated cells were collected and centrifuged at 3000× *g* for 10 min. The total RNA and protein samples were sent to Allwegene Technology Company Limited (Beijing, China) for further processing and bioinformatics analysis. The detailed process was performed as previously described [25,26]. For RNA-Seq, p value < 0.005 and $|\log2(\text{fold change})| \geq 1$ were set as the threshold for significantly differential expression. For proteomics, TMT coupled with liquid chromatography electrospray ionization tandem mass spectrometry (LC-MS/MS) analysis was referenced to the database of uniprot_*Candida_albicans*_strain_SC5314_6041_20230218.fasta. The expression fold change was > 1.2-fold (up-regulation greater than 1.2-fold or down-regulation less than 0.83-fold) and p value was < 0.05 (*t*-test or others).

2.11. Quantitative Real-Time PCR (qPCR)

1 μg of total RNA was extracted using the Fungal Total RNA Isolation Kit (Sangon Biotech, China). cDNA was synthesized with a Reverse Transcription System (Toyobo, Osaka, Japan) and detected using the Starlighter SYBR Green qPCR Mix (Foreverstar Biotech, Beijing, China) in a 7500 Real-Time PCR System (Applied Biosystem, San Francisco, CA, USA). The q-PCR was carried out for 35 cycles of 94 °C for 1 min, 60 °C for 1 min, and 72 °C for 1 min. Relative gene expression was calculated by the CT method using ACT1 as the reference gene.

Experiments were performed in biological duplicates and measured in technical triplicates. Primers used for real-time PCR are given in Table S1 in the Supplementary Materials.

2.12. A280 Absorbance Assay and Electrical Conductivity Assay

Protein concentration was determined via the A280 absorbance assay. After exposure to DC for 0.5, 1, 6 and 12 h, 2 μL supernatant of the treated *C. albicans* was taken to measure the absorbance at 280 nm using a NanoDrop instrument (Thermo Scientific NanoDrop, Wilmington, DE, USA).

The change of electrical conductivity is an important index to measure the change of fungi cell structure. The supernatant of the treated *C. albicans* was taken to measure its conductivity using the DDS–307 conductivity meter (Shanghai instrument, Shanghai, China).

2.13. Rh6G Absorption and Efflux Assay

In this study, we used the Rh6G tracer method to explore whether DC interfered with the drug absorption and efflux activity [27]. Planktonic *C. albicans* was grown to the exponential phase. After centrifugation (3000× *g*) for 10 min, the yeast cells were harvested and washed twice with glucose-free PBS (Solario, China) and resuspended to 1×10^7 CFU/mL. After oscillated in the shaker for 1 h to deplete cellular energy, 10 μM Rh6 G was added in the *C. albicans* suspension for the subsequent experiment. The *C. albicans* cells were resuspended in 1 mL medium and 100 μL diluted suspensions were measured at timepoint of 0, 10, 20, 30 and 50 min by microplate reader. For the Rh6G efflux, the treated *C. albicans* was placed in an ice bath for 10 min; then, after centrifugation (3000× *g*) for 10 min, the yeast cells were harvested and washed twice with glucose-free PBS. Subsequently, the intracellular Rh6 G was measured every 30 min. The Rh6 G-alone group was set as the control group. Then, the fluorescence intensity of intracellular Rh6G was measured with excitation at 488 nm and emission at 530 nm.

2.14. High-Performance Liquid Chromatography Mass Spectrometry (HPLC-DAD/MS) Analysis for Intracellular FLC and AMB

C. albicans cells were centrifuged at 3000× *g* for 5 min at 4 °C and washed with cold PBS twice. Similarly to Section 2.13, the supernatant was removed and centrifugation was repeated once. The sample processing was performed as previously described [24]. FLC and AMB were detected using authentic samples and mass ion peaks at 307.110 $[M + H]^+$ and 924.079 $[M–H]^-$.

2.15. Statistical Analysis

The data were presented as mean ± standard deviation (SD), and all experiments were performed three to six times. Significant differences between two or multiple groups were analyzed by the two-tailed Student's *t*-test or one-way ANOVA, in which post-hoc analysis was performed with the Tukey test. Data were analyzed by GraphPad Prism 9.4.1 software (GraphPad Software Inc., La Jolla, CA, USA). Differences were considered significant at a p value of < 0.05.

3. Results

3.1. The Dose-Dependent Effect of FLC/AMB against Planktonic and Biofilm States of C. albicans

The MIC of FLC and AMB against planktonic *C. albicans* were 4 μg/mL and 0.5 μg/mL, and the minimum lethal concentration reached 1280 μg/mL and 256 μg/mL, respectively (Figure 1A). As for biofilms, the amount of viable *C. albicans* in biofilms decreased by less than 1-log killing as FLC concentration increased up to 16 μg/mL, and remained at a similar level even at higher concentrations (32–1280 μg/mL). As the concentration of AMB increased, the treatment killed the majority of *C. albicans* biofilms but failed to eradicate a tiny subpopulation of the biofilms, presenting a biphasic pattern. The fractions of biofilm persisters reached 0.01% even at lethal doses of AMB (64 to 256 μg/mL, Figure 1B). After consecutive treatment of the biofilms by FLC (1280 μg/mL) or AMB (256 μg/mL) for

another 72 h, the survival rate of AMB-treated biofilms was maintained at a relatively stable level and the MIC value did not show obvious changes, while the survival rate of FLC-treated biofilms decreased significantly as exposure times increased to 72 h and the MIC value did not change (Figure 1C–E).

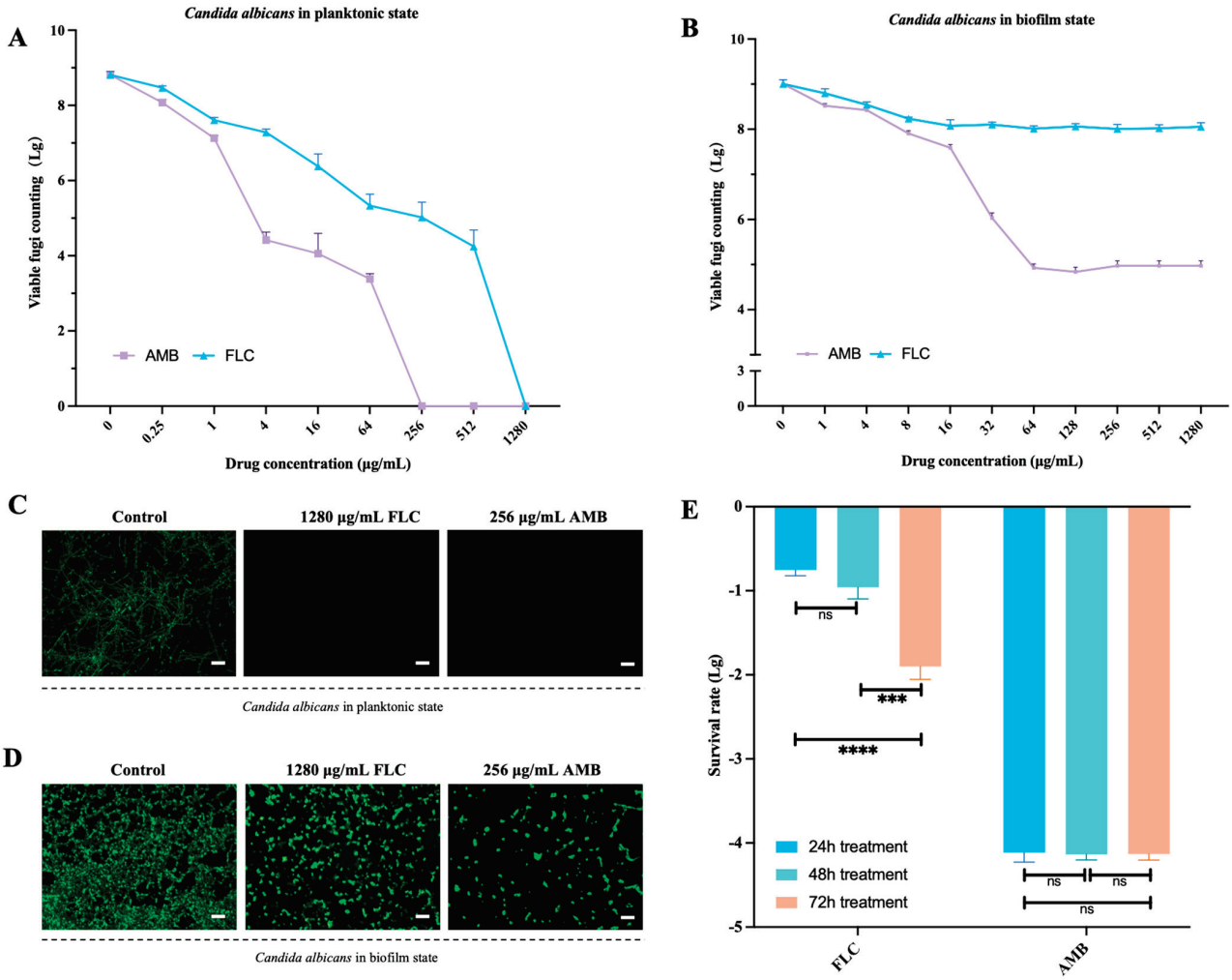

Figure 1. Dose-dependent inhibition of *C. albicans* BF-1 in planktonic state and biofilm state by FLC and AMB. Planktonic *C. albicans* were treated with various concentrations of FLC/AMB for 12 h. Next, the colonies were counted after 1 day of incubation (**A**). *C. albicans* biofilms were treated with various concentrations of FLC/AMB for 24 h. Next, the colonies were counted after 1 day of incubation (**B**) and recultured for the same stimulation and assay twice. The surviving cells were assessed using live/dead staining (scale bar 50 μm, (**C**) in planktonic state and (**D**) in biofilm state). The survival rate of *C. albicans* biofilms was calculated for comparison (**E**). *** and **** denote significant difference of $p < 0.001$, $p < 0.0001$, respectively. ns denotes no significant difference.

3.2. The Time-Dependent Killing Effect of 1000 μA DC against Planktonic and Biofilm States of C. albicans

For the planktonic *C. albicans*, compared to untreated control, the CFU counting was significantly decreased when treated with 1000 μA DC for 0.5 h, 1 h, 6 h and 12 h (Figure 2A), which reached 0.23, 0.35, 0.80 and 2.00-log killing, respectively. The dead staining showed consistent viable fungi count results (Figure 2B). The agar plate of *C. albicans* colonies showed the maximum killing when treated by DC for 12 h (Figure 2C). The SEM showed that the average cell density decreased and cellular structure wrinkled after 12 h-DC treatment (Figure 2D).

For the *C. albicans* biofilms, compared to untreated control, the CFU counting was significantly decreased when treated with 1000 μA DC for 6 h, 12 h and 24 h (Figure 2E), which reached 0.27, 0.94 and 0.97-log killing, respectively. The metabolic activity of DC-stimulated biofilms at 6 h, 12 h and 24 h was significantly lower than the controls(Figure 2F). Crystal violet staining showed significant decrease in the amount of biofilm mass after exposure to DC for 24 h, 48 h and 72 h (Figure 2G). SEM further demonstrated the biofilm density was decreased after continual DC stimulation for 24 h, 48 h and 72 h (Figure 2H). The dead staining (Figure 2I) and agar plates (Figure 2J) of *C. albicans* showed significant killing when treated by DC for 24 h.

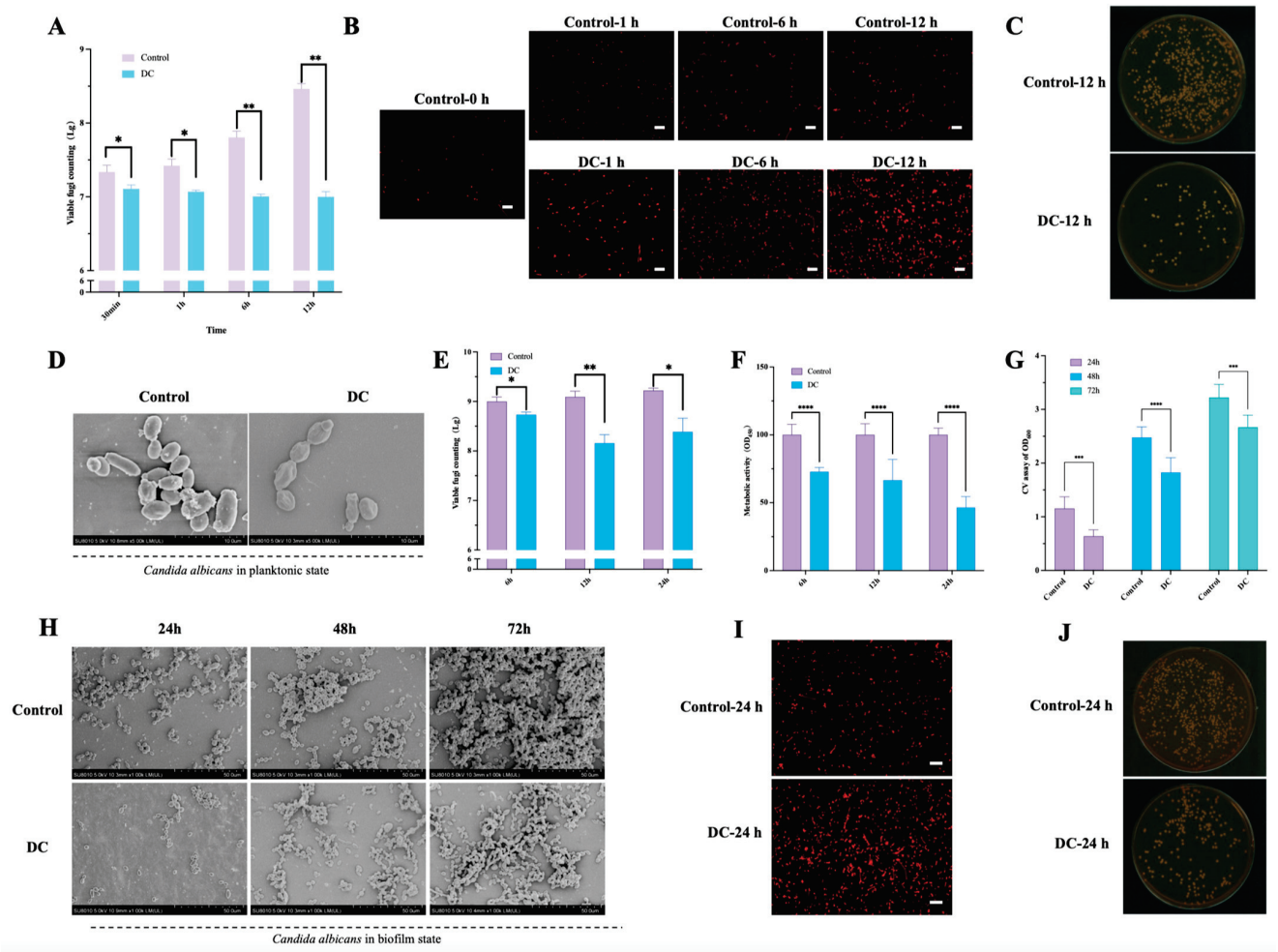

Figure 2. The killing effect of 1000 μA direct current (DC) with different stimulus durations on *C. albicans* in planktonic state and biofilm state. Viable fungi counting (**A**) and dead staining (stained red, (**B**)) after exposure to DC for 1 h, 6 h and 12 h in planktonic state. The SDA agar plate with *C. albicans* colonies (**C**) and scanning electron microscopy (SEM) observation (**D**) after exposure to DC for 12 h in planktonic state. Viable fungi counting (**E**) and metabolic activities assay (**F**) after exposure to DC for 6, 12 and 24 h. Total biofilm amount (**G**) and SEM observation at magnifications of ×1000 (scale bar 50 μm,(**H**)) at 24, 48 and 72 h of DC treatment. SEM observation at magnifications of ×5000 (scale bar 10 μm, (**I**)) , dead staining (stained red, scale bar 50 μm, (**F**)) and SDA agar plate with *C. albicans* colonies (**J**) after exposure to DC for 24 h. *, **, ***, **** denote significant difference of $p < 0.05$, $p < 0.01$, $p < 0.001$, $p < 0.0001$, respectively.

3.3. The mRNA and Protein Expression Profiles of DC-Treated Planktonic C. albicans

In the planktonic cells of *C. albicans* treated by DC for 6 h, 1200 genes and 49 proteins were found to be differentially expressed. Among these, 509 upregulated genes and 691

downregulated genes were observed, and 18 upregulated proteins and 31 downregulated proteins were involved in the response to DC. After conducting the combined analysis of transcriptomic and proteomic data, the top five GO terms of biological processes were oxidation-reduction process, lipid metabolic process, cellular lipid metabolic process, metal ion transport and fatty acid metabolic process (Figure 3A). Moreover, the top five GO terms of molecular function processes were oxidoreductase activity, NAD binding NADP binding, serine-type peptidase activity, hydrolase activity acting on acid phosphorus-nitrogen bonds and serine hydrolase activity (Figure 3A). The KEGG enrichment analysis revealed that the top 10 enriched pathways included metabolic pathways, biosynthesis of secondary metabolites, lysine biosynthesis, peroxisome, biosynthesis of antibiotics, biosynthesis of amino acids, alpha-linolenic acid metabolism, ABC transporters, biosynthesis of unsaturated fatty acids, and fructose and mannose metabolism (Figure 3B).

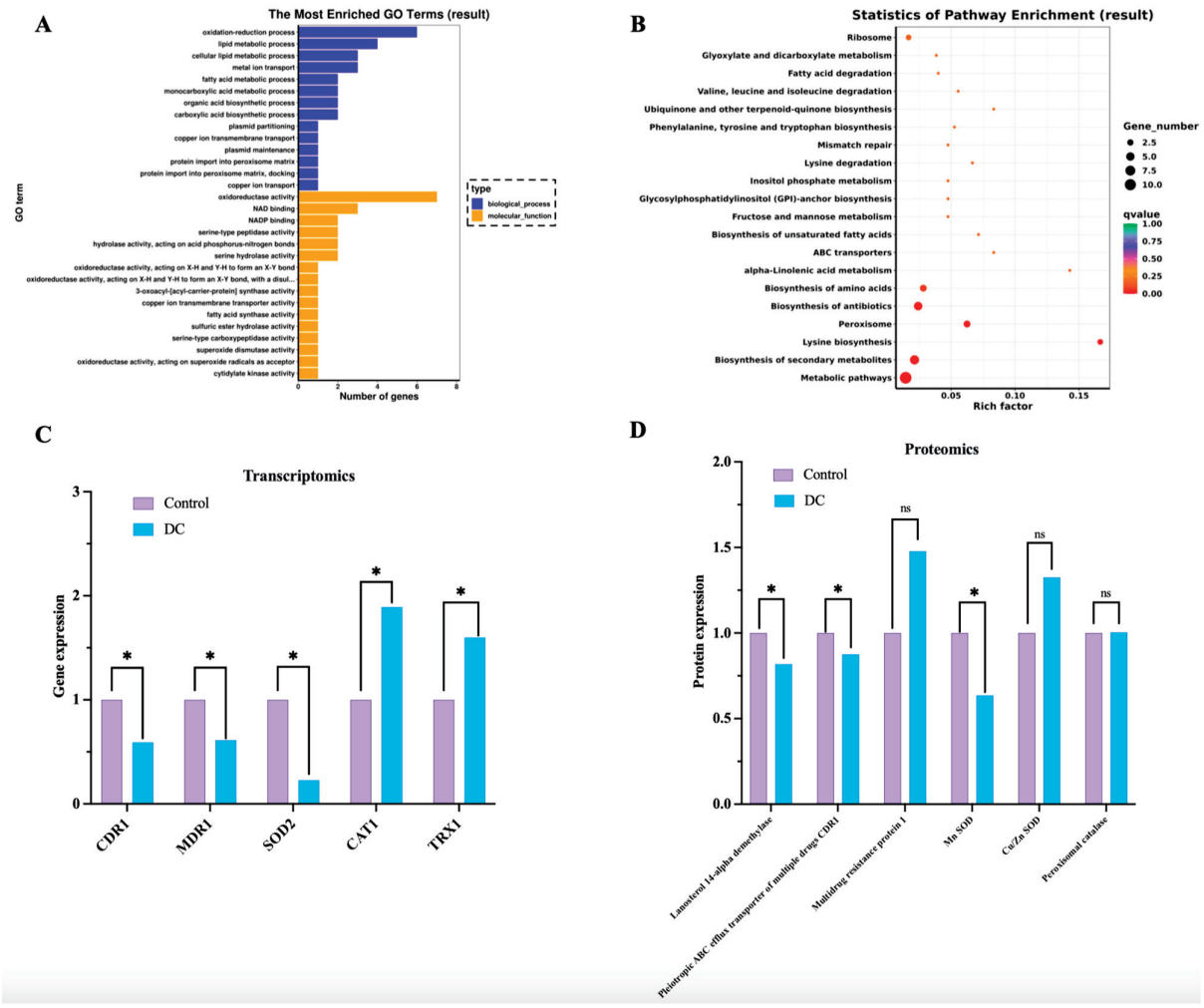

Figure 3. The transcriptomic and proteomic analysis of biological changes on planktonic *C. albicans* after DC treatment. Gene ontology (GO) functional analysis (**A**) and KEGG enrichment (**B**) of differentially expressed genes (DEGs) caused by 1000 μA DC (fold change FDR < 0.05). Selected differentially expressed genes (**C**) and proteins (**D**) involved in drug efflux and oxidative stress were listed. * denotes significant difference of $p < 0.05$. ns denotes no significant difference.

As for the pathways of oxidoreductase activity and ABC transporters, the mRNA level of EGR11, CDR1, MDR1 and SOD2 was significantly decreased after DC treatment, and the mRNA level of CAT1 and TRX1 was increased significantly (Figure 3C). The proteomic analysis showed significantly reduced expression of lanosterol 14-alpha demethylase, pleiotropic ABC efflux transporter of multiple drugs CDR1 and Mn SOD, which were in

accordance with the mRNA expression changes. The expression of multidrug resistance protein 1, Cu/Zn SOD and peroxisomal catalase increased with no significant difference after DC treatment (Figure 3D).

3.4. The Increased ROS Mediated the Killing Effect of DC on Planktonic and Biofilm States of C. albicans

For the planktonic *C. albicans*, 1000 μA DC treatment for 6 h markedly increased the intracellular ROS content by nearly 2.5-fold (Figure 4A) and caused significant upregulation of CAT1 and TRX1 (Figure 4C). In addition, DC downregulated the mRNA expression of SOD2 (Figure 4C) and exerted ~1-log killing (Figure 4B). Tempol treatment alone did not affect the viable fungi amount and the ROS content. Moreover, compared to DC treatment alone, DC combined with Tempol showed significant downregulation of CAT1 and TRX1 expression, lower oxidative stress and decreased CFU counting (Figure 4A–C). The ROS fluorescence view further confirmed that DC combined with Tempol treatment resulted in lower intracellular oxidative stress than DC only treatment group (Figure 4D).

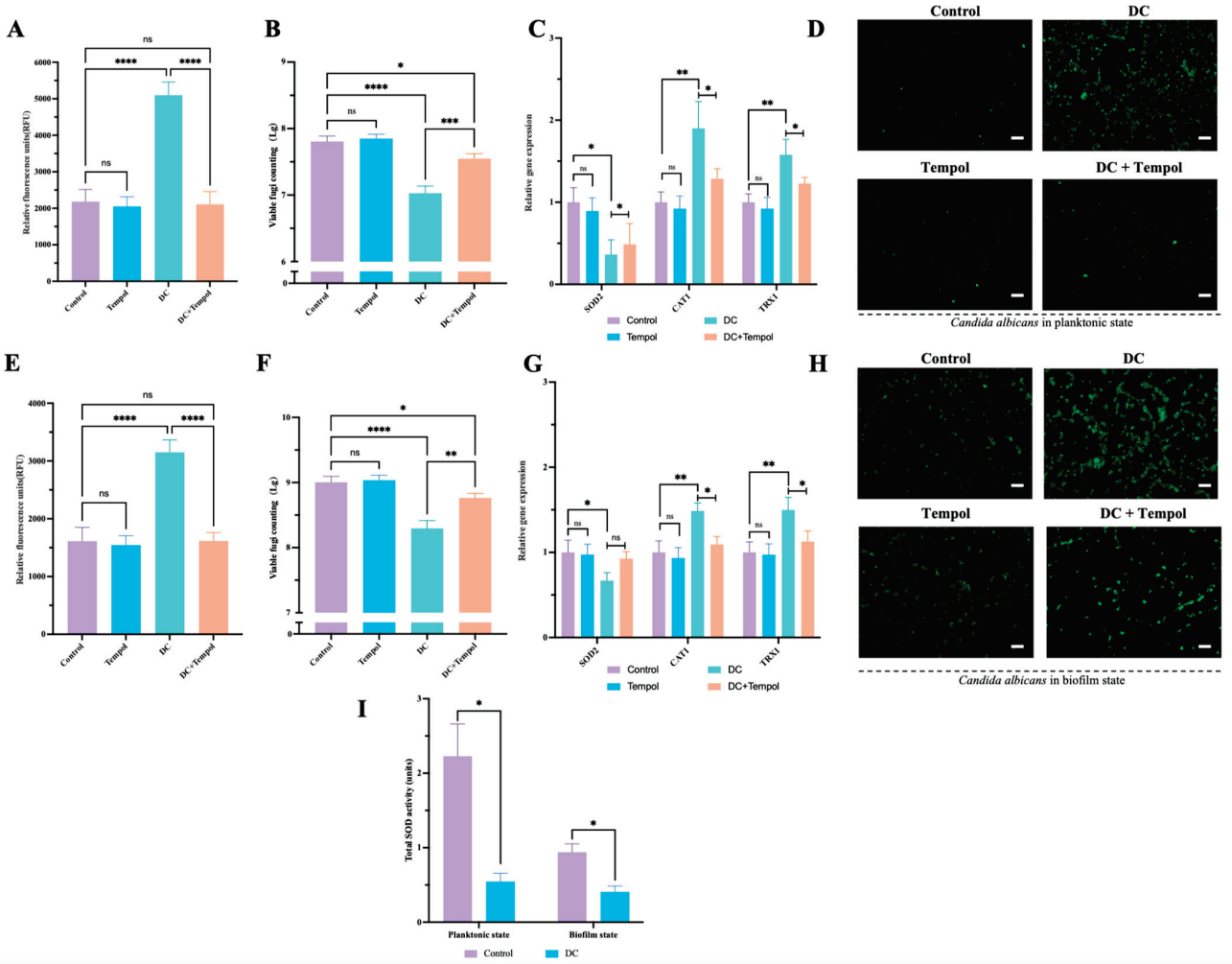

Figure 4. The role of ROS induced by DC on *C. albicans* in planktonic state and biofilm state. The *C. albicans* were treated by 0 μA DC (control), Tempol alone (15 μM for plankton, 30 μM for biofilms), 1000 μA DC combined with or without Tempol (15 μM for the plankton, 30 μM for biofilms), and subjected to analyses of ROS level in the form of RFU ((**A**) in plankton, (**E**) in biofilms), CFU counting ((**B**) in plankton, (**F**) in biofilms), relative gene expression assay ((**C**) in plankton, (**G**) in biofilms) , DCFH-DA staining ((**D**) in plankton, (**H**) in biofilms, scale bar: white line = 50 μm) and total SOD activity comparisons between the control group and DC treatment group (**I**). *, **, ***, **** denote significant difference of $p < 0.05$, $p < 0.01$, $p < 0.001$, $p < 0.0001$, respectively. ns denotes no significant difference.

For the *C. albicans* biofilms, 1000 μA DC treatment for 12 h showed obvious killing effect (less than 1-log killing, Figure 4F). In addition, DC increased the intracellular ROS content by nearly 2-fold (Figure 4E) and led to significant upregulation of CAT1 and TRX1 and downregulation of SOD2 (Figure 4G). Similarly, Tempol did not affect the survival of fungi in biofilms and decreased the ROS content with no greater significance than in the control group (Figure 4E,F). Interestingly, Tempol was able to partially reverse the killing effect of DC on *C. albicans* biofilms and the increased oxidative stress caused by DC treatment. The ROS fluorescence view further demonstrated that DC combined with Tempol treatment showed a lower level of intracellular oxidative stress than the DC only treatment group (Figure 4H). Moreover, DC decreased the total SOD activity of *C. albicans* significantly both in planktonic and biofilm cells (Figure 4I).

3.5. DC Showed Synergistic Effect with FLC/AMB against C. albicans in Planktonic and Biofilm States

For the planktonic *C. albicans*, 1000 μA DC, 1 μg/mL FLC, 1 μg/mL AMB, DC combined with 1 μg/mL FLC, and DC combined with 1 μg/mL AMB caused significant viable fungi reduction of 0.76, 0.23, 0.73, 4.46 and 3.17 $\log_{10}$ CFU/mL compared to control, respectively (Figure 5A). The killing effect of DC combined with 1 μg/mL FLC for 6 h reached a similar level to that achieved by the 256 μg/mL FLC for 12 h treatment. Similarly, the killing effect of DC combined with 1 μg/mL AMB for 6 h reached a similar level to that achieved by the 32 μg/mL AMB for 12 h treatment (Figure 5A). The live staining further confirmed these results (Figure 5B).

For the *C. albicans* biofilms, 1000 μA DC, 8 μg/mL FLC, 8 μg/mL AMB, DC combined with 8 μg/mL FLC, and DC combined with 8 μg/mL AMB caused significant viable fungi reduction of 0.79, 0.54, 1.03, 2.35 and 4.00 $\log_{10}$ CFU/mL compared to control, respectively (Figure 5C). The killing effect of DC combined with 8 μg/mL FLC for 12 h was even more effective than 1280 μg/mL FLC for 24 h group. Moreover, the killing effect of DC combined with 8 μg/mL AMB for 12 h reached a similar level to that achieved by the 64 μg/mL AMB for 24 h treatment (Figure 5C). The live staining further confirmed these results (Figure 5D).

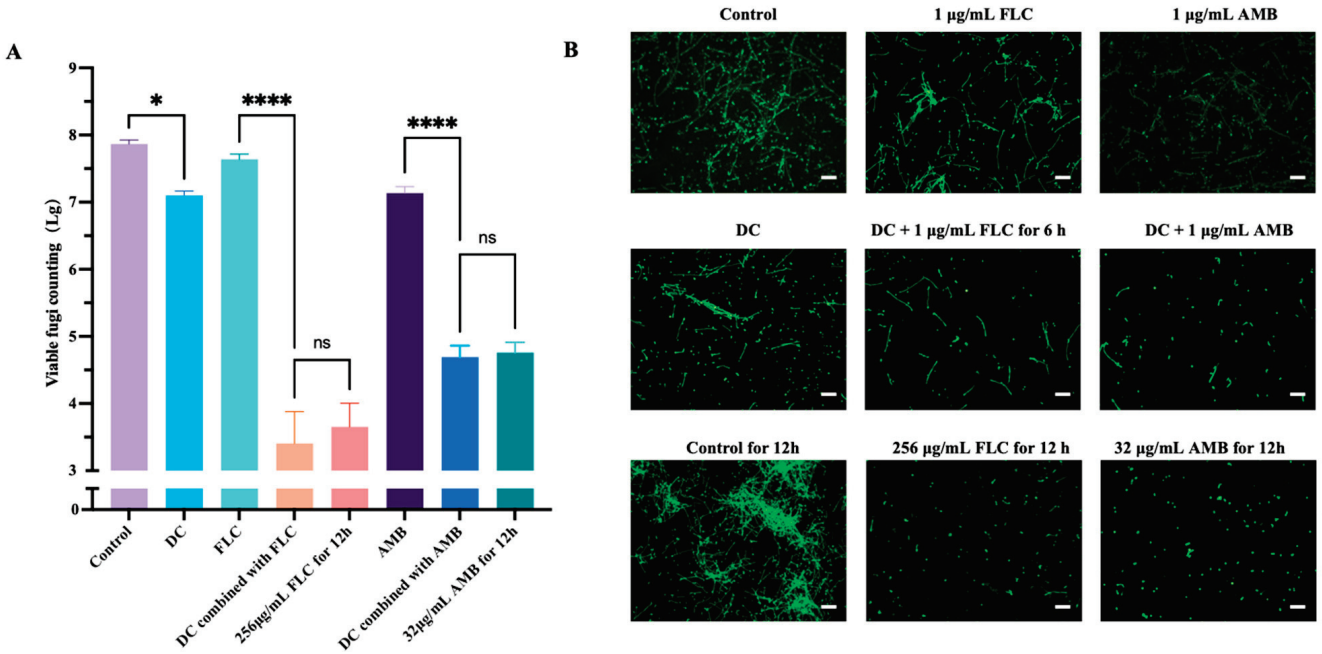

Figure 5. *Cont.*

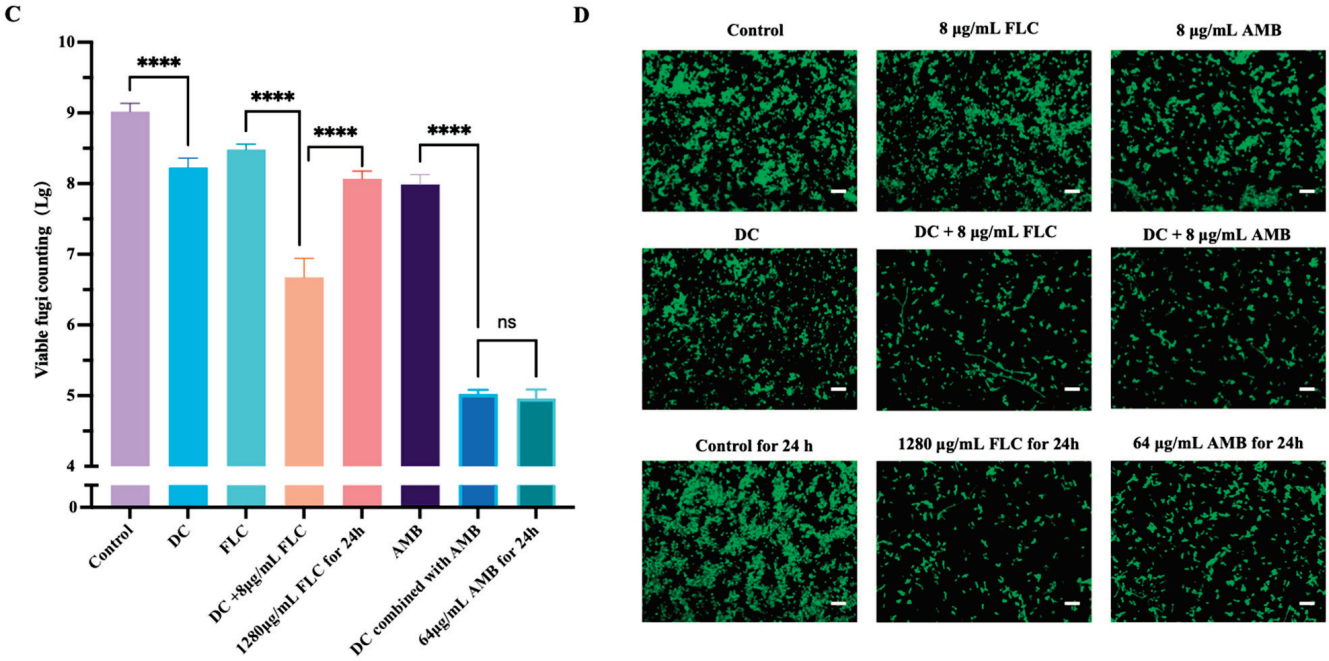

Figure 5. The synergistic effect of DC with FLC/AMB on *C. albicans* in planktonic state and biofilm state. The planktonic *C. albicans* were treated for 6 h by 0 μA DC (control), FLC alone (1 μg/mL), AMB alone (1 μg/mL) and 1000 μA DC combined with or without FLC/AMB (1 μg/mL). Moreover, 0 μA DC for 12 h were set as another negative control group, and 256 μg/mL FLC for 12 h and 32 μg/mL AMB for 12 h were set as the high-dose antifungal group. After stimulation, they were subjected to viable fungi count (**A**) and live staining (**B**). The *C. albicans* biofilms were treated for 12 h by 0 μA DC (control), FLC alone (8 μg/mL), AMB alone (8 μg/mL) and 1000 μA DC combined with or without FLC/AMB (8 μg/mL). Moreover, 0 μA DC for 24 h were set as another negative control group, and 1280 μg/mL FLC for 12 h and 64 μg/mL AMB for 24 h were set as the high-dose antifungal group. After stimulation, they were subjected to viable fungi count (**C**) and live staining (scale bar 50 μm, (**D**)). *, and **** denote significant difference of $p < 0.05$, $p < 0.0001$, respectively. ns denotes no significant difference.

3.6. DC Increased the Membrane Permeability and Intracellular Drug Concentrations of Planktonic C. albicans

The A280 assay showed that the number of external proteins increased with the prolonged stimulation time of DC, with reference to the controls (Figure 6A). The electrical conductivity assay further confirmed DC increased the conductivity of the solution and membrane permeability (Figure 6B); and TEM demonstrated aberrantly shaped membrane and uneven cell walls (Figure 6C). The Rh6G assay showed DC augmented the absorption of Rh6G by *C. albicans* as the DC stimulation time increased from 0 to 50 min, and DC also decreased the efflux of Rh6G continually from 60 to 240 min (Figure 6D,E). The HPLC-DAD/MS analysis showed DC treatment for 6 h significantly increased the cellular drug content of FLC and AMB by 2.56- and 2.92-fold relative to that of the drug alone group, respectively (Figure 6F,G); and DC treatment significantly downregulated the gene expression of CDR1 and MDR1 compared to the control group (Figure 6H). Moreover, DC was able to partially reverse the FLC-induced overexpression of CDR1 and MDR1 (Figure 6H).

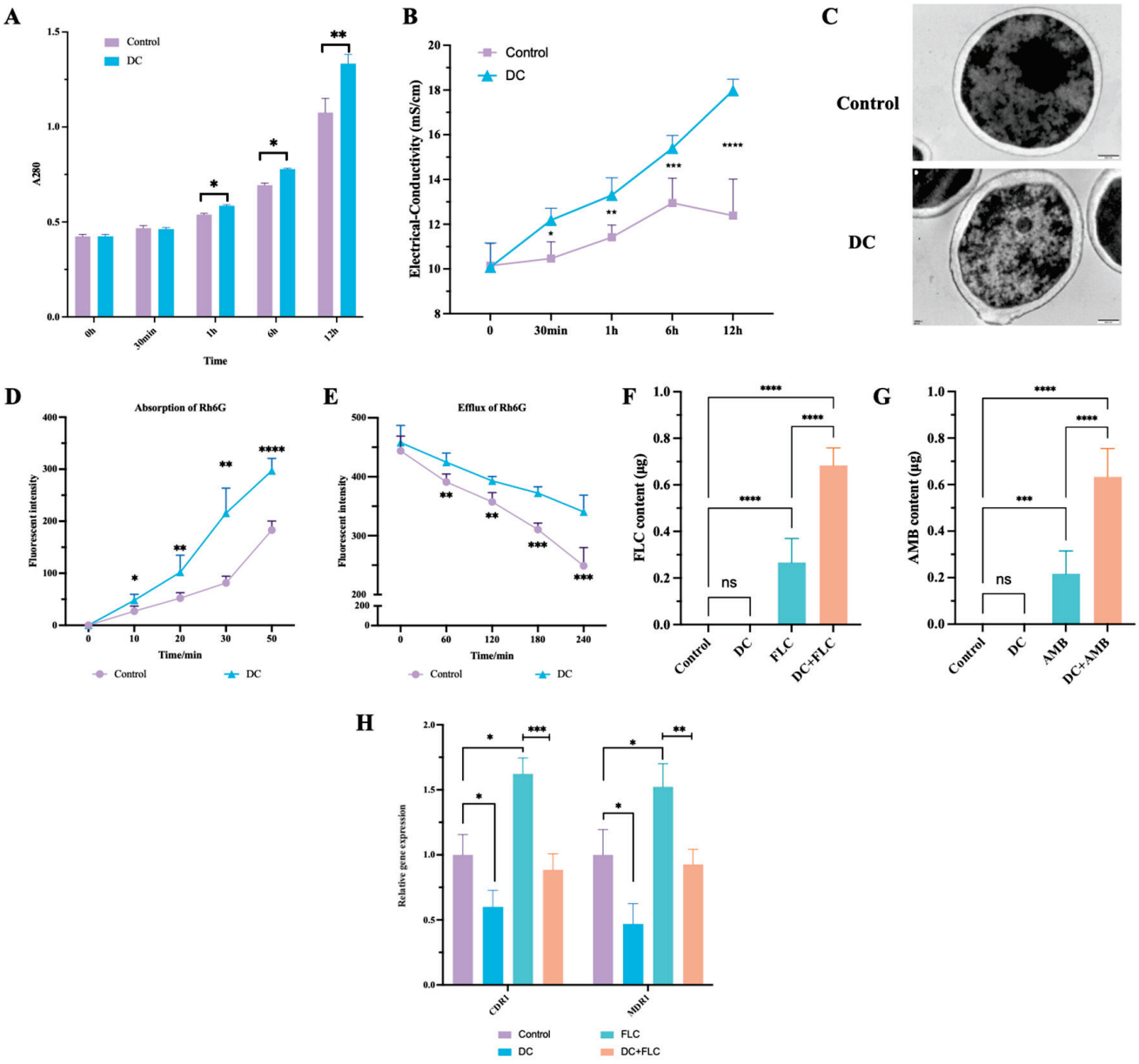

Figure 6. Effect of DC on the absorption and efflux of FLC/AMB. The planktonic *C. albicans* was treated by 0 μA and 1000 μA DC for 0, 0.5, 1, 6 and 12 h. The supernatant after centrifugation was subjected to the A280 assay (**A**) and electrical conductivity assay (**B**). In addition, DC-treated *C. albicans* for 12 h was analyzed by transmission electron microscopy (TEM) (**C**). The absorption (**D**) and efflux (**E**) of Rh6G were detected after DC treatment. The intracellular drug content of FLC (**F**) and AMB (**G**) were detected when treated for 6 h. The relative gene expression of CDR1 and MDR1 were detected after treated by 0 μA alone (control), 1000 μA DC alone, FLC alone, and 1000 μA DC combined with FLC (**H**). *, **, ***, **** denote significant difference of $p < 0.05$, $p < 0.01$, $p < 0.001$, $p < 0.0001$, respectively. ns denotes no significant difference.

3.7. SOD2 Gene and Mn SOD Mediated the Killing Effect of DC on AMB-Tolerant Biofilm Persisters of C. albicans

Lethal AMB (256 μg/mL) resulted in 0.01% biofilm persisters. After the addition of MnTMPyP, the proportion of persisters increased slightly with no significant difference (Figure 7A). Importantly, the level of persisters decreased 100-fold after adjunctive DC treatment (Figure 7A). However, after the addition of MnTMPyP, the proportion of persisters in the DC combined with MnTMPyP and AMB group increased significantly with reference

to the combination of DC and AMB (Figure 7A). Next, we explored the expression of SOD2, Mn SOD activity and ROS level in AMB-tolerant biofilm persisters. After exposure to 256 μg/mL AMB, the oxidative stress significantly increased, accompanied by higher SOD2 gene expression and Mn SOD activity than the control group. DC caused a more significant downregulation of SOD2 gene expression and Mn SOD activity than in the control group, and increased intracellular oxidative stress (Figure 7B–D). Although MnTMPyP alone did not affect SOD2 gene expression significantly, it inhibited the AMB-tolerant higher expression of SOD2 and the increased oxidative stress. Moreover, compared with the DC combined with AMB group, the addition of MnTMPyP weakened the oxidative stress and increased Mn SOD activity. (Figure 7C,D). The Mito-Sox Red staining further confirmed these results, and the treatment with DC or AMB led to mitochondrial ROS production (Figure 7E). MnTMPyP decreased the mitochondrial ROS in *C. albicans* biofilms treated by AMB alone or combined with DC (Figure 7E).

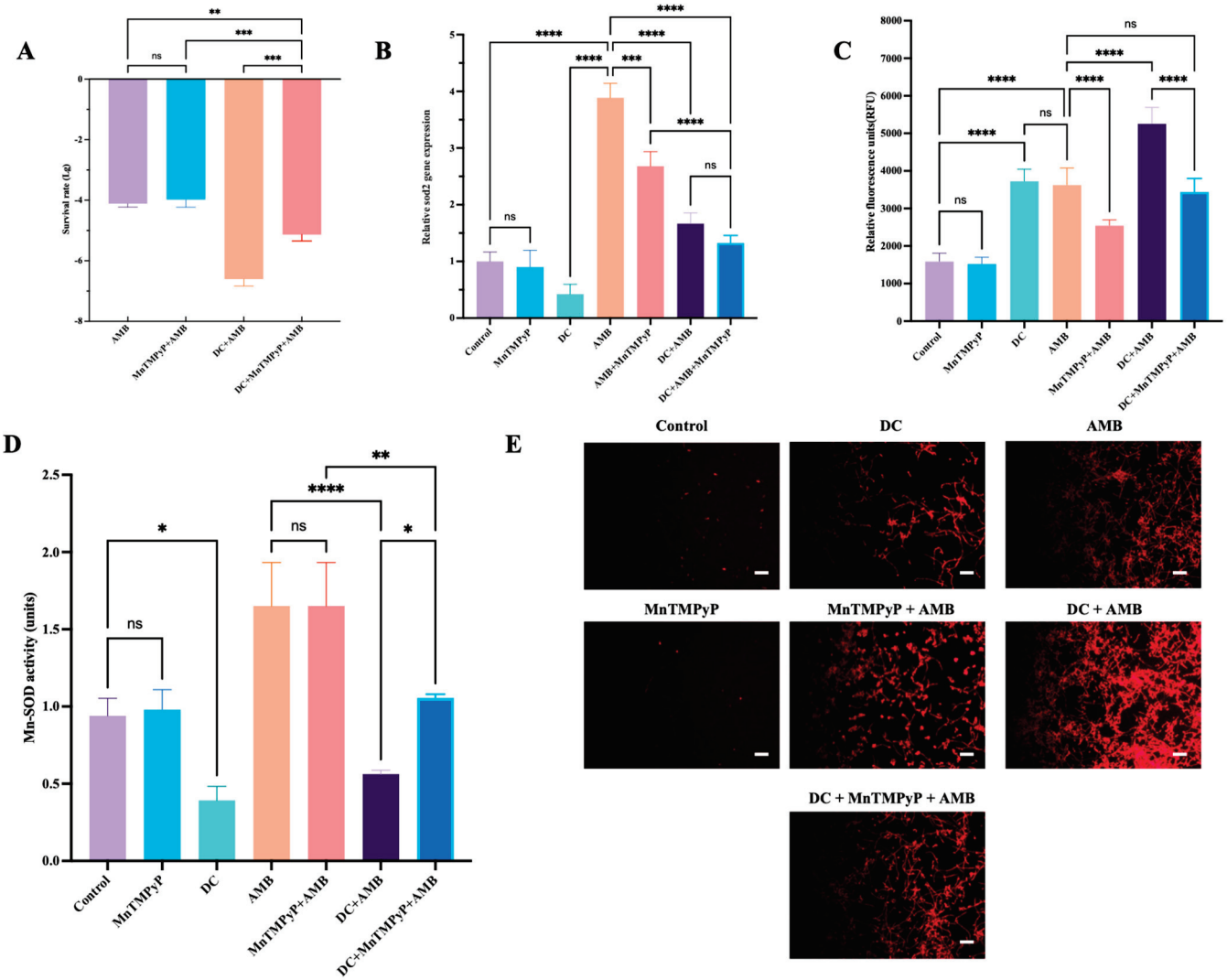

Figure 7. The role of manganese superoxide dismutase (Mn SOD) in the survival rate of AMB-tolerant *C. albicans* biofilm persisters. The *C. albicans* biofilms were treated for 24 h by 256 μg/mL AMB alone (Control), 256 μg/mL AMB combined with 10 μM MnTMPyP, 1000 μA DC or 1000 μA DC with 10 μM MnTMPyP. After the persisters assay, they were subjected to viable fungi count (**A**), relative SOD2 gene expression (**B**), ROS level assay (**C**), Mn SOD activity assay (**D**) and Mito-SOX Red staining (scale bar: white line = 50 μm, (**E**)). *, **, ***, **** denote significant difference of $p < 0.05$, $p < 0.01$, $p < 0.001$, $p < 0.0001$, respectively. ns denotes no significant difference.

4. Discussion

The present study first showed that constant DC (1000 μA) had a killing effect and synergistic effect with FLC/AMB on planktonic and biofilm states of *C. albicans.* High concentration of FLC and AMB were both able to kill all planktonic cells of *C. albicans*. However, *C. albicans* biofilms were highly resistant to FLC, with less than 1-log CFU reduction when stimulated by 1280 μg/mL FLC. In accordance with our prior research [5], 256 μg/mL AMB killed the majority of *C. albicans* biofilms and about 0.01% biofilm persisters remained alive without inheritable resistance. Notably, when DC and AMB were used in combination, the adjunctive DC treatment was capable of eliminating AMB-tolerant *C. albicans* biofilm persisters. The findings indicate that DC is a novel potential strategy to combat *C. albicans* biofilms and their persisters.

Next, to investigate the mechanism of action of DC, transcriptomic and proteomic analyses were conducted. The results showed that oxidoreductase activity and process in DC-treated *C. albicans* was significantly enriched, suggesting that intracellular oxidative stress induced by DC might play a critical role in killing *C. albicans.* ROS are formed during normal oxygen metabolism and are byproducts of aerobic metabolism, which is necessary for gene expression, cell signaling, and redox homeostasis in certain amounts [28, 29]. The antioxidant system is able to scavenge overproduced ROS to maintain adequate amounts of ROS [30]. The balance between the production and scavenging of ROS in cells maintains stability of metabolism and cellular process. The oxidative stress occurs when ROS production overwhelms the scavenging capacity of antioxidants, which can oxidize or damage DNA, proteins, and lipids, thus leading to cellular damage and cell death [21,28,30]. It was reported that DC could induce excessive ROS production and cause bacterial death in *Staphylococcus aureus* and *Staphylococcus epidermidis* biofilms [31,32]. Similar results were observed in this study, in that the cellular ROS level of *C. albicans* was increased after DC treatment and decreased when Tempol was added. Tempol, as a ROS scavenger, is a membrane-permeable and redox-cycling (catalytic) superoxide dismutase mimetic. In this study, Tempol alleviated oxidative stress and was able to decrease ROS levels in DC-treated *C. albicans* to levels comparable to untreated controls. However, the killing efficacy was only partly reversed by the addition of Tempol, suggesting that other mechanisms may also be involved in the antifungal effect of DC.

To further confirm and validate the role of ROS in DC-associated cell death of *C. albicans*, we examined the gene expression of SOD2, CAT1 and TRX1 by qPCR and Mn SOD activity. Interestingly, we found that DC treatment markedly downregulated SOD2 expression and upregulated CAT1 and TRX1 expression, which could result in decreased total SOD activity and Mn SOD activity. These findings were consistent with the results of the transcriptomic and proteomic analysis. It is well known that Mn SOD is encoded by superoxide dismutase gene 2 (SOD2) and specifically present in the mitochondrial matrix and inner membrane. Mn SOD plays a crucial role in removing superoxide anions and acts as the first line of defense against the mitochondrial oxidative damage [21,33]. Moreover, Tempol was able to reduce oxidative stress and downregulate the expression of SOD2 in DC-treated *C. albicans*. Taken together, the increased oxidation stress induced by DC may be a critical mechanism underlying its antifungal effect.

We found that the combination of DC with FLC/AMB displayed a synergistic effect both in planktonic and biofilm states, the planktonic *C. albicans* being particularly sensitive to this. To understand the mechanisms underlying the synergism, the overall membrane permeability of *C. albicans* was assessed by TEM observation, A280 assay and electrical conductivity. Notably, the cell walls and membranes of *C. albicans* crumpled after DC treatment. Moreover, the protein content and extracellular conductivity rose with increasing treatment time, indicating that membrane permeability increased following DC stimulation. The increased cellular membrane permeability is able to enhance drug uptake and promote drug delivery and treatment efficacy [17,30,34]. Rh6G was used as a tracer of FLC to detect the intracellular FLC concentration, recording the changes in uptake and efflux transport of FLC [27]. As expected, DC treatment could increase the FLC uptake and inhibit the

FLC efflux. The HPLC-DAD/MS analysis further confirmed DC led to a nearly 3-fold increase of intracellular FLC relative to the FLC alone group. The overexpression of efflux pumps including CDR1 and MDR1 is one of the most common resistance mechanisms of *C. albicans* to FLC [7,27,35]. The transcriptome and qPCR data revealed that DC significantly suppressed expression of CDR1, which supported the theory of efflux pump inhibition by DC. These findings demonstrated that the synergism between DC and FLC may be related to membrane permeability increase and efflux pump suppression.

Consistent with our previous study [5], about 0.01% *C. albicans* biofilm persisters remained alive without inheritable resistance after exposure to 256 μg/mL AMB, confirming the limitation of single antifungal treatment in combating *C. albicans* biofilms. In this study, we found that the combination of DC and AMB caused a substantial decrease in the proportion of *C. albicans* biofilm persisters. DC significantly inhibited the expression of SOD2 gene and Mn SOD activity, and resulted in an increased ROS level in *C. albicans* biofilms. Interestingly, the addition of MnTMPyP partly reversed the persister-killing effect of DC. MnTMPyP, as a Mn SOD mimetic, exerted the ROS scavenging effects by increasing the Mn SOD activity in the biofilms. These findings indicate that DC mediated the killing of AMB-tolerant biofilm persisters partly by the inhibition of the SOD2-Mn SOD pathway and the overproduction of ROS. Moreover, our results were consistent with a recent study which showed the significant downregulation of sodB by rifampicin could contribute to greater generation of ROS and lead to clearance of polymyxin B-tolerant persister cells, revealing that the overproduction of ROS may promote the killing of persisters [21].

We found that the increased ROS mediated the killing effect of DC against *C. albicans*. In addition, DC could increase membrane permeability to promote the absorption of FLC and inhibit the efflux pump, thereby showing synergism with FLC against *C. albicans*. DC was also able to downregulate the mRNA expression of SOD2 and inhibit the superoxide scavenging activity of Mn SOD, leading to the overproduction of ROS and thus exerting a killing effect on *C. albicans*-tolerant biofilm persisters. The scheme of the proposed biological mechanisms of DC against *C. albicans* is demonstrated in Figure 8.

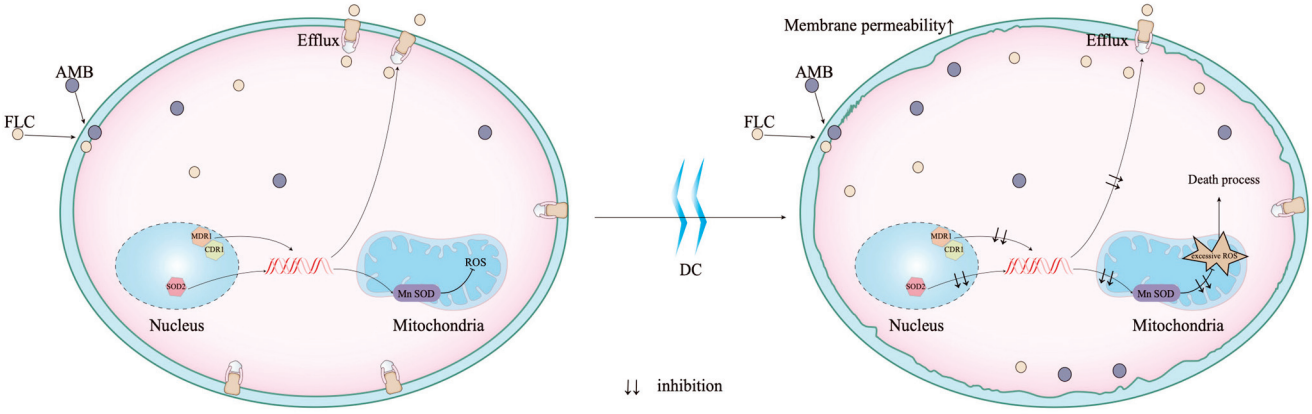

Figure 8. Proposed model for the fungicidal action mechanisms of DC in *C. albicans.* DC increases the membrane permeability, and inhibits the efflux activity by downregulating the gene expressions of CDR1 and MDR1, thus increasing the cellular drug concentrations and killing effect of FLC and AMB. Meanwhile, DC inhibits the expression of SOD2, and decreases Mn SOD activity of scavenging ROS in mitochondria, which leads to an oxidative stress disorder and accelerates the killing of AMB-tolerant persisters.

Our study had several limitations. To maintain the electric current at a harmless level, the current intensity of DC used in this study was no more than 1000 μA. It is unknown whether larger current intensity could result in a stronger antifungal effect and synergism with FLC/AMB. Moreover, animal studies may be needed prior to its application in the clinical environment in the future. Lastly, owing to the lack of a reliable primary antibody

against Mn SOD in *C. albicans* BF-1, the amount of Mn SOD may be difficult to assess quantitatively, further hindering the progress in understanding the nature of DC against *C. albicans*.

In summary, using DC to activate oxidative stress response pathways of SOD2–Mn SOD could harness their potential as efficient molecular targets to control *C. albicans* and persisters in *C. albicans* biofilms. From a certain point of view, DC may be seen as a SOD inhibitor, which induces oxidative stress in *C. albicans* by inhibiting SOD2 gene expression and Mn SOD activity, thus exerting a killing effect on *C. albicans* and AMB-tolerant persisters. The inhibition of the drug efflux pump and increase in membrane permeability caused by DC contribute to the enhanced killing efficacy of FLC and AMB. Hence, our findings suggest that low-intensity DC is a promising approach for controlling *C. albicans* and AMB-tolerant *C. albicans* persisters. In the future, the development of clinically suitable DC devices or charged material may become indicated in effective management of fungal infections.

Supplementary Materials: The following supporting information can be downloaded at: https://www.mdpi.com/article/10.3390/antibiotics13060521/s1, Table S1: List of genes and corresponding primers sequence.

Author Contributions: Conceptualization, P.Z.; methodology, P.Z., J.L., P.L. and Q.L.; validation, P.Z.; formal analysis, P.Z.; investigation, P.Z.; data curation, P.Z.; writing—original draft, P.Z.; writing—review and editing, P.Z., J.L., P.L. and Q.L.; supervision, J.L.; funding acquisition, P.Z., P.L. and Q.L. All authors have read and agreed to the published version of the manuscript.

Funding: The work was funded by grant PKUSS20220107 to Peihui Zou from Young and middle-aged scientific research fund of Peking University School, Hospital of Stomatology, grant PKUSSNMP-201905 to Qingxian Luan from the National Program for Multidisciplinary Cooperative Treatment on Major Diseases and grant 81700975 to Peng Li from the National Natural Science Foundation of China.

Institutional Review Board Statement: Not applicable.

Informed Consent Statement: Not applicable.

Data Availability Statement: All data supporting the findings of this study are available from the corresponding author upon reasonable request.

Acknowledgments: The authors are grateful to Lilian Li (KuShi Medical Technology Co., Ltd., Shanghai, China) for technical assistance.

Conflicts of Interest: The authors declare no conflicts of interest.

References

1. Lass-Flörl, C.; Samardzic, E.; Knoll, M. Serology anno 2021-fungal infections: From invasive to chronic. *Clin. Microbiol. Infect.* **2021**, *27*, 1230–1241. [CrossRef] [PubMed]
2. Bertolini, M.; Ranjan, A.; Thompson, A.; Diaz, P.I.; Sobue, T.; Maas, K.; Dongari-Bagtzoglou, A. *Candida albicans* induces mucosal bacterial dysbiosis that promotes invasive infection. *PLoS Pathog.* **2019**, *15*, e1007717. [CrossRef] [PubMed]
3. Pereira, R.; Dos Santos Fontenelle, R.O.; de Brito, E.H.S.; de Morais, S.M. Biofilm of Candida albicans: Formation, regulation and resistance. *J. Appl. Microbiol.* **2021**, *131*, 11–22. [CrossRef]
4. Kumar, D.; Kumar, A. Molecular Determinants Involved in *Candida albicans* Biofilm Formation and Regulation. *Mol. Biotechnol.* **2023**, 1–20. [CrossRef] [PubMed]
5. Li, P.; Seneviratne, C.J.; Alpi, E.; Vizcaino, J.A.; Jin, L. Delicate Metabolic Control and Coordinated Stress Response Critically Determine Antifungal Tolerance of *Candida albicans* Biofilm Persisters. *Antimicrob. Agents Chemother.* **2015**, *59*, 6101–6112. [CrossRef] [PubMed]
6. Wainwright, J.; Hobbs, G.; Nakouti, I. Persister cells: Formation, resuscitation and combative therapies. *Arch. Microbiol.* **2021**, *203*, 5899–5906. [CrossRef] [PubMed]
7. Suchodolski, J.; Krasowska, A. Fructose Induces Fluconazole Resistance in *Candida albicans* through Activation of Mdr1 and Cdr1 Transporters. *Int. J. Mol. Sci.* **2021**, *22*, 2127. [CrossRef] [PubMed]
8. Lu, H.; Shrivastava, M.; Whiteway, M.; Jiang, Y. *Candida albicans* targets that potentially synergize with fluconazole. *Crit. Rev. Microbiol.* **2021**, *47*, 323–337. [CrossRef] [PubMed]

9. Galdiero, E.; de Alteriis, E.; De Natale, A.; D'Alterio, A.; Siciliano, A.; Guida, M.; Lombardi, L.; Falanga, A.; Galdiero, S. Eradication of *Candida albicans* persister cell biofilm by the membranotropic peptide gH625. *Sci. Rep.* **2020**, *10*, 5780. [CrossRef]
10. Blenkinsopp, S.A.; Khoury, A.E.; Costerton, J.W. Electrical enhancement of biocide efficacy against Pseudomonas aeruginosa biofilms. *Appl. Environ. Microbiol.* **1992**, *58*, 3770–3773. [CrossRef]
11. Torgomyan, H.; Trchounian, A. Bactericidal effects of low-intensity extremely high frequency electromagnetic field: An overview with phenomenon, mechanisms, targets and consequences. *Crit. Rev. Microbiol.* **2013**, *39*, 102–111. [CrossRef] [PubMed]
12. Sultana, S.T.; Babauta, J.T.; Beyenal, H. Electrochemical biofilm control: A review. *Biofouling* **2015**, *31*, 745–758. [CrossRef] [PubMed]
13. Annamalai, S.; Futalan, C.C.; Ahn, Y. Electrochemical Disinfection of Simulated Ballast Water Using RuO(2)-TiO(2)/Ti Electrode. *Int. J. Environ. Res. Public Health* **2022**, *19*, 1835. [CrossRef] [PubMed]
14. Zou, P.; Li, P.; Liu, J.; Cao, P.; Luan, Q. Direct current exerts electricidal and bioelectric effects on *Porphyromonas gingivalis* biofilms partially via promoting oxidative stress and antibiotic transport. *J. Microbiol.* **2021**, *60*, 70–78. [CrossRef] [PubMed]
15. Zou, P.; Wang, Y.; Cao, P.; Li, P.; Liu, J.; Luan, Q. Weak direct current exerts synergistic effect with antibiotics and reduces the antibiotic resistance: An in vitro subgingival plaque biofilm model. *J. Periodontal Res.* **2023**, *58*, 143–154. [CrossRef] [PubMed]
16. Dusane, D.H.; Lochab, V.; Jones, T.; Peters, C.W.; Sindeldecker, D.; Das, A.; Roy, S.; Sen, C.K.; Subramaniam, V.V.; Wozniak, D.J.; et al. Electroceutical Treatment of *Pseudomonas Aeruginosa* Biofilms. *Sci. Rep.* **2019**, *9*, 2008. [CrossRef] [PubMed]
17. Parry-Nweye, E.; Onukwugha, N.E.; Balmuri, S.R.; Shane, J.L.; Kim, D.; Koo, H.; Niepa, T.H.R. Electrochemical Strategy for Eradicating Fluconazole-Tolerant *Candida albicans* Using Implantable Titanium. *ACS Appl. Mater. Interfaces* **2019**, *11*, 40997–41008. [CrossRef] [PubMed]
18. Prasad, D.; Sharma, A.K.; Sharma, H.C. Electric shock and human body. *Int. J. Electr. Power Eng.* **2010**, *4*, 177–181. [CrossRef]
19. Li, P.; Seneviratne, C.J.; Luan, Q.; Jin, L. Proteomic Analysis of Caspofungin-Induced Responses in Planktonic Cells and Biofilms of Candida Albicans. *Front. Microbiol.* **2021**, *12*, 639123. [CrossRef]
20. Humphries, R.; Bobenchik, A.M.; Hindler, J.A.; Schuetz, A.N. Overview of Changes to the Clinical and Laboratory Standards Institute *Performance Standards for Antimicrobial Susceptibility Testing*, M100, 31st Edition. *J. Clin. Microbiol.* **2021**, *59*, e0021321. [CrossRef]
21. Dubey, V.; Gupta, R.; Pathania, R. Targeting Superoxide dismutase confers enhanced Reactive Oxygen Species mediated eradication of Polymyxin B induced Acinetobacter baumannii persisters. *Antimicrob. Agents Chemother.* **2023**, *65*, 10–1128. [CrossRef] [PubMed]
22. Ling, S.; He, Y.; Li, X.; Hu, M.; Ma, Y.; Li, Y.; Lu, Z.; Shen, S.; Kong, B.; Zou, X.; et al. CircRHOT1 mediated cell proliferation, apoptosis and invasion of pancreatic cancer cells by sponging miR-125a-3p. *J. Cell. Mol. Med.* **2020**, *24*, 9881–9889. [CrossRef] [PubMed]
23. Zhao, S.; Gong, J.; Wang, Y.; Heng, N.; Wang, H.; Hu, Z.; Wang, H.; Zhang, H.; Zhu, H. Sirtuin 3 regulation: A target to alleviate β-hydroxybutyric acid-induced mitochondrial dysfunction in bovine granulosa cells. *J. Anim. Sci. Biotechnol.* **2023**, *14*, 18. [CrossRef] [PubMed]
24. Wu, Z.; Wu, Q.F.; Yuan, W.L.; Chen, Y.H.; Hu, D.; Deng, D.Y.; Zhang, L.L.; Niu, X.M. Arthrocolins Synergizing with Fluconazole Inhibit Fluconazole-Resistant *Candida albicans* by Increasing Riboflavin Metabolism and Causing Mitochondrial Dysfunction and Autophagy. *Microbiol. Spectr.* **2023**, *11*, e0405122. [CrossRef] [PubMed]
25. Kong, Y.; Wang, G.; Tang, H.; Yang, J.; Yang, Y.; Wang, J.; Li, G.; Li, Y.; Yuan, J. Multi-omics analysis provides insight into the phytotoxicity of chicken manure and cornstalk on seed germination. *Sci. Total Environ.* **2023**, *861*, 160611. [CrossRef] [PubMed]
26. Gao, Y.; Jian, L.; Lu, W.; Xue, Y.; Machaty, Z.; Luo, H. Vitamin E can promote spermatogenesis by regulating the expression of proteins associated with the plasma membranes and protamine biosynthesis. *Gene* **2021**, *773*, 145364. [CrossRef] [PubMed]
27. Lu, M.; Yan, H.; Yu, C.; Yuan, L.; Sun, S. Proton pump inhibitors act synergistically with fluconazole against resistant Candida albicans. *Sci. Rep.* **2020**, *10*, 498. [CrossRef]
28. Atriwal, T.; Chawla, M.; Hussain, A.; Alajmi, M.F.; Abid, M. Reactive oxygen mediated apoptosis as a therapeutic approach against opportunistic Candida albicans. *Adv. Protein Chem. Struct. Biol.* **2021**, *125*, 25–49. [PubMed]
29. Broxton, C.N.; He, B.; Bruno, V.M.; Culotta, V.C. A role for *Candida albicans* superoxide dismutase enzymes in glucose signaling. *Biochem. Biophys. Res. Commun.* **2018**, *495*, 814–820. [CrossRef]
30. Demirci-Çekiç, S.; Özkan, G.; Avan, A.N.; Uzunboy, S.; Çapanoğlu, E.; Apak, R. Biomarkers of Oxidative Stress and Antioxidant Defense. *J. Pharm. Biomed. Anal.* **2022**, *209*, 114477. [CrossRef]
31. Niepa, T.H.R.; Snepenger, L.M.; Wang, H.; Sivan, S.; Gilbert, J.L.; Jones, M.B.; Ren, D. Sensitizing Pseudomonas aeruginosa to antibiotics by electrochemical disruption of membrane functions. *Biomaterials* **2016**, *74*, 267–279. [CrossRef] [PubMed]
32. Sultana, S.T.; Call, D.R.; Beyenal, H. Eradication of Pseudomonas aeruginosa biofilms and persister cells using an electrochemical scaffold and enhanced antibiotic susceptibility. *NPJ Biofilms Microbiomes* **2016**, *2*, 2. [CrossRef] [PubMed]
33. Wildeman, A.S.; Patel, N.K.; Cormack, B.P.; Culotta, V.C. The role of manganese in morphogenesis and pathogenesis of the opportunistic fungal pathogen *Candida albicans*. *PLoS Pathog.* **2023**, *19*, e1011478. [CrossRef] [PubMed]
34. Kim, J.H.; Mahoney, N.; Chan, K.L.; Molyneux, R.J.; May, G.S.; Campbell, B.C. Chemosensitization of fungal pathogens to antimicrobial agents using benzo analogs. *FEMS Microbiol. Lett.* **2008**, *281*, 64–72. [CrossRef]
35. Zare-Bidaki, M.; Maleki, A.; Ghanbarzadeh, N.; Nikoomanesh, F. Expression pattern of drug-resistance genes ERG11 and TAC1 in *Candida albicans* Clinical isolates. *Mol. Biol. Rep.* **2022**, *49*, 11625–11633. [CrossRef]

Disclaimer/Publisher's Note: The statements, opinions and data contained in all publications are solely those of the individual author(s) and contributor(s) and not of MDPI and/or the editor(s). MDPI and/or the editor(s) disclaim responsibility for any injury to people or property resulting from any ideas, methods, instructions or products referred to in the content.

antibiotics

MDPI

Article

Anti-*Staphylococcus aureus* Activity of Volatile Phytochemicals and Their Combinations with Conventional Antibiotics Against Methicillin-Susceptible *S. aureus* (MSSA) and Methicillin-Resistant *S. aureus* (MRSA) Strains

Isidora Nikolic, Verica Aleksic Sabo, Damir Gavric and Petar Knezevic *

Department of Biology and Ecology, Faculty of Sciences, University of Novi Sad, Trg Dositeja Obradovica 3, 21000 Novi Sad, Serbia; isidoran@dbe.uns.ac.rs (I.N.); verica.aleksic@dbe.uns.ac.rs (V.A.S.); damir.gavric@dbe.uns.ac.rs (D.G.)

* Correspondence: petar.knezevic@dbe.uns.ac.rs; Tel.: +381-21-485-2685

Abstract: Background: MSSA and MRSA strains are challenging human pathogens that can develop resistance to antibiotics, highlighting the need for alternative antimicrobial agents. Plant metabolites, particularly volatile phytochemicals, may offer promising antimicrobial properties. The aim was to evaluate the antimicrobial and antibiofilm efficacy of various commercial volatile phytochemicals from the terpene and terpenoid groups against reference MSSA and MRSA strains, focusing on synergistic effects in both binary combinations and combinations with antibiotics. Methods: The microdilution method was used to determine the minimum inhibitory concentrations (MICs) for antibiotics and phytochemicals. The checkerboard method assessed synergistic interactions between phytochemicals and between phytochemicals and antibiotics, while the time-kill method was used to confirm these results. Biofilm quantification was performed using the microtiter plate method to evaluate the effects of phytochemicals, antibiotics, and their binary combinations on the eradication of 48-h-old biofilms. Results: Carvacrol and thymol demonstrated the strongest anti-staphylococcal activity, while other terpene compounds showed weaker effects. In binary combinations, carvacrol and thymol exhibited synergy against one MSSA strain (FICI = 0.50) and with tetracycline and chloramphenicol (FICI = 0.28–0.50). Synergy was also noted with streptomycin sulfate against one MRSA strain (FICI = 0.31–0.50) and with other antibiotics, including gentamicin (FICI = 0.25–0.50) and oxacillin (FICI = 0.44). Additionally, effective combinations achieved over 50% biofilm removal at both minimum inhibitory and sub-inhibitory concentrations. Conclusions: Results showed that synergy varies based on strain sensitivity to chemical agents, highlighting their potential for personalized therapy. Despite the difficulty in removing preformed biofilms, the findings highlight the importance of combined treatments to enhance antibiotic effectiveness.

Keywords: antibiotics; biofilm; carvacrol; *S. aureus*; synergism; thymol

1. Introduction

Staphylococcus aureus is a Gram-positive coccoid bacterium commonly found on the skin and in the nasal mucosa of approximately 25–30% of asymptomatic individuals, as well as in other mucous membranes of humans and warm-blooded animals. These sites serve as a key reservoir for staphylococcal infections [1]. While it can cause mild skin infections and food poisoning, it is also responsible for serious nosocomial infections [2,3]. As a significant human pathogen, *S. aureus* has developed various resistance mechanisms and virulence factors, particularly through frequent antibiotic treatment. Notable resistance mechanisms include enzymatic inactivation (e.g., beta-lactamase), decreased affinity for target components (e.g., PBP2a protein in methicillin-resistant (MRSA) strains, d-Ala-d-Lac peptidoglycan precursor in vancomycin-resistant (VRSA) strains), alteration of cell

membrane permeability for antibiotics, efflux pumps, and the production of biofilms [4,5]. The emergence of MRSA and VRSA strains presents a major challenge in the treatment of staphylococcal infections, particularly due to their ability to form biofilms [6].

The biofilm itself represents the aggregation of bacterial cells adhered to different biotic or abiotic surfaces and embedded in an extracellular matrix made of polysaccharides, proteins, extracellular DNA, and other molecules. Biofilms contribute to a wide range of infections and are a significant barrier to treatment because they protect the bacterial community from the immune system and the antibiotics themselves [7]. Resistance of biofilms occurs due to spontaneous mutation, which is not uncommon in staphylococci either [8]. Additionally, agents may be neutralized, and decreased permeability due to the biofilm matrix can facilitate the transfer of plasmids through conjugation and transformation, promoting the horizontal exchange of resistance genes [9]. Biofilms formed by staphylococci exhibit antibiotic resistance that is 1000 times greater than that of planktonic cells [10]. This makes biofilm an important factor in antimicrobial resistance and difficult-to-treat nosocomial infections.

In the absence of adequate chemotherapeutics, attention is drawn to new antimicrobial agents, including plant metabolites. Most studies have focused on determining the antibacterial activity of essential oils, which are a mixture of volatile, lipophilic, and aromatic substances originating from secondary plant metabolites [11]. The composition of essential oils is highly diverse and can vary significantly depending on factors such as the extraction method, plant age, genetics, environmental conditions, geographical climate, and harvest time [12,13]. Because of this variability, the antimicrobial activity of essential oils can also differ, making it challenging to identify which specific compounds are responsible for their effects. Most bioactive compounds in essential oils are terpenes and terpenoids, which show a diverse range of biological activities, including antimicrobial, anticancer, antiparasitic, neuroprotective, phytotoxic, anti-inflammatory, antioxidant, and antiallergic effects [14,15]. When these compounds are isolated as pure substances, it becomes easier to monitor and study their biological activities.

Carvacrol and thymol, the prominent and extensively studied terpenoids found in the essential oils of oregano and thyme [16], exhibit significant anti-staphylococcal activity [16–23]. These compounds inhibit bacterial growth by disrupting cell membrane integrity, leading to increased permeability and cell lysis [24,25]. They also interfere with bacterial metabolism by inhibiting key enzymes and modulating virulence-related gene expression [25,26]. Notably, carvacrol acts as an efflux pump inhibitor in both MSSA and MRSA strains, enhancing its efficacy against resistant strains [27–29]. Additionally, both compounds effectively inhibit biofilm formation and disrupt established biofilms [30–35], thereby improving treatment outcomes, as biofilms are critical for the persistence and the pathogenicity of *S. aureus*.

Given that bioactive compounds exhibit promising anti-staphylococcal effects while the efficacy of antibiotics declines, combining antibiotics with phytochemicals such as carvacrol and thymol offers a potential strategy to enhance their antimicrobial activity [22,27,36–38]. However, there is insufficient information about the synergistic effects between these compounds and certain antibiotics. In this study, we aimed to investigate the anti-staphylococcal activity of ten volatile phytochemicals to identify those suitable for combination with antibiotics. The time-dependent effects of these combinations on bacterial growth kinetics were analyzed to predict how synergistic combinations could be utilized in future clinical trials. Additionally, we examined the anti-biofilm activity of confirmed synergistic combinations of phytochemicals and antibiotics on planktonic cells and preformed staphylococcal biofilms, which are also of clinical importance.

2. Results

2.1. Anti-S. aureus Activity of Conventional Antibiotics and Volatile Phytochemicals Alone

The antibacterial activity of the selected volatile phytochemicals was detected for six out of ten tested strains (Table 1). Among the phytochemicals, carvacrol (CAR) had

the best activity, with MIC values ranging from 128.0 to 203.2 μg mL^{-1} for MSSA and from 362.0 to 1024.0 μg mL^{-1} for MRSA. Thymol (THY) expressed slightly higher MICs compared to CAR for MSSA (256.0–724.01 μg mL^{-1}) and for MRSA (512.0 ≥ 2048 μg mL^{-1}). Compound (−)-terpinene-4-ol exhibited no activity against MRSA strains and weak activity against MSSA (1722.2–2048.0 μg mL^{-1}). The terpene compounds, 3-carene and sabinene, showed activity against MRSA strains at higher concentrations (1024.0 ≥ 2048.0 μg mL^{-1} and ≥2048.0 ≥ 2048 μg mL^{-1}, respectively). Also, 3-carene was active against one MSSA strain (1625.5 μg mL^{-1}), while sabinene exhibited activity against three MSSA strains (2048.0 μg mL^{-1}). Other compounds from terpene class—(R)-(+)-limonene, α-terpinene, γ-terpinene, and terpinolene—did not exhibit antimicrobial activity against any of the used *S. aureus* strains, even at the highest examined concentration (2048.0 μg mL^{-1}), while only α-pinene expressed weak activity against MSSA strains (≥2048.0 μg mL^{-1}) and one MRSA strain (2048.0 μg mL^{-1}).

2.2. Binary Combinations of Phytochemicals and Combinations with Conventional Antibiotics

2.2.1. Synergistic Combinations Determined by the Checkerboard Method

CAR and THY were used to characterize interactions between binary combinations or combinations with conventional antibiotics. Out of 28 examined binary combinations, 57.1% were characterized as synergistic (FICI ≤ 0.50). The combination of CAR and THY showed a synergistic effect against MSSA strain ATCC 6538 (FICI = 0.50) (Figure 1).

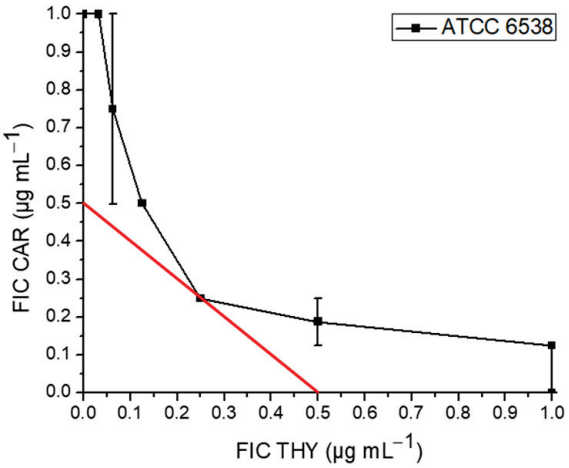

Figure 1. Effect of carvacrol (CAR) and thymol (THY) binary combination.

A synergistic effect was also observed for CAR or THY in combination with TET against MSSA strain ATCC 11632 (FICI = 0.28 and FICI = 0.38, respectively) (Figure 2A,B). Similarly, CHL also showed a synergistic effect in combination with these phytochemicals against MSSA strain ATCC 6538 (FICI = 0.50; Figure 2C,D).

Against MRSA strain ATCC 43300, synergy was observed only for the combination of CAR (FICI = 0.31; Figure 3A) or THY (FICI = 0.50; Figure 3B) with STR. Sinergy was also observed for MRSA strains ATCC 700699, ATCC 700698, ATCC BAA-1708, and ATCC BAA-2312 between CAR and STR (FICI = 0.50; FICI = 0.26, FICI = 0.32, and FICI = 0.26, respectively) (Figure 3D,E,J,K). Additionally, the combination of CAR and GEN showed synergy against MRSA strains ATCC BAA-1708, ATCC BAA-2312, and NCTC 12493 (FICI = 0.44, FICI = 0.50, and FICI = 0.25, respectively) (Figure 3C,F,H). Antibiotics CIP and OXC in combination with CAR also showed synergistic activity against MRSA strain NCTC 12493 (FICI = 0.38 and FICI = 0.44, respectively; Figure 3G,I).

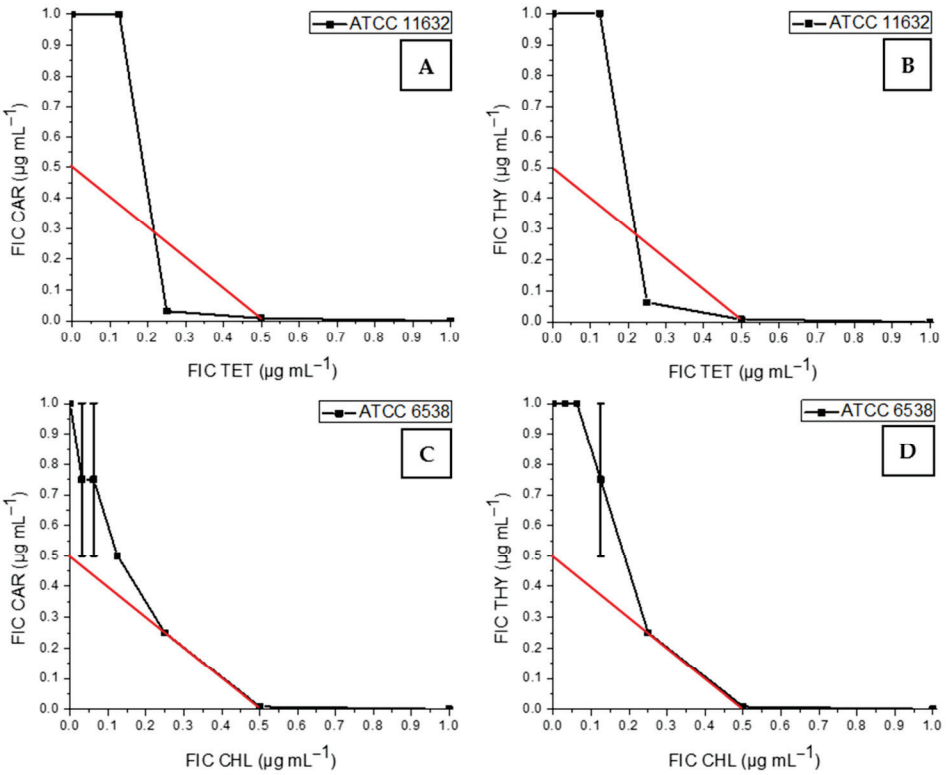

Figure 2. Synergistic effects of volatile phytochemicals and antibiotics against MSSA ATCC 11632 (**A**,**B**) and MSSA ATCC 6538 (**C**,**D**). CAR—carvacrol, THYthymol, TET—tetracycline, CHL—chloramphenicol.

2.2.2. Growth Inhibition Kinetics of Synergistic Binary Combinations

In order to further characterize the obtained synergistic interactions, the kinetic growth inhibition of staphylococcal strains over a period of time was determined using the time-kill method. Out of 16 tested binary combinations characterized as synergistic by the checkerboard method, 9 were confirmed by the time-kill method (56.30%).

For MSSA strain ATCC 11632, the CAR + TET combination maximally reduced the bacterial count by 0.50 log after 12 h compared to the initial count and by 0.85 log relative to the final count. Synergism was observed at 9, 12, and 15 h, with reductions of 1.70–2.40 log. However, after 24 h, there was no synergism (0.70 log reduction) (Figure 4A). The TYM + TET combination decreased the count by 0.30 log at 9 h and 1.00 log at 24 h, with similar transient synergisms (2.00–2.20 log) (Figure 4B). Although the combination of CAR or THY with CHL showed borderline synergism against MSSA (FICI = 0.50), the growth kinetics indicated a more additive to indifferent effect. After 24 h, bacterial counts increased by 2.60 log and 2.30 log for CAR + CHL and THY + CHL, respectively (Figure 4C,D).

For MRSA strain ATCC 43300, the CAR + STR combination reduced the bacterial count by 2.40 log after 15 h compared to the initial count, and by 4.70 log at 24 h compared to the final count. Synergism was observed from 12 to 24 h (2.10–4.10 log) (Figure 4E). The TYM + STR combination decreased the count by 2.00 log after 15 h, showing synergism at 12 and 15 h (3.20–3.90 log), but this was not maintained after 24 h (0.40 log reduction) (Figure 4F).

Significant synergism for combination CAR + GEN against MRSA strain ATCC BAA-1708 was observed, reducing the bacterial count by 2.50 log after 6 h and 7.30 log at 24 h (Figure 4G). In contrast, the CAR + STR combination did not show synergism against the same strain, with only a 0.50 log reduction after 9 h (Figure 4H).

Table 1. Geometric mean of minimum inhibitory concentration (MIC) of essential-oil-derived active compounds and antibiotics on *S. aureus* reference strains.

			MIC (μg mL^{-1})									
			MSSA					MRSA				
	Chemical Class	**Density (g mL^{-1})**	**ATCC 11632**	**ATCC 6538**	**ATCC 25923**	**ATCC 43300**	**ATCC 33591**	**ATCC BAA-1708**	**ATCC BAA-2312**	**ATCC 700699**	**ATCC 700698**	**NCTC 12493**
α-pinene	Terpene	0.0858	≥2048.0	≥2048.0	≥2048.0	>2048.0	>2048.0	>2048.0	>2048.0	>2048.0	>2048.0	2048
(R)-(+)-limonene		0.842	>2048.0	>2048.0	>2048.0	>2048.0	>2048.0	>2048.0	>2048.0	>2048.0	>2048.0	>2048.0
sabinene		0.842	2048.0	2048.0	2048.0	≥2048.0	≥2048.0	>2048.0	>2048.0	>2048.0	>2048.0	>2048.0
3-carene		0.857	1625.5	>2048.0	>2048.0	2048.0	1024.0	>2048.0	>2048.0	>2048.0	>2048.0	>2048.0
α-terpinene		0.837	>2048.0	>2048.0	>2048.0	>2048.0	>2048.0	>2048.0	>2048.0	>2048.0	>2048.0	>2048.0
γ-terpinene		0.850	>2048.0	>2048.0	>2048.0	>2048.0	>2048.0	>2048.0	>2048.0	>2048.0	>2048.0	>2048.0
terpinolene		0.861	>2048.0	>2048.0	>2048.0	>2048.0	>2048.0	>2048.0	>2048.0	>2048.0	>2048.0	>2048.0
(−)-terpinene-4-ol	Terpenoid	0.934	1722.2	2048.0	2048.0	>2048.0	>2048.0	>2048.0	>2048.0	>2048.0	>2048.0	>2048.0
thymol		0.965	256.0	512.0	724.1	512.0	512.0	>2048.0	>2048.0	2048	>2048.0	2048
carvacrol		0.976	128.0	203.2	181.0	430.0	362.0	861.1	1024.0	861.1	724.1	724.1
CAZ	Antibiotics [1]	-	16.0	8.0	32.0	≥64.0	>64.0	>64.0	>64.0	>64.0	>64.0	>64.0
CTX		-	8.0	>64.0	4.0	32.0	>64.0	32.0	32.0	>64.0	>64.0	>64.0
STR		-	8.0	2.0	4.0	4.0	>64.0	16.0	8.0	8.0	8.0	>64.0
CHL		-	16	8.0	16.0	8.0	64.0	16.0	8.0	4.0	8.0	8.0
TET		-	2	<0.5	0.5	1.0	>64.0	1.0	1.0	64.0	64.0	>64.0
AMC		-	1	<0.5	0.5	32.0	>64.0	>64.0	32.0	>64.0	>64.0	>64.0
GEN		-	<0.5	<0.5	<0.5	64.0	8.0	1.0	1.0	>64.0	>64.0	1.0
CIP		-	<0.5	<0.5	<0.5	0.5	0.5	64.0	<0.5	16.0	16.0	1.0
OXC		-	<0.5	<0.5	<0.5	4.0	4.0	2.0	1.0	>64.0	>64.0	32.0
VAN		-	2.0	2.0	2.0	2.0	2.0	1.0	1.0	8.0	2.0	1.0

[1] CAZ—ceftazidime, CTX—ceftriaxone, STR—streptomycin sulfate, CHL—chloramphenicol, TET—tetracycline, AMC—amoxicillin clavulanic acid, GEN—gentamicin, CIP—ciprofloxacin, OXC—oxacillin, and VAN—vancomycin.

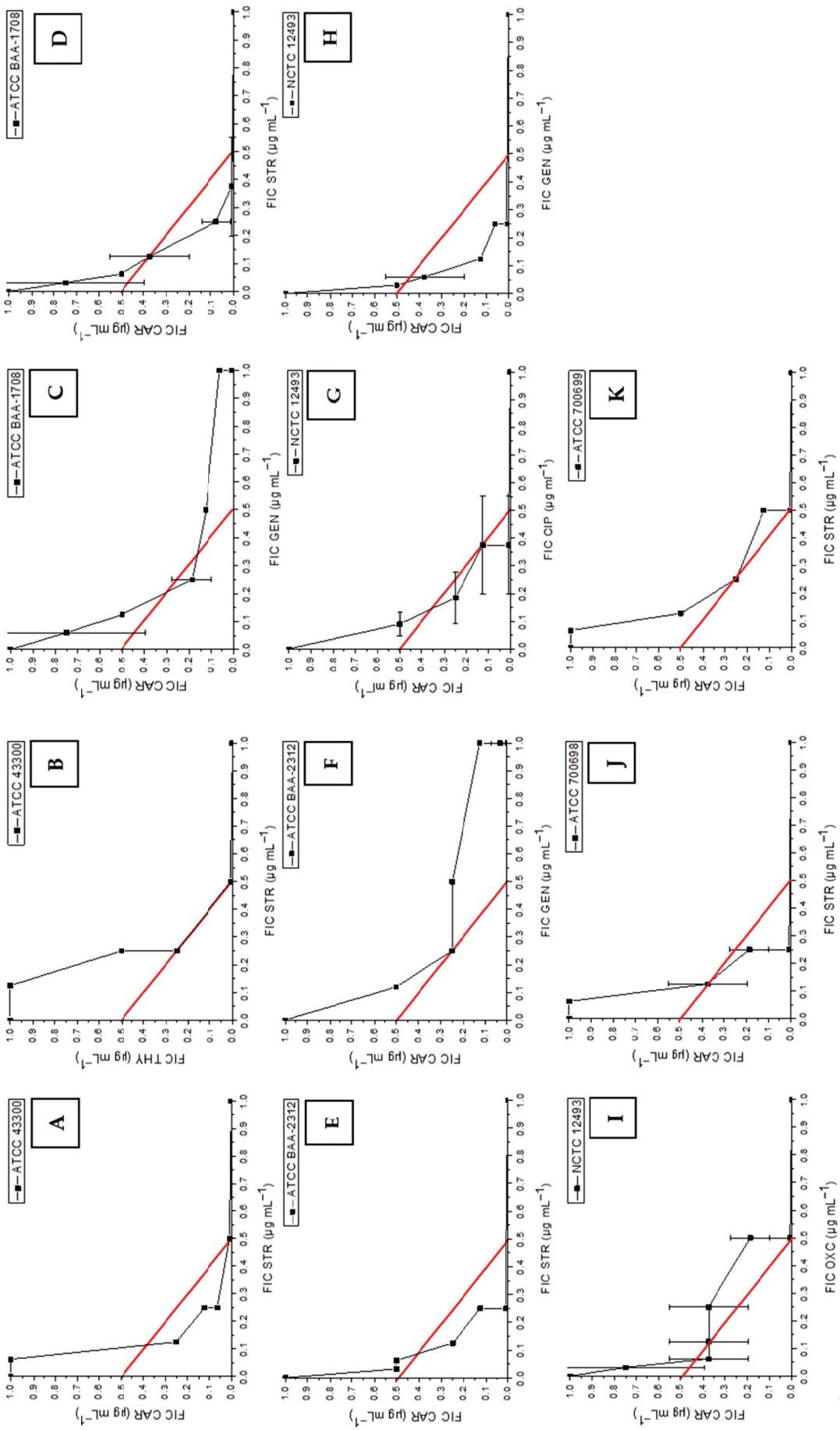

Figure 3. Synergistic effects of volatile phytochemicals and antibiotics against MRSA ATCC 43300 (**A**,**B**), ATCC BAA-1708 (**C**,**D**), ATCC BAA-2312 (**E**,**F**), ATCC 700699 (**K**), ATCC 700698 (**J**), and NCTC 12493 (**G**–**I**): CAR—carvacrol, THY—thymol, GEN—gentamicin, STR—streptomycin sulfate, CIP—ciprofloxacin, OXC—oxacillin.

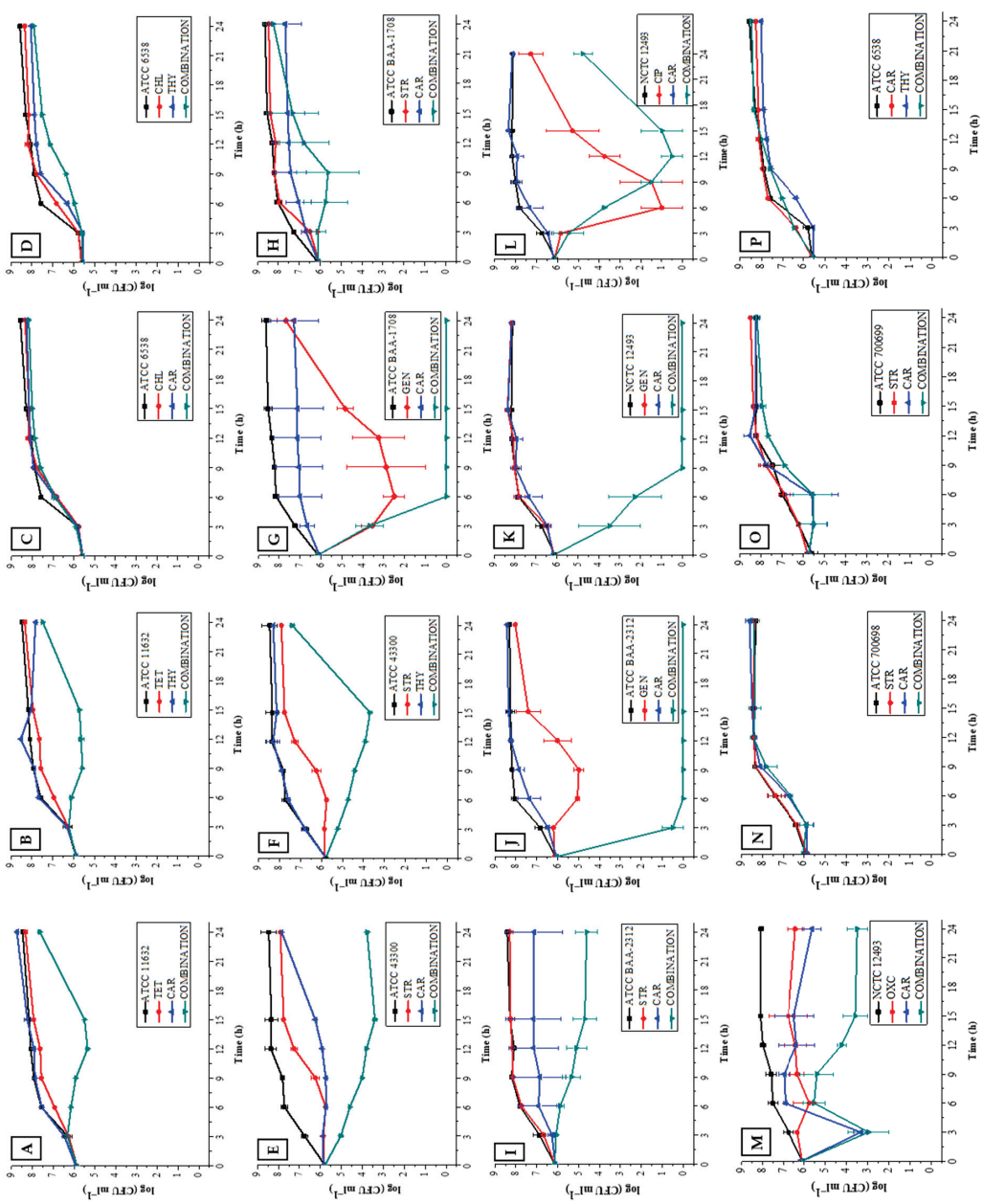

Figure 4. Time-kill assay for carvacrol and thymol in combination with antibiotics against MRSA ATCC 43300 (**E**,**F**), MRSA BAA-1708 (**G**,**H**), MRSA BAA-2312 (**I**,**J**), MRSA NCTC 12493 (**K**–**M**), MRSA ATCC 700698 (**N**), MRSA ATCC 700699 (**O**), MSSA 11632 (**A**,**B**), and MSSA ATCC 6538 (**C**,**D**), and in binary combination against MSSA ATCC 6538 (**P**). CAR—carvacrol, THY—thymol, TET—tetracycline, STR—streptomycin sulfate, CHL—chloramphenicol, GEN—gentamicin, CIP—ciprofloxacin, OXC—oxacillin.

For MRSA strain ATCC BAA-2312, the CAR + STR combination exhibited synergism, with reductions of 2.00–2.50 log from 12 to 24 h (Figure 4I). The CAR + GEN combination demonstrated a bacterial reduction of 6.10 log after 6 h, reaching 8.30 log after 24 h. This combination was most promising because synergism was detected after only 3 h of incubation, reducing the bacterial count by 6.30 log (Figure 4J).

The CAR + GEN combination on MRSA strain NCTC 12493 reduced bacteria by 2.60 log after 3 h and became undetectable after 9 h, exceeding 8.20 log by the end of incubation (Figure 4K). Against the same strain, the combination of CAR + CIP had the greatest reduction after 12 h of 5.60 log compared to the initial count. The synergism started after 12 h, with a 3.20 log reduction and 2.51 log after 24 h (Figure 4L). Similar to GEN + CAR, the OXC + CAR combination decreased the bacterial number by 3.10 log after 3 h compared to the initial number and the synergism started at 12 h, with a consistent reduction of 2.14 log after 24 h (Figure 4M).

No synergism was confirmed for CAR + STR against MRSA strains ATCC 700698 and ATCC 700699 (Figure 4N,O) or for CAR + THY against MSSA strain ATCC 6538 (Figure 4P). Increases in bacterial counts were noted for ATCC 700698 (0.10 log) and minimal reductions were noted for ATCC 700699 (0.05 log) and ATCC 6538 (0.11 log) after 24 h.

2.3. Biofilm Quantification

To evaluate the effects of antibiotics and essential oil compounds, both individually and in combination, it was necessary to examine the ability of biofilm formation. Based on the obtained results, the majority of strains produced biofilm better after 48 h, and the production was stronger in the presence of glucose (Table 2). Strains that expressed moderate to strong biofilm-forming ability under all experimental conditions were MSSA strain ATCC 6538 and MRSA strain ATCC BAA-2312, while MSSA strain ATCC 11632 did not form biofilm during the experiment.

Table 2. Quantification of biofilm.

Strains	MHB		MHB + 1% Glucose	
	Incubation Period (h)			
	24	48	24	48
ATCC 11632	nonadherent	nonadherent	nonadherent	nonadherent
ATCC 6538	strongly	strongly	strongly	strongly
ATCC 25923	nonadherent	nonadherent	strongly	strongly
ATCC 43300	nonadherent	nonadherent	weakly	moderately
ATCC 33591	nonadherent	nonadherent	weakly	nonadherent
ATCC BAA−1708	weakly	weakly	strongly	strongly
ATCC BAA−2312	moderately	moderately	strongly	strongly
ATCC 700699	weakly	nonadherent	weakly	moderately
ATCC 700698	weakly	nonadherent	nonadherent	weakly
NCTC 12493	weakly	moderately	strongly	strongly

2.3.1. Biofilm Eradication Activity of Antibiotics and Phytochemicals Alone

Strains MSSA ATCC 6538 and MRSA ATCC BAA-2312, characterized as strong biofilm producers, were selected for the experiment to emphasize the effectiveness of the compound on established biofilms. The biofilm eradication ability of the antibiotics and phytochemicals against MSSA strain ATCC 6538 was good when CHL or CAR was applied at MICs, removing 51.6 and 56.5% of the biofilm, respectively. Other antibiotics and THY were active against the same strain at super MICs (Table 3). The best planktonic cell removal activity was achieved by CAR at an MIC of 89.8%, so the PEC value was the same as the MIC value of CAR. Except for CAR, THY at 2 × MIC (PEC) removed 54.6% of planktonic cells, whereas CHL and other antibiotics showed no activity against planktonic cells.

Table 3. Biofilm eradication effect of antibiotics and phytochemicals alone.

Agent	Type of Effect	*S. aureus* Strains							
		MSSA ATCC 6538				MRSA ATCC BAA−2312			
		MIC	2 × MIC	4 × MIC	PEC (μg mL^{-1}) [3]	MIC	2 × MIC	4 × MIC	PEC (μg mL^{-1})
CAZ	I [1]	28.5	59.8	70.6	>32.0				
	II [2]	0.0	0.0	0.0					
CHL	I	51.6	56.6	60.3	>32.0	94.0	96.0	97.6	8.0
	II	0.0	0.0	0.0		65.0	53.5	74.3	
STR	I	34.8	39.4	64.9	>8.0	46.8	47.7	61.8	≤8.0
	II	0.0	0.0	0.0		47.0	30.4	0.0	
VAN	I	49.3	50.3	51.0	>16.0	23.2	96.6	98.4	2.0
	II	0.0	0.0	0.0		32.0	72.0	74.3	
CAR	I	56.5	41.6	22.6	256.0	44.2	88.5	89.6	2048.0
	II	89.8	95.4	95.6		32.6	80.3	86.0	
TYM	I	40.3	47.0	48.2	1024.0				
	II	0.0	54.6	65.4					
CTX	I					89.7	90.8	84.5	32.0
	II					82.2	85.5	86.2	
TET	I					92.2	94.7	96.8	1.0
	II					54.0	58.0	51.0	
GEN	I					20.5	21.0	51.4	2.0
	II					32.3	50.5	19.2	
OXC	I					91.0	92.3	96.2	1.0
	II					71.1	70.8	73.3	

[1] I—Biofilm eradication (%); [2] II—Planktonic cell eradication (%); [3] PEC—Planktonic cell eradication concentration.

For MRSA strain ATCC BAA-2312 (Table 3), the best biofilm eradication activity was achieved using CTX, CHL, TET, and OXC (87.7%, 94.0%, 92.2%, and 91.0%, respectively) at the MIC, with PEC values matching the MICs (82.2, 65.0, 54.0, and 71.1%, respectively). Similar to the MSSA strain, other antibiotics required higher concentrations to remove the biofilm and planktonic cells of MRSA strain ATCC BAA-2312, as well as CAR.

2.3.2. Biofilm Eradication Activity of Antibiotics, and Phytochemicals in Combination

For the current study, binary combinations were tested based on the synergistic effects observed using the checkerboard method.

All three combinations—CHL + THY, CHL + CAR, and CAR + THY—expressed synergism because 1/4 × MIC combinations of both agents were sufficient for biofilm removal of MSSA ATCC 6538 (78.3, 79.3, and 74.6%, respectively). Also, the combination of CHL + THY led to a decrease in the concentrations required for the removal of planktonic cells (1/4 × MIC for both agents), while CAR in combination with CHL or THY led to a decrease in their PEC values (1/4 × MIC). The biofilm of MRSA strain ATCC BAA-2312 was more resistant to combinations of CAR with STR or GEN (Table 4). This study hypothesizes that CAR influences the ability of antibiotics to eradicate biofilms and remove planktonic cells at MICs compared to using antibiotics alone at their MICs. However, no synergistic effect was observed. Unlike the MSSA strain, increasing the concentrations of the combinations simultaneously increased the percentage of biofilm eradication and removal of planktonic cells of the MRSA strain, indicating the necessity of applying MICs and super MICs for these binary combinations.

Table 4. CAR + STR and CAR + GEN against biofilm formed by ATCC BAA-2312 and CHL + TYM, CHL + CAR, and CAR + TYM against biofilm formed by ATCC 6538.

MIC Combinations	CAR + STR		CAR + GEN		CHL + TYM		CHL + CAR		CAR + TYM	
	BR [1] (%)	PCR [2] (%)	BR (%)	PCR (%)	BR (%)	PCR (%)	BR (%)	PCR (%)	BR (%)	PCR (%)
4 × MIC	83.5	85.6	0.0	96.1	0.0	92.4	0.0	93.1	0.0	92.4
2 × MIC	87.1	85.3	34.7	96.6	0.0	94.8	47.0	90.2	0.0	94.8
MIC	87.6	76.3	38.3	90.7	52.1	89.3	44.0	89.4	52.1	89.3
1/2 × MIC	75.0	34.6	64.4	85.1	68.1	87.0	83.4	81.6	68.1	87.0
1/4 × MIC	31.0	24.1	78.3	56.2	74.6	44.7	79.3	83.9	74.6	44.7
PEC [3] (μg mL^{-1})	1024.0 + 8.0		1024.0 + 1.0		2.0 + 128.0		2.0 + 50.8		101.5 + 256.0	

[1] BR—Biofilm removal, [2] PCR—Planktonic cell removal, [3] PEC—Planktonic cell eradication concentration.

3. Discussion

3.1. Anti-S. aureus Activity of Volatile Phytochemicals

Staphylococcal antibiotic resistance is becoming an increasingly significant concern for human health, highlighting the need to explore alternative antimicrobial agents. Phytochemicals, natural compounds derived from plants, have emerged as promising solutions due to their diverse biological activities.

This study investigates the antimicrobial effects of specific phytochemicals, among which CAR and THY have shown significant activity against various MSSA and MRSA strains. Previous studies have reported comparable MICs for CAR against various strains, including ATCC 25923, ATCC 6538, and certain MRSA strains [17,18,30,39–41]. However, varying MIC values have been observed for MRSA strains ATCC 43300, ATCC 700698, and ATCC 33591 [17,19,42], as well as for MSSA strain ATCC 6538 [43].

For THY, similar results have been noted against ATCC MSSA and MRSA strains [17, 30,39,40,43], although some studies indicate lower MICs for MRSA strains ATCC 33591, ATCC 43300, and ATCC 700698 [19,41,42]. These discrepancies may arise from variations in the methods used for MIC determination.

Data on other reference strains examined in this study are limited in the literature. Terpinene-4-ol exhibited weaker activity compared to CAR and THY, consistent with findings from studies involving strains ATCC 25923, ATCC 6538, and ATCC 43300 [44–48]. Although terpinene-4-ol exhibits antimicrobial activity against *S. aureus* through mechanisms such as membrane disruption and enzymatic inhibition, its lower effectiveness compared to CAR or THY may be attributed to differences in chemical structure, hydrophobicity, stability, and mechanisms of action [46,49].

Higher concentrations of terpene compounds, such as 3-carene and sabinene, were required to inhibit MRSA strains, as confirmed for MRSA ATCC 43300 [42]. Also, the weak activity of other terpene compounds like (R)-(+)-limonene, α-terpinene, γ-terpinene, and terpinolene has been reported for ATCC MSSA and MRSA strains [39,40,42–44,47,50–54].

Based on the results obtained and the available literature, only CAR and THY, among the examined phytochemicals, demonstrate significant anti-staphylococcal activity. This may be attributed to the presence of functional groups in terpenoids, which generally enhance their antimicrobial efficacy against staphylococci compared to terpenes.

Additionally, CAR was effective against both MSSA and MRSA strains, indicating its potential as a single-agent treatment for staphylococcal infections. In contrast, THY's effectiveness was more limited, which may restrict its use for MRSA infections. While higher concentrations of both agents might be necessary, the potential toxicity of these concentrations should be tested. Considering that antibiotics can cause various side effects, combining them with these phytochemicals could provide mutual benefits by reducing the required concentrations of both agents and decreasing the emergence of resistance in bacteria.

3.2. Anti-S. aureus Activity of Antibiotics and Phytochemicals in Combination

3.2.1. Anti-*S. aureus* Activity of Combinations

Due to emerging staphylococcal resistance, combined therapy presents an effective strategy for enhancing antibiotic efficacy. This approach involves using antibiotics in combination with other agents, such as phytochemicals. Additionally, phytochemicals can also be combined to explore potential synergistic effects. Previous studies have reported a predominant additive effect for the combination of CAR and THY against various *S. aureus* strains [16,17,20,55]. However, some studies noted indifferent or even antagonistic effects against different strains [21,56]. These variations highlight that CAR–THY interactions depend on multiple factors, emphasizing the need for further characterization.

In contrast to our findings, Miladi et al. reported a two-fold decrease in TET concentration when combined with CAR or THY against MSSA strain 25923 [27], which we did not observe. Similar reductions in TET concentrations with these phytochemicals were noted for other *S. aureus* strains [28,36]. Discrepancies may be attributed to differences in methods, concentrations used in binary combinations, strain sensitivities, and unspecified methodological variations. For instance, borderline synergism was observed for CAR or THY combined with TET on MSSA strain ATCC 29213 (FICI = 0.53) and MRSA strain ATCC 43300 (FICI = 0.38) [57], contrasting with our results. Similar inconsistencies are noted with combinations of CAR or THY with GEN, where synergism was reported for MSSA ATCC 29213 (FICI = 0.25 and FICI = 0.19, respectively) and MRSA ATCC 43300 (FICI = 0.19 and FICI = 0.25, respectively).

Previous studies demonstrated that THY + GEN reduced the MIC of GEN by 16 times on ATCC 12624 [37], while the same combination's FICI was 0.38 on ATCC 9144 [22]. Our study uniquely identified significant effects of CAR + GEN and THY + GEN combinations against *S. aureus* strains. Additionally, we highlight substantial synergistic activity of CAR or THY with CIP, resulting in an eight-fold reduction in the MIC of CIP. This aligns with previous findings and supports reported additive interactions for THY + CIP combinations against MSSA ATCC 25923 and two MRSA strains [38,58].

Additionally, our results support the synergistic effect of CAR's combination with CIP against *Bacillus cereus* ATCC 11778 and *Escherichia coli* ATCC 11775 [59], while THY and VAN exhibited additive effects against MRSA ATCC BAA-1717 [31]. However, CAR or THY showed indifferent or antagonistic effects with methicillin and penicillin G against MRSA ATCC 43300 [60]. Since these antibiotics target cell wall synthesis, similarly to CAR and THY, synergism may not occur when they target the same sites in certain *S. aureus* strains.

To the best of our knowledge, no data exist on the effects of CAR combined with STR, or CAR or THY combined with CHL and OXC on *S. aureus* strains. Our results indicate a significant effect of these combinations. It is crucial to note that the diversity of results among researchers can be attributed to the lack of standardized methods for testing binary combinations. Adhering to established principles is essential for the reproducibility of experiments and the effective clinical application of phytochemicals.

3.2.2. Time Kinetics of Bacterial Growth Inhibition for Synergistic Interaction

While checkerboard assays provide a quick preliminary assessment, time-kill assays offer a more accurate representation of an antibiotic's effectiveness over time and help identify the time point at which synergism occurs. For instance, Aleksic Sabo et al. confirmed synergy between CAR or THY and CIP against multidrug-resistant *Acinetobacter baumannii* strains [61], highlighting the potential of these combinations against drug-resistant bacteria, while Gan et al. observed synergy for THY + STR and THY + GEN combinations against *S. aureus* ATCC 9144 [22].

Our time-kill assay results indicate that the most effective antibiotics in combination with CAR or THY against staphylococci were GEN, STR, and TET, while CIP and OXC exhibited slightly weaker activity. Notably, GEN, STR, and TET target the 30S subunit of the ribosome. The enhanced activity of these antibiotics, when combined with terpenoids

such as CAR and THY, which act on the bacterial cell membrane, suggests a potential mechanism where terpenoids facilitate the antibiotics' entry into the cytoplasm.

Future research should focus on elucidating the mechanisms underlying these synergistic interactions and evaluating the cytotoxicity of these combinations to ensure their safe application in clinical settings. Given that CAR and THY are food additives with low toxicity and are listed as Generally Recognized As Safe (GRAS) by the U.S. Food and Drug Administration (US FDA), they hold promise for both food and medical applications, provided safe dosages are established [62–65].

For effective therapy that combines antibiotics and phytochemicals, it is essential to consider resistance to both types of agents. Investigating potential cross-resistance is crucial, as understanding how *S. aureus* strains respond to each can inform treatment strategies, mitigate resistance risks, and enhance the effectiveness of combination therapy.

3.3. Biofilm Formation

The choice of growth medium is crucial for studying biofilm formation. While MHB is commonly used, other media such as Brain Heart Infusion Broth (BHIB) and Tryptic Soy Broth (TSB) can also be effective. The addition of glucose, particularly at a concentration of 1% in TSB, can promote and stabilize biofilm formation in MSSA and MRSA strains [66]. This may explain why the strains tested in our study formed better biofilms in the presence of glucose in MHB.

However, enhanced biofilm formation due to glucose poses significant risks in hospital settings, particularly for patients with diabetes. Waldrop et al. demonstrated that clinical isolates have been shown to develop strong biofilms at glucose concentrations commonly encountered in clinical practice [67]. It is speculated that biofilm growth may be induced by the lower pH resulting from glucose utilization by bacterial cells [67]. This situation can be particularly dangerous due to the reduced efficacy of antibiotics against these stronger biofilms, leading to recurrent infections, as biofilms are a source of infection and contribute to the spread of antibiotic resistance.

These findings highlight the diverse phenotypic and genotypic characteristics of each strain and species under varying conditions, which can affect biofilm development. This is consistent with Croes et al., who demonstrated that staphylococcal biofilm formation depends on clonal lineage and genetic background [68].

To account for these variations, different assays for biofilm quantification are necessary [16,18–22,27,28,31,36–38,41–65,69]. It is important to note that each step in the microtiter method is crucial for the success of the experiment [70]. Key factors include the substrate used for inoculation (along with the size of the bacterial inoculum) and the number of washes between biofilm formation, fixation, staining, and decolorization. The rinsing technique employed also plays a significant role.

While this method, like other in vitro approaches, may not accurately reflect biofilm formation under in vivo conditions, it can be instrumental in identifying new anti-biofilm solutions through the combined effects of different agents.

3.3.1. Biofilm Eradication Effects of Individual Agents

Staphylococcal biofilms present significant challenges in medicine, veterinary practices, and various industries, highlighting the urgent need to identify compounds capable of disrupting established biofilms resistant to antibiotics and disinfectants. The removal of mature biofilms is more challenging than inhibiting early-stage formation [18,30,32,55,71]. Using super MICs of CAR against MRSA strains and THY against MSSA strains resulted in higher biofilm removal rates. However, higher CAR concentrations decreased biofilm removal and increased planktonic cell removal of MSSA strains. This could be a defense mechanism that promotes biofilm formation to protect planktonic cells, which were barely present in the medium. Additionally, while higher concentrations of STR removed the biofilm, they decreased planktonic cell removal, suggesting that the biofilm was detached

while the cells were in the stationary phase, during which they were sufficiently resistant to the action of a super MIC of STR.

3.3.2. Biofilm Eradication Effects of Combinations

It is important to note that the sub-inhibitory concentrations, in almost all combinations of CAR with THY and antibiotics (1/2 and 1/4 × MIC), did not stimulate biofilm production, contrasting with typical effects seen with essential oils [72]. The CAR + THY combination showed potential against both monospecies and mixed biofilms [33], and according to our results on *S. aureus* monospecies, biofilms at super MICs. The choice and concentration of antibiotics are critical in addressing persisters within biofilms [73]. Certain antibiotics like CIP and GEN allow survival at sub-inhibitory levels, while others like VAN and OXC may enhance biofilm production [74].

A combination of antibiotics and phytochemicals may provide a synergistic approach to mitigate survivor cells, although many studies have yet to investigate the underlying mechanisms of this synergy. It is suggested that synergistic effects often arise from multi-target actions, where antibiotics primarily inhibit DNA or protein synthesis, while phytochemicals disrupt cell membranes [75]. Due to its hydrophobic nature, CAR interacts with the lipid bilayer, causing leakage of cellular components [23,76] and THY damages membranes by altering NADPH levels and increasing lipid peroxidation [24,77]. However, the mechanisms are likely more complex within biofilms. Our findings suggest that future strategies to combat biofilm formation may involve the use of synergistic combinations of natural products with antibiofilm properties. This approach could potentially provide more effective and targeted treatments for biofilm-related infections. However, researchers face significant challenges due to experimental variability and strain differences, underscoring the need for standardized terminology and methodologies in biofilm research [34,35,71,78].

4. Materials and Methods

4.1. Materials

4.1.1. Bacterial Strains and Culture Conditions

Three reference strains of MSSA (ATCC 11632, ATCC 25923, and ATCC 6538) and seven reference strains of MRSA (ATCC 43300, ATCC 33591, ATCC BAA-1708, ATCC BAA-2312, ATCC 700699, ATCC 700698, and NCTC 12493) from the American Type Culture Collection (Rockville, MD, USA) were used for the antimicrobial tests. Bacterial strains were stored in Luria Bertani broth (LBB) (HiMedia, Mumbai, India) with glycerol supplementation (10% v/v) at −70 °C.

4.1.2. Antimicrobial Agents

In total, ten commercially available volatile phytochemicals were examined: α-pinene, (R)-(+)-limonene, sabinene, 3-carene, α-teprinene, γ-terpinene, terpinolene, (-)-terpinene-4-ol, thymol, and carvacrol (Sigma-Aldrich, Steinheim, Germany), as well as ten conventional antibiotics: ceftazidime (CAZ) (PharmaSwiss, Beograd, Serbia), ceftriaxone (CTX) (Galenika, Zemun, Serbia), streptomycin sulfate (STR) (Sigma-Aldrich, Germany), chloramphenicol (CHL) (Sigma-Aldrich, Germany), tetracycline (TET) (Sigma-Aldrich, Germany), amoxicillin clavulanic acid (AMC) (Medochemie, Limassol, Cyprus), gentamicin (GEN) (Galenika, Serbia), ciprofloxacin (CIP) (Acros Organics, Geel, Belgium), oxacillin (OXC) (Sigma-Aldrich, Germany), and vancomycin (VAN) (Liophilchem, Roseto degli Abruzzi, Italy).

4.2. Anti-S. aureus Activity of Conventional Antibiotics and Volatile Phytochemicals Alone

Microdilution Method

In order to determine minimal inhibitory concentrations (MICs) of the tested antibiotics and phytochemicals, the microdilution susceptibility testing method was used [79], slightly modified for both types of compounds. Overnight cultures were grown on Müller Hinton

agar (MHA) for 24 h at 37 °C before MIC determination. Müller Hinton broth (MHB) was inoculated with the bacteria to obtain a final concentration of 2×10^6 CFU mL^{-1}.

Stock solutions of the tested antibiotics were prepared in sterile distilled water, while phytochemicals were dissolved in 100% dimethyl sulfoxide (DMSO), ensuring a final DMSO concentration of $\leq$0.8%. Phytochemicals were tested in two-fold serial dilutions ranging from 2048.0 to 16.0 μg mL^{-1}, and antibiotics were diluted from 64.0 to 0.5 μg mL^{-1}. After the addition of equal volumes of bacterial inoculum (1:1, *v*/*v*) into each well, the final bacterial count was approximately 1×10^6 CFU mL^{-1}. The microtiter plates were tightly sealed with parafilm and incubated for 24 h at 37 °C. MIC was visually determined as the lowest concentration of agent that inhibited bacterial growth, with final confirmation using triphenyltetrazolium chloride (TTC) (0.1% *w*/*v*) and optical density (OD) measurement at 540 nm.

Phytochemical concentrations were recalculated from μL mL^{-1} or percentage to μg mL^{-1} based on their densities (Table 1) to ensure comparability [80].

4.3. Anti-S. aureus Activity of Binary Combinations

4.3.1. Pre-Checkerboard Method and Checkerboard Method

The checkerboard method was used to determine interactions between antibiotics and phytochemicals, and binary combinations between different phytochemicals [80]. Before checkerboard testing, the potential synergistic interactions were examined by combining 1/4 × MIC of both agents (pre-checkerboard method). If bacterial growth was not observed for a combination, the checkerboard method was applied (Supplementary Materials Table S1).

Only antibiotics with MICs ranging from 1.0 to 64.0 μg mL^{-1} and phytochemicals with MICs from 128.0 to 1024.0 μg mL^{-1} were used in the pre-checkerboard and checkerboard methods. These ranges were selected to include concentrations that can be used in vivo and for clinical purposes. Antibiotics and phytochemicals were two-fold serially diluted in the checkerboard method, ranging from 1 × MIC to 1/32 × MIC and 1 × MIC to 1/128 × MIC, respectively.

The Fractional Inhibitory Concentration Index (FICI) [81] was calculated to assess the interaction type between agents:

$$\text{FICI} = \frac{\text{MIC of component A in mixture}}{\text{MIC of component A}} + \frac{\text{MIC of component B in mixture}}{\text{MIC of component B}}$$

4.3.2. Time-Kill Curve Method

The kinetics of bacterial growth inhibition for synergistic interaction, over a period of time, between volatile phytochemicals and antibiotics were performed using a slightly modified time-kill method [80,82]. Modifications were made during the setup of the experiment, which was conducted in parallel across four test tubes. The specific modifications were as follows: (I) bacterial count was 5×10^5 CFU mL^{-1}: MSSA strains (ATCC 11632, ATCC 6538) and MRSA strains (ATCC 43300, ATCC BAA-1708, ATCC BAA-2312, ATCC 700699, ATCC 700698, NCTC 12493); (II) sub-inhibitory antibiotic concentration and bacteria (1/4 × MIC): MSSA strains with TET or CHL and MRSA strains with STR, GEN, CIP, or OXC; (III) sub-inhibitory concentration of volatile phytochemical and antibiotics (1/4 × MIC): MSSA and MRSA strains with CAR or THY; and (IV) sub-inhibitory concentrations of antibiotics and volatile phytochemicals with bacteria (1/4 × MICs for both agents). After incubation periods of 0, 3, 6, 9, 12, 15, and 24 h at 37 °C, the bacterial counts (CFU mL^{-1}) were determined on MHA by the spreading plate method. A reduction in bacterial count of $\geq$2 log compared to a more effective agent administered alone was considered a synergistic interaction [83].

4.4. Biofilm Quantification Assay

The microtiter plate method described by [84] was used for biofilm quantification of three MSSA and seven MRSA strains. The test was performed using 24-h-old cultures. To compare biofilm production, bacterial suspensions were adjusted to a cell density of 2×10^6 CFU mL^{-1} in MHB and MHB supplemented with 1% glucose. Microtiter plates were incubated for 24 h and 48 h at 37 °C, and optical density (OD) was measured at 570 nm using a MultiscanGo microtiter plate reader (Thermo Scientific, Vantaa, Finland).

The biofilm production intensity was classified into four categories according to the cut-off of ODc values for negative controls: (I) nonadherent: OD $\leq$ ODc; (II) weakly adherent: ODc $\leq$ OD $\leq 2 \times$ ODc; (III) moderately adherent: $2 \times$ ODc $\leq$ OD $\leq 4 \times$ ODc; (IV) strongly adherent: $4 \times$ ODc $\leq$ OD.

4.4.1. Single-Agent Biofilm Eradication Assay

The effect of phytochemicals and antibiotics alone on the eradication of 48-h-old biofilm was examined using a modified microtiter plate method [84]. Two strains, MSSA ATCC 6538 and MRSA ATCC BAA-2312, were grown on MHB supplemented with 1% glucose for 48 h at 37 °C.

Only antibiotics with MICs ranging from 1.0 to 64.0 μg mL^{-1} and phytochemicals with MICs ranging from 128.0 to 1024.0 μg mL^{-1} were used. Based on this, for MSSA biofilm eradication, four antibiotics (CHL, CAZ, VAN, STR) and two phytochemicals (CAR, THY) were tested; for MRSA biofilm eradication, six antibiotics (CHL, VAN, STR, CTX, TET, GEN, OXC) and one phytochemical (CAR) was tested.

Prepared concentrations of agents for single treatments ranged from $1 \times$ MIC to $4 \times$ MIC and were added (200 μL per well) after the biofilm was washed and the plates dried. The microtiter plates were then incubated at 37 °C for 24 h. The planktonic cell eradication (PEC) assay was performed first by transferring 100 μL of the well content to a new microtiter plate, followed by the addition of 90 μL of double-strengthened MHB supplemented with 1% glucose and 10 μL of 1% TTC. The plates were incubated at 37 °C for 3 h, and absorbance was read spectrophotometrically at 540 nm. PEC (planktonic eradication concentration) was defined as the minimum concentration that prevented the appearance of red color from TTC, indicating inhibition of planktonic cell release.

Biofilm eradication concentration (BEC) was quantified using the method described in Section 4.4. BEC was determined after the PEC assay and expressed as a percentage, with the percentage of biofilm and planktonic cell removal calculated based on the mean OD values for treatments in relation to the control. Obtained negative OD values were considered as zero.

4.4.2. Binary Combination Biofilm Eradication Assay

The principle of the experiment remains the same as described in Section 4.3.2, where the eradication of biofilms was investigated using single agents. For the MSSA strain, three binary combinations (CAR + THY, CAR + CHL, and THY + CHL) were selected, while for the MRSA strain, two binary combinations (CAR + GEN and CAR + STR) were examined. For the synergistic combinations, the concentration range was from $1/4 \times$ MIC to $4 \times$ MIC.

4.5. Data Analysis

Each experiment was performed in triplicate and independently repeated at least twice. MIC values were calculated as geometric means (GMs) to reduce the impact of extreme outliers.

$$\mathrm{GM} = \sqrt[n]{x_1 \times x_2 \times \ldots \times x_n}$$

Other results were averaged and expressed as means ± standard errors. The FICI of the antibiotic and phytochemical combinations, as well as the kinetics of bacterial growth inhibition, were graphically represented using Origin Pro 8 software (OriginLab, Northampton, MA, USA).

5. Conclusions

The terpenoid compounds CAR and THY effectively inhibit the growth of both MSSA and MRSA strains. In contrast, compounds from the terpene group, such as sabinene, 3-carene, and α-pinene, exhibit limited activity against MRSA, even at higher concentrations. The observed synergistic interactions between CAR and THY when combined with conventional antibiotics highlight their potential to enhance antibacterial efficacy and combat antibiotic resistance. Furthermore, these terpenoids were effective against biofilms formed by MSSA and MRSA, which are critical for their pathogenicity. Results indicate that CAR and THY can disrupt established biofilms, with CAR specifically improving the efficacy of antibiotics, presenting a promising solution for biofilm eradication.

Given the strain-dependent nature of these interactions, it is essential to carefully evaluate specific combinations against individual strains, particularly in MRSA infections, to develop personalized treatment strategies. Future research should focus on elucidating the mechanisms of action, optimizing these combinations for clinical application, and conducting in vivo studies to validate the findings. In conclusion, this study offers significant insights into potential alternative antimicrobial strategies/approaches and underscores the potential of plant-derived compounds as promising agents in addressing the growing challenge of antibiotic-resistant bacterial infections.

Supplementary Materials: The following supporting information can be downloaded at: https://www.mdpi.com/article/10.3390/antibiotics13111030/s1, Table S1. Pre-checkerboard combination of phytochemicals and antibiotics against MSSA and MRSA strains.

Author Contributions: Data curation, I.N. and V.A.S.; formal analysis, I.N., V.A.S., D.G. and P.K.; investigation, I.N. and P.K.; methodology I.N., V.A.S., D.G. and P.K.; visualization, I.N., D.G. and P.K.; writing—original draft, I.N.; writing—review and editing, V.A.S. and P.K.; conceptualization, P.K.; funding acquisition, P.K.; project administration, P.K.; supervision, P.K. All authors have read and agreed to the published version of the manuscript.

Funding: This research was funded by the Ministry of Science, Technological Development and Innovation of the Republic of Serbia, Grants No. 451-03-66/2024-03/200125 and 451-03-65/2024-03/200125.

Institutional Review Board Statement: Not applicable.

Informed Consent Statement: Not applicable.

Data Availability Statement: The data that support the findings of this study are available from the corresponding author upon reasonable request.

Conflicts of Interest: The authors declare no conflicts of interest.

References

1. Okesola, A.O. Community-acquired methicillin-resistant *Staphylococcus aureus*-a review of literature. *Afr. J. Med. Health Sci.* **2011**, *40*, 97–107.
2. Klein, E.; Smith, D.L.; Laxminarayan, R. Hospitalizations and deaths caused by methicillin-resistant *Staphylococcus aureus*, United States, 1999–2005. *Emerg. Infect. Dis.* **2007**, *13*, 1840–1846. [CrossRef] [PubMed]
3. Scallan, E.; Hoekstra, R.M.; Angulo, F.J.; Tauxe, R.V.; Widdowson, M.-A.; Roy, S.L.; Jones, J.L.; Griffin, P.M. Foodborne illness acquired in the United States-Major pathogens. *Emerg. Infect. Dis.* **2011**, *17*, 7–15. [CrossRef] [PubMed]
4. Davies, D. Understanding biofilm resistance to antibacterial agents. *Nat. Rev. Drug Discov.* **2003**, *2*, 114–122. [CrossRef] [PubMed]
5. Pantosti, A.; Sanchini, A.; Monaco, M. Mechanisms of antibiotic resistance in *Staphylococcus aureus*. *Future Microbiol.* **2007**, *2*, 323–334. [CrossRef]
6. Gould, I.M. Treatment of bacteremia: Meticillin-resistant *Staphylococcus aureus* (MRSA) to vancomycin-resistant *S. aureus* (VRSA). *Int. J. Antimicrob. Agents* **2013**, *42*, S17–S21. [CrossRef]
7. Mishra, A.; Tabassum, N.; Aggarwal, A.; Kim, Y.-M.; Khan, F. Artificial intelligence-driven analysis of antimicrobial-resistant and biofilm-forming pathogens on biotic and abiotic surfaces. *Antibiotics* **2024**, *13*, 788. [CrossRef]
8. Ryder, V.J.; Chopra, I.; O'Neill, A.J. Increased mutability of staphylococci in biofilms as a consequence of oxidative stress. *PLoS ONE* **2012**, *7*, e47695. [CrossRef]
9. Savage, V.J.; Chopra, I.; O'Neill, A.J. *Staphylococcus aureus* biofilms promote horizontal transfer of antibiotic resistance. *Antimicrob. Agents Chemother.* **2013**, *57*, 1968–1970. [CrossRef]

10. Mah, T.C.; O'Toole, G.A. Mechanisms of biofilm resistance to antimicrobial agents. *Trends Microbiol.* **2001**, *9*, 34–39. [CrossRef]
11. da Silva, A.C.R.; Monteiro Lopes, P.; de Azevedo, M.M.B.; Machado Costa, D.C.; Sales Alviano, C.; Sales Alviano, D. Biological activities of α-pinene and β-pinene enantiomers. *Molecules* **2012**, *17*, 6305–6316. [CrossRef] [PubMed]
12. Diniz do Nascimento, L.; Moraes, A.A.B.; Costa, K.S.D.; Pereira Galúcio, J.M.; Taube, P.S.; Costa, C.M.L.; Neves Cruz, J.; de Aguiar Andrade, E.H.; Faria, L.J.G. Bioactive natural compounds and antioxidant activity of essential oils from spice plants: New findings and potential applications. *Biomolecules* **2020**, *10*, 988. [CrossRef] [PubMed]
13. de Oliveira, M.S.; Vostinaru, O.; Rigano, D.; de Aguiar Andrade, E.H. Editorial: Bioactive compounds present in essential oils: Advances and pharmacological applications. *Front. Pharmacol.* **2023**, *14*, 1130097. [CrossRef] [PubMed]
14. Masyita, A.; Mustika Sari, R.; Dwi Astuti, A.; Yasir, B.; Rahma Rumata, N.; Emran, T.B.; Nainu, F.; Simal-Gandara, J. Terpenes and terpenoids as main bioactive compounds of essential oils, their roles in human health and potential application as natural food preservatives. *Food Chem. X* **2022**, *13*, 100217. [CrossRef]
15. Rout, S.; Tambe, S.; Deshmukh, R.K.; Mali, S.; Cruz, J.; Srivastav, P.P.; Amin, P.D.; Gaikwad, K.K.; Andrade, E.H.d.A.; de Oliveira, M.S. Recent trends in the application of essential oils: The next generation of food preservation and food packaging. *Trends Food Sci. Technol.* **2022**, *129*, 421–439. [CrossRef]
16. Gavaric, N.; Smole Mozina, S.; Kladar, N.; Bozin, B. Chemical profile, antioxidant and antibacterial activity of thyme and oregano essential oils, thymol and carvacrol and their possible synergism. *J. Essent. Oil Bear.* **2015**, *18*, 1013–1021. [CrossRef]
17. Netopilova, M.; Houdkova, M.; Rondevaldova, J.; Kmet, V.; Kokoska, L. Evaluation of in vitro growth-inhibitory effect of carvacrol and thymol combination against *Staphylococcus aureus* in liquid and vapour phase using new broth volatilization chequerboard method. *Fitoterapia* **2018**, *129*, 185–190. [CrossRef]
18. Vasconcelos, S.E.C.B.; Melo, H.M.; Cavalcante, T.T.A.; Júnior, F.E.A.C.; de Carvalho, M.G.; Menezes, F.G.R.; de Sousa, O.V.; Costa, R.A. *Plectranthus amboinicus* essential oil and carvacrol bioactive against planktonic and biofilm of oxacillin- and vancomycin-resistant *Staphylococcus aureus*. *BMC Complement. Altern. Med.* **2017**, *17*, 462. [CrossRef]
19. Rani, S.; Singh, H.; Ram, C. Efficacy and mechanism of carvacrol with octanoic acid against mastitis causing multi-drug-resistant pathogens. *Braz. J. Microbiol.* **2022**, *53*, 385–399. [CrossRef]
20. Lambert, R.J.W.; Skandamis, P.N.; Coote, P.J.; Nychas, G.-J.E. A study of the minimum inhibitory concentration and mode of action of oregano essential oil, thymol and carvacrol. *J. Appl. Microbiol.* **2001**, *91*, 453–462. [CrossRef]
21. Rúa, J.; Del Valle, P.; De Arriaga, D.; Fernández-Álvarez, L.; García-Armesto, M.R. Combination of carvacrol and thymol: Antimicrobial activity against *Staphylococcus aureus* and antioxidant activity. *Foodborne Pathog. Dis.* **2019**, *16*, 622–629. [CrossRef] [PubMed]
22. Gan, C.; Langa, E.; Valenzuela, A.; Ballestero, D.; Pino-Otín, M.R. Synergistic activity of thymol with commercial antibiotics against critical and high WHO priority pathogenic bacteria. *Plants* **2023**, *12*, 1868. [CrossRef] [PubMed]
23. Trombetta, D.; Castelli, F.; Sarpietro, M.G.; Venuti, V.; Cristani, M.; Daniele, C.; Saija, A.; Mazzanti, G.; Bisignano, G. Mechanisms of antibacterial action of three monoterpenes. *Antimicrob. Agents Chemother.* **2005**, *49*, 2474–2478. [CrossRef] [PubMed]
24. Li, Q.; Huang, K.X.; Pan, S.; Su, C.; Bi, J.; Lu, X. Thymol disrupts cell homeostasis and inhibits the growth of *Staphylococcus aureus*. *Contrast Media Mol. Imaging* **2022**, *2022*, 8743096. [CrossRef]
25. Souza, E.L.; Oliveira, C.E.; Stamford, T.L.; Conceição, M.L.; Neto, N.J. Influence of carvacrol and thymol on the physiological attributes, enterotoxin production and surface characteristics of *Staphylococcus aureus* strains isolated from foods. *Braz. J. Microbiol.* **2013**, *44*, 29–35. [CrossRef]
26. Abdel-Raheem, S.M.; Abd El-Hamid, M.I.; Ibrahim, D.; El-Malt, R.M.S.; El-Ghareeb, W.R.; Ismail, H.A.; Al-Sultan, S.I.; Meligy, A.M.A.; ELTarabili, R.M. Future scope of plant-derived bioactive compounds in the management of methicillin-resistant *Staphylococcus aureus*: In vitro antimicrobial and antivirulence prospects to combat MRSA. *Microb. Pathog.* **2023**, *183*, 106301. [CrossRef]
27. Miladi, H.; Zmantar, T.; Chaabouni, Y.; Fedhila, K.; Bakhrouf, A.; Mahdouani, K.; Chaieb, K. Antibacterial and efflux pump inhibitors of thymol and carvacrol against food-borne pathogens. *Microb. Pathog.* **2016**, *99*, 95–100. [CrossRef]
28. Silveira, Z.d.S.; Macêdo, N.S.; dos Santos, J.F.S.; de Freitas, T.S.; Barbosa, C.R.d.S.; Júnior, D.L.d.S.; Muniz, D.F.; de Oliveira, L.C.C.; Júnior, J.P.S.; da Cunha, F.A.B.; et al. Evaluation of the antibacterial activity and efflux pump reversal of thymol and carvacrol against *Staphylococcus aureus* and their toxicity in *Drosophila melanogaster*. *Molecules* **2020**, *25*, 2103. [CrossRef]
29. Mouwakeh, A.; Kincses, A.; Nové, M.; Mosolygó, T.; Mohácsi-Farkas, C.; Kiskó, G.; Spengler, G. *Nigella sativa* essential oil and its bioactive compounds as resistance modifiers against *Staphylococcus aureus*. *Phytother. Res.* **2019**, *33*, 1010–1018. [CrossRef]
30. Nostro, A.; Roccaro, A.S.; Bisignano, G.; Marino, A.; Cannatelli, M.A.; Pizzimenti, F.C.; Cioni, P.L.; Procopio, F.; Blanco, A.R. Effects of oregano, carvacrol and thymol on *Staphylococcus aureus* and *Staphylococcus epidermidis* biofilms. *J. Med. Microbiol.* **2007**, *56*, 519–523. [CrossRef]
31. Yuan, Z.; Dai, Y.; Ouyang, P.; Rehman, T.; Hussain, S.; Zhang, T.; Yin, Z.; Fu, H.; Lin, J.; He, C.; et al. Thymol inhibits biofilm formation, eliminates pre-existing biofilms, and enhances clearance of methicillin-resistant *Staphylococcus aureus* (MRSA) in a mouse peritoneal implant infection model. *Microorganisms* **2020**, *8*, 99. [CrossRef] [PubMed]
32. Peng, Q.; Tang, X.; Dong, W.; Zhi, Z.; Zhong, T.; Lin, S.; Ye, J.; Qian, X.; Chen, F.; Yuan, W. Carvacrol inhibits bacterial polysaccharide intracellular adhesin synthesis and biofilm formation of mucoid *Staphylococcus aureus*: An in vitro and in vivo study. *RSC Adv.* **2023**, *13*, 28743–28752. [CrossRef] [PubMed]

33. Swetha, T.K.; Vikraman, A.; Nithya, C.; Prasath, N.H.; Pandian, S.K. Synergistic antimicrobial combination of carvacrol and thymol impairs single and mixed-species biofilms of *Candida albicans* and *Staphylococcus epidermidis*. *Biofouling* **2021**, *36*, 1256–1271. [CrossRef] [PubMed]
34. Nostro, A.; Cellini, L.; Zimbalatti, V.; Blanco, A.R.; Marino, A.; Pizzimenti, F.; Giulio, M.D.; Bisignano, G. Enhanced activity of carvacrol against biofilm of *Staphylococcus aureus* and *Staphylococcus epidermidis* in an acidic environment. *APMIS* **2012**, *120*, 967–973. [CrossRef]
35. Kifer, D.; Mužinić, V.; Ševgić Klarić, M. Antimicrobial potency of single and combined mupirocin and monoterpenes, thymol, menthol and 1,8-cineole against *Staphylococcus aureus* planktonic and biofilm growth. *J. Antibiot.* **2016**, *69*, 689–696. [CrossRef]
36. Cirino, I.C.S.; Menezes-Silva, S.M.P.; Silva, H.T.D.; De Souza, E.L.; Siqueira-Júnior, J.P. The essential oil from *Origanum vulgare* L. and its individual constituents carvacrol and thymol enhance the effect of tetracycline against *Staphylococcus aureus*. *Chemotherapy* **2014**, *60*, 290–293. [CrossRef]
37. Veras, H.N.H.; Rodrigues, F.F.G.; Botelho, M.A.; Menezes, I.R.A.; Coutinho, H.D.M.; Costa, J.G.M. Enhancement of aminoglycosides and β-lactams antibiotic activity by essential oil of *Lippia sidoides* Cham. and the thymol. *Arab. J. Chem.* **2017**, *10*, S2790–S2795. [CrossRef]
38. Grădinaru, A.C.; Trifan, A.; Şpac, A.; Brebu, M.; Miron, A.; Aprotosoaie, A.C. Antibacterial activity of traditional spices against lower respiratory tract pathogens: Combinatorial effects of *Trachyspermum ammi* essential oil with conventional antibiotics. *Lett. Appl. Microbiol.* **2018**, *67*, 449–457. [CrossRef]
39. Miladi, H.; Zmantar, T.; Kouidhi, B.; Al Qurashi, Y.M.A.; Bakhrouf, A.; Chaabouni, Y.; Mahdouani, K.; Chaieb, K. Synergistic effect of eugenol, carvacrol, thymol, p-cymene and γ-terpinene on inhibition of drug resistance and biofilm formation of oral bacteria. *Microb. Pathog.* **2017**, *112*, 156–163. [CrossRef]
40. Peng, L.; Xiong, Y.; Wang, M.; Han, M.; Cai, W.; Li, Z. Chemical composition of essential oil in *Mosla chinensis* Maxim cv. Jiangxiangru and its inhibitory effect on *Staphylococcus aureus* biofilm formation. *Open Life Sci.* **2018**, *13*, 1–10. [CrossRef]
41. Wang, T.-H.; Hsia, S.-M.; Wu, C.-H.; Ko, S.-Y.; Chen, M.Y.; Shih, Y.-H.; Shieh, T.-M.; Chuang, L.-C.; Wu, C.-Y. Evaluation of the antibacterial potential of liquid and vapor phase phenolic essential oil compounds against oral microorganisms. *PLoS ONE* **2016**, *11*, e0163147. [CrossRef] [PubMed]
42. İşcan, G. Antibacterial and anticandidal activities of common essential oil constituents. *Rec. Nat. Prod.* **2017**, *11*, 374–388.
43. Cristani, M.; D'Arrigo, M.; Mandalari, G.; Castelli, F.; Sarpietro, M.G.; Micieli, D.; Venuti, V.; Bisignano, G.; Saija, A.; Trombetta, D. Interaction of four monoterpenes contained in essential oils with model membranes: Implications for their antibacterial activity. *J. Agric. Food Chem.* **2007**, *55*, 6300–6308. [CrossRef] [PubMed]
44. Angioni, A.; Barra, A.; Russo, T.M.; Coroneo, V.; Dessí, S.; Cabras, P. Chemical composition of the essential oils of Juniperus from ripe and unripe berries and leaves and their antimicrobial activity. *J. Agric. Food Chem.* **2003**, *51*, 3073–3078. [CrossRef] [PubMed]
45. Cheng, F.; Mo, Y.; Chen, K.; Shang, X.; Yang, Z.; Hao, B.; Shang, R.; Liang, J.; Liu, Y. Integration of metabolomics and transcriptomics indicates changes in MRSA exposed to terpinen-4-ol. *BMC Microbiol.* **2021**, *21*, 305. [CrossRef] [PubMed]
46. Cordeiro, L.; Figueiredo, P.; Souza, H.; Sousa, A.; Andrade-Júnior, F.; Medeiros, D.; Nóbrega, J.; Silva, D.; Martins, E.; Barbosa-Filho, J.; et al. Terpinen-4-ol as an antibacterial and antibiofilm agent against *Staphylococcus aureus*. *Int. J. Mol. Sci.* **2020**, *21*, 4531. [CrossRef]
47. Ghazal, T.S.A.; Schelz, Z.; Vidács, L.; Szemerédi, N.; Veres, K.; Spengler, G.; Hohmann, J. Antimicrobial, multidrug resistance reversal and biofilm formation inhibitory effect of *Origanum majorana* extracts, essential oil and monoterpenes. *Plants* **2022**, *11*, 1432. [CrossRef]
48. Hammer, K.A.; Carson, C.F.; Riley, T.V. Effects of *Melaleuca alternifolia* (Tea Tree) essential oil and the major monoterpene component terpinen-4-ol on the development of single- and multistep antibiotic resistance and antimicrobial susceptibility. *Antimicrob. Agents. Chemother.* **2012**, *56*, 909–915. [CrossRef]
49. Sun, L.M.; Zhang, C.L.; Li, P. Characterization, antibiofilm, and mechanism of action of novel PEG-stabilized lipid nanoparticles loaded with terpinen-4-ol. *J. Agric. Food Chem.* **2012**, *60*, 6150–6156. [CrossRef]
50. Filipowicz, N.; Kamiński, M.; Kurlenda, J.; Asztemborska, M.; Ochocka, J.R. Antibacterial and antifungal activity of juniper berry oil and its selected components. *Phytother. Res.* **2003**, *17*, 227–231. [CrossRef]
51. Gambino, E.; Maione, A.; Guida, M.; Albarano, L.; Carraturo, F.; Galdiero, E.; Di Onofrio, V. Evaluation of the pathogenic-mixed biofilm formation of *Pseudomonas aeruginosa*/*Staphylococcus aureus* and treatment with limonene on three different materials by a dynamic model. *Int. J. Environ. Res. Public Health* **2022**, *19*, 3741. [CrossRef] [PubMed]
52. Leite, A.M.; Lima, E.D.O.; Souza, E.L.D.; Diniz, M.D.F.F.M.; Trajano, V.N.; Medeiros, I.A.D. Inhibitory effect of β-pinene, α-pinene and eugenol on the growth of potential infectious endocarditis causing Gram-positive bacteria. *Braz. J. Pharm. Sci.* **2007**, *43*, 121–126. [CrossRef]
53. Ngassapa, O.D.; Runyoro, D.K.B.; Vagionas, K.; Graikou, K.; Chinou, I.B. Chemical composition and antimicrobial activity of *Geniosporum rotundifolium* Briq and *Haumaniastrum villosum* (Bene) AJ Paton (Lamiaceae) essential oils from Tanzania. *Trop. J. Pharm. Res.* **2016**, *15*, 107–113. [CrossRef]
54. Salinas, C.; Florentín, G.; Rodríguez, F.; Alvarenga, N.; Guillén, R. Terpenes combinations inhibit biofilm formation in *Staphylococcus aureus* by interfering with initial adhesion. *Microorganisms* **2022**, *10*, 1527. [CrossRef]
55. García-Salinas, S.; Elizondo-Castillo, H.; Arruebo, M.; Mendoza, G.; Irusta, S. Evaluation of the antimicrobial activity and cytotoxicity of different components of natural origin present in essential oils. *Molecules* **2018**, *23*, 1399. [CrossRef]

56. Ahmad, A.; Van Vuuren, S.; Viljoen, A. Unravelling the complex antimicrobial interactions of essential oils-The case of *Thymus vulgaris* (Thyme). *Molecules* **2014**, *19*, 2896–2910. [CrossRef]
57. Özel, Y.; Yilmaz, U.; Ünlü, M.; Vardar Ünlü, G. Antibacterial activity and synergistic interaction of various essential oil components and antibiotics. *Mikrobiyol. Bul.* **2022**, *56*, 95–102. [CrossRef]
58. Fadli, M.; Saad, A.; Sayadi, S.; Chevalier, J.; Mezrioui, N.E.; Pagès, J.-M.; Hassani, L. Antibacterial activity of *Thymus maroccanus* and *Thymus broussonetii* essential oils against nosocomial infection-Bacteria and their synergistic potential with antibiotics. *Phytomedicine* **2012**, *19*, 464–471. [CrossRef]
59. Van Zyla, R.L.; Tsietsi Seatlholo, S.; Van Vuuren, S.F.; Viljoen, A. Pharmacological interactions of essential oil constituents on the viability of micro-organisms. *Nat. Prod. Commun.* **2010**, *5*, 1381–1386.
60. Kwiatkowski, P.; Łopusiewicz, Ł.; Pruss, A.; Kostek, M.; Sienkiewicz, M.; Bonikowski, R.; Wojciechowska-Koszko, I.; Dołęgowska, B. Antibacterial activity of selected essential oil compounds alone and in combination with β-lactam antibiotics against MRSA strains. *Int. J. Mol. Sci.* **2020**, *21*, 7106. [CrossRef]
61. Aleksic Sabo, V.; Nikolic, I.; Mimica-Dukic, N.; Knezevic, P. Anti-*Acinetobacter baumannii* activity of selected phytochemicals alone, in binary combinations and in combinations with conventional antibiotics. *Nat. Prod. Res.* **2020**, *35*, 5964–5967. [CrossRef] [PubMed]
62. Cohen, S.M.; Eisenbrand, G.; Fukushima, S.; Gooderham, N.J.; Guengerich, P.; Hecht, S.S.; Rietjens, I.M.C.M.; Rosol, T.J.; Davidsen, M.; Harman, C.L.; et al. FEMA GRAS assessment of natural flavor complexes: Origanum oil, thyme oil and related phenol derivative-containing flavoring ingredients. *Food Chem. Toxicol.* **2021**, *155*, 112378. [CrossRef] [PubMed]
63. Imran, M.; Aslam, M.; Alsagaby, S.A.; Saeed, F.; Ahmad, I.; Afzaal, M.; Arshad, U.M.; Abdelgawad, M.A.; El-Ghorab, A.H.; Ahmed, K.; et al. Therapeutic application of carvacrol: A comprehensive review. *Food Sci. Nutr.* **2022**, *10*, 3529–4088. [CrossRef] [PubMed]
64. Nagoor Meeran, F.M.; Javed, H.; Al Taee, H.; Azimullah, S.; Ojha, S. Pharmacological properties and molecular mechanisms of thymol: Prospects for its therapeutic potential and pharmaceutical development. *Front. Pharmacol.* **2017**, *8*, 380. [CrossRef]
65. Xie, K.; Tashkin, D.P.; Luo, M.Z.; Zhang, J.Y. Chronic toxicity of inhaled thymol in lungs and respiratory tracts in mouse model. *Pharmacol. Res. Perspect.* **2019**, *7*, e00516. [CrossRef]
66. Lade, H.; Park, J.H.; Chung, S.H.; Kim, I.H.; Kim, J.M.; Joo, H.S.; Kim, J.S. Biofilm formation by *Staphylococcus aureus* clinical isolates is differentially affected by glucose and sodium chloride supplemented culture media. *J. Clin. Med.* **2019**, *8*, 1853. [CrossRef]
67. Waldrop, R.; McLaren, A.; Calara, F.; McLemore, R. Biofilm growth has a threshold response to glucose in vitro. *Clin. Orthop. Relat. Res.* **2014**, *472*, 3305–3310. [CrossRef]
68. Croes, S.; Deurenberg, R.H.; Boumans, M.L.; Beisser, P.S.; Neef, C.; Stobberingh, E.E. *Staphylococcus aureus* biofilm formation at the physiologic glucose concentration depends on the *S. aureus* lineage. *BMC Microbiol.* **2009**, *9*, 229. [CrossRef]
69. Cruz, C.D.; Shah, S.; Tammela, P. Defining conditions for biofilm inhibition and eradication assays for Gram-positive clinical reference strains. *BMC Microbiol.* **2018**, *18*, 173. [CrossRef]
70. Stepanović, S.; Vuković, D.; Hola, V.; Bonaventura, G.D.; Djukić, S.; Ćirković, I.; Ruzicka, F. Quantification of biofilm in microtiter plates: Overview of testing conditions and practical recommendations for assessment of biofilm production by staphylococci. *APMIS* **2007**, *115*, 891–899. [CrossRef]
71. Kostoglou, D.; Protopappas, I.; Giaouris, E. Common plant-derived terpenoids present increased anti-biofilm potential against *Staphylococcus* bacteria compared to a quaternary ammonium biocide. *Foods* **2020**, *9*, 697. [CrossRef] [PubMed]
72. Vetas, D.; Dimitropoulou, E.; Mitropoulou, G.; Kourkoutas, Y.; Giaouris, E. Disinfection efficiencies of sage and spearmint essential oils against planktonic and biofilm *Staphylococcus aureus* cells in comparison with sodium hypochlorite. *Int. J. Food Microbiol.* **2017**, *257*, 19–25. [CrossRef] [PubMed]
73. Johnson, P.J.T.; Levin, B.R. Pharmacodynamics, population dynamics, and the evolution of persistence in *Staphylococcus aureus*. *PLoS Genet.* **2013**, *9*, e1003123. [CrossRef] [PubMed]
74. Hsu, C.Y.; Lin, M.H.; Chen, C.C.; Chien, S.C.; Cheng, Y.H.; Su, I.N.; Shu, J.C. Vancomycin promotes the bacterial autolysis, release of extracellular DNA, and biofilm formation in vancomycin-non-susceptible *Staphylococcus aureus*. *FEMS Microbiol. Immunol.* **2011**, *63*, 236–247. [CrossRef] [PubMed]
75. Langeveld, W.T.; Veldhuizen, E.J.; Burt, S.A. Synergy between essential oil components and antibiotics: A review. *Crit. Rev. Microbiol.* **2014**, *40*, 76–94. [CrossRef]
76. Swamy, M.K.; Akhtar, M.S.; Sinniah, U.R. Antimicrobial properties of plant essential oils against human pathogens and their mode of action: An updated review. *Evid. Based Complement. Alternat. Med.* **2016**, *2016*, 3012462. [CrossRef]
77. Zhou, W.; Wang, Z.; Mo, H.; Zhao, Y.; Li, H.; Zhang, H.; Hu, L.; Zhou, X. Thymol mediates bactericidal activity against *Staphylococcus aureus* by targeting an aldo-keto reductase and consequent depletion of NADPH. *J. Agric. Food Chem.* **2019**, *67*, 8382–8392. [CrossRef]
78. Thieme, L.; Hartung, A.; Tramm, K.; Klinger-strobel, M.; Jandt, K.D.; Makarewicz, O.; Pletz, M.W. MBEC versus MBIC: The lack of differentiation between biofilm reducing and inhibitory effects as a current problem in biofilm methodology. *Biol. Proced. Online* **2019**, *21*, 18. [CrossRef]
79. Clinical and Laboratory Standards Institute (CLSI). *Methods for Dilution Antimicrobial Susceptibility Tests for Bacteria That Grow Aerobically*, 10th ed.; Clinical and Laboratory Standards Institute (CLSI): Malvern, PA, USA, 2015; M07-A10.

80. Knezevic, P.; Aleksic, V.; Simin, N.; Svircev, E.; Petrovic, A.; Mimica-Dukic, N. Antimicrobial activity of *Eucalyptus camaldulensis* essential oils and their interactions with conventional antimicrobial agents against multi-drug resistant *Acinetobacter baumannii*. *J. Ethnopharmacol.* **2016**, *178*, 125–136. [CrossRef]
81. Fratini, F.; Mancini, S.; Turchi, B.; Frisciaa, E.; Pistelli, L.; Giusti, G.; Cerri, D. A novel interpretation of the Fractional Inhibitory Concentration Index: The case *Origanum vulgare* L. and *Leptospermum scoparium* J. R. et G. Forst essential oils against *Staphylococcus aureus* strains. *Microbiol. Res.* **2017**, *195*, 11–17. [CrossRef]
82. Aleksic, V.; Mimica-Dukic, N.; Simin, N.; Nedeljkovic, N.S.; Knezevic, P. Synergistic effect of *Myrtus communis* L. essential oils and conventional antibiotics against multi-drug resistant *Acinetobacter baumannii* wound isolates. *Phytomedicine* **2014**, *21*, 1666–1674. [CrossRef] [PubMed]
83. Knezevic, P.; Curcin, S.; Aleksic, V.; Petrusic, M.; Vlaski, L. Phage-antibiotic synergism: A possible approach to combatting *Pseudomonas aeruginosa*. *Res. Microbiol.* **2013**, *164*, 55–60. [CrossRef] [PubMed]
84. Stepanovic, S.; Vukovic, D.; Dakic, I.; Savic, B.; Svabic-Vlahovic, M. A modified microtiter-plate test for quantification of staphylococcal biofilm formation. *J. Microbiol. Methods* **2000**, *40*, 175–179. [CrossRef] [PubMed]

Disclaimer/Publisher's Note: The statements, opinions and data contained in all publications are solely those of the individual author(s) and contributor(s) and not of MDPI and/or the editor(s). MDPI and/or the editor(s) disclaim responsibility for any injury to people or property resulting from any ideas, methods, instructions or products referred to in the content.

antibiotics

MDPI

Article

Synergistic Antibiofilm Effects of Chestnut and Linden Honey with Lavender Essential Oil Against Multidrug-Resistant Otitis Media Pathogens

Virág D. Ángyán [1], Viktória L. Balázs [1], Marianna Kocsis [2], Béla Kocsis [3], Györgyi Horváth [1], Ágnes Farkas [1,*] and Lilla Nagy-Radványi [1]

[1] Department of Pharmacognosy, Faculty of Pharmacy, University of Pécs, 7624 Pécs, Hungary; angyan.virag@edu.pte.hu (V.D.Á.); viktoria.balazs@aok.pte.hu (V.L.B.); horvath.gyorgyi@gytk.pte.hu (G.H.); lilla.radvanyi@aok.pte.hu (L.N.-R.)
[2] Department of Agricultural Biology, Institute of Biology, University of Pécs, 7624 Pécs, Hungary; kocsis.marianna@pte.hu
[3] Department of Medical Microbiology and Immunology, Medical School, University of Pécs, 7624 Pécs, Hungary; kocsis.bela@pte.hu
* Correspondence: agnes.farkas@aok.pte.hu

Abstract: Background/Objectives: Bacterial resistance to antibiotics is a major problem in healthcare, complicated by the ability of bacteria to form biofilms. Complementary therapy for infectious diseases can rely on natural substances with antibacterial activity, e.g., essential oils and honeys. The aim of the study was to investigate the effects of linden and chestnut honeys, lavender essential oil, and their combinations against the multidrug-resistant otitis media pathogens *Haemophilus influenzae*, *H. parainfluenzae*, *Moraxella catarrhalis*, *Pseudomonas aeruginosa*, and *Streptococcus pneumoniae*. The efficacy of these natural substances was compared with each other and antibiotics used in clinical practice. Methods: Microscopic pollen analysis and physicochemical traits were used to confirm the botanical origin of honey samples. The antibiotic sensitivity of bacteria was tested with a disk diffusion assay. Minimum inhibitory concentrations were determined using a microdilution assay. A 24 h immature biofilm eradication test was performed with a crystal violet assay. The efficacy of combinations was tested with a checkerboard titration method. The DNA release of damaged bacterial cells was measured using a membrane degradation assay. Results: Lavender essential oil displayed more potent antibacterial activity compared to the honey samples. However, honey–essential oil combinations showed higher inhibition rates for biofilm eradication, with *P. aeruginosa* being the most resistant bacterium. The combined use of chestnut honey and lavender oil resulted in a higher degree of membrane degradation in a shorter time, and their synergistic effect was proven with checkerboard titration. Conclusions: The combination of linden or chestnut honey with lavender essential oil was shown to be effective in the eradication of a 24 h immature biofilm formed by *H. parainfluenzae*, *M. catarrhalis*, and *S. pneumoniae*.

Keywords: chestnut honey; linden honey; lavender essential oil; antibacterial effect; biofilm eradication

1. Introduction

Bacterial resistance to antibiotics appears in three main forms: intrinsic, acquired, and adaptive resistance. Through intrinsic resistance, the bacterium naturally resists the effects of certain antibiotics due to its innate structural and functional characteristics (the structure

of the bacterial cell membrane, efflux pumps, and enzymatic processes, e.g., penicillin-degrading beta-lactamase) [1,2]. In case of acquired resistance, a bacterium previously sensitive to an antibiotic loses its sensitivity, which can develop through genomic mutations or horizontal gene transfer (HGT). During HGT, bacterial cells are able to transfer resistance-carrying genes to each other; thus, it is not necessary to develop resistance from generation to generation, which complicates treatment of the infection [3]. Adaptive resistance is a phenomenon in which bacteria are able to adapt to environmental stressors and the presence of an antibiotic without undergoing genetic change. In contrast to intrinsic and acquired resistance, adaptive resistance ceases when the trigger is removed [4].

Biofilm formation can be observed in many bacterial strains and has given bacteria a huge advantage, as bacterial biofilms provide optimal conditions and protection for the entire bacterial community, thus contributing greatly to the development of antibiotic resistance [5,6]. The dense polymer matrix of biofilms provides physical protection for the bacterium against the antibiotic; its cohesive structure mainly consists of extracellular polysaccharides, DNA fragments, and proteins [7]. Until recently, only biomaterial bound to the surface has been considered a biofilm, but, today, free-floating, aggregated bacterial cells are also recognized as biofilms [8]. Bacterial colonies that do not adhere to the surface have also been observed in children with persistent soft tissue infections or serous otitis media. In the latter case, a bacterial biofilm formed not only on the mucous membrane but also in the fluid of the middle ear [9,10].

Acute otitis media is the most common childhood illness and the most frequent reason for antibiotics to be prescribed in this age group to treat the infection [11]. It is a disease that occurs at least once in 50–85% of children by the age of three [12]. In many cases, it is a condition that develops after an upper respiratory viral infection, which can be accompanied by ear pain, hearing loss, fever, and the appearance of purulent ear discharge. As a result of the infection, the Eustachian tube loses its normal function, i.e., drainage of accumulated fluid, ventilation of the middle ear, and equalization of pressure. The accumulation of fluid caused by a blocked ear horn provides favorable conditions for the growth of bacteria [13]. The infection is often caused by biofilm-forming bacteria, which can reduce the success of antibiotic therapy, thereby slowing down the recovery process. The most common multidrug-resistant, biofilm-forming pathogens causing otitis media include Gram-negative *Haemophilus influenzae*, *H. parainfluenzae*, *Moraxella catarrhalis*, and *Pseudomonas aeruginosa* and Gram-positive *Streptococcus pneumoniae* [14]. Patients with acute otitis media have a high risk of the infection re-flaring, so it is very important to keep the ear canal clean and isolated and to promote the regeneration of the eardrum. Plant-based active ingredients with antibacterial activity (e.g., essential oil, honey) can play a significant role as a complementary treatment accompanying antibiotic therapies, as they can prevent the re-emergence of inflammation and superinfection.

Essential oils (EOs) are mainly composed of volatile hydrocarbons and oxygen-containing compounds, which are classified based on their biosynthetic pathways. Terpenoids are produced via the mevalonate pathway, while phenylpropanoids are synthesized through the shikimate pathway [15]. Many EOs penetrate cell membranes and, thanks to this, are able to influence the functioning of molecular targets [16]. Due to its anti-inflammatory, soothing, and antiseptic effects, lavender essential oil (Leo) can be used in dermatology to treat eczema and psoriasis. During upper respiratory infections, inhalation of Leo disinfects the airways [17]. Leo distilled during the early flowering period was proven to have a more significant anti-inflammatory effect compared to Leo distilled in the main flowering period or after flowering [18]. Its main components include the monoterpenes linalool, linalyl acetate, 1,8-cineole, terpinen-4-ol, β-ocimene, and camphor [19].

Honey is a natural medicinal substance that contains the active ingredients of the nectar source plant and the special enzymes and hormones of bees. The bactericidal hydrogen peroxide produced through the dilution of honey, the plant-derived polyphenols that increase the permeability of the bacterial cell membrane, the peptides synthesized by bees (e.g., defensin-1 peptide), the slightly acidic pH (bacteriostatic effect), and the high sugar content (osmotic stress) all contribute to honey's antibacterial activity [20–24]. The strong antibacterial effect of linden honey (Lh) and chestnut honey (Ch) has been confirmed by several research groups, suggesting that their use as adjunctive therapy may also be effective in the case of otitis media [25–30]. In terms of polyphenols, lindenine was identified as a marker compound in Lhs, accompanied by higher amounts of ferulic acid and methyl syringate [31–33], while kynurenic acid content was prominent in Chs [34–36].

The therapeutic use and combination of medicinal substances that contain different types of active components are justified by their diverse and complex active ingredient composition [37]. Honeys and EOs might achieve their antibacterial effect through several modes of action, which in turn might hinder acquired bacterial resistance to these complex mixtures of compounds [38,39]. The basic question of our research is how effectively the combinations Leo–Lh or Leo–Ch can eradicate the biofilm formed by the most common multidrug-resistant otitis media bacterial strains in comparison to antibiotics and Leo, Lh, or Ch applied alone. To achieve these objectives, minimum inhibitory concentrations (MICs) were measured using microdilution assay, and biofilm eradication was investigated with crystal violet staining. To investigate the mode of action, a membrane degradation study was performed, and the level of interaction between honey and essential oil was determined through checkerboard titration.

2. Results

2.1. Pollen Profile and Physicochemical Parameters of Honey Samples

Based on the melissopalynological analysis, our Lh and Ch samples can clearly be regarded as varietal honeys, as they contained the pollen of the supposed nectar source plant in the percentage described in the literature (Table 1) [40]. In the case of Lh, linden (*Tilia* spp.) pollen (Figure 1A) was present in the largest proportion, but a significant part of pollen grains was identified as acacia (*Robinia pseudoacacia*) and oilseed rape (*Brassica napus*) pollen. Complying with requirements regarding Ch, chestnut (*Castanea sativa*) pollen (Figure 1B) was present in more than 90% in our honey sample. The sensory and physicochemical properties of the honey samples (Table 2) also supported their monofloral origin, in accordance with the results of the microscopic pollen analysis.

Table 1. Pollen spectrum of linden honey and chestnut honey.

	Pollen Type—Relative Frequency (%)				
Honey Sample	***Tilia* spp.**	***Robinia pseudoacacia***	***Brassica napus***	***Castanea sativa***	**Other**
Linden	36.0	25.7	20.4	6.2	11.7
Chestnut	0.2	4.3	1.4	93.1	1.0

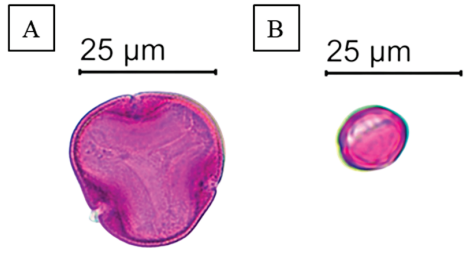

Figure 1. Microscopic pollen images of linden pollen (**A**) and chestnut pollen (**B**).

Table 2. Sensory characteristics and physicochemical parameters of honey samples. Data are presented as means ± standard deviation (n = 3).

Honey Type, Plant Name	Sensory Characteristics (Color, Odor, and Consistency)	$ABS_{450–720}$ (mAU)	Electrical Conductivity (mS/cm)	pH
Linden, *Tilia* spp.	Light amber, strong odor, semisolid, fine, granulated	107 ± 1.4	0.528 ± 0.01	4.1 ± 0.01
Chestnut, *Castanea sativa*	Dark amber, intense odor, semisolid, fine, granulated	215.3 ± 1.4	0.598 ± 0.01	4.7 ± 0.01

2.2. Antibiotic Sensitivity of Test Bacteria

Table 3 and Table S1 summarize the resistance profile of the pathogens included in the study. Based on these results, amikacin was used for *H. influenzae* and *H. parainfluenzae* bacteria, imipenem for *M. catarrhalis* and *S. pneumoniae*, and gentamicin for *P. aeruginosa*.

Table 3. Antibiotic sensitivity of test bacteria according to the disk diffusion assay.

Antibiotics	1	2	3	4	5
Amikacin	-	R	S	S	S
Ampicillin	R	R	S	R	R
Amoxicillin/ clavulanic acid	-	S	S	R	R
Ciprofloxacin	R	S	S	S	S
Ceftazidim	-	S	S	-	-
Eritromicin	-	-	R	-	S
Gentamicin	S	S	S	S	S
Imipenem	S	S	S	S	S
Levofloxacin	-	-	R	-	-
Oxacillin	R	-	-	-	-
Penicillin	R	-	-	-	-
Piperacillin/ tazobactam	-	S	S	-	-
Vankomicin	S	-	-	-	-

1: Moraxella catarrhalis, 2: Pseudomonas aeruginosa, 3: Streptococcus pneumoniae, 4: Haemophilus influenzae, 5: H. parainfluenzae; R: resistant, S: sensitive, "-": no data.

2.3. Minimum Inhibitory Concentrations (MICs)

The MIC values of the studied samples (Lh, Ch, and Leo) and the antibiotic controls are summarized in Table 4. The most resistant bacterium was *P. aeruginosa* in the case of both the honey samples and the essential oil, while Gram-negative *Haemophilus* species and Gram-positive *S. pneumoniae* bacteria were the most sensitive in the case of honeys and essential oil, respectively. Antibiotics were more effective against each bacterial strain included in the study compared to Lh, Ch, and Leo. Comparing the efficacy of honeys and Leo, the antibacterial activity of Leo was more significant. The Tween40 used for the emulsification of Leo had no antibacterial effect.

Table 4. The minimum inhibitory concentrations (MICs) of linden and chestnut honey, lavender essential oil, and the antibiotic controls (amikacin for *H. influenzae* and *H. parainfluenzae*; imipenem for *M. catarrhalis* and *S. pneumoniae*; gentamicin for *P. aeruginosa*) against the investigated bacterial strains.

	MIC Values (mg/mL)				
	S. pneumoniae	***H. influenzae***	***H. parainfluenzae***	***M. catarrhalis***	***P. aeruginosa***
Linden honey	142.86	111.11	111.11	142.86	176.47
Chestnut honey	142.86	111.11	111.11	111.11	176.47
Lavender essential oil	0.31	0.63	0.63	1.25	2.50
Antibiotics	0.0008	0.0031	0.0016	0.0002	0.0063

2.4. Biofilm Eradication Activity

In this experiment, Lh, Ch, Leo, and the antibiotics were used at MIC/2 concentration when tested alone, but in the case of honey–essential oil combinations, MIC/4 values were used, as our goal was to reveal the effect of the combinations on biofilm eradication, not to destroy the bacterial cells. Based on our observations, all samples had antibiofilm activity, but they had a different effect on the biofilm eradication of the five bacterial strains included in the study (Figure 2). The biofilm formation of *H. influenzae* (Figure 2A) and *H. parainfluenzae* (Figure 2B) was inhibited to a greater degree by the honey samples, with Lh displaying higher inhibition rates compared to Leo. In the case of *M. catarrhalis* (Figure 2C), however, the essential oil had a higher inhibition rate compared to the honey samples, and here Ch was the stronger inhibitor from the honey samples. Similar tendencies were observed in the case of *P. aeruginosa* (Figure 2D) and *S. pneumoniae* (Figure 2E) bacteria, where Ch and Leo exerted the same level of inhibition, while the inhibition activity of Lh was somewhat lower. For each bacterial strain, the combinations had the strongest antibiofilm activity (Ch + Leo inhibition rate: 74–93%). The antibiotic had the lowest inhibitory effect on biofilm formation (inhibition rate: 28–34%). Gram-negative *P. aeruginosa* was the most resistant, while the Gram-positive *S. penumoniae* bacterium was the most sensitive. Biofilm formation was not affected by the emulsifier (Tween40) used in the case of essential oil.

2.5. Checkerboard Assay

The results of checkerboard titration are summarized in Tables 5 and 6. Table 5 shows the combination MIC values of the test substances, which were used to calculate the FICI values. Based on the FICI values, the interactions between the test substances were determined, taking into account the following value ranges: FICI $\leq$ 0.5: synergist; 0.5–1: additive; >1: negative interaction; >4: antagonist [41].

Table 5. Combination MIC values of test samples (μg/mL).

Bacterial Strains	Test Samples	Combination MIC
P. aeruginosa	Leo	0.3125
	Lh	88.235
	Leo	0.3125
	Ch	44.1175
S. pneumoniae	Leo	0.0775
	Lh	71.43
	Leo	0.0775
	Ch	35.715

Leo: lavender essential oil; Lh: linden honey; Ch: chestnut honey.

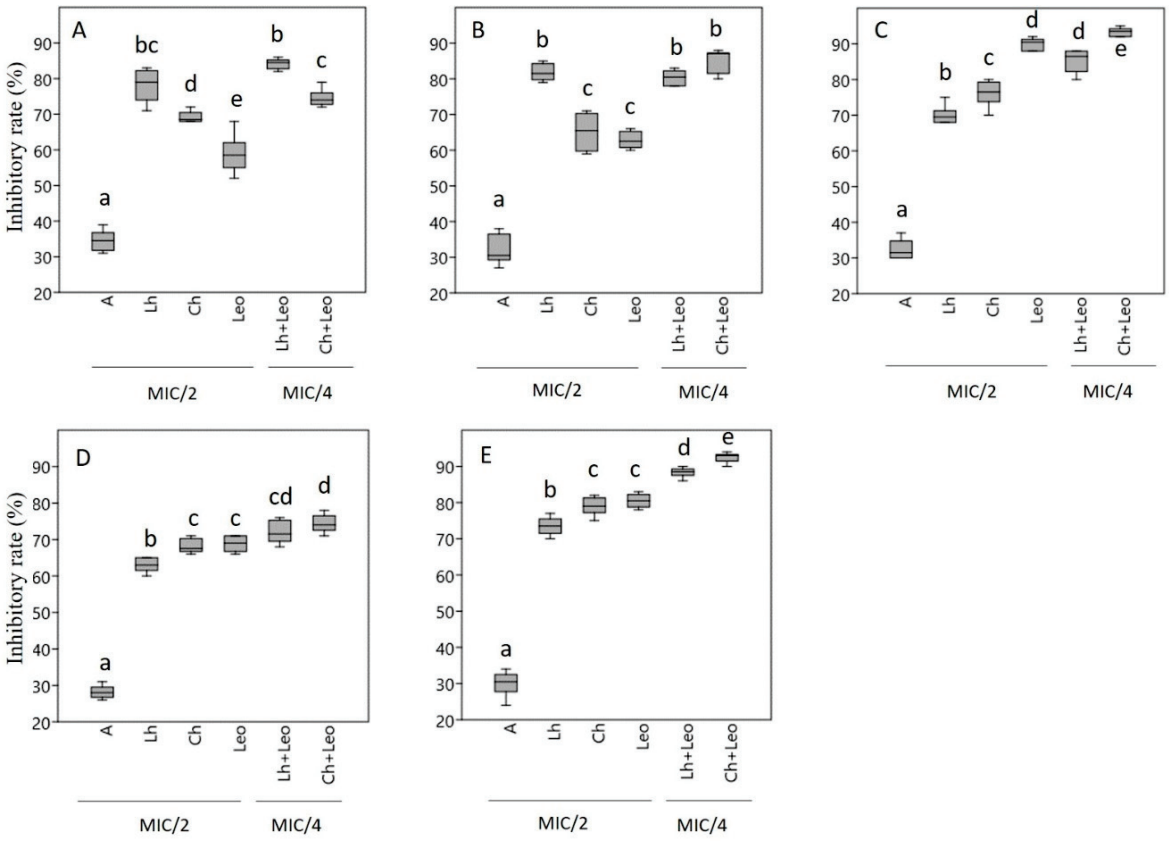

Figure 2. The biofilm degradation effects of linden and chestnut honeys and lavender essential oil alone and in combination against five bacteria. *H. influenzae* (**A**), *H. parainfluenzae* (**B**), *M. catarrhalis* (**C**), *P. aeruginosa* (**D**), and *S. pneumoniae* (**E**); antibiotic (A), linden honey (Lh), chestnut honey (Ch), lavender essential oil (Leo), combination of linden honey and lavender essential oil (Lh + Leo), combination of chestnut honey and lavender essential oil (Ch + Leo). Data were expressed using box plots with minimum to maximum values presented by vertical lines, with the median in the plot as a horizontal line. Different lowercase letters above the boxes indicate significant differences between the means of inhibitory rates of different components against the given bacteria, according to the Tukey's test ($p < 0.05$), based on results of 6 parallel measurements (n = 6).

Table 6. FICI values and combination effects of test samples.

Bacterial Strains	Test Samples	FICI	Combination Effect
P. aeruginosa	Leo Lh	0.625	additive effect
	Leo Ch	0.375	synergistic effect
S. pneumoniae	Leo Lh	0.75	additive effect
	Leo Ch	0.5	synergistic effect

Leo: lavender essential oil; Lh: linden honey; Ch: chestnut honey.

Based on the FICI values, Ch used together with Leo resulted in a synergistic effect against both Gram-negative and Gram-positive bacteria. When Leo was combined with Lh, an additive effect was detected (Table 6).

2.6. Membrane Degradation Assay

The checkerboard titration supported the synergistic effect of Ch and Leo (Table 6), so membrane degradation studies were performed with these two samples and their

combinations. In addition, Ch was chosen for these experiments because of its high antibacterial and antibiofilm activity against *S. pneumoniae* (Gram-positive) and *P. aeruginosa* (Gram-negative) bacteria (Table 4, Figure 2).

Using Ch and Leo separately at MIC × 2 concentrations, bacterial DNA release was above 60% (60.7–68.4%) for both bacterial strains included in the study. In the case of the combination, half of the concentration of the two natural substances (MIC, 1:1 ratio) resulted in DNA leakage of 67.9% (*P. aeruginosa*) and 69.8% (*S. pneumoniae*) (Table 7). In the study of DNA release kinetics, Ch and Leo were used separately at MIC × 2 concentrations at different time intervals (20, 40, 60, and 90 min) (Table 8). For the combination, in this case too, we worked with the MIC concentration for both samples (1:1 ratio). In each measurement, bacterial DNA was detected already at 20 min (34.4–53.6%), and the highest values were obtained at 90 min (66.6–71.2%). In this study, as well, the most DNA was released during treatment with the combination (90th minute: 70.9 and 71.2%). Based on our results, *P. aeruginosa* proved to be a more resistant bacterium compared to *S. pneumoniae* (Tables 7 and 8).

Table 7. Effect of chestnut honey, lavender essential oil, and their combination on the release of DNA in Gram-negative (*P. aeruginosa*) and Gram-positive (*S. pneumoniae*) bacteria.

DNA Release from Bacterial Cells (%)			
Samples	**Concentrations**	***P. aeruginosa***	***S. pneumoniae***
Chestnut honey (Ch)	MIC/2	11.7 ± 1.2	14.3 ± 1.3
	MIC	26.9 ± 2.3	31.6 ± 1.7
	MIC × 2	60.7 ± 2.5	66.3 ± 2.3
	MIC × 4	100	100
Lavender essential oil (Leo)	MIC/2	15.6 ± 1.8	18.1 ± 1.3
	MIC	36.5 ± 2.2	42.2 ± 2.1
	MIC × 2	67.1 ± 2.5	68.4 ± 2.3
	MIC × 4	100	100
Combination	MIC Ch + MIC Leo (1:1 ratio)	67.9 ± 2.8	69.8 ± 3.0

Data are means ± standard deviations of six independent determinations (n = 6).

Table 8. Kinetics of 260 nm absorbing material released from Gram-negative (*P. aeruginosa*) and Gram-positive (*S. pneumoniae*) bacteria treated with chestnut honey, lavender essential oil, and their combination.

DNA Release from Bacterial Cells (%)			
Samples	**Time (min)**	***P. aeruginosa***	***S. pneumoniae***
Chestnut honey (Ch) conc.: MIC × 2	0	0	0
	20	34.4 ± 2.1	39.2 ± 2.2
	40	55.2 ± 2.3	58.9 ± 2.1
	60	60.7 ± 2.5	66.3 ± 2.3
	90	66.6 ± 2.2	68.0 ± 2.6
Lavender essential oil (Leo) conc.: MIC × 2	0	0	0
	20	40.3 ± 2.2	49.1 ± 2.0
	40	62.8 ± 2.5	64.4 ± 2.6
	60	67.1 ± 2.5	68.4 ± 2.3
	90	69.2 ± 2.3	70.5 ± 2.8
Combination conc.: MIC Ch + MIC Leo (1:1 ratio)	0	0	0
	20	46.2 ± 2.4	53.6 ± 1.9
	40	63.7 ± 2.2	68.0 ± 2.1
	60	67.9 ± 2.8	69.8 ± 3.0
	90	70.9 ± 2.6	71.2 ± 2.2

Data are means ± standard deviations of six independent determinations (n = 6).

3. Discussion

Investigating the antibacterial and biofilm inhibition activities of natural substances is vital to explore new therapeutic options to curb the increasing spread of antibiotic resistance. In our study, we applied a novel approach by exploring the possibility of using two natural substances, honey and essential oil, together. Chestnut and linden honey, which were included in our experiment, have proven antibacterial and biofilm formation inhibitory effects against respiratory bacteria. Combining them with Leo not only resulted in an increased antibacterial effect, but the anti-inflammatory effect of lavender essential oil can also contribute to the success of the complementary therapy. Both honey and essential oil have been hypothesized to achieve their antibacterial efficacy through several modes of action.

Essential oils are multicomponent, lipophilic liquids with characteristic aroma, as they comprise volatile compounds. Up to 20–60 different bioactive components can be present in essential oils [42]. Their mechanisms of action are diverse; some essential oils can kill bacteria (bactericidal effect), but there are some that only slow down their division (bacteriostatic effect) [43]. The general bacteriostatic effect of essential oils is based on several mechanisms. They cause the disintegration of the bacterial outer membrane or the phospholipid bilayer. They increase the permeability of the bacterial cell membrane and promote the leakage of intracellular components from the cell, which leads to an upset in the ionic balance. In addition, they can interfere with the cellular metabolism (glucose and fatty acid metabolism) and enzyme kinetics of pathogens [44,45]. According to some researchers, there is a significant difference between the sensitivity of Gram-negative and Gram-positive bacteria. Essential oil components with hydrophobic properties are more effective on Gram-positive bacteria [46,47]. This phenomenon can be explained by the fact that Gram-positive bacteria have a thick peptidoglycan layer linked to apolar molecules through which lipophilic components can easily pass; meanwhile, in the cell envelope of Gram-negative bacteria, proteins linked to the outer membrane and lipopolysaccharides prevent this [48]. Understanding the mechanism of action of a given essential oil or one of its components is of paramount importance, as this allows us to develop new therapeutic procedures and identify new areas of indication. The antibacterial effect of lavender is well-known, and numerous studies have supported the antibacterial and anti-inflammatory effects of Leo [18,49,50]. However, there are few studies on the antibacterial and anti-biofilm effects of Leo against pathogens that cause upper respiratory tract diseases. The activity of Leo against *Haemophilus* strains was first described by our research group. Due to the overuse of antibiotics and the increasing phenomenon of antibiotic resistance, which can largely be attributed to the ability of bacteria to form biofilms, research is directed towards bacteria that cause problems in the nosocomial area [51–53]. Leo has been shown to be effective against both MRSA (methicillin-resistant *Staphylococcus aureus*) and VRE (vancomycin-resistant *Enterococcus faecalis*) at concentrations below 1% [54]. In the study by de Rapper, the efficacy of Leo was tested in combination with antibiotics and antifungals, and the individual MIC value of Leo was also determined using the microdilution method. The MIC values obtained against the bacteria *P. aeruginosa* and *S. aureus* were 1 mg/mL, and values against the fungus (*C. albicans*) were 3 mg/mL. Another research group measured 2.33 mg/mL as the MIC value of Leo against the pathogen *P. aeruginosa* [55]. The MIC value of Leo against *P. aeruginosa* in our study was 2.5 mg/mL, which shows that our data are comparable with the results of other research groups [56]. A veterinary study indicated that Leo may be effective as a topical treatment for canine otitis externa promoted by biofilm-producing *P. aeruginosa* [57]. The antipseudomonal effect of *L. angustifolia*, *L. intermedia*, *L. pyrenaica*, and *L. stoechas* essential oils was confirmed by Végh et al. (2012) [58]. The anti-*Pseudomonas* activity of essential oils obtained from *L. sumian* and *L. grosso* was

supported by Donadu's research group. Their results confirmed that *L. sumian* essential oil showed lower antimicrobial activity (MIC: 16% solution) than *L. grosso* (MIC: 8% solution). None of the Leos tested showed cytotoxic effects at the tested concentrations [59].

In biofilm inhibition studies, *P. aeruginosa* was the most resistant pathogen in each test system. This may be due to the fact that this bacterium has three exopolysaccharides: Psl, Pel, and alginate. Psl is a neutral pentasaccharide that typically contains D-glucose, D-mannose, and L-rhamnose moieties. Psl acts as a signaling molecule and promotes the production of c-di-GMP (bis-(3′-5′)-cyclic dimeric guanosine monophosphate), the levels of which, when elevated, result in thicker and more robust biofilms [60]. In addition, Psl protects biofilm bacteria from antimicrobial agents and neutrophil phagocytosis [61]. Pel is a cationic polysaccharide polymer of partially deacetylated N-acetyl-D-glucosamine and N-acetyl-D-galactosamine. Pel promotes the tolerance of bacteria embedded in biofilms to aminoglycoside antibiotics [62]. Alginic acids are mixtures of uronic acid polymers, the main components of which are β-D-mannuronic acid and α-L-guluronic acid. The salts of alginic acids are alginates. Alginate has a wide range of functions, including biofilm maturation, protection against phagocytosis, and reduced diffusion of antibiotics through the biofilm [63]. The aforementioned units contribute to the increased resistance of *P. aeruginosa* biofilm to treatment. The other pathogens included in the study (*Haemophilus* spp., *M. catarrhalis*, *S. pneumoniae*) do not have such resistant biofilms, so higher inhibition rate values were detected for these pathogens.

Among the possible mechanisms of action underlying the effectiveness of Leo, in addition to membrane-degrading activity, the inhibition of quorum sensing (QS) should also be mentioned. Although we do not have enough data regarding the anti-QS effect of Leo, a study written in 2014 supports this fact [64]. The antibacterial effect of vaporizing Leo was also confirmed against *Staphylococcus* strains (*S. hominis*, *S. haemolyticus*, *S. epidermidis*, *S. aureus*) in hospital environments. The data showed that Leo reduced the number of bacteria in all hospital areas compared to the untreated control [65].

Based on the microbiological studies conducted to date, it can be concluded that similar studies related to *Haemophilus* strains and *M. catharralis* and *S. pneumoniae* bacteria are not available. Furthermore, it should be emphasized that few studies investigate the biofilm inhibitory effect of Leo [66]. In addition to the above, another novelty of our work is that we also examined the biofilm eradication activity of Leo in combination with two types of honey. Honeys, just like essential oils, are promising antibacterial and antiviral agents due to their diverse plant-derived compounds and multiple modes of action.

The antimicrobial activities of honey have recently been reviewed by Luca et al. (2024) [67]. Honey's antibacterial activity was reported against numerous bacteria, including *Acinetobacter*, *Escherichia*, *Klebsiella*, *Pseudomonas*, *Staphylococcus,* and *Streptococccus* strains. The antifungal effect of honey was investigated mainly against various *Candida* and *Aspergillus* species. The antiviral activity of honeys requires further research; however, honey seems to be active against SARS-CoV-2, human immunodeficiency virus, herpes simplex virus types 1 and 2, viral hepatitis virus, and others [68,69]. The antimicrobial properties of honey are attributed partly to plant-derived compounds, like polyphenols [23], and partly to bee-derived components, like defensin-1 peptide [20]. The antibacterial activity of honey is usually in correlation with its hydrogen peroxide content [70], e.g., in acacia, rapeseed, and sunflower honeys harvested in Europe but not in linden honey. The synergistic effect of polyphenols and hydrogen peroxide has been proposed to determine a honey's antibacterial qualities [71]. New Zealand's manuka honey is characterized by non-peroxide antibacterial activity, which can be attributed to its methylglyoxal content [72]. In addition, the physicochemical traits of honeys, like acidity (low pH), high sugar concentration, low water content, phenolic acids and flavonoids, as well as proteins, all contribute

to honey's antibacterial properties. It must be emphasized that individually none of these factors would be sufficient to achieve antimicrobial activity, as their complex interaction is required [67]. Exposure to honey can induce physiological changes in bacteria related to membrane integrity and polarization and can lead to metabolic disruption [29]. High levels of carbohydrates in honey can cause the dehydration of bacterial cells through osmosis [67]. Damage to the cytoplasmic membrane can result in the easy release of nucleic acids, amino acids, K+, proteins, and inorganic phosphates from the bacterial cell, leading to cell lysis and death [73]. Lh and Ch contain higher proportions of the polyphenolic components ferulic acid and gallic acid, which can cause irreversible damage to membrane properties of various pathogenic bacteria (e.g., *P. aeruginosa*), such as physicochemical characteristics or intra- and extracellular permeability [74–76]. Increased pore formation, local tearing, or a decrease in negative surface charge may occur [23,77]. Membrane-bound efflux pumps (proteins) fulfill many functions in bacterial cells; for example, they promote the development of resistance to antibacterial agents, biofilm stabilization, and protection against oxidative stress [78–80]. Efflux pump inhibitors are used to prevent antibiotic resistance of multidrug-resistant bacterial strains with increased efflux activity. These compounds significantly reduce tolerance and biofilm formation and thus increase the effectiveness of antibiotics [81,82]. Phenolic compounds found in honey (e.g., ferulic, gallic, caffeic and salicylic acids, quercetin, kaempferol, galangin) can act as efflux pump inhibitors by inhibiting ATPases involved in antibiotic efflux [79,83]. In order to increase their chances of survival, bacterial cells constantly communicate with each other using signal molecules. It has been observed that the QS mechanism (local cell density sensing) of bacteria directly affects the development of antibiotic resistance through the expression of different efflux pumps [84]. QS activity is significantly inhibited by many unifloral honeys (e.g., by degrading the N-acyl homoserine lactone signaling molecule in Gram-negative bacteria); however, the extent of the inhibitory effect depends significantly on the type of honey, the place of collection, or the different phenolic acid content. For example, chestnut and linden honeys show higher QS inhibitory activity than orange or rosemary honeys [79,85,86].

There are a few studies available on the combination of honey and essential oil. Imtara and his research group used checkerboard titration to explore the possible synergistic effect of oregano (*Origanum vulgare*) essential oil and different honey samples on *E. coli*, *P. aeruginosa*, *S. faecalis,* and *Staphylococcus aureus* by calculating fractional inhibitory concentrations. The most pronounced synergistic effect was achieved with the combination of oregano essential oil and *Euphorbia* honey against the pathogens *E. coli* and *Streptococcus faecalis* [87]. Another study supports the synergistic effect of combining eucalyptus honey and eucalyptus essential oil against the pathogens *E. coli*, *Proteus mirabilis*, *Salmonella* Typhimurium, *Bacillus subtilis*, *Staphylococcus aureus*, *Listeria monocytogenes*, *Candida albicans*, *Trichophyton rubrum,* and *Aspergillus niger*. The study tested honey and essential oil separately and in combination. The results confirmed that the combination of the two substances was more effective [37]. The research team of Qasem tested the combination of chamomile essential oil and chamomile honey against similar pathogens. The results showed that the most sensitive pathogens were *S. aureus* and *L. monocytogenes*, and the most resistant ones were *E. coli*, *P. mirabilis*, *S.* Typhimurium, and *P. aeruginosa*. In all cases, the combination of chamomile honey and chamomile essential oil showed higher efficacy compared to the use of honey or essential oil separately [88]. Increased efficacy of honey–essential oil combinations can be attributed to the fact that complexity makes it difficult for bacteria to develop tolerance, as adapting to several different active ingredients is a much more time-consuming and complicated task.

Our study demonstrated the synergistic effect of Ch and Leo against otitis media pathogens through a series of in vitro experiments. Using only in vitro assays poses a

limitation for the usability of our data; thus, further experiments should be planned to test the honey–essential oil combinations in either in vivo or clinical settings. Further research should be directed to clarifying which constituents of honeys and essential oils are responsible for their respective antibacterial and antibiofilm effect and how these bioactive compounds can enhance each other's efficacy in combination, resulting in synergistic effects. The current study revealed the membrane degrading potential of Lh, Ch, and Leo. This is, however, only one of the mechanisms of honeys' and essential oils' antibacterial action; thus, further experiments are needed to shed light on whether these complex natural substances or their bioactive compounds are able to inhibit other defense lines of bacteria, such as efflux pumps and quorum-sensing mechanisms. In addition, the study could be broadened to include several other bacterial strains causing multiple types of infections to reveal the width of the antibacterial spectrum of honeys and essential oils.

4. Materials and Methods

4.1. Honey and Essential Oil Samples

For our investigations, linden (*Tilia* spp.) and chestnut (*Castanea sativa* Mill.) honeys were purchased in 2021 from Hungarian apiaries in the South Transdanubian region; Lh was purchased from the Reith Apiary (Baranya County) and Ch was purchased from the Németh Apiary (Zala County). The aerial parts of lavender (*Lavandula angustifolia* Mill.) were collected before the flowering period in Bolhó village (N46.0408 E17.3034, Somogy County, Hungary) in 2021. The plant material was prepared for essential oil extraction, as described in our previous publication [18]. The herba was dried at room temperature for 1 week, and then the essential oil was extracted through hydrodistillation [89]. The lavender essential oil (Leo) distilled in the pre-bloom period was selected for this study based on our previous experiments, where Leo from this phenophase exhibited greater antibacterial and anti-inflammatory activity compared to Leo obtained during and after the flowering period [18,90]. The chemical composition of Leo was characterized in Balázs et al. (2025), with the main components being linalool (31.02%) and linalyl acetate (23.66%), followed by terpinen-4-ol (6.44%), α-terpineol (5.54%), and geranyl acetate (3.45%) [90].

4.2. Melissopalynological Analysis

Following the work of Nagy-Radványi et al. (2024—A) [91], we chose microscopic pollen analysis as one of the most effective methods to determine the botanical origin of honeys. Honey pollen samples were prepared according to the methodology developed by Von der Ohe et al. (2004) [92]. Ten grams of honey was measured into a 50 mL centrifuge tube and then mixed with 20 mL of distilled water using a Combi-spin FVL-2400N vortex (Biocenter Ltd., Szeged, Hungary). The centrifuge tube was placed into a Neofuge 15R centrifuge (Lab-Ex Ltd., Budapest, Hungary) and centrifuged at 3000 rpm for 10 min. After removing the supernatant, the remaining sediment was supplemented with 10 mL of distilled water, and the mixture was centrifuged again at 3000 rpm for 5 min. After the second centrifugation, 250 µL of distilled water was added to the sediment remaining in the centrifuge tube and vortexed, and then 20 µL of this pollen suspension was pipetted onto slides on an OTS 40 heating plate (Tiba Ltd., Győr, Hungary) set to 40 °C. A piece of Kaiser's glycerin jelly with fuchsine (Merck Life Science Ltd., Budapest, Hungary) was placed onto the pollen preparations, thus staining the pollen grains. The pollen preparations were covered with a coverslip and analyzed with a Nikon Eclipse E200 light microscope connected to a Michrome 20 MP CMOS camera (Auro-Science Consulting Ltd., Budapest, Hungary) at 400× magnification using the 4.3.0.605 version of TCapture software [93]. Five hundred pollen grains were counted for each honey sample, and the plant species or family

the particular pollen grain belonged to was recorded. The relative frequency of pollen types was given as a percentage of all pollen grains.

4.3. Physicochemical Parameters of Honey

The physicochemical properties of the honey samples were determined based on the research of Nagy-Radványi et al. (2024—A) [91]. For the determination of pH and electrical conductivity, we used a DSZ-708 multiparameter analyzer (Simex Ltd., Budapest, Hungary). The pH of the honey samples was measured according to the Hungarian Food Codex, and the pH meter was calibrated using buffer solutions with pH values of 4 and 9 [94]. For the determination of electrical conductivity, 20% (*w*/*w*) aqueous honey solutions were prepared, while for pH measurement, 10 g of honey was dissolved in 75 mL of carbon-dioxide-free distilled water. The electrical conductivity of honey, which is related to its mineral content, was measured at 20 °C, and the results were expressed in milli-Siemens per centimeter (mS/cm) [95].

To analyze the color intensity of varietal honeys, 50% (*w*/*w*) aqueous honey solutions were prepared, placed in an ultrasonic water bath (45–50 °C) for 5 min, and then filtered (0.45 μm pore size, Agilent Technologies, Milan, Italy). Spectrophotometric analysis was carried out using a Shimadzu UV-1800 spectrophotometer (Shimadzu Schweiz GmbH, Reinach, Switzerland). The results, expressed in milliabsorbance units (mAU), were calculated from the difference in absorbance values measured at 450 nm and 720 nm [96].

4.4. Bacterial Strains

In our research, multidrug-resistant bacteria that play a significant role in the development of otitis media were used. The pathogens *Moraxella catarrhalis* (DSM 9143), *Pseudomonas aeruginosa* (ATCC 27853), and *Streptococcus pneumoniae* (DSM 20566) were cultured using Brain Heart Infusion (BHI) Broth (Sigma-Aldrich Ltd., Budapest, Hungary) as the liquid medium. For culturing two members of the *Haemophilus* genus, *H. influenzae* (DSM 4690) and *H. parainfluenzae* (DSM 8978), a specialized growth medium was prepared. Specifically, 3750 μL of Mueller-Hinton II Broth (MHB, OXOID Ltd., London, UK) was supplemented with 750 μL of NAD solution (1 mg/mL) and 500 μL of *Haemophilus* Supplement B (Diagon Ltd., Budapest, Hungary). The bacterial cultures were incubated in a shaking incubator (at 60 rpm) at 37 °C for 12 h using a C25 Incubator Shaker (New Brunswick Scientific, Edison, NJ, USA) [97].

4.5. Determination of Antibiotic Sensitivity of Test Bacteria

The antibiotic sensitivity of the microorganisms was evaluated using the Kirby–Bauer disk diffusion method, based on the work of Nagy-Radványi et al. (2024—B) [98] and following the guidelines of the Clinical and Laboratory Standards Institute (CLSI) and the Manual of Clinical Microbiology [99,100]. Susceptibility to the following antibiotics (OXOID Ltd.) was examined: amikacin (30 μg), ampicillin (10 μg), amoxicillin/clavulanic acid (20/10 μg), ceftazidime (10 μg), ciprofloxacin (5 μg), erythromycin (15 μg), gentamicin (30 μg), imipenem (10 μg), levofloxacin (5 μg), oxacillin (1 μg), penicillin (1 μg), piperacillin–tazobactam (100/10 μg), and vancomycin (5 μg) [101]. A filter paper disk impregnated with the specified antibiotic concentration was placed onto the surface of the culture medium (in the case of *P. aeruginosa*, *M. catarrhalis* and *S. pneumoniae*: Mueller-Hinton Agar, Sigma-Aldrich Ltd., Budapest, Hungary; in case of *Haemophilus* spp.: chocolate agar) that had been inoculated with a bacterial suspension (equal to the visual turbidity of a no. 0.5 McFarland standard). After 15 min, the Petri dishes were incubated at 35 ± 2 °C for 16–18 h, after which the inhibition zones were measured under visible light.

4.6. Determination of Minimum Inhibitory Concentration (MIC)

To determine the MIC, the microdilution method was used in accordance with the guidelines of the CLSI [102]. The procedure was carried out on 96-well microtiter plates, and, to ensure accuracy, all tests were performed in six replicates. For linden and chestnut honey, the following dilution series was prepared using BHI broth: 22.5, 20, 17.5, 15, 12.5, and 10% (*w*/*w*). To emulsify the essential oil, a Tween40-containing medium was used, and the following dilution series was prepared: 10, 5, 2.5, 1.25, 0.625, and 0.3125 mg/mL. To each well, 100 µL of a 10^5 CFU/mL bacterial suspension prepared in the appropriate growth medium was added, followed by 100 µL of honey solution or essential oil solution at varying concentrations. During our study, an antibiotic specific to each bacterial strain was used as the positive control. In the case of *Haemophilus* spp., amikacin (Likacin 250 mg/mL solution for injection (Lisapharma S.P.A., Erba, Italy), in the case of *M. catharralis* and *S. pneumoniae*, imipenem (Imipenem/Cilastatin Kabi 500 mg/500 mg powder for solution for infusion), and in the case of *P. aeruginosa*, gentamicin (Gentamicin Sandoz 80 mg injection, Sandoz) antibiotics were used. Bacterial cells were also treated with BHI solution containing 1% Tween40 without the addition of essential oil in order to exclude the effect of Tween40. The plates were incubated for 24 h at 37 °C, and then absorbance values were measured at 600 nm using a microplate reader (BMG Labtech, Budapest, Hungary) [98]. We considered the lowest honey or essential oil concentration as the MIC value, in which case no bacterial growth was visible in the wells of the microtiter plate.

4.7. Biofilm Eradication Assay

In order to investigate the effect of honey samples and Leo on biofilm eradication, biofilms were formed on 96-cell microtiter plates, similarly to Balázs et al. (2023) [103]. In these experiments, MIC/2 concentrations determined in previous MIC studies were applied for honey and essential oil samples, while MIC/4 concentrations were used for combinations.

To initiate biofilm formation, 200 µL of bacterial suspension at 10^8 CFU/mL was pipetted into individual wells of the microtiter plates. As a negative control, BHI medium was applied, while untreated bacterial suspensions (10^8 CFU/mL) served as the positive control. During a 24 h incubation period (37 °C), bacterial cells formed adherent and cohesive biofilms (24 h immature biofilm). Unattached cells were washed out with physiological saline, followed by the treatment step. Treatments involved adding 200 µL of honey or essential oil solutions or 100 µL of each solution for the combination (MIC/4 concentrations). Tween40-containing medium was used to emulsify the essential oil. After incubation (24 h at 37 °C), the wells were washed again with physiological saline to remove non-adherent cells, and the adhered cells were fixed with 99% methanol (Molar Chemicals Ltd., Halásztelek, Hungary) for 15 min at room temperature (23 °C). After removing the methanol, the biofilms were stained with 0.1% crystal violet for 20 min. The crystal violet binds to negatively charged molecules in the extracellular matrix of biofilms, enabling the quantitative determination of total biofilm biomass. As a final step, the dye bound to the biofilm was dissolved in 33% acetic acid. Absorbance was measured at 595 nm using a SPECTROstar Nano microplate reader (BMG Labtech, Budapest, Hungary) [104,105]. In the series of experiments, the following antibiotic controls were used: *H. influenzae* and *H. parainfluenzae*—amikacin, *M. catarrhalis* and *S. pneumoniae*—imipenem, and *P. aeruginosa*—gentamicin.

The inhibition rate was calculated using the formula [106]

$$\text{Inhibition rate} = (1 - S/C) \times 100\%$$

where C is the absorbance of the control and S is the absorbance of the sample.

4.8. Checkerboard Assay

The combination studies were performed using the checkerboard titration method. This method is particularly suitable for studying the combination effect of substances with antibacterial effects. The selected bacterial strains were *P. aeruginosa* and *S. pneumoniae*; thus, the interaction between different substances was tested in the case of both Gram-negative and Gram-positive pathogens. BHI medium (Sigma-Aldrich Ltd.) was used for cultivation; the germ count was 10^5 CFU/mL. Furthermore, 96-well microtiter plates were used for the studies, and 3 parallel measurements were performed. In this study, Leo was combined with Lh and Ch for both pathogens. In each study design, a halving dilution series was prepared at concentrations corresponding to predetermined MIC values, which were as follows: MIC × 2, MIC, MIC/2, MIC/4, and MIC/8. Subsequently, according to the test layouts, 100 µL of bacterial suspension and then 50 µL of essential oil sample (substance A) and 50 µL of honey sample (substance B) were applied to the cells of the microtiter plates. In parallel, a bacterial suspension without samples was applied to a microtiter plate as the positive control, and only BHI medium was used as the negative control. The prepared microtiter plates were incubated (for 24 h at 37 °C), and then their absorbance was measured at a wavelength of 600 nm with a plate reader (BMG Labtech, Budapest, Hungary; Bio-Tek Ltd., Winooski, Vermont, USA). Following the test, combination MIC values were calculated. The concentration at which the absorbance of the positive control was reduced to ±10% was considered the combination MIC value. From the combination MIC values calculated in this way, the fractional inhibitory concentration index (FICI) was calculated, which is a dimensionless numerical value that helps to evaluate the combination effect of pharmacons.

$$\mathrm{FICI} = \mathrm{FICA} + \mathrm{FICB} = \frac{\text{MIC A combination}}{\text{MIC A}} + \frac{\text{MIC B combination}}{\text{MIC B}}$$

4.9. Membrane Degradation Assay

During the study of membrane degradation, bacterial suspensions (10^8 CFU/mL) were prepared in phosphate buffer solution (PBS), and untreated bacterial cells were used as controls. Samples (Ch, Leo, and honey—essential oil combination) with concentrations of MIC/4, MIC/2, MIC, MIC × 2, and MIC × 4 were added to the cells (incubation time: 1 h). The time dependence of DNA release was also investigated; in this test, the bacterial cells were suspended in PBS containing honey or essential oil with a concentration of MIC × 2. In the case of the combination, Ch and Leo were used in MIC concentration (1:1 ratio). Treatments lasted 0, 20, 40, 60, and 90 min. In both cases, these steps were followed by centrifugation (Neofuge 15R, Lab-Ex Ltd., Budapest, Hungary) at 12,000× *g* for 2 min. The absorbance of the supernatant liquid containing nucleic acid was determined at 260 nm with a Metertech SP-8001 (Abl&e-Jasco Ltd., Budapest, Hungary) spectrophotometer, and the results were expressed as a percentage compared to the control [107].

4.10. Statistical Analysis

Statistical analyses were carried out using Microsoft Excel® 2016 MSO (16.0.4266.1001 version) (Microsoft Corp., Redmond, WA, USA) and the PAST software package version 3.11 [108]. The effects of honey types, essential oil, and their combinations were compared with each other using one-way ANOVA. If the null hypothesis of the ANOVA was rejected, we used Tukey's test to establish a difference between the given groups ($p < 0.05$).

5. Conclusions

Based on our results and a few other studies conducted so far, it can be stated that the combined use of essential oil and honey may be promising for suppressing pathogens and eradicating biofilms. Demonstrating the synergistic effect of Ch and Leo supports that combinations of the two natural substances could be used in adjunctive therapy for otitis media. Our in vitro experiments provide a good starting point for the development of an ear drop or ear spray with the honey–essential oil combination that would speed up the healing time by preventing the infection from becoming chronic.

Supplementary Materials: The following supporting information can be downloaded at https://www.mdpi.com/article/10.3390/antibiotics14020146/s1, Table S1: Antibiotic sensitivity of test bacteria (1-5) measured by disk diffusion assay.

Author Contributions: Conceptualization, Á.F. and V.L.B.; methodology, V.D.Á., B.K., V.L.B. and L.N.-R.; software, M.K. and V.L.B.; validation, M.K. and Á.F.; formal analysis, M.K.; investigation, V.D.Á., B.K. and L.N.-R.; resources, V.D.Á. and L.N.-R.; data curation, M.K. and V.D.Á.; writing—original draft preparation, V.L.B., Á.F., B.K. and G.H.; writing—review and editing, Á.F., B.K. and V.L.B.; visualization, M.K.; supervision, Á.F., L.N.-R. and V.L.B.; project administration, M.K., Á.F. and V.L.B.; funding acquisition, Á.F., V.L.B., G.H. and V.D.Á. All authors have read and agreed to the published version of the manuscript.

Funding: This research was supported by the Fund of National Research, Development and Innovation Office NKFIH PD 147156 (Balázs V.L.) and NKFIH K18 128217 (Horvath G.), the Research Grant of the Faculty of Pharmacy University of Pécs, GYTK KA-2024-05 (Farkas Á.), the University Research Scholarship Program of the Ministry for Culture and Innovation from the Source of the National Research, Development and Innovation Fund (Nagy-Radványi L.: EKÖP-24-4-I-PTE-113; Balázs V.L.: EKÖP-24-4-II-PTE-114), and the Kriszbacher Ildikó Talent Management Programme of the University of Pécs: PTE-KITEP-2023-262 and PTE-KITEP-2024-385 (Ángyán V.D.).

Institutional Review Board Statement: Not applicable.

Informed Consent Statement: Not applicable.

Data Availability Statement: The original contributions presented in this study are included in the article. Further inquiries can be directed to the corresponding author.

Conflicts of Interest: The authors declare no conflicts of interest.

References

1. Webber, M.A.; Piddock, L.J. The importance of efflux pumps in bacterial antibiotic resistance. *J. Antimicrob. Chemother.* **2003**, *51*, 9–11. [CrossRef]
2. Varela, M.F.; Stephen, J.; Lekshmi, M.; Ojha, M.; Wenzel, N.; Sanford, L.M.; Hernandez, A.J.; Parvathi, A.; Kumar, S.H. Bacterial Resistance to Antimicrobial Agents. *Antibiotics* **2021**, *10*, 593. [CrossRef]
3. Moura de Sousa, J.; Lourenço, M.; Gordo, I. Horizontal gene transfer among host-associated microbes. *Cell Host Microbe* **2023**, *31*, 513–527. [CrossRef]
4. D'Aquila, P.; De Rango, F.; Paparazzo, E.; Passarino, G.; Bellizzi, D. Epigenetic-Based Regulation of Transcriptome in Escherichia coli Adaptive Antibiotic Resistance. *Microbiol. Spectr.* **2023**, *11*, e0458322. [CrossRef]
5. López, D.; Vlamakis, H.; Kolter, R. Biofilms. *Cold Spring Harb. Perspect. Biol.* **2010**, *2*, a000398. [CrossRef] [PubMed]
6. Lv, X.; Wang, L.; Mei, A.; Xu, Y.; Ruan, X.; Wang, W.; Shao, J.; Yang, D.; Dong, X. Recent Nanotechnologies to Overcome the Bacterial Biofilm Matrix Barriers. *Small* **2023**, *19*, e2206220. [CrossRef] [PubMed]
7. Zhang, L.; Bera, H.; Wang, H.; Wang, J.; Guo, Y.; Shi, C.; Cun, D.; Moser, C.; Høiby, N.; Yang, M. Combination and nanotechnology based pharmaceutical strategies for combating respiratory bacterial biofilm infections. *Int. J. Pharm.* **2022**, *616*, 121507. [CrossRef]
8. Kragh, K.N.; Tolker-Nielsen, T.; Lichtenberg, M. The non-attached biofilm aggregate. *Commun. Biol.* **2023**, *6*, 898. [CrossRef] [PubMed]

9. Van Hoecke, H.; De Paepe, A.S.; Lambert, E.; Van Belleghem, J.D.; Cools, P.; Van Simaey, L.; Deschaght, P.; Vaneechoutte, M.; Dhooge, I. Haemophilus influenzae biofilm formation in chronic otitis media with effusion. *Eur. Arch. Oto-Rhino-Laryngol.* **2016**, *273*, 3553–3560. [CrossRef] [PubMed]
10. Sauer, K.; Stoodley, P.; Goeres, D.M.; Hall-Stoodley, L.; Burmølle, M.; Stewart, P.S.; Bjarnsholt, T. The biofilm life cycle: Expanding the conceptual model of biofilm formation. *Nat. Rev. Microbiol.* **2022**, *20*, 608–620. [CrossRef] [PubMed]
11. Scott, A.M.; Clark, J.; Julien, B.; Islam, F.; Roos, K.; Grimwood, K.; Little, P.; Del Mar, C.B. Probiotics for preventing acute otitis media in children. *Cochrane Database Syst. Rev.* **2019**, *6*, CD012941. [CrossRef] [PubMed]
12. Gaddey, H.L.; Wright, M.T.; Nelson, T.N. Otitis Media: Rapid Evidence Review. *Am. Fam. Physician* **2019**, *100*, 350–356.
13. Danishyar, A.; Ashurst, J.V. *Acute Otitis Media*; StatPearls Publishing: Treasure Island, FL, USA, 2024.
14. Paramasivan, S.; Bassiouni, A.; Shiffer, A.; Dillon, M.R.; Cope, E.K.; Cooksley, C.; Ramezanpour, M.; Moraitis, S.; Ali, M.J.; Bleier, B.; et al. The international sinonasal microbiome study: A multicentre, multinational characterization of sinonasal bacterial ecology. *Allergy* **2020**, *75*, 2037–2049. [CrossRef]
15. de Sousa, D.P.; Damasceno, R.O.S.; Amorati, R.; Elshabrawy, H.A.; de Castro, R.D.; Bezerra, D.P.; Nunes, V.R.V.; Gomes, R.C.; Lima, T.C. Essential Oils: Chemistry and Pharmacological Activities. *Biomolecules* **2023**, *13*, 1144. [CrossRef]
16. Sharifi-Rad, J.; Sureda, A.; Tenore, G.C.; Daglia, M.; Sharifi-Rad, M.; Valussi, M.; Tundis, R.; Sharifi-Rad, M.; Loizzo, M.R.; Ademiluyi, A.O.; et al. Biological activities of essential oils: From plant chemoecology to traditional healing systems. *Molecules* **2017**, *22*, 70. [CrossRef]
17. Kim, N.S.; Lee, D.S. Comparison of different extraction methods for the analysis of fragrances from Lavandula species by gas chromatography–mass spectrometry. *J. Chromatogr. A* **2002**, *982*, 31–47. [CrossRef]
18. Pandur, E.; Balatinácz, A.; Micalizzi, G.; Mondello, L.; Horváth, A.; Sipos, K.; Horváth, G. Anti-inflammatory effect of lavender (*Lavandula angustifolia* Mill.) essential oil prepared during different plant phenophases on THP-1 macrophages. *BMC Complement. Med. Ther.* **2021**, *21*, 287. [CrossRef] [PubMed]
19. Koulivand, P.H.; Ghadiri, M.K.; Gorji, A. Lavender and the nervous system. *Evid. -Based Complement. Altern. Med.* **2013**, *2013*, 681304. [CrossRef]
20. Keitel, U.; Schilling, E.; Knappe, D.; Al-Mekhlafi, M.; Petersen, F.; Hoffmann, R.; Hauschildt, S. Effect of antimicrobial peptide from Apis mellifera hemolymph and its optimized version Api88 on biological activities of human monocytes and mast cells. *Innate Immun.* **2013**, *19*, 355–367. [CrossRef]
21. Kurek-Górecka, A.; Górecki, M.; Rzepecka-Stojko, A.; Balwierz, R.; Stojko, J. Bee Products in Dermatology and Skin Care. *Molecules* **2020**, *25*, 556. [CrossRef] [PubMed]
22. Liu, Y.; Han, L.; Yang, H.; Liu, S.; Huang, C. Effect of apigenin on surface associated characteristics and adherence of Streptococcus mutans. *Dent. Mater. J.* **2020**, *39*, 933–940. [CrossRef] [PubMed]
23. Olas, B. Honey and its phenolic compounds as an effective natural medicine for cardiovascular diseases in humans? *Nutrients* **2020**, *12*, 283. [CrossRef] [PubMed]
24. Khatami, S.H.; Vakili, O.; Ahmadi, N.; Soltani Fard, E.; Mousavi, P.; Khalvati, B.; Maleksabet, A.; Savardashtaki, A.; Taheri-Anganeh, M.; Movahedpour, A. Glucose oxidase: Applications, sources, and recombinant production. *Biotechnol. Appl. Biochem.* **2021**, *69*, 939–950. [CrossRef]
25. Balázs, V.L.; Nagy-Radványi, L.; Filep, R.; Kerekes, E.; Kocsis, B.; Kocsis, M.; Farkas, Á. In vitro antibacterial and antibiofilm activity of Hungarian honeys against respiratory tract bacteria. *Foods* **2021**, *10*, 16–32. [CrossRef] [PubMed]
26. Farkas, Á.; Balázs, V.L.; Kőszegi, T.; Csepregi, R.; Kerekes, E.; Horváth, G.; Szabó, P.; Gaál, K.; Kocsis, M. Antibacterial and Biofilm Degradation Effects of Hungarian Honeys Linked with Botanical Origin, Antioxidant Capacity and Mineral Content. *Front. Nutr.* **2022**, *9*, 953470. [CrossRef] [PubMed]
27. Sakač, M.; Jovanov, P.; Marić, A.; Četojević-Simin, D.; Novaković, A.; Plavšić, D.; Škrobot, D.; Kovač, R. Antioxidative, Antibacterial and Antiproliferative Properties of Honey Types from the Western Balkans. *Antioxidants* **2022**, *11*, 1120. [CrossRef] [PubMed]
28. Oliveira, A.; Sousa, J.C.; Silva, A.C.; Melo, L.D.; Sillankorva, S. Chestnut Honey and Bacteriophage Application to Control *Pseudomonas aeruginosa* and *Escherichia coli* Biofilms: Evaluation in an ex vivo Wound Model. *Front. Microbiol.* **2018**, *9*, 1725. [CrossRef]
29. Combarros-Fuertes, P.; Estevinho, L.M.; Teixeira-Santos, R.; Rodrigues, A.G.; Pina-Vaz, C.; Fresno, J.M.; Tornadijo, M.E. Antibacterial action mechanisms of honey: Physiological Effects of Avocado, Chestnut, and Polyfloral Honey upon Staphylococcus aureus and Escherichia coli. *Molecules* **2020**, *25*, 1252. [CrossRef] [PubMed]
30. Cumhur, A.; Hakan, A.; Tuğrul, Y.; Ahmet, T.; Nuray, T.D. Determination of the superior quality properties of randomly selected chestnut honey samples from the Sinop region. *Spectrosc. Lett.* **2023**, *56*, 353–363. [CrossRef]
31. Qiao, J.; Chen, L.; Kong, L.; Dong, J.; Zhou, Z.; Zhang, H. Characteristic Components and Authenticity Evaluation of Rape, Acacia, and Linden Honey. *J. Agric. Food Chem.* **2020**, *68*, 9776–9788. [CrossRef]

32. Farkas, Á.; Horváth, G.; Kuzma, M.; Mayer, M.; Kocsis, M. Phenolic compounds in Hungarian acacia, linden, milkweed and goldenrod honeys. *Curr. Res. Food Sci.* **2023**, *6*, 100526. [CrossRef]
33. Skadiņš, I.; Labsvārds, K.D.; Grava, A.; Amirian, J.; Tomsone, L.E.; Ruško, J.; Viksna, A.; Bandere, D.; Brangule, A. Antimicrobial and Antibiofilm Properties of Latvian Honey against Causative Agents of Wound Infections. *Antibiotics* **2023**, *12*, 816. [CrossRef] [PubMed]
34. Alissandrakis, E.; Tarantilis, P.A.; Pappas, C.; Harizanis, P.C.; Polissiou, M. Investigation of Organic Extractives from Unifloral Chestnut (*Castanea sativa* L.) and Eucalyptus (*Eucalyptus globulus* Labill.) Honeys and Flowers to Identification of Botanical Marker Compounds. *LWT-Food Sci. Technol.* **2011**, *44*, 1042–1051. [CrossRef]
35. Mayda, N.; Ozok, A.; Sorkun, K. Some Characteristic Properties of Chestnut and Rhododendron Honeys in Turkey. *J. Biol. Chem.* **2018**, *1*, 135–145. [CrossRef]
36. Turska, M.; Paluszkiewicz, P.; Turski, W.A.; Parada-Tuska, J. A Review of the Health Benefits of Food Enriched with Kynurenic Acid. *Nutrients* **2022**, *14*, 4182. [CrossRef] [PubMed]
37. Assaggaf, H.M.; Naceiri, M.H.; Rajab, B.S.; Attar, A.A.; Hamed, M.; Sheikh, R.A.; Omari, N.E.; Menyiy, N.E.; Belmehdi, O.; Mahmud, S.; et al. Singular and Combined Effects of Essential Oil and Honey of Eucalyptus Globulus on Anti-Inflammatory, Antioxidant, Dermatoprotective, and Antimicrobial Properties: In Vitro and In Vivo Findings. *Molecules* **2022**, *27*, 5121. [CrossRef]
38. Almasaudi, S. The antibacterial activities of honey. *Saudi J. Biol. Sci.* **2021**, *28*, 2188–2196. [CrossRef]
39. Millezi, A.F.; Piccoli, R.H.; Oliveira, J.M.; Pereira, M.O. Anti-biofilm and Antibacterial Effect of Essential Oils and Their Major Compounds. *J. Essent. Oil Bear. Plants* **2016**, *19*, 624–631. [CrossRef]
40. Oddo, L.P.; Piro, R.; Bruneau, É.; Guyot-Declerck, C.; Ivanov, T.; Piskulová, J.; Flamini, C.; Lheritier, J.; Morlot, M.; Russmann, H.; et al. Main European unifloral honeys: Descriptive sheets. *Apidologie* **2004**, *35*, 38–81. [CrossRef]
41. Odds, F.C. Synergy, antagonism, and what the chequerboard puts between them. *J. Antimicrob. Chemother.* **2003**, *52*, 1. [CrossRef] [PubMed]
42. Swamy, M.K.; Akhtar, M.S.; Sinniah, U.R. Antimicrobial Properties of Plant Essential Oils against Human Pathogens and Their Mode of Action: An Updated Review. *Evid. Based Complement. Altern. Med.* **2016**, *2016*, 3012462. [CrossRef] [PubMed]
43. Pezantes-Orellana, C.; German, B.F.; De la Cruz, C.M.; Montalvo, J.L.; Orellana-Manzano, A. Essential oils: A systematic review on revolutionizing health, nutrition, and omics for optimal well-being. *Front. Med.* **2024**, *16*, 1337785. [CrossRef] [PubMed]
44. Burt, S. Essential oils: Their antibacterial properties and potential applications in foods—A review. *Int. J. Food Microbiol.* **2004**, *94*, 223–253. [CrossRef] [PubMed]
45. Cho, T.; Park, S.M.; Yu, H.; Seo, G.; Kim, H.; Kim, S.A.; Rhee, M. Recent Advances in the Application of Antibacterial Complexes Using Essential Oils. *Molecules* **2020**, *25*, 1752. [CrossRef]
46. Plesiat, P.; Nikaido, H. Outer membranes of Gram-negative bacteria are permeable to steroid probes. *Mol. Microbiol.* **1992**, *6*, 1323–1333. [CrossRef] [PubMed]
47. Angane, M.; Swift, S.; Huang, K.; Butts, C.A.; Quek, S.Y. Essential Oils and Their Major Components: An Updated Review on Antimicrobial Activities, Mechanism of Action and Their Potential Application in the Food Industry. *Foods* **2022**, *11*, 464. [CrossRef] [PubMed]
48. Nikaido, H. Prevention of drug access to bacterial targets: Permeability barriers and active efflux. *Science* **1994**, *264*, 382–388. [CrossRef]
49. Huang, M.Y.; Liao, M.H.; Wang, Y.K.; Huang, Y.S.; Wen, H.C. Effect of lavender essential oil on LPS-stimulated inflammation. *Am. J. Chin. Med.* **2012**, *40*, 845–859. [CrossRef]
50. Todorova, D.; Yavorov, N.; Lasheva, V.; Damyanova, S.; Kostova, I. Lavender Essential Oil as Antibacterial Treatment for Packaging Paper. *Coatings* **2023**, *13*, 32. [CrossRef]
51. Kollef, M.H.; Torres, A.; Shorr, A.F.; Martin-Loeches, I.; Micek, S.T. Nosocomial Infection. *Crit. Care Med.* **2021**, *49*, 169–187. [CrossRef]
52. Sousa, S.A.; Feliciano, J.R.; Pita, T.; Soeiro, C.F.; Mendes, B.L.; Alves, L.G.; Leitão, J.H. Bacterial Nosocomial Infections: Multidrug Resistance as a Trigger for the Development of Novel Antimicrobials. *Antibiotics* **2021**, *10*, 942. [CrossRef] [PubMed]
53. Shivshankar, P.; Collum, S.; Bi, W. Haemophilus influenzae is associated with fibrotic phenotype of COVID-19 and idiopathic pulmonary fibrosis. *ERJ Open Res.* **2022**, *8*, 236. [CrossRef]
54. Cavanagh, H.M.; Wilkinson, J.M. Biological activities of lavender essential oil. *Phytother. Res.* **2002**, *16*, 301–308. [CrossRef] [PubMed]
55. Nikolić, M.; Jovanović, K.K.; Marković, T.; Marković, D.; Gligorijević, N.; Radulović, S.; Soković, M. Chemical composition, antimicrobial, and cytotoxic properties of five Lamiaceae essential oils. *Ind. Crops Prod.* **2014**, *61*, 225–232. [CrossRef]
56. de Rapper, S.; Viljoen, A.; van Vuuren, S. The In Vitro Antimicrobial Effects of Lavandula angustifolia Essential Oil in Combination with Conventional Antimicrobial Agents. *Evid. Based Complement. Altern. Med.* **2016**, *2016*, 2752739. [CrossRef]
57. Mourão, A.; Serrano, I.; Cunha, E.; Tavares, L.; Lourenco, A.; Oliveira, M. In vitro efficacy of lavender oil, otological gel and gentamicin to eradicate biofilm produced by Pseudomonas aeruginosa. *Vet. Dermatol.* **2024**, *35*, 726–735. [CrossRef] [PubMed]

58. Végh, A.; Bencsik, T.; Molnár, P.; Böszörményi, A.; Lemberkovics, É.; Kovács, K.; Kocsis, B.; Horváth, G. Composition and antipseudomonal effect of essential oils isolated from different lavender species. *Nat. Prod. Commun.* **2012**, *7*, 1393–1396. [CrossRef]
59. Donadu, M.; Usai, D.; Pinna, A.; Porcu, T.; Mazzarello, V.; Fiamma, M.; Marchetti, M.; Cannas, S.; Delogu, G.; Zanetti, S.; et al. In vitro activity of hybrid lavender essential oils against multidrug resistant strains of Pseudomonas aeruginosa. *J. Infect. Dev. Ctries.* **2018**, *12*, 9–14. [CrossRef] [PubMed]
60. Irie, Y.; Borlee, B.R.; O'Connor, J.R.; Hill, P.J.; Harwood, C.S.; Wozniak, D.J.; Parsek, M.R. Self-produced exopolysaccharide is a signal that stimulates biofilm formation in Pseudomonas aeruginosa. *Proc. Natl. Acad. Sci. USA* **2012**, *109*, 20632–20636. [CrossRef] [PubMed]
61. Mishra, M.; Byrd, M.S.; Sergeant, S.; Azad, A.K.; Parsek, M.R.; McPhail, L.; Schlesinger, L.S.; Wozniak, D.J. Pseudomonas aeruginosa Psl polysaccharide reduces neutrophil phagocytosis and the oxidative response by limiting complement-mediated opsonization. *Cell. Microbiol.* **2012**, *14*, 95–106. [CrossRef]
62. Jennings, L.K.; Storek, K.M.; Ledvina, H.E.; Coulon, C.; Marmont, L.S.; Sadovskaya, I.; Secor, P.R.; Tseng, B.S.; Scian, M.; Filloux, A.; et al. Pel is a cationic exopolysaccharide that cross-links extracellular DNA in the Pseudomonas aeruginosa biofilm matrix. *Proc. Natl. Acad. Sci. USA* **2015**, *112*, 11353–11358. [CrossRef] [PubMed]
63. Hay, I.D.; Rehman, Z.U.; Moradali, M.F.; Wang, Y.; Rehm, B.H.A. Microbial alginate production, modification and its applications. *Microb. Biotechnol.* **2013**, *6*, 637–650. [CrossRef]
64. Yap, P.S.X.; Krishnan, T.; Yiap, B.C.; Hu, C.P.; Chan, K.-G.; Lim, S.H.E. Membrane disruption and anti-quorum sensing effects of synergistic interaction between Lavandula angustifolia (lavender oil) in combination with antibiotic against plasmid-conferred multi-drug-resistant *Escherichia coli*. *J. Appl. Microbiol.* **2014**, *116*, 1119–1128. [CrossRef] [PubMed]
65. Gismondi, A.; Di Marco, G.; Redi, E.L.; Ferrucci, L.; Cantonetti, M.; Canini, A. The antimicrobial activity of *Lavandula angustifolia* Mill. essential oil against Staphylococcus species in a hospital environment. *J. Herb. Med.* **2021**, *26*, 100426. [CrossRef]
66. Leigh-de Rapper, S.; van Vuuren, S.F. Odoriferous Therapy: A Review Identifying Essential Oils against Pathogens of the Respiratory Tract. *Chem. Biodivers.* **2020**, *17*, 6. [CrossRef]
67. Luca, L.; Pauliuc, D.; Oroian, M. Honey microbiota, methods for determining the microbiological composition and the antimicrobial effect of honey—A review. *Food Chem.* **2024**, *23*, 101524. [CrossRef]
68. Al-Hatamleh, M.A.I.; Hatmal, M.M.; Sattar, K.; Ahmad, S.; Mustafa, M.Z.; Bittencourt, M.D.C.; Mohamud, R. Antiviral and immunomodulatory effects of phytochemicals from honey against COVID-19: Potential mechanisms of action and future directions. *Molecules* **2020**, *25*, 5017. [CrossRef] [PubMed]
69. Asma, S.T.; Bobis, O.; Bonta, V.; Acaroz, U.; Shah, S.R.A.; Istanbullugil, F.R.; Arslan Acaroz, D. General nutritional profile of bee products and their potential antiviral properties against mammalian viruses. *Nutrients* **2022**, *14*, 3579. [CrossRef] [PubMed]
70. Farkasovska, J.; Bugarova, V.; Godocikova, J.; Majtan, V.; Majtan, J. The role of hydrogen peroxide in the antibacterial activity of different floral honeys. *Eur. Food Res. Technol.* **2019**, *245*, 2739–2744. [CrossRef]
71. Sawicki, T.; Starowicz, M.; Kłębukowska, L.; Hanus, P. The profile of polyphenolic compounds, contents of total phenolics and flavonoids, and antioxidant and antimicrobial properties of bee products. *Molecules* **2022**, *27*, 1301. [CrossRef] [PubMed]
72. Johnston, M.; McBride, M.; Dahiya, D.; Owusu-Apenten, R.; Nigam, P.S. Antibacterial activity of Manuka honey and its components: An overview. *AIMS Microbiol.* **2018**, *4*, 655–664. [CrossRef] [PubMed]
73. Al-Sayaghi, A.M.; Al-Kabsi, A.M.; Abduh, M.S.; Saghir, S.A.M.; Alshawsh, M.A. Antibacterial Mechanism of Action of Two Types of Honey against *Escherichia coli* through Interfering with Bacterial Membrane Permeability, Inhibiting Proteins, and Inducing Bacterial DNA Damage. *Antibiotics* **2022**, *11*, 1182. [CrossRef] [PubMed]
74. Borges, A.; Ferreira, C.; Saavedra, M.J.; Simoes, M. Antibacterial activity and mode of action of ferulic and gallic acids against pathogenic bacteria. *Microb. Drug Resist.* **2013**, *19*, 256–265. [CrossRef] [PubMed]
75. Zou, S.; Tao, H.; Chang, Y.-N. Characterization of antioxidant activity and analysis of phenolic acids and flavonoids in linden honey. *Food Sci. Technol.* **2022**, *42*, e76621. [CrossRef]
76. Kim, J.; Uy, N.P.; Kim, D.; Lee, S. Analysis of Phenolic Acid Content and Antioxidant Activity of Chestnut Honey from Different Regions of Korea. *Natl. Prod. Sci.* **2023**, *29*, 127–131. [CrossRef]
77. Anand, S.; Deighton, M.; Livanos, G.; Morrison, P.D.; Pang, E.C.K.; Mantri, N. Antimicrobial Activity of Agastache Honey and Characterization of Its Bioactive Compounds in Comparison with Important Commercial Honeys. *Front. Microbiol.* **2019**, *10*, 263. [CrossRef] [PubMed]
78. Bogomolnaya, L.M.; Andrews, K.D.; Talamantes, M.; Maple, A.; Ragoza, Y.; Vazquez-Torres, A.; Andrews, H. Polymenis The ABC-type efflux pump MacAB protects Salmonella enterica serovar typhimurium from oxidative stress. *mBio* **2013**, *4*, e00630-13. [CrossRef] [PubMed]
79. Khataybeh, B.; Jaradat, Z.; Ababneh, Q. Anti-bacterial, anti-biofilm and anti-quorum sensing activities of honey: A review. *J. Ethnopharmacol.* **2023**, *317*, 116830. [CrossRef]

80. Nishino, K.; Yamasaki, S.; Nakashima, R.; Zwama, M.; Hayashi-Nishino, M. Function and inhibitory mechanisms of multidrug efflux pumps. *Front. Microbiol.* **2021**, *12*, 737288. [CrossRef] [PubMed]
81. Babin, B.M.; Atangcho, L.; van Eldijk, M.B.; Sweredoski, M.J.; Moradian, A.; Hess, S.; Tolker-Nielsen, T.; Newman, D.K.; Tirrell, D.A. Selective proteomic analysis of antibiotic-tolerant cellular subpopulations in pseudomonas aeruginosa biofilms. *mBio* **2017**, *8*, e01593-17. [CrossRef]
82. Zimmermann, S.; Klinger-Strobel, M.; Bohnert, J.A.; Wendler, S.; Rödel, J.; Pletz, M.W.; Löffler, B.; Tuchscherr, L. Clinically approved drugs inhibit the Staphylococcus aureus multidrug norA efflux pump and reduce biofilm formation. *Front. Microbiol.* **2019**, *10*, 2762. [CrossRef] [PubMed]
83. Jaganathan, S.K. Can flavonoids from honey alter multidrug resistance? *Med. Hypotheses* **2011**, *76*, 535–537. [CrossRef]
84. Preda, V.G.; Sandulescu, O. Communication is the key: Biofilms, quorum sensing, formation and prevention. *Discoveries* **2019**, *7*, e100. [CrossRef]
85. Truchado, P.; Gil-Izquierdo, A.; Tomás-Barberán, F.; Allende, A. Inhibition by chestnut honey of N-Acyl-L-homoserine lactones and biofilm formation in Erwinia carotovora, Yersinia enterocolitica, and Aeromonas hydrophila. *J. Agric. Food Chem.* **2009**, *57*, 11186–11193. [CrossRef] [PubMed]
86. Nazzaro, F.; Fratianni, F.; Coppola, R. Quorum sensing and phytochemicals. *Int. J. Mol. Sci.* **2013**, *14*, 12607–12619. [CrossRef] [PubMed]
87. Imtara, H.; Elamine, Y.; Lyoussi, B. Honey Antibacterial Effect Boosting Using *Origanum vulgare* L. Essential Oil. *Evid.-Based Complement. Altern. Med.* **2018**, *7842583*, 14. [CrossRef] [PubMed]
88. Qasem, A.; Assaggaf, H.; Montesano, D.; Khalil, Z.; Al-Mijalli, S.H.; Baaboua, A.E.; El Omari, N.; El Menyiy, N.; Bakrim, S.; Sheikh, R.A.; et al. Determination of Chemical Compounds and Investigation of Biological Properties of *Matricaria chamomilla* Essential Oils, Honey, and Their Mixture. *Molecules* **2022**, *27*, 5850. [CrossRef]
89. Katekar, V.P.; Rao, A.B.; Sardeshpande, V.R. A hydrodistillation-based essential oils extraction: A quest for the most effective and cleaner technology. *Sustain. Chem. Pharm.* **2023**, *36*, 101270. [CrossRef]
90. Balázs, V.L.; Bordás, B.; Nagy-Radványi, L.; Ormai, E.; Kocsis, M.; Kocsis, B.; Farkas, Á.; Micalizzi, G.; Mondello, L.; Bencsik-Kerekes, E.; et al. Efficacy of lavender essential oil against respiratory tract bacteria is influenced by harvesting time. *Sci. Rep.* 2025; *under review*.
91. Nagy-Radványi, L.; Balázs, V.L.; Kocsis, B.; Csikós, E.; Ángyán, V.D.; Szabó, P.; Biró, V.; Kocsis, M.; Farkas, Á. Antibacterial activity of Hungarian varietal honeys against respiratory pathogens as a function of storage time. *Sci. Rep.* **2024**, *14*, 10200. [CrossRef]
92. Von Der Ohe, W.; Oddo, L.P.; Piana, M.L.; Morlot, M.; Martin, P. Harmonized Methods of Melissopalynology. *Apidologie* **2004**, *35*, 18–25. [CrossRef]
93. TCapture V4.3.0.605. 2022. Available online: https://www.tucsen.com/uploads/TCapture4.3.0.605.zip (accessed on 20 October 2022).
94. *Codex STAN 12-1981*; Revised Codex Standard for Honey. Codex Alimentarius Commission: Rome, Italy, 2001.
95. Bogdanov, S.; Lüllmann, C.; Martin, P. Harmonised methods of the European Honey Commission. *Apidologie* **1997**, *extra issue*, 1–59.
96. Beretta, G.; Granata, P.; Ferrero, M.; Orioli, M.; Facino, R.M. Standardization of antioxidant properties of honey by a combination of spectrophotometric/fluorimetric assays and chemometrics. *Anal. Chim. Acta* **2005**, *533*, 185–191. [CrossRef]
97. Hindler, J.A.; Jorgensen, J.H. Susceptibility test methods: Fastidious bacteria. In *Manual of Clinical Microbiology*, 10th ed.; Versalovic, J., Ed.; ASM Press: Washington, DC, USA, 2011; pp. 1180–1187.
98. Nagy-Radványi, L.; Ormai, E.; Koloh, R.; Ángyán, V.D.; Kocsis, B.; Bencsik-Kerekes, E.; Szabó, P.; Csikós, E.; Farkas, Á.; Horváth, G.; et al. Biofilm Inhibition Activity of Fennel Honey, Fennel Essential Oil and Their Combination. *Microorganisms* **2024**, *12*, 2309. [CrossRef]
99. *CLSI Document M 2-A10*; Performance Standards for Antimicrobial Disk Susceptibility Tests. 10th ed, Approved Standard. CLSI (Clinical and Laboratory Standards Institute): Wayne, PA, USA, 2009.
100. *CLSI Document M 100-S20*; Performance Standards for Antimicrobial Susceptibility Testing; 19th Informational Supplement. CLSI (Clinical and Laboratory Standards Institute): Wayne, PA, USA, 2010.
101. Patel, J.B.; Tenover, F.C.; Turnidge, J.D.; Jorgensen, J.H. Susceptibility test methods: Dilution and disk diffusion methods. In *Manual of Clinical Microbiology*, 10th ed.; Versalovic, J., Ed.; ASM Press: Washington, DC, USA, 2011; Volume 1, pp. 1122–1143.
102. *CLSI Document M07-A9*; Methods for Dilution Antimicrobial Susceptibility Tests for Bacteria That Grow Aerobically; Approved Standard, 9th ed. Clinical and Laboratory Standards Institute: Wayne, PA, USA, 2012.
103. Balázs, V.L.; Nagy-Radványi, L.; Bencsik-Kerekes, E.; Koloh, R.; Szabó, D.; Kocsis, B.; Kocsis, M.; Farkas, Á. Antibacterial and Antibiofilm Effect of Unifloral Honeys against Bacteria Isolated from Chronic Wound Infections. *Microorganisms* **2023**, *11*, 509. [CrossRef] [PubMed]
104. Peeters, E.; Nelis, H.J.; Coenye, T. Comparison of multiple methods for quantification of microbial biofilms grown in microtiter plates. *J. Microbiol. Methods* **2008**, *72*, 157–165. [CrossRef] [PubMed]

105. Kerekes, E.; Deák, É.; Takó, M.; Tserennadmid, R.; Petkovits, T.; Vágvölgyi, C.; Krisch, J. Anti-biofilm formatting and anti-quorum sensing activity of selected essential oils and their main components on food related microorganisms. *J. Appl. Microbiol.* **2013**, *115*, 933–942. [CrossRef] [PubMed]
106. Sun, Y.; Chen, S.; Zhang, C.; Liu, Y.; Ma, L.; Zhang, X. Effects of sub-minimum inhibitory concentrations of lemon essential oil on the acid tolerance and biofilm formation of Streptococcus mutans. *Arch. Oral Biol.* **2018**, *87*, 235–241. [CrossRef] [PubMed]
107. Bennis, S.; Chami, F.; Chami, N.; Bouchikhi, T.; Remmal, A. Surface Alteration of Saccharomyces Cerevisiae Induced by Thymol and Eugenol. *Lett. Appl. Microbiol.* **2004**, *38*, 454–458. [CrossRef]
108. Hammer, Ø.; Harper, D.A.; Ryan, P.D. PAST: Paleontological statistics software package for education and data analysis. *Palaeontol. Electron.* **2001**, *4*, 1–9.

Disclaimer/Publisher's Note: The statements, opinions and data contained in all publications are solely those of the individual author(s) and contributor(s) and not of MDPI and/or the editor(s). MDPI and/or the editor(s) disclaim responsibility for any injury to people or property resulting from any ideas, methods, instructions or products referred to in the content.

antibiotics

MDPI

Article

Pulsed Blue Light and Phage Therapy: A Novel Synergistic Bactericide

Amit Rimon [1,2,3], Jonathan Belin [1], Ortal Yerushalmy [1,3], Yonatan Eavri [4], Anatoly Shapochnikov [5], Shunit Coppenhagen-Glazer [1,3], Ronen Hazan [1,3,†] and Lilach Gavish [4,5,6,*,†]

1 Institute of Biomedical and Oral Research (IBOR), Faculty of Dental Medicine, The Hebrew University of Jerusalem, Jerusalem 9112102, Israel; amit.rimon@mail.huji.ac.il (A.R.); jonathan.belin@mail.huji.ac.il (J.B.); ortal.yerushalmy@mail.huji.ac.il (O.Y.); shunitc@ekmd.huji.ac.il (S.C.-G.); ronenh@ekmd.huji.ac.il (R.H.)
2 Tzameret, The Military Track of Medicine, The Hebrew University-Hadassah Medical School, Jerusalem 9112001, Israel
3 The Israeli Phage Therapy Center (IPTC) of the Hebrew University and Hadassah Medical Center, Jerusalem 9112001, Israel
4 Institute for Research in Military Medicine (IRMM), Faculty of Medicine, The Hebrew University of Jerusalem, Jerusalem 9112001, Israel; yonatan.eavri@gmail.com
5 The Department of Medical Neurobiology, Institute for Medical Research (IMRIC), Faculty of Medicine, The Hebrew University of Jerusalem, Jerusalem 9112001, Israel; anatolys@ekmd.huji.ac.il
6 The Saul and Joyce Brandman Hub for Cardiovascular Research, Jerusalem 9112001, Israel
* Correspondence: lilachg@ekmd.huji.ac.il; Tel.: +972-2-6758623; Fax: +972-2-6757660
† These authors contributed equally to this work.

Abstract: Background: Antibiotic-resistant *Pseudomonas aeruginosa* (*P. aeruginosa*) strains are an increasing cause of morbidity and mortality. Pulsed blue light (PBL) enhances porphyrin-induced reactive oxygen species and has been clinically shown to be harmless to the skin at low doses. Bacteriophages, viruses that infect bacteria, offer a promising non-antibiotic bactericidal approach. This study investigates the potential synergism between low-dose PBL and phage therapy against *P. aeruginosa* in planktonic cultures and preformed biofilms. **Methods:** We conducted a factorial dose–response in vitro study combining *P. aeruginosa-specific* phages with PBL (457 nm, 33 kHz) on both PA14 and multidrug-resistant PATZ2 strains. After excluding direct PBL effects on phage titer or activity, we assessed effectiveness on planktonic cultures using growth curve analysis (via *growth_curve_outcomes*, a newly developed, Python-based tool available on GitHub), CFU, and PFU. Biofilm efficacy was evaluated using CFU post-sonication, crystal violet staining, and live/dead staining with confocal microscopy. Finally, we assessed reactive oxygen species (ROS) as a potential mechanism using the nitro blue tetrazolium reduction assay. ANOVA or Kruskal–Wallis tests with post hoc Tukey or Conover–Iman tests were used for comparisons (n = 5 biological replicates and technical triplicates). **Results:** The bacterial growth lag phase was significantly extended for phage alone or PBL alone, with a synergistic effect of up to 144% ($p < 0.001$ for all), achieving a 9 log CFU/mL reduction at 24 h ($p < 0.001$). In preformed biofilms, synergistic combinations significantly reduced biofilm biomass and bacterial viability (% Live, median (IQR): Control 80%; Phage 40%; PBL 25%; PBL&Phage 15%, $p < 0.001$). Mechanistically, PBL triggered transient ROS in planktonic cultures, amplified by phage co-treatment, while a biphasic ROS pattern in biofilms reflected time-dependent synergy. **Conclusions:** Phage therapy combined with PBL demonstrates a synergistic bactericidal effect against *P. aeruginosa* in both planktonic cultures and biofilms. Given the strong safety profile of PBL and phages, this approach may lead to a novel, antibiotic-complementary, safe treatment modality for patients suffering from difficult-to-treat antibiotic-resistant infections and biofilm-associated infections.

Keywords: bacteriophage; phage therapy; photobiomodulation; blue light; biofilm; *Pseudomonas*

1. Introduction

1.1. Antibiotic-Resistant Bacteria and Biofilms

The rise in the prevalence and spread of antibiotic-resistant bacteria is a critical health concern, directly contributing to 1.27 million deaths in 2019 alone [1]. The genetic plasticity of bacterial populations, driven by selective pressures from the overuse of antibiotics in clinical, agricultural, and environmental settings, facilitates rapid bacterial adaptation and resistance mechanisms [2]. This phenomenon significantly diminishes the effectiveness of conventional antibiotic therapies, particularly in biofilms—structured bacterial communities encased in a self-produced extracellular matrix. These microbial aggregates enhance resistance to both antimicrobial agents and host immune responses, presenting substantial challenges in clinical and industrial environments [3]. *Pseudomonas aeruginosa* (PA), a Gram-negative rod, is one of the six leading pathogens responsible for antibiotic resistance-related deaths [1], and it frequently forms biofilms, especially in burns and other wounds [4]. Therefore, novel treatments, strategies, or combinations of approaches are urgently needed to combat this pathogen. In this study, we explore two such approaches and demonstrate their synergistic effects against PA.

1.2. Phage Therapy

A growing and revitalized approach to combat resistant bacteria is the use of bacteriophages (phages) [5], viruses that specifically target bacteria without harming eukaryotic cells. Phages are the most abundant biological entities on Earth, with an estimated 10^{31} particles worldwide [5]. Unlike antibiotics, which can affect a broad range of bacteria, phages target specific bacterial strains while largely sparing other microbiota [5]. One key advantage of phages as therapeutic agents is their ability to penetrate biofilm structures [6,7]. Furthermore, bacterial resistance to phages can be managed through novel phage isolation, phage engineering, or naturally through evolutionary changes [8]. Phage therapy has shown effectiveness against several antibiotic-resistant pathogens including *Pseudomonas aeruginosa*, *Staphylococcus aureus*, and *Cutibacterium acnes* [9–11], particularly in skin-related infections. Additionally, phage therapy has been successfully used in compassionate cases and case series [9,12] including by our team in the Israeli Phage Therapy Center (IPTC) to treat non-healing infections caused by antibiotic-resistant bacteria [13].

1.3. Pulsed Blue Light (PBL)

Another promising approach to combat resistant bacteria is antimicrobial blue light, which has been shown to be effective against both Gram-positive and Gram-negative bacteria, particularly antibiotic-resistant *P. aeruginosa* strains [14]. Blue light photons are absorbed by bacterial chromophores, such as porphyrins (notably coproporphyrin in *P. aeruginosa* [15,16]), leading to the generation of reactive oxygen species (ROS) that induce oxidative damage including to the bacterial membranes [17]. In addition to ROS-mediated effects, blue light has also been reported to directly depolarize the membrane potential and disrupt membrane integrity [17,18]. Clinical studies have demonstrated that blue light at low doses is harmless to the skin [19]. Pulsed blue light (PBL) has been found to have greater bactericidal efficacy compared to continuous blue light, requiring much lower power intensity and energy doses in planktonic cultures [20]. Additionally, PBL has been shown to partially disrupt and disassemble biofilm structures [21].

1.4. Study Rationale and Objective

The rise in antibiotic-resistant bacteria and the limited availability of new antibiotics [5] have created an urgent need for alternative treatments. In response, we explored the combination of pulsed blue light (PBL) and phage therapy as a novel non-antibiotic strategy. These two approaches target bacteria through distinct, complementary mechanisms: PBL generates reactive oxygen species (ROS) that disrupt bacterial membranes and biofilm structures [17,20], while phages specifically infect and lyse bacteria, including those within biofilms [6]. Given that both PBL and phages are effective against antibiotic-resistant pathogens, combining them may provide a synergistic effect that enhances bacterial eradication without contributing to the growing problem of antibiotic resistance.

This study aimed to assess the efficacy of combining PBL and phage therapy on both planktonic and biofilm cultures of *Pseudomonas aeruginosa*, a model organism frequently associated with antibiotic-resistant infections. By demonstrating the potential for synergy between these two non-antibiotic treatments, we hope to provide a new approach to combating resistant bacterial infections, particularly in biofilm-associated cases.

2. Results

2.1. Effect of PBL on Phage Number and Activity

To rule out the direct effect of 450 nm PBL on phages, we first exposed phages to the extended duration of PBL and quantified their titer and bactericidal activity. This was important for determining the timing of PBL administration in relation to phage administration. As expected, no reduction in the titer of either PAShipCat1 or PASA16 was observed after up to 3 h of PBL irradiation ($p > 0.5$ for both phages, by 1-way ANOVA). Furthermore, the bactericidal activity of the irradiated phages against planktonic cultures or preformed biofilms was not impaired, as assessed by CFU ($p < 0.001$ for all PBL doses) (Figure 1 and Supplemental Table S1).

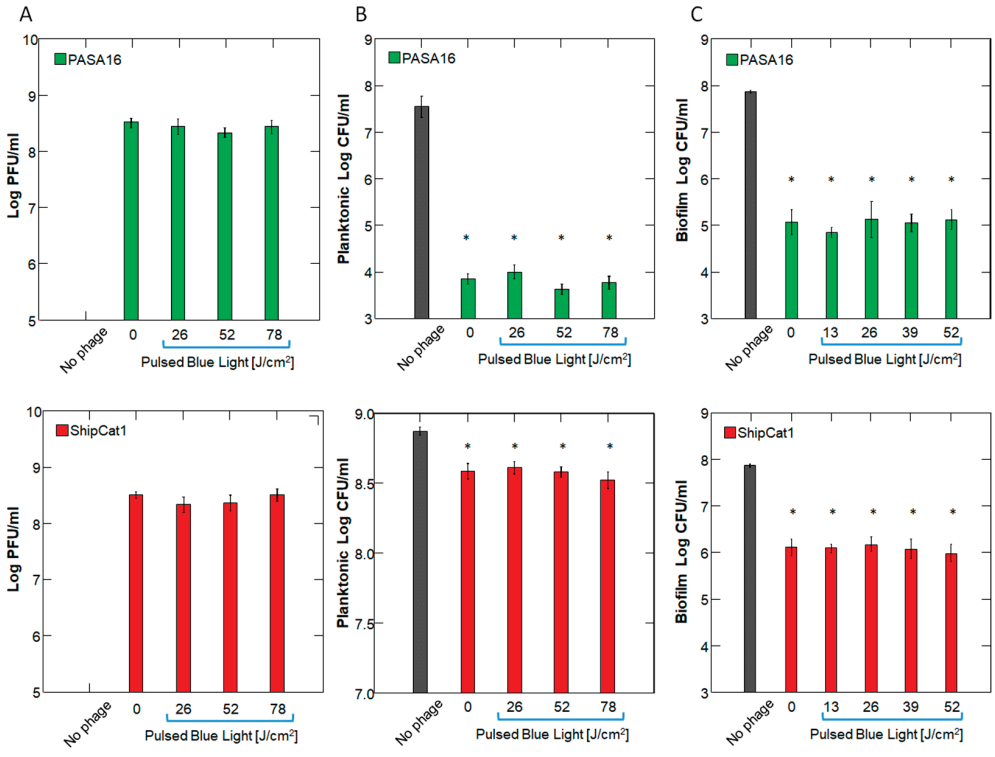

Figure 1. Effect of Direct Pulsed Blue Light (PBL) on Phage Stability. Phages PASA16 (upper row in green) and ShipCat1 (lower row in red) a were pre-exposed to PBL at 7.2 mW/cm^2 for 0, 1, 2, or 3 h

(0–78 J/cm^2). PA14 bacteria, either in planktonic cultures or in preformed biofilms, were then incubated with irradiated phages for 24 h. Bar graphs represent mean ± SEM for (**A**) viral titer (PFU/mL), (**B**) planktonic bacterial count, and (**C**) biofilm bacterial count post-sonication (CFU/mL). n = 5 biological repeats per dose (average of triplicates for each). Note that while both phages significantly reduced bacterial count, PBL did not affect viral count or bactericidal efficacy. * $p < 0.001$ compared to no phages, by ANOVA with Tukey's post hoc.

2.2. Timing of Administration and Dose/Concentration Response

After confirming that 457 nm 33 kHz PBL irradiation does not directly affect phage activity, we proceeded to evaluate the combination of PBL and phage treatments. Initially, we tested the combination using the lytic phage PASA16; however, due to its complete bactericidal effect (See Section 4 below), we isolated a novel, less effective phage with a lysogenic lifecycle, PAShipCat1, to assess the potential synergism between phage and PBL. The timing of phage addition to planktonic *P. aeruginosa* in relation to PBL was evaluated using PAShipCat1 (10^6 PFU) at 10, 90, and 150 min post-PBL treatment (8.5 J/cm^2). While PBL and phage treatments alone reduced the area under the curve (AUC) at the 20 h post-PBL treatment compared to the controls by 28% and 51%, respectively, their combination resulted in a 73% reduction, with the most effective timing being the 10 min post-PBL treatment (Figure 2A and Supplemental Table S2).

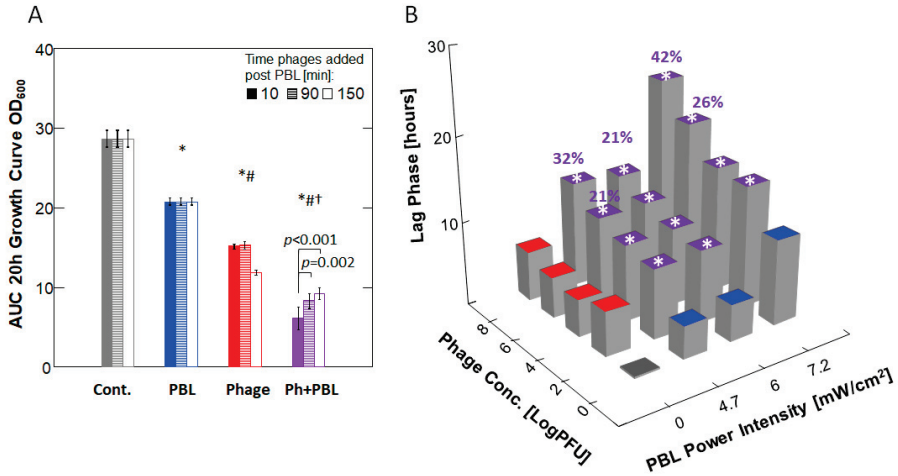

Figure 2. PBL and Phage Synergism Depend on Timing and Dose. (**A**) Bar graph showing the bactericidal effect in response to 8.5 J/cm^2 PBL, followed by the addition of 10^6 PFU Phage at 10, 90, or 150 min later. Bars represent the mean ± SD area under the growth curve (AUC) at 20 h; n = 4 (each data point is the average of triplicate technical repeats). The addition of phage at 10 min was the most effective. Statistical significance is indicated by *, #, and †, where $p < 0.001$ compared to control, PBL, and phage alone, respectively, as determined by a 2-way ANOVA with Tukey's post hoc test. (**B**) Three-dimensional bar graph showing the bactericidal effect in response to various dose combinations of PBL followed by phage addition. Bars represent the mean lag time (in hours) compared to control, with n = 5 (each data point is the average of triplicate technical repeats). All comparisons were statistically significant ($p < 0.001$), as determined by a 2-way ANOVA with Tukey's post hoc test. Additive effect: ±10% of expected; % synergistic effect: >20% over expected.

Using the above protocol, we tested the effect of different phage concentrations combined with various PBL power intensities. Phage treatment alone significantly extended the lag phase, as did PBL alone ($p < 0.001$ for all concentrations and power intensities). When PBL and phages were combined, an additive effect was observed at $10^2/10^4$ PFU/mL, while a synergistic effect of up to 144% was noted at higher phage concentrations (Figure 2B). This combination reduced CFU by 9 log in PA14 and also produced significant

results when applied to the multidrug-resistant (MDR) strain PATZ2, although to a lesser extent (Figure 3 and Supplemental Table S3).

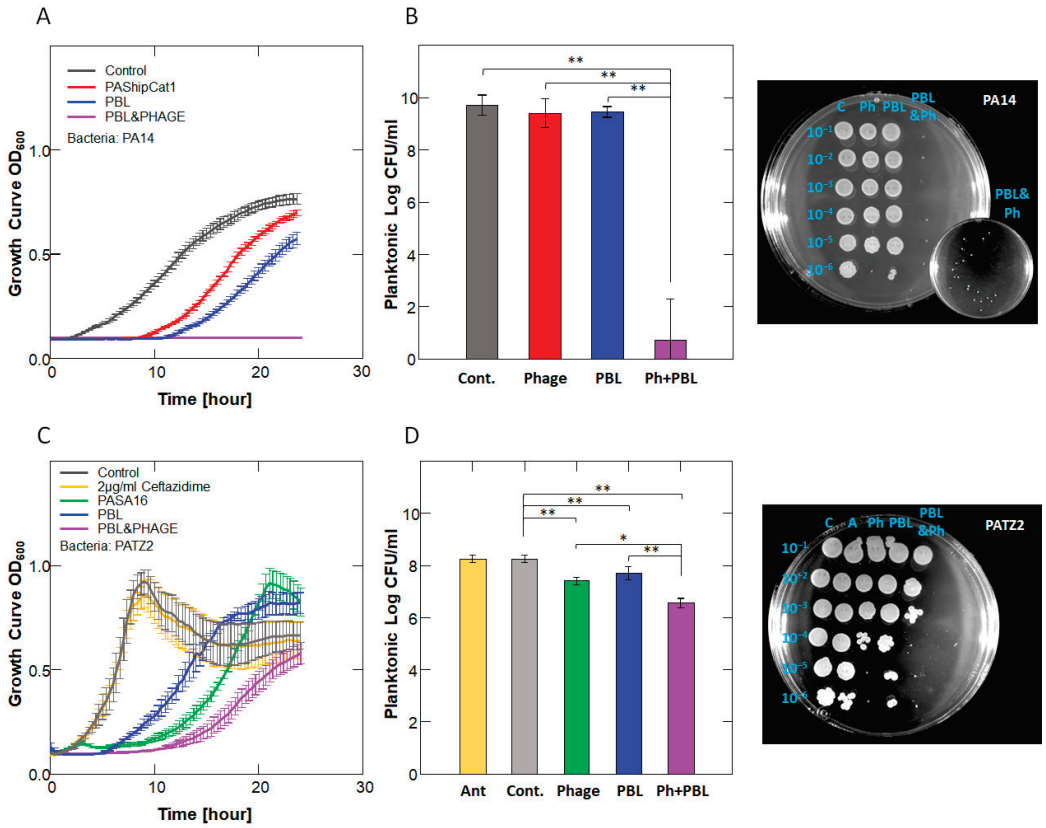

Figure 3. Differential Effects of PBL and Phage on *P. aeruginosa* Strains. *P. aeruginosa* strains were treated with or without 30 min of PBL (7.2 mW/cm^2) followed by phage (10^8 PFU/mL). Growth curves and CFU results are shown. (**A**,**B**) PA14 with PAShipCat1 + PBM: 9-log reduction. (**C**,**D**) Antibiotic-resistant PATZ2 with PASA16 + PBL: 1.5-log reduction. $n = 5$; representative spot titer plates for PA14 and PATZ2 (right) show serial dilutions (10^{-1} to 10^{-6}) after treatment with control, phage alone, PBL alone, or PBL plus phage. The PBL + Ph group shows the most pronounced reduction in viable colonies. Inset in PA14 plate shows rare surviving colonies from the combination treatment. * $p < 0.05$; ** $p < 0.001$. Bars represent mean ± SD.

2.3. Bacterial Viability and Biomass

Next, we assessed the effect of the PBL–phage combination on preformed biofilms. First, we evaluated the optimal timing for phage addition relative to the PBL doses. PASA16 phage was used, as it has greater anti-biofilm activity than PAShipcat1. Using crystal violet staining, we found that both PBL and phage treatments reduced biofilm biomass, with the most effective protocol being the addition of phage immediately before PBL regardless of the dose ($p < 0.001$ across doses, presence of phage, and timing of phage addition, by 3-way ANOVA) (Figure 4A and Supplemental Figure S1). Based on these results, we chose to add phage immediately before a 26 J/cm^2 PBL treatment for subsequent experiments.

CFU analysis revealed that this combination achieved a synergistic 3-log reduction (Figure 4B). Using live/dead staining, we found that all treatments significantly decreased bacterial viability ($p < 0.001$ vs. controls). However, while phage alone reduced bacterial viability by 50% compared to controls, the addition of PBL further reduced bacterial viability to 19% ($p = 0.012$ for PBL&Phage vs. Phage alone) (Figure 4C,D and Supplemental Table S4).

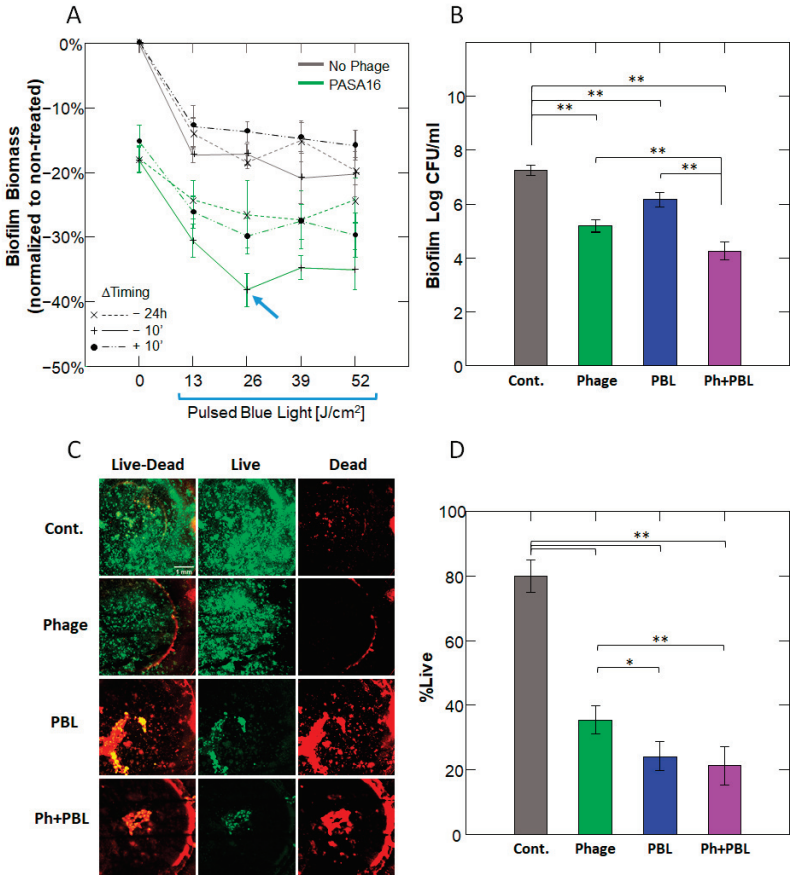

Figure 4. Biofilm Viability and Biomass Are Effectively Reduced Following PBL and Phage Treatment. (**A**) Percent reduction in biofilm biomass, normalized to non-treated controls, in response to different doses of PBL (0–52 J/cm^2) with phage added either 10 min before PBL or 10 min or 24 h after PBL, as determined by crystal violet staining. Lines were added for visualization. The most effective combination was a PBL dose of 26 J/cm^2 immediately after phage administration (blue arrow). Data points represent mean ± SEM. (**B**) CFU levels correspond to the most effective combination. ** $p < 0.001$, by 2-way ANOVA with Tukey's post hoc test. (**C**,**D**) Representative live-dead fluorescently stained biofilm samples from each experimental group, visualized at 4× magnification. The percent of live bacteria was determined according to Robertson et al. [22]. Maximal intensity projections of the Z-stack, constructed by confocal microscopy, were extracted from 17 sections at 12.5 µm intervals. Bars represent mean ± SD; $n = 5$; * $p < 0.05$; ** $p < 0.001$.

2.4. Reactive Oxidant Species

Finally, to determine the mechanism underlying the synergistic effect, we measured the level of intracellular reactive oxygen species. In planktonic culture, PBL induced an immediate increase in ROS that was significantly amplified to 169% of the controls with the addition of phage ($p < 0.001$). In the biofilm, no change in ROS levels was observed with PBL or phage alone. However, ROS levels following the addition of the combination exhibited a biphasic modulation over time, with a significant decrease at 1 h after the addition of phage but a significant increase at 3 h (65% and 154% of controls; $p = 0.012$ and $p = 0.002$, respectively, Figure 5 and Supplemental Table S5).

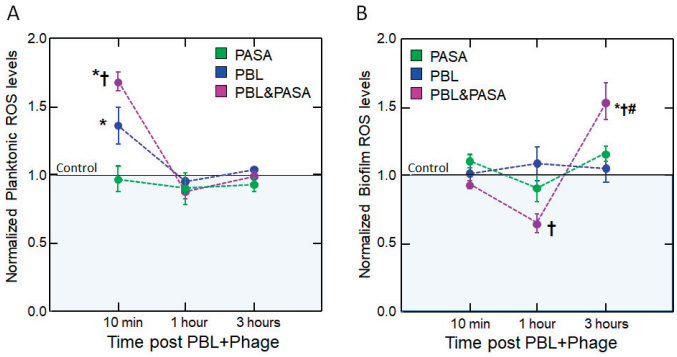

Figure 5. Reactive oxygen species (ROS) levels are altered following PBL and phage treatment. ROS levels (normalized to untreated controls; horizontal line = 1) were measured at 10 min, 1 h, and 3 h after pulsed blue light (PBL) treatment, with or without subsequent phage addition, in *P. aeruginosa* cultures. (**A**) In planktonic cultures, PBL induced an immediate increase in ROS, further enhanced by phage. (**B**) In biofilms, combined PBL and phage treatment triggered a biphasic ROS response. Points represent mean ± SEM; $n = 5$ (average of triplicates); $p < 0.05$ * vs. control, † vs. PBL, and # vs. PASA by ANOVA + Tukey.

3. Discussion

Antibiotic-resistant bacteria are a major health concern. In this study, we explored a combination of two non-antibiotic bactericidal techniques: pulsed blue light (PBL) and phage therapy. While combining antibiotics with phages has shown promise, the overuse of antibiotics is driving resistance, making non-antibiotic options increasingly important [23].

PBL and phage therapy are innovative because both therapies act independently of antibiotics. PBL damages bacterial cell structures and increases susceptibility to phages, which specifically target bacteria for lysis. Additionally, whereas antibiotics can harm beneficial bacteria and promote resistance [23,24], PBL can be applied locally, minimizing systemic side effects, and phages are strain-specific. Thus, PBL and phage therapy offer a focused, non-antibiotic alternative that could address antibiotic resistance while maintaining high bactericidal efficacy.

The results of this study show that both planktonic and biofilm cultures of *P. aeruginosa* are highly susceptible to combined treatment of phage therapy and pulsed blue light. The synergistic effect of this combination led to a 9-log reduction in planktonic cultures and a 40% reduction in preformed biofilms. The most effective bactericidal results were observed at a dose of 26 J/cm^2, with 10^8 PFU/mL phage added within 10 min of PBL administration. This combination of PA-targeted phage therapy and low-dose, no-risk pulsed blue light presents a promising strategy for treating superficial wound infections, such as burns, acne, diabetic foot ulcers, and cellulitis. Additionally, it could enhance biofilm management, a growing escalating challenge in the context of antibiotic resistance [1].

3.1. Phages and Antibiotics

Phage therapy has a well-established safety profile, supported by numerous clinical trials and compassionate use cases, and has shown efficacy with minimal adverse effects in treating *Pseudomonas aeruginosa* infections [25]. Currently, phage therapy is usually combined with antibiotic treatment [26]. Lin et al. reported that the effectiveness of the combination depends on the *P. aeruginosa* strain and the antibiotic used. For example, phage PEV20 achieved complete inhibition in planktonic cultures when combined with ciprofloxacin but not with amikacin or colistin [27]. However, Knezevic et al. reported that the combination with ciprofloxacin led to only a 3.3-log reduction in PA [28]. Similarly, in this study, we observed complete inhibition of planktonic PA14 but partial inhibition of MDR PATZ2. Interestingly, antibiotics alone were ineffective in reducing *Pseudomonas*

biofilm biomass [29,30]. However, Chaudhry et al. demonstrated that combining 10 μg/mL ciprofloxacin with phages resulted in a 47–74% reduction in biofilm biomass from a clinical cystic fibrosis *P. aeruginosa* strain, which was higher than the 40% synergistic effect observed in the current study [29]. Although increasing the PBL dose did not further reduce biomass (Figure 4A), increasing the power intensity may enhance eradication efficacy (Figure 3B), which will be the focus of future studies.

3.2. Blue Light

While blue light may be harmful to the eyes, skin exposure has been clinically determined to be harmless [19]. Clinical studies demonstrate that low doses of PBL is harmless to the skin, and LED patches with similar specifications are FDA-approved and available for consumer use in the USA [19]. Pulsed blue light in similar frequencies and doses is sold commercially as LED patches (in combination with red LEDs) for personal health-related use in the USA and has FDA approval (https://www.carewear.net/). In a clinical study, healthy volunteers were exposed to a daily dose of 100 J/cm^2 of 420 nm blue light for 5 consecutive days. No indication of DNA damage, inflammation, or apoptosis was detected in their skin biopsies, although transient keratinocyte melanogenesis and vacuolization were observed [31]. The bactericidal effect of continuous blue light has been extensively studied, with special attention given to the trade-off between power and dose to avoid a photothermal effect: Rupel et al. used 455 nm blue light with an irradiance of 300 mW/cm^2 and a dose of 60 or 120 J/cm^2 to irradiated planktonic cultures of *P. aeruginosa* achieving inhibition for 24 h [32]. In the current study, we achieved a post-infection 9-log CFU/mL reduction using a similar wavelength, 7.2 mW/cm^2 irradiance, and a dose of 13 J/cm^2. Pulsed light allows for higher peak power densities compared to those used in continuous wave treatments, without exposing the skin to excessive tissue heating [20]. Indeed, PBL in very low average irradiances and doses has been shown to be superior to continuous wave light. Bumah et al. demonstrated that PBL, using multiple 30 min sessions of 450 nm PBL at doses of 7.6 J/cm^2 or lower, was more effective than continuous wave light at similar doses. They reported a 7-log CFU/mL reduction in planktonic cultures and 64% and 53% suppression of biofilms in *C. acnes* and MRSA, respectively [21]. In comparison, we achieved a 9-log reduction in planktonic *P. aeruginosa* culture and 40% suppression of pre-formed *P. aeruginosa* biofilms, highlighting the variability of the response between different bacterial species.

3.3. Practical Considerations

We found that the most effective timing for treatment was administering PBL immediately after phage administration in biofilm cultures (Figures 3 and 4). The synergistic effect remained significant even when phage was administered 24 h before PBL, as would be the case with intravenous or oral phage delivery [33]. Our study utilized pulsed blue light with clinically applicable power density and pulse frequency [21,34], making our findings relevant to potential clinical applications [35]. Notably, one of the two phages used, PASA16, has previously been involved in various compassionate clinical treatments [9].

3.4. Possible Mechanisms

The proposed synergy between phage therapy and pulsed blue light (PBL) likely involves multiple mechanisms, including lysogen activation, which similar to ultraviolet light [36] and overwhelms the cell's DNA repair mechanisms, as both treatments cause DNA damage [37], and ROS induction, which we tested as part of this study. In planktonic cultures, we observed that PBL immediately induces ROS, which is known to activate bacterial antioxidant defenses [38], and has also been shown to cause membrane perturbations (Enwemeka et al., 2017 and 2021 [17,18]). The increased ROS levels may facilitate

phage entry, intensifying oxidative stress. However, biofilms present a more complex scenario. Repeated PBL exposure likely triggered early antioxidant responses in biofilm-residing cells, buffering ROS levels and preventing detectable accumulation. Meanwhile, phage infection was delayed due to the expected interference of virion diffusion via the extracellular polymeric substance [39]. In the combined treatment, membrane damage by PBL facilitated phage entry and likely accelerated the infection rate, prompting a stronger antioxidant surge that suppressed ROS at 1 h. By 3 h, progressing phage replication and cell lysis may have released secondary ROS [40]. Future experiments should aim to validate this hypothesis by measuring antioxidant gene expression, intracellular iron levels, and membrane integrity at key time points.

3.5. Limitations

This study was limited by its focus on only two phages (PASA16 and PAShipCat1) and two *P. aeruginosa* strains (PA14 and PATZ2), which restricts the generalizability of our findings. The treatment duration of 30 min may also be considered lengthy in practical applications. However, we used very low-dose PBL, which was effective and presented the opportunity to explore higher doses that could reduce treatment time, all while remaining harmless to the skin.

4. Materials and Methods

4.1. Study Design

In this study, we employed a factorial dose–response design involving combinations of phage concentrations and PBL power densities to test their bactericidal effect against *P. aeruginosa* planktonic cultures during the logarithmic phase and on pre-formed biofilms (Figure 6A–E).

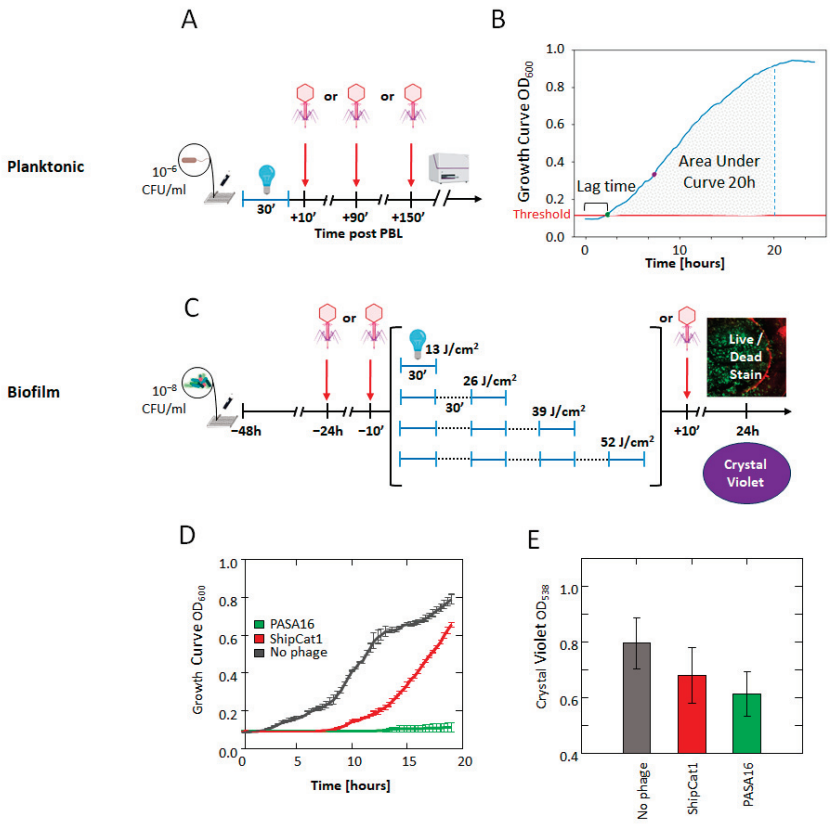

Figure 6. Study Design. (**A**) Phage was added to planktonic *P. aeruginosa* (PA14) at 10, 90, or 150 min after 30 min pulsed blue light (PBL) treatment. The bacteria were transferred to a spectrophotometer

for 24 h to generate growth curves. (**B**) Measures of bactericidal effect were extracted from the growth curves, including lag time (the duration until reaching the threshold) and area under the curve at 20 h (AUC 20). (**C**) Biofilms of PA14 were formed, and phage was added 24 h and 10 min before PBL or 10 min after. PBL consisted of multiple 30 min irradiations with 30 min intervals. Crystal violet or live/dead staining was used to evaluate biofilm biomass and bacterial viability. (**D**) Phage selection for experiments with planktonic bacteria: Growth curve analysis revealed that PASA16 completely eradicated PA14, while PAShipCat1 exhibited moderate effectiveness, allowing for further investigation of its synergistic potential with PBL. (**E**) Phage selection for biofilm experiments: Crystal violet staining showed that PAShipCat1 reduced biofilm biomass with limited efficacy, whereas PASA16 demonstrated moderate efficacy and was selected for subsequent biofilm analysis. This figure was created with Biorender.com.

4.2. Bacteria and Growth Conditions

4.2.1. Bacterial Strains

The bacteria used in this study were the reference *Pseudomonas aeruginosa* strain PA14 [41], obtained from our laboratory stock collection, and the multidrug-resistant strain MDR PATZ2, which was isolated from a clinical phage therapy case in our institution [9]. MDR PATZ2 was determined to be resistant to 2 μg/mL Ceftazidime (Panpharma Z.I, Luitre, France). Antibiotic resistance was assessed by the Hadassah Medical Center Clinical Microbiology Laboratory.

4.2.2. Planktonic Bacteria

Bacteria were grown from a −80 °C stock overnight in Luria Bertani (LB) medium at 37 °C under continuous agitation at 60 RPM. The cultures were then diluted 1:1000 and re-grown in LB. Bacteria at the mid-logarithmic phase ($OD_{600} \cong 0.5$) were used for the experiments.

4.2.3. Biofilm

Bacteria (200 μL/well, 10^8 CFU/mL) were grown overnight and then transferred into the inner wells of a 96-well plate made from virgin polypropylene, where they were incubated for 48 h. The outer wells were filled with double-distilled water to prevent uneven evaporation [42].

4.3. Phage Strains

In this study, we used two phage strains specific for PA: one lytic and the other lysogenic (PASA16 and PAShipCat1, respectively).

The phage PASA16 was previously isolated and characterized in our lab [43] and has been used in various clinical compassionate treatments [9]. As described previously [43], PAShipCat1 is a novel lysogenic phage isolated and characterized in this work [44].

These phages were deliberately chosen due to their moderate effects, which allowed us to observe potential synergistic effects with the PBL, despite their varying efficacy.

4.4. PBL

The light source was designed in-house to provide uniform irradiation over a 96-well plate inside a humid incubator (Figure 7). The irradiating surface consisted of 457 nm blue LED strips (Shenzhen Dengsum Optoelectronics Co., Ltd., Shenzhen, China) with high-lumen 2835 SMD chips (Epistar Corp., Hsinchu, Taiwan) arranged at a density of 120 LEDs/m. The device was powered by an LED driver (LCM-40, Mean Well Enterprises Co., Ltd., New Taipei City, Taiwan). Pulses, with a frequency of 33 kHz and a 50% duty cycle, were generated using an electronic circuit based on a 555 pulse generator module. Power density was measured at the plane of the cells using a LaserMate power meter (Coherent, Auburn group, Coherent-Europe, Utrecht, The Netherlands). The PBL frequency and initial

power density were based on published experiments by Enwemeka et al. in collaboration with CareWear company (Reno, NV, USA) [17,20,21].

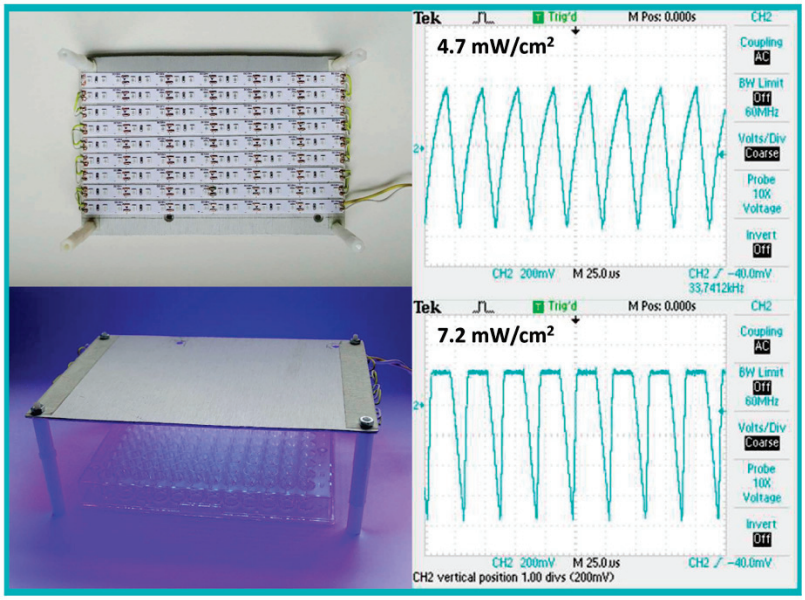

Figure 7. Pulsed Blue Light Source. Photograph of the pulsed blue light source used in this study, designed to uniformly irradiate a 96-well plate at a distance of 5 cm within a humid incubator. Stripes of 460 nm LEDs (A total of 153 LEDs) were attached to an aluminum surface and electrically interconnected. Power was supplied through an LED driver with a 555 pulse generator module. Waveform and frequency were measured using an oscilloscope connected to a light detector. Pulses were generated at a frequency of 33 kHz with a 50% duty cycle, and their waveforms were triangular and rectangular, corresponding to intensities of 4.7 and 7.2 mW/cm^2, respectively.

4.5. Quantification Methods

4.5.1. CFU

Samples were serially diluted 10-fold onto LB agar plates and incubated overnight at 37 °C. The number of colonies was counted, and the concentration of CFU was calculated.

4.5.2. PFU

The lysate was diluted 10-fold in LB broth and spotted onto a PA14 bacterial lawn grown on soft 0.6% agar, then incubated overnight at 37 °C. Plaques were observed and counted, and the concentration of PFU was calculated.

4.5.3. Growth Curves

Lytic activity was assessed by inoculating logarithmic *P. aeruginosa* (10 CFU/mL) with the experimental samples and measuring turbidity with a plate reader (Synergy, Gen5; BioTek, Winooski, VT, USA) at OD_{600nm} at 37 °C, with 5- s shaking every 20 min for 24 h. The data were smoothed using a 4-point rolling average. The threshold for growth curve detection was based on the measurements of the control group. The lag time is defined as the time (in hours) required for the OD to exceed the detection threshold, and the area under the curve at 20 h (AUC 20 h), which represents the growth potential (Figure 5B), was automatically extracted using the Python code *growth_curve_outcomes version 1.0* developed for this study. This code can be easily applied to plate reader growth curve data and is freely accessible on GitHub (https://github.com/bioimagehuji/growth_curve_outcomes/) (accessed on 5 May 2025).

4.5.4. Biofilm CFU

Biofilms were washed with a saline solution and then mechanically removed using a sterile tip. The contents of each well were transferred into a 1.5 mL tube, and the tubes were placed in a SONOREX sonication water bath (Bandelin, Berlin, Germany) for 5 min to effectively disrupt the biofilm. Next, 5 µL of 10-fold serial dilutions were plated on LB agar plates and incubated for 24 h, and colonies were counted.

4.5.5. Biofilm Biomass Detection

Biofilm biomass was measured using crystal violet staining [45] (Glentham Life Sciences, Corsham, UK). The liquid containing unattached bacteria was removed by pipetting, and the wells were rinsed with 100 µL of 0.9% NaCl and dried. A solution of 0.1% crystal violet was added to the wells (125 µL per well) and incubated for 15 min at room temperature. The dye was removed, and the wells were rinsed twice in a distilled water bath. The plate was dried at 37 °C for 1 h, and color was extracted with 30% acetic acid (100 µL per well). The purple-colored solution was transferred into a new plate, and OD_{550nm} was determined using The Synergy H1 plate reader (Agilent Technologies, Winooski, VE, USA) [45].

4.5.6. Live-Dead Stain

Bacterial viability was measured using the Live/Dead Cell Viability Kit (Invitrogen, Waltham, MA, USA) according to the manufacturer's instructions. Propidium iodide stained the dead cells red, while SYTO9 stained the live cells green (measured at 630 nm and 520 nm, respectively). The fluorescence emissions of the samples were detected using a Zeiss LSM410 confocal laser microscope (Carl Zeiss, Oberkochen, Germany) at ×4 and ×20 magnification. The maximal intensity of the Z-stack for each color was determined from multiple horizontal optical sections (17 sections at 12.5 µm intervals for ×4 and 9 sections at 10 µm intervals for ×20). Three separate fields per sample were measured using ImageJ, version 1.54 and the percentage of live bacteria was calculated as the proportion of the total bacteria following Robertson et al. [22].

4.5.7. ROS Determination

Intracellular ROS levels were assessed using the nitro blue tetrazolium (NBT) assay (Cayman Chemical, Ann Arbor, MI, USA), which measures the reduction in NBT to formazan. At 10 min, 1 h, and 3 h posttreatment, 10 µL of NBT solution (2 mg/mL, freshly prepared by 1:10 dilution of a 20 mg/mL stock in DMSO) was added directly to each sample well. Absorbance at 560 nm was recorded using the Synergy H1 plate reader [46].

4.5.8. Statistics

Data are presented as mean ± SD or median (interquartile range) as appropriate. The results represent the mean of five independent experiments, each with triplicate measurements (unless otherwise stated). ANOVA or Kruskal–Wallis was used to compare the groups with Tukey or Conover–Iman post hoc tests, as appropriate. A p-value < 0.05 was considered statistically significant. Statistical analyses were performed using SYSTAT, version 13 (Systat Software, Chicago, IL, USA).

5. Conclusions

We present a novel bactericidal synergistic combination of phage therapy and low-dose pulsed blue light, demonstrating effectiveness against both planktonic and preformed biofilms of *Pseudomonas aeruginosa* and proposing a mechanistic explanation for the synergistic effect based on the initial stimulation of ROS generation. Future research should

include a broader range of bacterial strains, additional phages, and a comprehensive exploration of the underlying mechanisms. Regarding safety, although both phage therapy and low-dose PBL each have a high safety profile and were applied to humans, biocompatibility studies of the combined treatment in wound models are warranted. Finally, clinical trials should assess the clinical implications of the treatment proposed here for patients suffering from antibiotic-resistant superficial infections.

Supplementary Materials: The following supporting information can be downloaded at https://www.mdpi.com/article/10.3390/antibiotics14050481/s1. Supplementary Table S1: PBL effect on phage stability; Supplementary Table S2: The effect of timing of phage addition; Supplementary Table S3: The effect of combinatorial treatment on antibiotic resistance bacteria PATZ2; Supplementary Table S4: The effect of PBL and phage on bacterial viability; Supplementary Table S5: The effect of PBL and phage on ROS levels; Supplementary Figure S1: The effect of PBL and either PASA16 or PAShipcat1 on biofilm biomass.

Author Contributions: Conceptualization, A.R., S.C.-G., R.H. and L.G.; methodology, A.R., J.B., O.Y., A.S., S.C.-G., R.H. and L.G.; software, Y.E. and L.G.; resources, R.H. and L.G.; data curation, A.R. and J.B.; writing—original draft, A.R. All authors have read and agreed to the published version of the manuscript.

Funding: The Milgrom Family Fund Grant#3015005877 (L.G., A.R., and R.H.); The United States–Israel Binational Science Foundation Grant #2017123 (R.H.); The Israel Science Foundation IPMP Grant #ISF1349/20 (R.H.); The Rosetrees Trust Grant A2232 (R.H.); The Stuart Roden Family (Lansdowne Partners) Research Fund, London, UK (L.G.); The Alexander Grass Family Research Fund (L.G.); The Bruce and Baila Waldholtz Research Fund (L.G.); The Foulks Foundation scholarship for MD-PhD students (A.R.).

Institutional Review Board Statement: Not applicable.

Informed Consent Statement: Not applicable.

Data Availability Statement: Phage genomes were deposited in the https://www.ncbi.nlm.nih.gov/genbank/ (accessed on 5 May 2025), and the accession numbers are MT933737.1 (PASA16) and PP067092 (PAShipCat1). The datasets generated during and/or analyzed during the current study are available from the corresponding author upon reasonable request. The *growth_curve_outcomes* Python tool version 1.0 can be accessed in Git Hub (https://github.com/bioimagehuji/growth_curve_outcomes/).

Acknowledgments: The authors gratefully acknowledge the expert technical assistance of Eduard Berenshtein from the Electron Microscopy Laboratory, Abed Nasereddin and Idit Shiff from the Genomics Applications Laboratory, and Yariv Marom of The Core Research Facility (CRF), Faculty of Medicine. During the preparation of this work, the author(s) used ChatGPT to improve the readability and language of the manuscript. After using this tool/service, the author(s) reviewed and edited the content as needed and take(s) full responsibility for the content of the published article.

Conflicts of Interest: The authors declare that they have no conflicts of interest.

References

1. Murray, C.J.L.; Ikuta, K.S.; Sharara, F.; Swetschinski, L.; Aguilar, G.R.; Gray, A.; Han, C.; Bisignano, C.; Rao, P.; Wool, E. Global Burden of Bacterial Antimicrobial Resistance in 2019: A Systematic Analysis. *Lancet* **2022**, *399*, 629–655. [CrossRef] [PubMed]
2. Schuts, E.C.; Hulscher, M.E.J.L.; Mouton, J.W.; Verduin, C.M.; Stuart, J.W.T.C.; Overdiek, H.W.P.M.; van der Linden, P.D.; Natsch, S.; Hertogh, C.M.P.M.; Wolfs, T.F.W.; et al. Current Evidence on Hospital Antimicrobial Stewardship Objectives: A Systematic Review and Meta-Analysis. *Lancet Infect. Dis.* **2016**, *16*, 847–856. [CrossRef] [PubMed]
3. Flemming, H.-C.; Wingender, J. The Biofilm Matrix. *Nat. Rev. Microbiol.* **2010**, *8*, 623–633. [CrossRef] [PubMed]
4. Mulcahy, L.R.; Isabella, V.M.; Lewis, K. *Pseudomonas aeruginosa* Biofilms in Disease. *Microb. Ecol.* **2014**, *68*, 1–12. [CrossRef]
5. Strathdee, S.A.; Hatfull, G.F.; Mutalik, V.K.; Schooley, R.T. Phage Therapy: From Biological Mechanisms to Future Directions. *Cell* **2023**, *186*, 17–31. [CrossRef]

6. Pires, D.P.; Meneses, L.; Brandão, A.C.; Azeredo, J. An Overview of the Current State of Phage Therapy for the Treatment of Biofilm-Related Infections. *Curr. Opin. Virol.* **2022**, *53*, 101209. [CrossRef] [PubMed]
7. Chang, C.; Yu, X.; Guo, W.; Guo, C.; Guo, X.; Li, Q.; Zhu, Y. Bacteriophage-Mediated Control of Biofilm: A Promising New Dawn for the Future. *Front. Microbiol.* **2022**, *13*, 825828. [CrossRef]
8. Meile, S.; Du, J.; Dunne, M.; Kilcher, S.; Loessner, M.J. Engineering Therapeutic Phages for Enhanced Antibacterial Efficacy. *Curr. Opin. Virol.* **2022**, *52*, 182–191. [CrossRef]
9. Onallah, H.; Hazan, R.; Nir-Paz, R.; Brownstein, M.J.; Fackler, J.R.; Hopkins, R.; Basu, S.; Yerushalmy, O.; Alkalay-Oren, S.; Braunstein, R. Refractory *Pseudomonas aeruginosa* Infections Treated with Phage PASA16: A Compassionate Use Case Series. *Med* **2023**, *4*, 600–611. [CrossRef]
10. Technophage, S. Bacteriophage Therapy TP-102 in Diabetic Foot Ulcers (REVERSE). Available online: https://clinicaltrials.gov/ct2/show/NCT04803708 (accessed on 5 May 2025).
11. Rimon, A.; Rakov, C.; Lerer, V.; Sheffer-Levi, S.; Oren, S.A.; Shlomov, T.; Shasha, L.; Lubin, R.; Zubeidat, K.; Jaber, N. Topical Phage Therapy in a Mouse Model of *Cutibacterium acnes*-Induced Acne-like Lesions. *Nat. Commun.* **2023**, *14*, 1005. [CrossRef]
12. Onallah, H.; Hazan, R.; Nir-Paz, R. Compassionate Use of Bacteriophages for Failed Persistent Infections During the First 5 Years of the Israeli Phage Therapy Center. In *Open Forum Infectious Diseases*; Oxford University Press: New York, NY, USA, 2023; Volume 10, p. ofad221.
13. Yerushalmy, O.; Braunstein, R.; Alkalay-Oren, S.; Rimon, A.; Coppenhagn-Glazer, S.; Onallah, H.; Nir-Paz, R.; Hazan, R. Towards Standardization of Phage Susceptibility Testing: The Israeli Phage Therapy Center "Clinical Phage Microbiology"—A Pipeline Proposal. *Clin. Infect. Dis.* **2023**, *77*, S337–S351. [CrossRef] [PubMed]
14. Wang, Y.; Wu, X.; Chen, J.; Amin, R.; Lu, M.; Bhayana, B.; Zhao, J.; Murray, C.K.; Hamblin, M.R.; Hooper, D.C. Antimicrobial Blue Light Inactivation of Gram-Negative Pathogens in Biofilms: In Vitro and in Vivo Studies. *J. Infect. Dis.* **2016**, *213*, 1380–1387. [CrossRef] [PubMed]
15. Hamblin, M.R.; Abrahamse, H. Can Light-based Approaches Overcome Antimicrobial Resistance? *Drug Dev. Res.* **2019**, *80*, 48–67. [CrossRef]
16. Amin, R.M.; Bhayana, B.; Hamblin, M.R.; Dai, T. Antimicrobial Blue Light Inactivation of *Pseudomonas aeruginosa* by Photo-excitation of Endogenous Porphyrins: In Vitro and in Vivo Studies. *Lasers Surg. Med.* **2016**, *48*, 562–568. [CrossRef] [PubMed]
17. Bowman, C.; Bumah, V.V.; Niesman, I.R.; Cortez, P.; Enwemeka, C.S. Structural Membrane Changes Induced by Pulsed Blue Light on Methicillin-Resistant *Staphylococcus aureus* (MRSA). *J. Photochem. Photobiol. B* **2021**, *216*, 112150. [CrossRef]
18. Biener, G.; Masson-Meyers, D.S.; Bumah, V.V.; Hussey, G.; Stoneman, M.R.; Enwemeka, C.S.; Raicu, V. Blue/Violet Laser Inactivates Methicillin-Resistant *Staphylococcus aureus* by Altering Its Transmembrane Potential. *J. Photochem. Photobiol. B* **2017**, *170*, 118–124. [CrossRef]
19. Hadi, J.; Wu, S.; Brightwell, G. Antimicrobial Blue Light versus Pathogenic Bacteria: Mechanism, Application in the Food Industry, Hurdle Technologies and Potential Resistance. *Foods* **2020**, *9*, 1895. [CrossRef]
20. Masson-Meyers, D.S.; Bumah, V.V.; Castel, C.; Castel, D.; Enwemeka, C.S. Pulsed 450 Nm Blue Light Significantly Inactivates *Propionibacterium acnes* More than Continuous Wave Blue Light. *J. Photochem. Photobiol. B* **2020**, *202*, 111719. [CrossRef]
21. Bumah, V.V.; Masson-Meyers, D.S.; Enwemeka, C.S. Pulsed 450 Nm Blue Light Suppresses MRSA and *Propionibacterium acnes* in Planktonic Cultures and Bacterial Biofilms. *J. Photochem. Photobiol. B* **2020**, *202*, 111702. [CrossRef]
22. Robertson, J.; McGoverin, C.; Vanholsbeeck, F.; Swift, S. Optimisation of the Protocol for the LIVE/DEAD® BacLightTM Bacterial Viability Kit for Rapid Determination of Bacterial Load. *Front. Microbiol.* **2019**, *10*, 801. [CrossRef]
23. Kumar, M.; Sarma, D.K.; Shubham, S.; Kumawat, M.; Verma, V.; Nina, P.B.; Jp, D.; Kumar, S.; Singh, B.; Tiwari, R.R. Futuristic Non-Antibiotic Therapies to Combat Antibiotic Resistance: A Review. *Front. Microbiol.* **2021**, *12*, 609459. [CrossRef]
24. Chen, X.; Mendes, B.G.; Alves, B.S.; Duan, Y. Phage Therapy in Gut Microbiome. *Prog. Mol. Biol. Transl. Sci.* **2023**, *201*, 93–118. [PubMed]
25. Stacey, H.J.; De Soir, S.; Jones, J.D. The Safety and Efficacy of Phage Therapy: A Systematic Review of Clinical and Safety Trials. *Antibiotics* **2022**, *11*, 1340. [CrossRef] [PubMed]
26. Segall, A.M.; Roach, D.R.; Strathdee, S.A. Stronger Together? Perspectives on Phage-Antibiotic Synergy in Clinical Applications of Phage Therapy. *Curr. Opin. Microbiol.* **2019**, *51*, 46–50. [CrossRef]
27. Lin, Y.; Chang, R.Y.K.; Britton, W.J.; Morales, S.; Kutter, E.; Chan, H.-K. Synergy of Nebulized Phage PEV20 and Ciprofloxacin Combination against *Pseudomonas aeruginosa*. *Int. J. Pharm.* **2018**, *551*, 158–165. [CrossRef] [PubMed]
28. Knezevic, P.; Curcin, S.; Aleksic, V.; Petrusic, M.; Vlaski, L. Phage-Antibiotic Synergism: A Possible Approach to Combatting *Pseudomonas aeruginosa*. *Res. Microbiol.* **2013**, *164*, 55–60. [CrossRef]
29. Chaudhry, W.N.; Concepcion-Acevedo, J.; Park, T.; Andleeb, S.; Bull, J.J.; Levin, B.R. Synergy and Order Effects of Antibiotics and Phages in Killing *Pseudomonas aeruginosa* Biofilms. *PLoS ONE* **2017**, *12*, e0168615. [CrossRef]
30. Ciofu, O.; Rojo-Molinero, E.; Macià, M.D.; Oliver, A. Antibiotic Treatment of Biofilm Infections. *Apmis* **2017**, *125*, 304–319. [CrossRef]

31. Kleinpenning, M.M.; Smits, T.; Frunt, M.H.A.; Van Erp, P.E.J.; Van De Kerkhof, P.C.M.; Gerritsen, R.M.J.P. Clinical and Histological Effects of Blue Light on Normal Skin. *Photodermatol. Photoimmunol. Photomed.* **2010**, *26*, 16–21. [CrossRef]
32. Rupel, K.; Zupin, L.; Ottaviani, G.; Bertani, I.; Martinelli, V.; Porrelli, D.; Vodret, S.; Vuerich, R.; Passos da Silva, D.; Bussani, R. Blue Laser Light Inhibits Biofilm Formation in Vitro and in Vivo by Inducing Oxidative Stress. *NPJ Biofilms Microbiomes* **2019**, *5*, 29. [CrossRef]
33. Ryan, E.M.; Gorman, S.P.; Donnelly, R.F.; Gilmore, B.F. Recent Advances in Bacteriophage Therapy: How Delivery Routes, Formulation, Concentration and Timing Influence the Success of Phage Therapy. *J. Pharm. Pharmacol.* **2011**, *63*, 1253–1264. [CrossRef] [PubMed]
34. Bumah, V.V.; Masson-Meyers, D.S.; Enwemeka, C.S. Blue 470 Nm Light Suppresses the Growth of *Salmonella enterica* and Methicillin-resistant *Staphylococcus aureus* (MRSA) in Vitro. *Lasers Surg. Med.* **2015**, *47*, 595–601. [CrossRef]
35. Turner, P.E.; Azeredo, J.; Buurman, E.T.; Green, S.; Haaber, J.K.; Haggstrom, D.; Kameda de Figueiredo Carvalho, K.; Kirchhelle, C.; Gonzalez Moreno, M.; Pirnay, J.-P. Addressing the Research and Development Gaps in Modern Phage Therapy. *Phage* **2024**, *5*, 30–39. [CrossRef] [PubMed]
36. Yang, P.; Wang, N.; Wang, C.; Yao, Y.; Fu, X.; Yu, W.; Cai, R.; Yao, M. 460nm Visible Light Irradiation Eradicates MRSA via Inducing Prophage Activation. *J. Photochem. Photobiol. B* **2017**, *166*, 311–322. [CrossRef]
37. Godley, B.F.; Shamsi, F.A.; Liang, F.-Q.; Jarrett, S.G.; Davies, S.; Boulton, M. Blue Light Induces Mitochondrial DNA Damage and Free Radical Production in Epithelial Cells. *J. Biol. Chem.* **2005**, *280*, 21061–21066. [CrossRef]
38. Orlandi, V.T.; Martegani, E.; Bolognese, F. Catalase A Is Involved in the Response to Photooxidative Stress in *Pseudomonas aeruginosa*. *Photodiagn. Photodyn. Ther.* **2018**, *22*, 233–240. [CrossRef] [PubMed]
39. Abedon, S.T. Ecology and Evolutionary Biology of Hindering Phage Therapy: The Phage Tolerance vs. Phage Resistance of Bacterial Biofilms. *Antibiotics* **2023**, *12*, 245. [CrossRef]
40. Chua, S.L.; Ding, Y.; Liu, Y.; Cai, Z.; Zhou, J.; Swarup, S.; Drautz-Moses, D.I.; Schuster, S.C.; Kjelleberg, S.; Givskov, M. Reactive Oxygen Species Drive Evolution of Pro-Biofilm Variants in Pathogens by Modulating Cyclic-Di-GMP Levels. *Open Biol.* **2016**, *6*, 160162. [CrossRef]
41. Hazan, R.; Que, Y.A.; Maura, D.; Strobel, B.; Majcherczyk, P.A.; Hopper, L.R.; Wilbur, D.J.; Hreha, T.N.; Barquera, B.; Rahme, L.G. Auto Poisoning of the Respiratory Chain by a Quorum-Sensing-Regulated Molecule Favors Biofilm Formation and Antibiotic Tolerance. *Curr. Biol.* **2016**, *26*, 195–206. [CrossRef]
42. Müsken, M.; Di Fiore, S.; Römling, U.; Häussler, S. A 96-Well-Plate–Based Optical Method for the Quantitative and Qualitative Evaluation of *Pseudomonas aeruginosa* Biofilm Formation and Its Application to Susceptibility Testing. *Nat. Protoc.* **2010**, *5*, 1460–1469. [CrossRef]
43. Alkalay-Oren, S.; Yerushalmy, O.; Adler, K.; Khalifa, L.; Gelman, D.; Coppenhagen-Glazer, S.; Nir-Paz, R.; Hazan, R. Complete Genome Sequence of *Pseudomonas aeruginosa* Bacteriophage PASA16, Used in Multiple Phage Therapy Treatments Globally. *Microbiol. Resour. Announc.* **2022**, *11*, e00092-22. [CrossRef] [PubMed]
44. Rimon, A.; Yerushalmy, O.; Belin, J.; Alkalay-Oren, S.; Gavish, L.; Coppenhagen-Glazer, S.; Hazan, R. Six Novel *Pseudomonas aeruginosa* Phages: Genomic Insights and Therapeutic Potential. *Phage* **2025**, *6*, 32–40. [CrossRef]
45. Shteindel, N.; Yankelev, D.; Gerchman, Y. High-Throughput Quantitative Measurement of Bacterial Attachment Kinetics on Seconds Time Scale. *Microb. Ecol.* **2019**, *77*, 726–735. [CrossRef] [PubMed]
46. Banerjee, S.; Ghosh, D.; Vishakha, K.; Das, S.; Mondal, S.; Ganguli, A. Photodynamic Antimicrobial Chemotherapy (PACT) Using Riboflavin Inhibits the Mono and Dual Species Biofilm Produced by Antibiotic Resistant *Staphylococcus aureus* and *Escherichia coli*. *Photodiagn. Photodyn. Ther.* **2020**, *32*, 102002. [CrossRef]

Disclaimer/Publisher's Note: The statements, opinions and data contained in all publications are solely those of the individual author(s) and contributor(s) and not of MDPI and/or the editor(s). MDPI and/or the editor(s) disclaim responsibility for any injury to people or property resulting from any ideas, methods, instructions or products referred to in the content.

antibiotics

MDPI

Article

Temperature Adaptive Biofilm Formation in *Yersinia enterocolitica* in Response to pYV Plasmid and Calcium

Yunah Oh and Tae-Jong Kim *

Department of Forest Products and Biotechnology, Kookmin University, Seoul 02707, Republic of Korea; oya010111@kookmin.ac.kr

* Correspondence: bigbell@kookmin.ac.kr

Abstract: Background/Objectives: *Yersinia enterocolitica* is a pathogenic bacterium that forms biofilms, enhancing its persistence and resistance to antimicrobial agents. Biofilm formation in *Y. enterocolitica* is influenced by environmental factors such as temperature, calcium, and the presence of the virulence plasmid pYV. This study aims to explore how temperature, calcium, and pYV modulate biofilm formation in *Y. enterocolitica*, with a focus on motility and extracellular polymeric substance (EPS) production as key factors. **Methods**: *Y. enterocolitica* strains with and without the pYV plasmid were cultured at two different temperatures (26 °C and 37 °C). The effect of calcium (5 mM) on biofilm formation was tested at both temperatures. Biofilm formation was measured using crystal violet staining, motility was assessed using soft agar plates, and EPS production was quantified to determine its role in biofilm stabilization. **Results**: At 26 °C, biofilm formation increased in pYV-negative strains, driven primarily by motility and flagellar expression. In contrast, at 37 °C, pYV-positive strains showed strong biofilm formation despite reduced growth, with EPS production as the key stabilizing factor. Calcium modulated biofilm formation in a temperature-dependent manner: at 26 °C, 5 mM calcium modestly reduced biofilm formation in pYV-negative strains, while at 37 °C, it significantly suppressed both EPS production and biofilm formation by approximately 50% in pYV-positive strains. **Conclusions**: This study reveals a novel regulatory switch where temperature, calcium, and pYV modulate biofilm formation in *Y. enterocolitica*. These findings suggest that *Y. enterocolitica* can adapt between motility- and EPS-dominated biofilm strategies depending on environmental conditions. Understanding these mechanisms offers potential targets for controlling biofilm-related persistence in clinical and food safety contexts.

Keywords: *Yersinia enterocolitica*; biofilm formation; virulence plasmid; extracellular polymeric substances; motility; calcium; temperature adaptation

1. Introduction

Yersinia enterocolitica is a Gram-negative, facultative anaerobic bacterium responsible for gastroenteritis in humans. It can also lead to systemic complications such as mesenteric lymphadenitis, septicemia, or reactive arthritis, collectively referred to as yersiniosis [1]. The ability of *Y. enterocolitica* to survive and proliferate in diverse environments, including refrigerated foods and host tissues, makes it a significant environmental pathogen and a public health concern [2,3]. A critical factor contributing to *Y. enterocolitica*'s persistence in various environments is its ability to form biofilms—structured microbial communities encased in a self-produced extracellular polymeric substance (EPS) matrix [4,5]. While biofilm formation enhances environmental resilience and survival, it is not necessarily a

central virulence determinant in human infections. Biofilms provide resistance to environmental stresses, antibiotics, and host immune defenses, allowing *Y. enterocolitica* to endure in diverse ecological niches. Understanding biofilm formation is essential for controlling *Y. enterocolitica* persistence in both clinical and food safety contexts.

In this study, *Y. enterocolitica* strains KT0001 and KT0003, belonging to biotype 1B and serotype O:8, were used. These strains possess distinct lipopolysaccharide (LPS) structures, which play a crucial role in their interaction with the host immune system and influence biofilm formation [6]. The LPS structure, particularly the O-antigen composition, affects bacterial surface properties and biofilm-related behaviors. Understanding the strain characteristics is critical as they directly impact biofilm phenotypes.

Several genes and regulatory pathways are known to regulate biofilm formation in *Y. enterocolitica*. These include the expression of flagella [7], the type III secretion system (T3SS) [8], and the production of extracellular polymeric substances (EPS). While the *flhDC* gene plays a key role in motility and biofilm regulation, a *flhDC* mutant and complementation strain were not included in this study due to experimental scope limitations. Future studies could benefit from including such mutants to further investigate the role of *flhDC* in biofilm regulation and motility. These factors are controlled by regulatory systems such as Rcs [9] and cyclic-di-GMP signaling [10], which contribute to biofilm architecture and its response to environmental conditions. For example, the *flhDC* operon, which regulates flagellar biosynthesis, influences biofilm formation by promoting motility at lower temperatures [11]. Moreover, the T3SS encoded by the pYV plasmid has been implicated in biofilm maturation under host-like conditions, particularly at 37 °C [12].

Environmental factors, including temperature, calcium availability, and nutrient conditions, significantly impact biofilm formation in *Y. enterocolitica*. At 26 °C, motility-driven biofilm formation predominates [7], whereas at 37 °C, EPS production and T3SS activation become more pronounced [12]. Calcium plays a key role in modulating T3SS function and biofilm stability by influencing the secretion of *Yersinia* outer proteins (Yops). Furthermore, quorum sensing and nutrient availability also play crucial roles in regulating biofilm formation. These environmental cues, along with genetic factors, determine how *Y. enterocolitica* establishes biofilms in different ecological niches.

Temperature is particularly important in regulating *Y. enterocolitica*'s behavior, as it shifts from motility-driven strategies at 26 °C to virulence-associated mechanisms at 37 °C. At ambient temperatures (26 °C), flagellar synthesis and motility drive colonization [7,13], whereas at 37 °C, mimicking the host environment, motility is suppressed, and virulence factors are activated [14]. A key genetic determinant of these adaptations is the virulence plasmid pYV, which encodes the T3SS and *Yersinia* outer proteins (Yops), facilitating immune evasion and bacterial survival during infection.

Calcium is another critical environmental factor influencing *Y. enterocolitica* physiology, particularly through its role in regulating T3SS function. A calcium-depleted environment is necessary for efficient Yop secretion, which mimics conditions encountered in intracellular host niches or the calcium-restricted gut environment [15]. The 5 mM calcium concentration used in this study was chosen because it has been shown to inhibit T3SS activation in *Y. enterocolitica* and serves as a standard high-calcium condition [16]. We observed both cell density and biofilm formation under TYE medium and 5 mM Ca^{2+} conditions and found that 5 mM Ca^{2+} treatment did not lead to significant changes in cell growth or biofilm formation. No growth inhibition or other notable physiological changes were observed, supporting the idea that the observed reduction in biofilm formation is due to calcium-specific signaling rather than osmotic stress. This concentration suppresses T3SS function and provides a physiologically relevant model for studying calcium's regulatory effects on bacterial virulence mechanisms.

This study investigates the combined effects of temperature, the pYV plasmid, and calcium on *Y. enterocolitica* biofilm formation and associated processes, including cell growth, motility, flagellar expression, and EPS production. We hypothesize that *Y. enterocolitica* employs distinct strategies for biofilm formation depending on environmental conditions. Specifically, we aim to determine how calcium modulates these processes in relation to pYV-mediated regulation. While previous studies have examined temperature regulation of virulence and calcium-dependent T3SS activation separately, the integrated influence of these factors on biofilm development and matrix composition—especially in the context of plasmid carriage—remains poorly understood. This study fills that gap by revealing a novel regulatory switch between motility-driven and EPS-driven biofilm formation, coordinated by temperature, calcium, and the pYV plasmid.

Understanding the mechanisms regulating biofilm formation in *Y. enterocolitica* offers valuable insights into its adaptive strategies for persistence in both environmental reservoirs and host tissues. Our findings also support the development of novel antibiofilm strategies targeting temperature- or calcium-responsive virulence pathways, including EPS inhibition or T3SS regulation. These strategies could be critical for controlling *Y. enterocolitica* biofilm-mediated infections in clinical and food safety settings.

2. Results

2.1. Effects of Temperature, the Virulence Plasmid (pYV100), and Calcium on Cell Growth and Biofilm Formation

This study investigated the influence of the temperature, the virulence plasmid pYV100, and calcium on the growth and biofilm formation of *Y. enterocolitica* (Figure 1). At 26 °C, all cells grow well, reaching Abs_{600} values above 1.2 regardless of whether they possessed the pYV plasmid or calcium depletion, suggesting that bacterial proliferation is relatively unaffected by these factors at environmental temperatures. However, at 37 °C, strain KT0003, which possessed pYV100, exhibited significantly reduced growth, with Abs_{600} values below 0.23 regardless of the calcium concentration, while strain KT0001, which did not contain pYV100, showed only moderately reduced growth, with mean Abs_{600} values of 0.95 of at 0 mM calcium and 0.80 at 5 mM calcium. Such temperature and virulence plasmid (pYV100)-dependent growth changes are consistent with the pattern seen in a previous study [17].

At 26 °C, strain KT0001 (without pYV100) exhibited robust biofilm formation, producing an Abs_{600} value exceeding 1.0. In contrast, strain KT0003 (with pYV100) displayed significantly lower biofilm formation, producing an Abs_{600} value below 0.5. At 37 °C, the biofilm formation pattern reversed; strain KT0003 with 0 mM calcium displayed strong biofilm formation, with a mean Abs_{600} of 1.9, while strain KT0001 with 0 mM calcium produced only minimal amounts of biofilm, with Abs_{600} values below 0.2. Notably, the biofilm formation of strain KT0003 was reduced by more than half in the 5 mM calcium media.

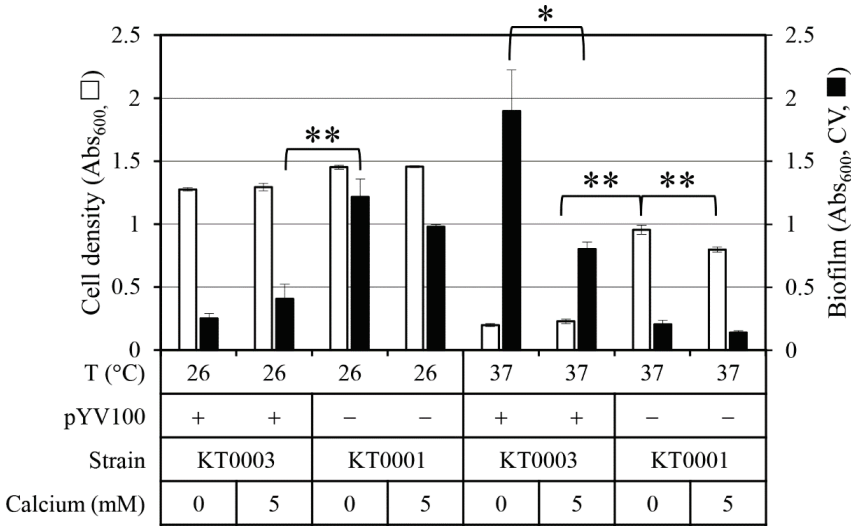

Figure 1. Effect of calcium concentration, virulence plasmid presence (pYV100), and temperature on cell growth and biofilm formation in *Y. enterocolitica*. Cell density (open bars, primary *Y*-axis) was measured as Abs_{600}. Biofilm formation (closed bars, secondary *Y*-axis) was quantified as Abs_{600} following crystal violet (CV) staining of biomass attached to the walls of the 96-well microplates, after removal of planktonic cells. Calcium concentrations tested were 0 mM and 5 mM; temperatures tested were 26 °C and 37 °C. Data represent means ± standard deviations from three biological replicates. Statistical significance was assessed using an unpaired two-tailed Student's *t*-test. Statistical significance is indicated by single asterisk (*) for $p < 0.05$ and double asterisks (**) for $p < 0.01$.

2.2. Effects of Temperature, the Virulence Plasmid, and Calcium on Motility and Flagellar Expression

Previous studies have suggested that in *Y. enterocolitica*, flagella actively rotate at environmental temperatures such as 26 °C and contribute significantly to biofilm formation [7]. To explore this relationship, we examined cell motility (Figure 2) and flagellar expression (Figures 3 and 4) under biofilm-forming conditions to assess their correlation.

Figure 2 presents the results of the motility assays. Active swimming motility was observed at 26 °C, regardless of the presence of the virulence plasmid. In contrast, motility was nearly absent at 37 °C across all strains and conditions. Under calcium-chelated conditions (0 mM calcium), motility was most pronounced at 26 °C, with cells covering the entire Petri dish within 24 h. However, supplementation with 5 mM calcium significantly reduced motility, indicating that motility is strongly influenced by both temperature and calcium availability. Figure 3 displays the results of the flagellar expression analysis. As expected, few flagella were observed at 37 °C, while flagella were readily detected at 26 °C. Strain KT0003 exhibited a significantly higher proportion of flagellated cells than KT0001 at 26 °C ($p < 0.01$), suggesting that the presence of the virulence plasmid positively influences flagellar expression. Notably, over 40% of KT0003 cells expressed flagella in the calcium-chelated medium, and this proportion increased to over 50% in the presence of 5 mM calcium. However, calcium treatment did not significantly affect the percentage of cells with flagella, indicating that the effect of calcium on flagellar expression is relatively modest. Taken together, these findings demonstrate a clear temperature-dependent relationship between motility and flagellar expression. However, at 26 °C, no significant correlation was observed between motility and flagellar presence when considering the effects of plasmid status and calcium concentration. To quantitatively assess these relationships, Pearson correlation analyses were conducted. A moderate correlation was found between motility zone diameter and the percentage of flagellated cells at 26 °C ($r = 0.62$), but this did not reach statistical significance ($p > 0.05$). A statistically significant correlation ($r = 0.78$,

$p < 0.05$) was observed between *flhDC* expression levels and biofilm formation, supporting the association shown in Figure 1.

To further investigate the molecular basis of these motility patterns, we analyzed the expression of *flhDC*—the master regulator of flagellar genes—using qPCR (Figure 4). At 26 °C, *flhDC* expression was significantly higher in strain KT0001 than in KT0003, particularly under calcium-chelated conditions, where *flhDC* transcript levels in KT0001 were more than 10.4-fold greater than in KT0003. This difference decreased to 3.7-fold when 5 mM calcium was added. At 37 °C, KT0003 showed a 43% increase in *flhDC* expression in the calcium-supplemented condition. Interestingly, a discrepancy was observed: at 26 °C, *flhDC* expression in KT0003 was relatively low in the presence of 5 mM calcium, yet flagellar presence was highest under this condition (Figure 3). This suggests the involvement of post-transcriptional regulation or additional unknown mechanisms influencing flagellar assembly beyond the transcriptional level governed by FlhDC. Further studies are required to elucidate these mechanisms. To better understand these relationships, we performed additional Pearson correlation analyses. A strong positive correlation ($r = 0.81$) was observed between *flhDC* expression and motility, while the correlation between *flhDC* expression and biofilm formation was moderate ($r = 0.59$). These results indicate that motility is likely to contribute to the biofilm phenotype at 26 °C, though it may not be the sole determining factor.

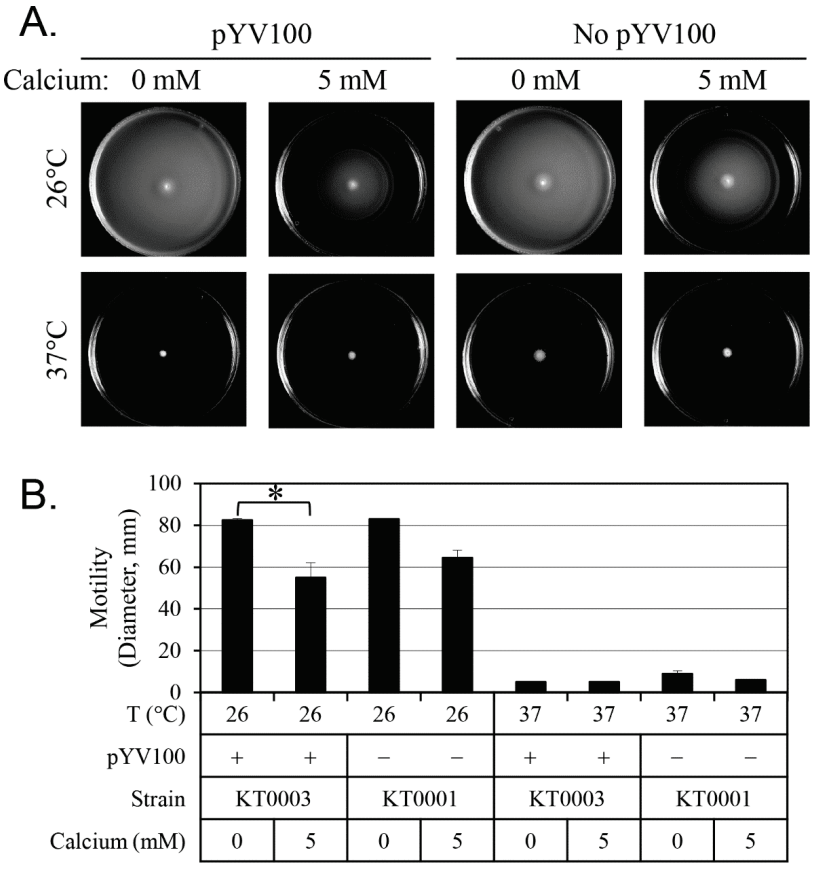

Figure 2. Effect of calcium concentration, pYV plasmid presence, and temperature on motility of *Y. enterocolitica*. (**A**) Representative images show radial spread from the inoculation center on soft agar plates. (**B**) Motility diameters (in mm) were measured and are presented as means ± standard deviations. Five biological replicates were analyzed per condition. Conditions tested include 0 mM and 5 mM calcium and incubation temperatures of 26 °C and 37 °C. Statistical significance was assessed using an unpaired two-tailed Student's *t*-test. Statistical significance is indicated by single asterisk (*) for $p < 0.05$.

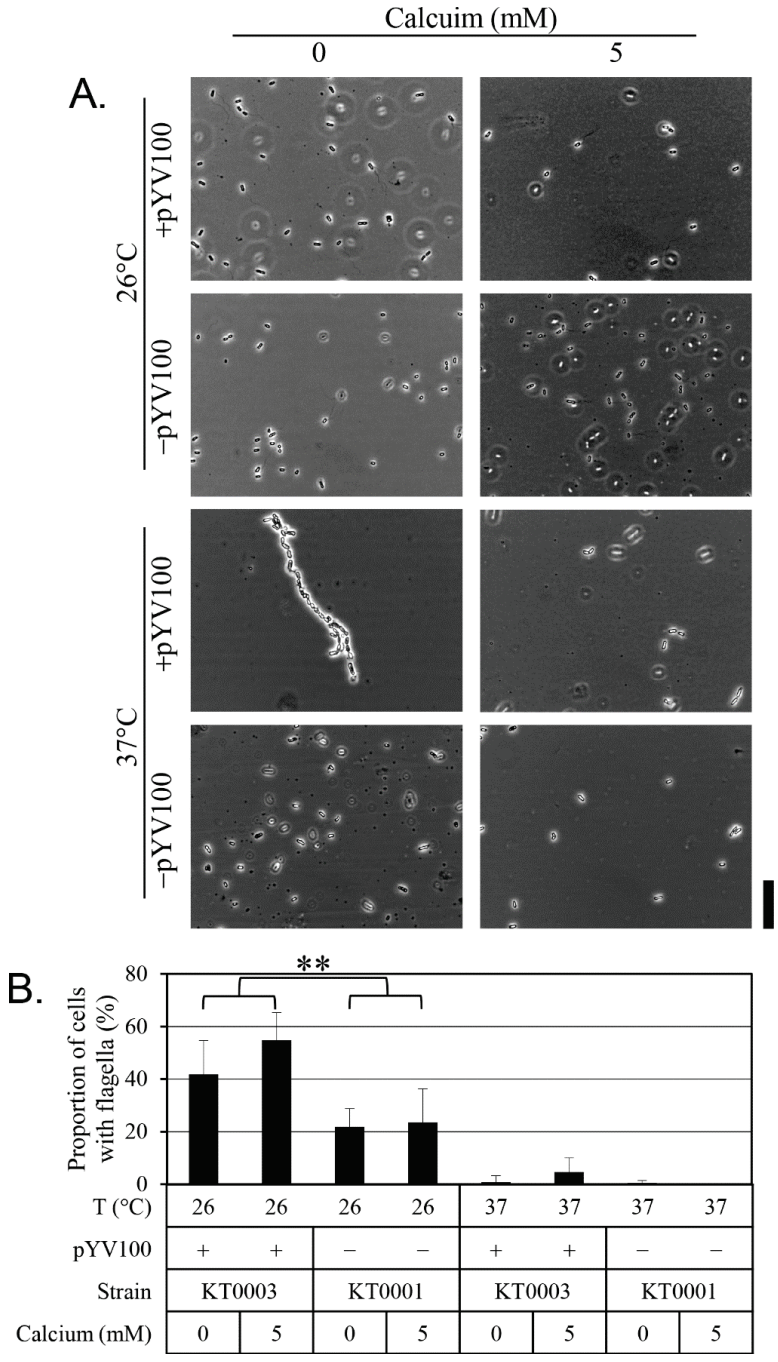

Figure 3. Impact of calcium, pYV plasmid presence, and temperature on flagellar expression in *Y. enterocolitica*. (**A**) Flagella were visualized by microscopy after specific staining. (**B**) Percentages of flagellated cells were quantified and are presented as means ± standard deviations from five independent experiments. Calcium concentrations tested were 0 mM and 5 mM; temperatures tested were 26 °C and 37 °C. Statistical significance was assessed using unpaired two-tailed Student's *t*-test; $p < 0.01$ is indicated by double asterisks (**).

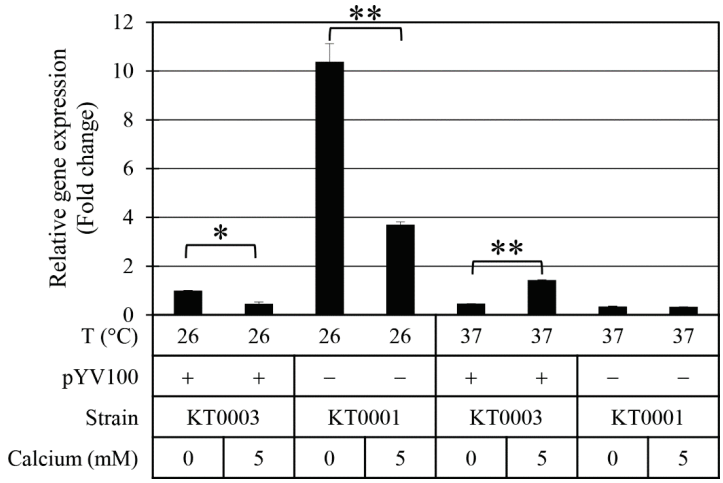

Figure 4. Relative expression of *flhDC*, the master regulator of flagellar synthesis, in response to calcium, pYV plasmid status, and temperature. Fold-change values were calculated by qPCR and are shown as means ± standard deviations from three independent experiments. Statistical significance was assessed using an unpaired two-tailed Student's *t*-test. Statistical significance is indicated by single asterisk (*) for $p < 0.05$ and double asterisks (**) for $p < 0.01$.

2.3. Effect of Temperature, the pYV Plasmid, and Calcium on Extracellular Polymeric Substance Production

To investigate the role of EPSs in *Y. enterocolitica* biofilm formation, EPS production was analyzed in relation to temperature, the presence of the virulence plasmid, and calcium availability (Figure 5). At 26 °C, the production of EPSs—including proteins, polysaccharides, and eDNA—was limited. At 37 °C, EPS production remained low in strain KT0001, but the production of all three EPS components increased dramatically in strain KT0003, though their levels were reduced by approximately 50% in the presence of 5 mM calcium. These results show that EPS production is tightly regulated by temperature, the virulence plasmid, and calcium availability, suggesting a coordinated mechanism that integrates environmental cues with biofilm formation and virulence strategies.

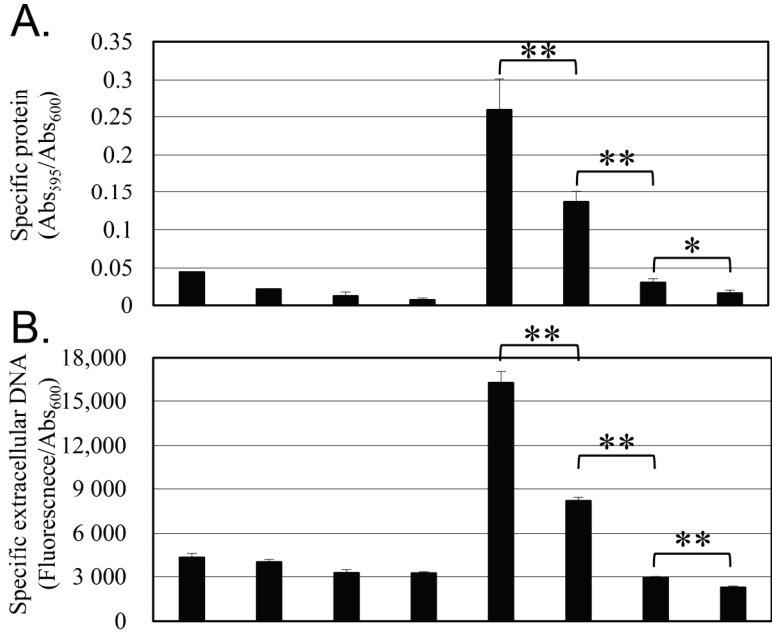

Figure 5. *Cont.*

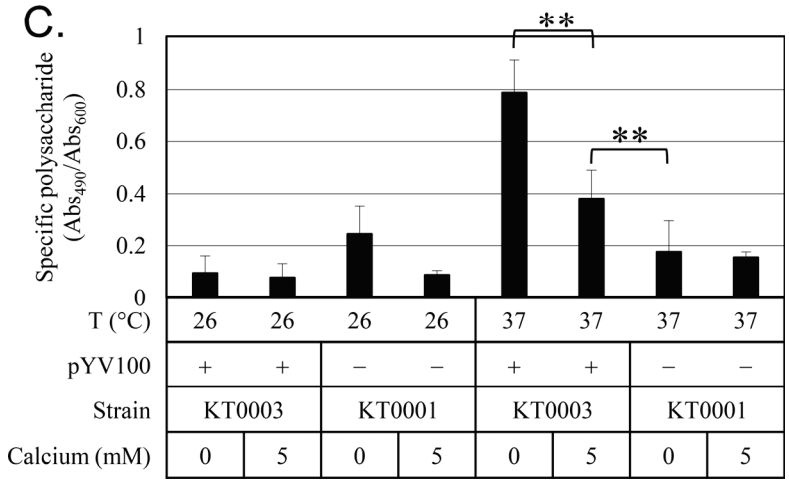

Figure 5. Effect of calcium, pYV plasmid status, and temperature on extracellular polymeric substance (EPS) production in *Y. enterocolitica*. (**A**) Protein content measured by Coomassie blue absorbance at 595 nm (Abs_{595}). (**B**) Extracellular DNA content assessed by fluorescence at 528 nm using SYTOX™ Green dye. (**C**) Polysaccharide content measured by phenol-sulfuric acid assay at 490 nm (Abs_{490}). All EPS component levels were normalized to cell density (Abs_{600}). Conditions included 0 mM and 5 mM calcium and incubation at 26 °C or 37 °C. Data represent means ± standard deviations from four biological replicates. Statistical significance was assessed using an unpaired two-tailed Student's *t*-test. Statistical significance is indicated by single asterisk (*) for $p < 0.05$ and double asterisks (**) for $p < 0.01$.

3. Discussion

This study provides new insights into how temperature and calcium co-regulate biofilm formation in a virulence plasmid-dependent manner. Importantly, our unique contribution lies in showing that *Y. enterocolitica* regulates biofilm formation differently depending on environmental temperature. At 26 °C, representing natural environmental conditions, biofilm formation is primarily motility-driven and largely independent of T3SS activity. In contrast, at 37 °C, mimicking the host infection environment, calcium modulates EPS-driven biofilm formation through pYV-dependent T3SS regulation. This temperature-dependent dual strategy distinguishes our work from previous studies and highlights the adaptive versatility of *Y. enterocolitica* in both environmental and host settings.

By comparing pYV-positive and -negative strains, we identified a regulatory shift: in pYV-positive cells, elevated temperature and calcium limitation suppress motility while promoting EPS-driven biofilm maturation—a likely adaptation for host colonization. In contrast, pYV-negative strains maintain a motility-dominant strategy under the same conditions, suggesting alternative survival tactics shaped by plasmid carriage.

At 26 °C, biofilm formation was highest in strain KT0001 and appeared independent of T3SS activity, regardless of calcium levels. This supports previous findings that biofilm development under environmental conditions is primarily driven by flagella-mediated surface attachment [7]. In contrast, at 37 °C, the pYV-positive strain showed significantly enhanced biofilm formation under calcium-deficient conditions, consistent with the known activation of T3SS under host-mimicking conditions [18]. Calcium supplementation suppressed this phenotype, likely by inhibiting Yop secretion. These findings suggest a context-specific biofilm strategy, wherein EPS-dependent stabilization dominates under host-like conditions.

Interestingly, in the pYV-negative strain at 37 °C, both motility and biofilm formation were reduced, indicating that, in the absence of the plasmid, the bacterium lacks the capacity to produce compensatory EPS. This observation supports a dual-regulatory model in which biofilm formation requires either flagellar motility (at 26 °C) or pYV-dependent EPS production (at 37 °C), but not both simultaneously. Temperature also plays a central role in

modulating motility. The pronounced reduction in swimming activity at 37 °C aligns with earlier reports showing transcriptional repression of flagellar genes at host temperature [19]. Flagella are antigenic and energetically costly; therefore, their expression may be downregulated during host infection. Consistent with this, both pYV-positive and -negative strains exhibited minimal flagellar gene expression at 37 °C (Figure 3B), reinforcing the concept of temperature-sensitive repression of motility genes. These data collectively support a model in which motility is prioritized at environmental temperatures and downregulated at host temperatures, where virulence factors such as T3SS take precedence.

Beyond FlhDC, other regulatory systems likely contribute to the observed phenotypes. One candidate is the Rcs phosphorelay system, which responds to envelope stress and regulates exopolysaccharide synthesis in *Yersinia* and other Gram-negative bacteria [20]. Cyclic-di-GMP is another global regulator that orchestrates the switch between motility and sessility [21]. Although c-di-GMP was not directly measured in this study, the temperature- and plasmid-dependent changes in biofilm architecture suggest its possible involvement. Moreover, it remains unclear whether virulence regulators such as VirF directly influence matrix gene expression, particularly under calcium-limited conditions at 37 °C. Further studies using transcriptomics and regulatory mutants will be needed to investigate these pathways.

The observed differences in EPS production between 26 °C and 37 °C further highlight the adaptive flexibility of *Y. enterocolitica*. EPS production was minimal in both strains at 26 °C, supporting the idea that motility dominates biofilm formation under environmental conditions. At 37 °C, EPS synthesis increased significantly in the pYV-positive strain under calcium-limited conditions, correlating with enhanced biofilm formation. This supports the hypothesis that EPS production is promoted by T3SS activation and is essential for biofilm stabilization under host-like conditions. However, the molecular links between T3SS activity and EPS gene expression remain unclear. It is plausible that T3SS signaling influences global regulators such as Rcs or c-di-GMP, leading to coordinated EPS upregulation.

Extracellular polymeric substances are known to shield bacteria from immune responses, including phagocytosis and antimicrobial peptides [22]. Our results suggest that calcium deficiency may enhance EPS synthesis via T3SS activation, contributing to immune evasion. The exceptionally high EPS production in pYV-positive strains under calcium-limited conditions supports a functional connection between Yop secretion and EPS biosynthesis. Furthermore, calcium ions may stabilize the Yop secretion system and thereby indirectly influence biofilm architecture—consistent with earlier studies that demonstrated calcium-dependent regulation of Yop activity and function. Importantly, although our current data provide indirect evidence, we propose potential mechanisms whereby T3SS activity could influence EPS synthesis. One possibility is that T3SS activation modulates global transcriptional regulators such as the Rcs phosphorelay system or cyclic-di-GMP signaling, both of which are known to orchestrate exopolysaccharide biosynthesis and biofilm maturation in Gram-negative bacteria [20,21]. Another possibility is post-transcriptional regulation, in which secretion-associated chaperones or small RNAs may stabilize or destabilize EPS-related transcripts. While further experimental validation is required, we believe these hypotheses provide a mechanistic framework to guide future investigations.

While our study provides robust endpoint comparisons across experimental variables, it is limited by its parallel design, which does not capture temporal changes in regulatory events or biofilm maturation. Mechanistic progressions, such as the sequential activation of matrix components or EPS dynamics, were not directly observed. A longitudinal experimental design—incorporating time-course analyses of gene expression, EPS composition, and T3SS/Yop activity—will be essential to uncover the regulatory hierarchy over time. We

acknowledge this limitation and suggest that future studies incorporate such approaches to resolve stage-specific regulatory transitions.

Additionally, the antimicrobial effects of calcium itself were not addressed. Determining the minimum inhibitory concentration (MIC) of calcium for *Y. enterocolitica*, and testing sub-MIC, would help clarify whether calcium affects biofilm formation through physiological stress or regulatory signaling. Another limitation is the absence of an empty vector control. Because pYV100 is a mobilizable derivative of the naturally occurring virulence plasmid pYV8081 rather than a recombinant plasmid constructed with a cloning backbone, there is no equivalent empty vector available for this system. Therefore, we relied on comparisons between plasmid-cured and plasmid-carrying strains to evaluate phenotypic differences. Future studies may consider constructing artificial vector-based systems if backbone-specific control is required. This would be particularly relevant for assessing the use of calcium-modulating strategies in food or clinical settings.

Finally, pH was not monitored or controlled in our assays. While the TYE medium is expected to remain near neutral, we acknowledge that local pH shifts during bacterial growth could influence gene expression, motility, or matrix synthesis. Future work should include pH-controlled conditions to clarify its role in biofilm regulation.

In summary, this study identifies a novel plasmid-dependent regulatory switch in *Y. enterocolitica* biofilm development—shifting from flagella-driven colonization at 26 °C to T3SS- and EPS-dominated biofilms at 37 °C. This dual-strategy model has not been previously reported and offers new insight into how environmental and genetic factors shape virulence and persistence. The integration of temperature, calcium signaling, and pYV plasmid function defines a complex regulatory network that balances motility, T3SS activation, and matrix production in response to niche-specific demands. These findings advance our understanding of *Y. enterocolitica* pathogenesis and suggest that targeting EPS synthesis or T3SS activity may offer effective strategies to mitigate biofilm-mediated infections.

4. Materials and Methods

4.1. Strains and Culture Conditions

The bacterial strains used in this study are listed in Table 1. Strain KT0001 (*Yersinia enterocolitica* KCCM 41657) is a plasmid-cured variant lacking the virulence plasmid pYV. To obtain the nalidixic acid-resistant mutant strain KT0002, the plasmid-cured parental strain KT0001 was cultured in 5 mL of tryptone-yeast extract (TYE) medium at 26 °C for 48 h. After incubation, cells were streaked onto TYE agar plates containing 25 μg/mL nalidixic acid. If no colonies appeared, the culture was subjected to an additional round of incubation in fresh 5 mL TYE medium under the same conditions, followed by re-plating on selective agar. This subculturing process was repeated until colonies capable of growing on the selective plates were observed. Colonies that emerged on nalidixic acid-containing plates were isolated and subjected to 16S rRNA gene sequencing to confirm their identity as *Y. enterocolitica*. The resulting strain was designated KT0002. Strain KT0003 was generated by introducing pYV100 into KT0002 via a triparental mating procedure. For this, *E. coli* HB101/pYV100 (streptomycin^R/spectinomycin^R) served as the donor, *E. coli* DH5α/pRK2013 (kanamycin^R) as the helper, and KT0002 (nalidixic acid^R) as the recipient strain. The three cultures were combined with $MgSO_4$, passed through a sterile filter, and incubated on LB agar for 3 h at 26 °C. After washing, cells were plated on LB agar containing streptomycin (15 μg/mL), spectinomycin (15 μg/mL), and nalidixic acid (25 μg/mL) to select for transconjugants. Colonies were screened for kanamycin sensitivity to confirm loss of the helper plasmid, and the presence of functional pYV100 was confirmed by detecting Yops secretion under Mg-oxalate culture conditions. pYV (plasmid of *Yersinia* virulence) generally refers to the family of virulence plasmids that encode the T3SS responsible for

secreting Yops. In this study, pYV100 denotes the specific artificial derivative of pYV that was reintroduced into the plasmid-cured strain KT0002 to restore virulence capacity. Hereafter, we use pYV to describe the plasmid in general, and pYV100 only when referring specifically to this engineered derivative.

Table 1. Bacterial strain, plasmid, and primer information.

Name	Description	Source/ Reference
Yersinia enterocolitica		
KT0001	biotype 1B, serotype O:8, Sal/Esc-Ptz-CRMOX-	KCCM 41657
KT0002	KCCM 41657, Nal^R	In this study
KT0003	KT0002 with pYV100, Nal^R	In this study
Plasmid		
pYV100	mob^+, mobilizable derivative of pYV8081, Str/Spc^R	[23]
Primers		
flhDC-F	CCTCAGCGATGTTTCGTCTC	[20]
flhDC-R	CTGCAAGTCATCCACACGAG	[20]
16S rRNA-F	GCACGTAATGGTGGGAACTC	[20]
16S rRNA-R	CTCCAATCCGGACTACGACA	[20]

All strains were cultured in TYE medium, consisting of 1% tryptone (catalog number: 211705, Becton Dickinson Korea Co., Ltd., Seoul, Republic of Korea) and 0.5% yeast extract (catalog number: 2509110, Becton Dickinson Korea Co., Ltd.) dissolved in distilled water. For preparation of TYE agar plates, 1.5% Bacto agar (catalog number: 214010, Becton Dickinson Korea Co., Ltd.) was added to the medium before autoclaving.

Strains KT0001 and KT0003 were streaked onto TYE agar plates and incubated at 26 °C for 48 h. Single colonies were then inoculated into liquid TYE medium and grown overnight at 26 °C. These overnight cultures were subcultured into fresh TYE medium at an initial optical density of Abs_{600} = 0.05 and used for all subsequent experiments. All bacterial cultures for assays were incubated in 96-well microplates (SPL Life Sciences, Pocheon, Republic of Korea).

To investigate the effect of calcium, two media conditions were prepared: calcium-depleted (0 mM) and calcium-supplemented (5 mM). Cell growth was not inhibited under the 5 mM calcium condition when compared to the calcium-depleted medium (TYE). Furthermore, previous studies, such as that by DeBord et al. [16], have used 5 mM calcium to inhibit Type III secretion in *Y. enterocolitica*, suggesting that the observed changes in biofilm formation in our study are due to specific regulatory effects rather than physiological stress. For the 0 mM calcium condition, calcium ions were removed by adding 0.8 mL of 2 M $MgCl_2$ and 8 mL of 0.2 M sodium oxalate to 91 mL of TYE medium. This mixture was incubated at room temperature for 24 h prior to use. For the 5 mM calcium condition, calcium chloride ($CaCl_2$) was added directly to the TYE medium. The pH of the TYE medium was not specifically monitored or adjusted during the experiments. It was assumed to remain near neutral under the experimental conditions at both 26 °C and 37 °C.

4.2. Cell Density and Biofilm Quantification

Subcultures of each strain (in TYE media at an Abs_{600} of 0.05) were incubated at either 26 °C or 37 °C for 24 h, and then cell density and biofilm formation were measured. Three independent biological replicates were performed for each strain to ensure reproducibility. Cell density was determined by measuring the absorbance at 600 nm. Biofilm formation was quantified using a modified version of the 1% crystal violet assay described in a previous study [24], measuring only biomass that was firmly attached to the walls and bottom surfaces of the 96-well microplates. Planktonic (non-adherent) cells were removed

during the washing steps and were not included in the quantification. Briefly, the cultures in the 96-well plates were washed three times with distilled water. Then, 100 µL of 1% crystal violet solution was added to each well, and the plates were incubated at room temperature for 15 min. After staining, the wells were again washed three times with distilled water, and the remaining crystal violet, which was bound in the biofilms, was solubilized by adding 100 µL of 95% ethanol. After incubating at room temperature for another 15 min, the cultures' Abs_{600} values were measured using a Synergy™ LX Multi-Mode Reader (BioTek Instruments Korea Ltd., Seoul, Republic of Korea).

4.3. Cell Motility Measurement

Motility was measured using TYE agar plates containing 0.3% agar using a procedure adapted from a previous study [7]. Cells from a single colony on a TYE plate were inoculated onto the center of a plate containing 0.3% agar, and the plate was incubated at 26 °C or 37 °C for 24 h. After incubation, images of the plates were captured using a Gel Doc™ XR+ (Bio-Rad Laboratories Inc., Hercules, CA, USA), and the diameter of the motility zone was measured using the Image Lab™ software version 3.0 (Bio-Rad Laboratories Inc.).

4.4. Flagellar Staining

The presence and distribution of flagella were observed via flagellar staining using a method modified from a previous study [7]. The staining solution was prepared immediately before use by mixing 10 parts of mordant solution (2 g of tannic acid, 10 mL of 5% phenol, and 10 mL of saturated aqueous $AlKO_8S_2{\cdot}12H_2O$) with 1 part of dye solution (12% crystal violet in ethanol). Three µL bacterial culture samples were placed on a 50 × 24 mm glass slip and covered with a cover slip. Ten µL of staining solution was added to the edge of the coverslip to be drawn into the sample by capillary action. Flagella were then observed under an AXIO Scope.A1 microscope (ZEISS Korea, Seoul, Republic of Korea).

The percentage of flagella-forming cells was calculated according to a previous study [25]. All cells and cells with flagella within a certain area of microscope field were counted, and if necessary, additional areas were observed the same way until 100 cells were counted. The number of flagellated cells was divided by the total number of cells and multiplied by 100 to obtain the percentage of flagellated cells.

4.5. Measuring flhDC Expression Level Using Real-Time Polymerase Chain Reaction (qPCR)

The cells were prepared by inoculating the strains, as described in Figure 4, and incubating them for 24 h under the specified conditions. Total RNA was extracted using the AccuPrep® Bacterial RNA Extraction Kit (Catalog number: K-3142, Bioneer Co., Daejeon, Republic of Korea) according to the manufacturer's instructions. The amount of total cDNA was adjusted to a range of 1 ng to 5 µg based on the Abs_{260}/Abs_{280} ratio using a GENESYS 150 UV-Vis spectrophotometer (Catalog number: 840-300300, ThermoFisher Scientific Korea Inc., Seoul, Republic of Korea). Then, complementary DNA (cDNA) synthesis was performed using the SuPrimeScript cDNA Synthesis Kit (Catalog number: SRK-1000, Genetbio Co., Ltd., Daejeon, Republic of Korea). The mRNA transcripts of *flhDC* were quantitatively analyzed using PowerUp™ SYBR™ Green Master Mix for qPCR (Catalog number: A25742, ThermoFisher Scientific Korea Inc.) in QuantStudio 5 Real-Time PCR System (Catalog number: A28574, ThermoFisher Scientific Korea Inc.) and the primer pair detailed in Table 1. The thermocycler protocol began at 50 °C for 2 min, followed by initial denaturation at 95 °C for 2 min, and then 40 cycles of 95 °C for 15 s, 59 °C for 15 s, and 72 °C for 1 min. The qPCR product size for the *flhDC* gene was 176 base pairs, and for the 16S rRNA gene, it was 183 base pairs. To confirm the quality of the amplified products, a melt curve analysis was performed at 95 °C for 15 s, followed by 60 °C for 1 min, and then a gradual temperature increases of 1.6 °C per second until reaching 95 °C, which

was maintained for 15 s. The reference control for calculating relative gene expression was strain KT0003 (pYV^+) cultured at 26 °C under calcium-free (0 mM) conditions. RNA was harvested at 24 h post-inoculation, corresponding to the same timepoint used for cell growth and biofilm quantification assays. The cycle threshold (Ct) values for the *flhDC* gene were calculated, and the 16S rRNA gene was used as the housekeeping gene for normalization. Relative gene expression levels were analyzed using the $2^{-\Delta\Delta Ct}$ method. Raw Ct values and replicate data are provided in Supplementary Table S1 to allow readers to evaluate variability across biological replicates.

4.6. Extracellular Polymeric Substance Quantification

The production of EPSs was measured to evaluate the major biofilm components: proteins, polysaccharides, and extracellular DNA (eDNA). We used a previously reported method [26] with some modifications. Strains were cultured as described in the Section 4.2. To ensure that EPS from both planktonic cells and surface-attached biofilms was included, the biofilm biomass adhering to the walls of the 96-well plates was gently scraped and suspended into the culture medium prior to centrifugation. Then, 1 mL of this mixture (containing both planktonic and detached biofilm cells) was centrifuged at 9279× *g* for 10 min to obtain a pellet and a cell-free culture supernatant. The pellet was washed once with phosphate-buffered saline, centrifuged at 9279× *g* for 10 min, and resuspended in 1 mL of isotonic buffer. The resuspended solution was incubated at 4 °C for 12 h. Then, after vortexing for 3 min, the solution was centrifuged at 9279× *g* for 15 min, and the supernatant was combined with the previously obtained cell-free cultures. This mixture was treated with 3 times its volume of iced ethanol and incubated at 20 °C for 12 h to precipitate the EPSs. The EPSs were then pelleted by centrifugation at 9279× *g* for 15 min, dried, and stored at 4 °C. The dried EPS was dissolved in distilled water for further analyses. For protein quantification, 100 µL of EPS sample was mixed with 1 mL of Bradford reagent (Biosesang, Yongin, Republic of Korea) and vortexed. Then, the mixture was incubated at room temperature for 2 min, and its Abs_{595} was measured. For polysaccharide quantification, a phenol–sulfuric acid method was used [26]. Fifty µL of EPS sample was mixed with 150 µL of sulfuric acid, followed by 30 µL of 5% phenol. The mixture was incubated at room temperature for 10 min, and its Abs_{490} was measured. For eDNA quantification, SYTOX™ Green Nucleic Acid Stain (Catalog number: S7020, ThermoFisher Scientific Korea Inc.) was used according to the manufacturer's protocol. Fifty µL of EPS sample was mixed with 50 µL of 5 µM SYTOX™ Green Stain solution. After incubating at room temperature for 40 min, fluorescence was measured with excitation at 485 nm and measurement at 528 nm. For all three EPS constituent analyses, the measured absorbances were divided by the Abs_{600} of the corresponding culture to calculate the relative EPS production per unit cell.

4.7. Statistical Analysis

All data were derived from three independent biological replicates unless otherwise specified. Statistical significance between experimental groups was assessed using unpaired two-tailed Student's *t*-tests, with *p*-values less than 0.05 considered statistically significant. Results are presented as mean ± standard deviation (SD). Statistically significant differences are indicated in the figures using either asterisks (* for $p < 0.05$ and ** for $p < 0.01$).

5. Conclusions

This study demonstrates that biofilm formation in *Y. enterocolitica* is regulated by a combination of environmental factors—temperature and calcium—and the presence of the pYV virulence plasmid. At 26 °C, biofilm development is primarily driven by flagella-mediated motility, especially in pYV-negative strains. In contrast, at 37 °C, the presence of

pYV promotes EPS-mediated biofilm formation despite reduced bacterial growth, reflecting a temperature-dependent regulatory shift that supports adaptation to both environmental and host-associated niches. Calcium further modulates these processes in a temperature- and plasmid-dependent manner. It enhances EPS production and biofilm formation in pYV-positive strains at 37 °C, while suppressing biofilm formation at 26 °C. These findings support a regulatory framework in which environmental cues are integrated through the pYV plasmid—potentially involving the Rcs phosphorelay system or cyclic-di-GMP signaling—to coordinate biofilm architecture. Targeting EPS biosynthesis or disrupting calcium-responsive regulatory pathways may offer promising strategies for controlling *Y. enterocolitica* persistence in both clinical and food safety contexts.

Supplementary Materials: The following supporting information can be downloaded at: https://www.mdpi.com/article/10.3390/antibiotics14090857/s1, Table S1: RT-qPCR raw Ct values of *flhDC* and housekeeping gene (16S rRNA) in *Yersinia enterocolitica*.

Author Contributions: Conceptualization, Y.O. and T.-J.K.; methodology, Y.O. and T.-J.K.; software, Y.O. and T.-J.K.; validation, T.-J.K.; formal analysis, Y.O. and T.-J.K.; investigation, Y.O.; resources, T.-J.K.; data curation, T.-J.K.; writing—original draft preparation, Y.O.; writing—review and editing, T.-J.K.; visualization, T.-J.K.; supervision, T.-J.K.; project administration, T.-J.K.; funding acquisition, Y.O. and T.-J.K. All authors have read and agreed to the published version of the manuscript.

Funding: This research was supported by a National Research Foundation of Korea (NRF) grant (No. 2021R1F1A1061888) funded by the Korean government (MSIT).

Institutional Review Board Statement: Not applicable.

Informed Consent Statement: Not applicable.

Data Availability Statement: The original contributions presented in this study are included in the article/Supplementary Materials. Further inquiries can be directed to the corresponding author.

Conflicts of Interest: The authors declare no conflicts of interest.

Abbreviations

The following abbreviations are used in this manuscript:

EPS	Extracellular polymeric substance
T3SS	Type III secretion system
Yops	*Yersinia* outer proteins
TYE	Tryptone-yeast extract
eDNA	Extracellular DNA
SD	Standard deviation
MIC	Minimum inhibitory concentration

References

1. Abdel-Haq, N.M.; Asmar, B.I.; Abuhammour, W.M.; Brown, W.J. *Yersinia enterocolitica* infection in children. *Pediatr. Infect. Dis. J.* **2000**, *19*, 954–958. [CrossRef] [PubMed]
2. Yue, Y.; Zheng, J.; Sheng, M.; Liu, X.; Hao, Q.; Zhang, S.; Xu, S.; Liu, Z.; Hou, X.; Jing, H.; et al. Public health implications of *Yersinia enterocolitica* investigation: An ecological modeling and molecular epidemiology study. *Infect. Dis. Poverty* **2023**, *12*, 41. [CrossRef] [PubMed]
3. Fredriksson-Ahomaa, M.; Grönthal, T.; Heljanko, V.; Johansson, V.; Rantala, M.; Heikinheimo, A.; Laukkanen-Ninios, R. Enteropathogenic *Yersinia* with public health relevance found in dogs and cats in Finland. *Pathogens* **2024**, *13*, 54. [CrossRef]
4. Wang, H.; Tay, M.; Palmer, J.; Flint, S. Biofilm formation of *Yersinia enterocolitica* and its persistence following treatment with different sanitation agents. *Food Control* **2017**, *73*, 433–437. [CrossRef]
5. Ham, Y.; Kim, T.-J. Inhibition of biofilm formation in *Yersinia enterocolitica* by edible plant extracts including Polygoni Multiflori Radix. *J. Korean Wood Sci. Technol.* **2022**, *50*, 448–457. [CrossRef]

6. Bengoechea, J.A.; Najdenski, H.; Skurnik, M. Lipopolysaccharide O antigen status of *Yersinia enterocolitica* O:8 is essential for virulence and absence of O antigen affects the expression of other *Yersinia* virulence factors. *Mol. Microbiol.* **2004**, *52*, 451–469. [CrossRef] [PubMed]
7. Kim, T.-J.; Young, B.M.; Young, G.M. Effect of flagellar mutations on *Yersinia enterocolitica* biofilm formation. *Appl. Environ. Microbiol.* **2008**, *74*, 5466–5474. [CrossRef]
8. Schwiesow, L.; Lam, H.; Dersch, P.; Auerbuch, V. *Yersinia* type III secretion system master regulator LcrF. *J. Bacteriol.* **2016**, *198*, 604–614. [CrossRef]
9. Fang, N.; Yang, H.; Fang, H.; Liu, L.; Zhang, Y.; Wang, L.; Han, Y.; Zhou, D.; Yang, R. RcsAB is a major repressor of *Yersinia* biofilm development through directly acting on *hmsCDE*, *hmsT* and *hmsHFRS*. *Sci. Rep.* **2015**, *5*, 9566. [CrossRef]
10. Liu, X.; Cao, B.; Yang, L.; Gu, J.-D. Biofilm control by interfering with c-di-GMP metabolism and signaling. *Biotechnol. Adv.* **2022**, *56*, 107915. [CrossRef]
11. Young, G.M.; Smith, M.J.; Minnich, S.A.; Miller, V.L. The *Yersinia enterocolitica* motility master regulatory operon, *flhDC*, is required for flagellin production, swimming motility, and swarming motility. *J. Bacteriol.* **1999**, *181*, 2823–2833. [CrossRef]
12. Wang, H.; Palmer, J.; Flint, S. Function of pYV plasmid on biofilm formation of *Yersinia enterocolitica* ERL032123 in the presence of Ca^{2+}. *J. Food Prot.* **2019**, *82*, 1683–1687. [CrossRef]
13. Meng, J.; Bai, J.; Chen, J. Transcriptomic analysis reveals the role of RcsB in suppressing bacterial chemotaxis, flagellar assembly and infection in *Yersinia enterocolitica*. *Curr. Genet.* **2020**, *66*, 971–988. [CrossRef]
14. Bottone, E.J. *Yersinia enterocolitica*: The charisma continues. *Clin. Microbiol. Rev.* **1997**, *10*, 257–276. [CrossRef] [PubMed]
15. Cornelis, G.; Vanootegem, J.C.; Sluiters, C. Transcription of the *yop* regulon from *Y. enterocolitica* requires trans acting pYV and chromosomal genes. *Microb. Pathog.* **1987**, *2*, 367–379. [CrossRef]
16. DeBord, K.L.; Galanopoulos, N.S.; Schneewind, O. The *ttsA* gene is required for low-calcium-induced yype III secretion of Yop proteins and virulence of *Yersinia enterocolitica* W22703. *J. Bacteriol.* **2003**, *185*, 3499–3507. [CrossRef] [PubMed]
17. Goverde, R.L.J.; Kusters, J.G.; Huis in't Veld, J.H.J. Growth rate and physiology of *Yersinia enterocolitica*; influence of temperature and presence of the virulence plasmid. *J. Appl. Bacteriol.* **1994**, *77*, 96–104. [CrossRef]
18. Gemski, P.; Lazere, J.R.; Casey, T. Plasmid associated with pathogenicity and calcium dependency of *Yersinia enterocolitica*. *Infect. Immun.* **1980**, *27*, 682–685. [CrossRef] [PubMed]
19. Kapatral, V.; Olson, J.W.; Pepe, J.C.; Miller, V.L.; Minnich, S.A. Temperature-dependent regulation of *Yersinia enterocolitica* Class III flagellar genes. *Mol. Microbiol.* **1996**, *19*, 1061–1071. [CrossRef]
20. Meng, J.; Xu, J.; Huang, C.; Chen, J. Rcs phosphorelay responses to truncated lipopolysaccharide-induced cell envelope stress in *Yersinia enterocolitica*. *Molecules* **2020**, *25*, 5718. [CrossRef]
21. Lamprokostopoulou, A.; Römling, U. Yin and Yang of biofilm formation and cyclic di-GMP signaling of the gastrointestinal pathogen *Salmonella enterica* serovar Typhimurium. *J. Innate Immun.* **2021**, *14*, 275–292. [CrossRef]
22. Flemming, H.-C.; van Hullebusch, E.D.; Little, B.J.; Neu, T.R.; Nielsen, P.H.; Seviour, T.; Stoodley, P.; Wingender, J.; Wuertz, S. Microbial extracellular polymeric substances in the environment, technology and medicine. *Nat. Rev. Microbiol.* **2025**, *23*, 87–105. [CrossRef] [PubMed]
23. Warren, S.M.; Young, G.M. An amino-terminal secretion signal Is required for YplA export by the Ysa, Ysc, and flagellar type III secretion systems of *Yersinia enterocolitica* biovar 1B. *J. Bacteriol.* **2005**, *187*, 6075–6083. [CrossRef] [PubMed]
24. Ham, Y.; Xu, D.; Kim, T.-J. Effect of licorice extract on biofilm formation in two pathogenic bacteria: *Aeromonas hydrophila* and *Yersinia enterocolitica*. *J. Korean Wood Sci. Technol.* **2025**, *53*, 77–88. [CrossRef]
25. Hidese, R.; Nishikawa, R.; Gao, L.; Katano, M.; Imai, T.; Kato, S.; Kanai, T.; Atomi, H.; Imanaka, T.; Fujiwara, S. Different roles of two transcription factor B proteins in the hyperthermophilic archaeon *Thermococcus kodakarensis*. *Extremophiles* **2014**, *18*, 573–588. [CrossRef]
26. Kim, S.; Kim, T.-J. Inhibitory effect of *Moringa oleifera* seed extract and its behenic acid component on *Staphylococcus aureus* biofilm formation. *Antibiotics* **2025**, *14*, 19. [CrossRef]

Disclaimer/Publisher's Note: The statements, opinions and data contained in all publications are solely those of the individual author(s) and contributor(s) and not of MDPI and/or the editor(s). MDPI and/or the editor(s) disclaim responsibility for any injury to people or property resulting from any ideas, methods, instructions or products referred to in the content.

antibiotics

MDPI

Review

Lactic Acid Bacteria as Natural Antimicrobials: Biofilm Control in Food and Food Industry

Minji Kim [1,2], Jesmina Khatun [3], Fazlurrahman Khan [1,2,4,5,*] and Young-Mog Kim [1,2,3,*]

1 Research Center for Marine Integrated Bionics Technology, Pukyong National University, Busan 48513, Republic of Korea
2 Marine Integrated Biomedical Technology Center, The National Key Research Institutes in Universities, Pukyong National University, Busan 48513, Republic of Korea
3 Department of Food Science and Technology, Pukyong National University, Busan 48513, Republic of Korea
4 Ocean and Fisheries Development International Cooperation Institute, Pukyong National University, Busan 48513, Republic of Korea
5 International Graduate Program of Fisheries Science, Pukyong National University, Busan 48513, Republic of Korea
* Correspondence: fkhan055@pknu.ac.kr (F.K.); ymkim@pknu.ac.kr (Y.-M.K.)

Abstract

Biofilm production by foodborne pathogens poses significant challenges to food safety and quality, leading to contamination, deterioration, and substantial economic losses for the food industry. Traditional biofilm control methods, such as chemical disinfectants, antibiotics, and preservatives, are sometimes ineffective against persistent biofilms, raising concerns about antimicrobial resistance and the accumulation of chemical residues. Lactic acid bacteria (LAB) have emerged as attractive natural biocontrol agents due to their ability to produce a wide range of antimicrobial secondary metabolites, including bacteriocins, organic acids, hydrogen peroxide, and biosurfactants. This paper thoroughly examines the effect of LAB and their metabolites in preventing and destroying biofilms generated by bacteria relevant to food systems, including *Listeria monocytogenes*, *Salmonella enterica*, *Escherichia coli*, and *Pseudomonas* spp. The processes causing LAB-mediated biofilm attenuation are thoroughly investigated, including competition for nutrients and adhesion sites, interference with quorum sensing (QS), and metabolic inhibition. Furthermore, recent breakthroughs in LAB-based techniques for food preservation and facility hygiene are discussed, including the creation of LAB-derived antimicrobial coatings, biosurfactant-based cleaning agents, and probiotic bio-coatings for industrial sanitation. The incorporation of nanotechnology has enhanced LAB applications by enabling the creation of LAB-mediated metallic nanoparticles and encapsulated formulations that improve metabolite stability and facilitate controlled release. The combination of LAB metabolites, natural preservatives, and eco-friendly materials in active packaging provides sustainable alternatives to synthetic chemicals. Overall, this review emphasizes the potential of LAB and their bioactive derivatives as environmentally friendly and practical tools for controlling biofilms and preserving food, thereby promoting safer food production systems and accelerating the food industry's transition to green, sustainable technologies.

Keywords: lactic acid bacteria; foodborne pathogens; biofilm control; nanoparticles; encapsulated formulations

1. Introduction

Microbial biofilms pose a critical challenge in food processing environments, consisting of structured microbial communities embedded within extracellular polymeric substances (EPS) matrices that adhere to various surfaces [1,2]. These EPS matrices, composed of polysaccharides, proteins, nucleic acids, and water, enable surface attachment and protect bacteria from environmental stresses, UV radiation, extreme pH, and antimicrobial agents [3]. Biofilms pose significant threats to food safety by facilitating cross-contamination, harboring pathogenic and spoilage microorganisms, and demonstrating enhanced resistance to traditional disinfectants and sanitizers [4]. The persistence of biofilms in food processing facilities leads to equipment corrosion, impaired heat transfer, reduced shelf life, and increased risk of foodborne disease transmission [5]. Effective control requires integrated approaches combining mechanical cleaning, chemical sanitation, and novel technologies to address this persistent contamination source [6].

Bacterial biofilms are complex surface-attached communities embedded in self-produced EPS composed of polysaccharides, proteins, nucleic acids, and lipids [7,8]. Biofilm development progresses through distinct phases: reversible attachment, irreversible adhesion, EPS production, maturation, and dispersal [8,9]. During initial attachment, planktonic cells adhere through weak interactions, followed by irreversible adhesion mediated by bacterial adhesins [8]. Mature biofilms develop three-dimensional architectures resembling coral reefs with microcolonies, channels, and nutrient gradients [9,10]. The EPS matrix provides mechanical stability, mediates surface adhesion, and acts as an external digestive system [7]. Biofilm-associated cells exhibit dramatically increased antimicrobial resistance compared to planktonic counterparts [11]. Active dispersal completes the biofilm lifecycle (Figure 1), enabling colonization of new surfaces through specialized dispersal cells [12]. This multicellular organization presents significant challenges in healthcare and industrial settings [13].

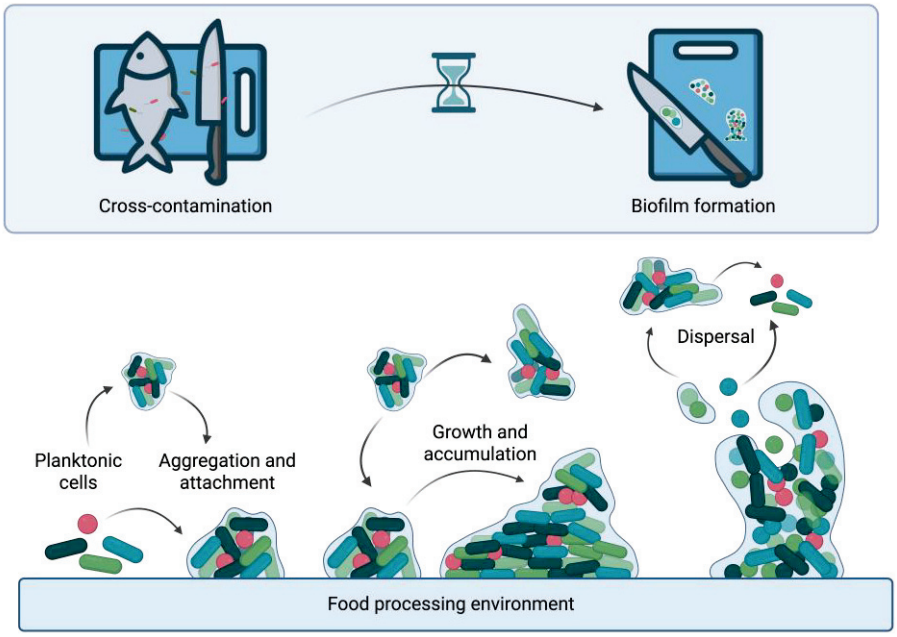

Figure 1. Biofilm formation in food processing environments. Planktonic cells aggregate and reversibly attach to a surface, initiating biofilm development. Cells then irreversibly adhere, mature into a structured community encased in extracellular matrix. Lastly, cells disperse to enable cross-contamination and colonize new sites, completing the cycle. Created in BioRender. Kim, M. (2026) https://www.biorender.com/ (accessed on 1 January 2026).

https://doi.org/10.3390/antibiotics15030248

Biofilm formation by foodborne pathogens on food-contact surfaces poses significant challenges in food processing environments. *Listeria monocytogenes* readily forms biofilms on various surfaces, including stainless steel, Teflon, nylon, and polyester floor sealant, with polyester showing the highest biofilm coverage [14]. These biofilms serve as persistent contamination sources, as microorganisms within biofilms demonstrate 10–1000 times greater resistance to antimicrobial agents compared to planktonic bacteria [15]. Key foodborne pathogens forming biofilms include *L. monocytogenes*, *Salmonella enterica*, *Escherichia coli*, *Staphylococcus aureus*, and *Pseudomonas aeruginosa* [16,17]. Persistent *L. monocytogenes* strains show enhanced surface adherence and biofilm formation capabilities, enabling survival for years in processing facilities [18]. Biofilm formation leads to cross-contamination, reduced shelf life, and increased foodborne illness risks [5,19]. Control strategies include mechanical cleaning, chemical sanitizers, thermal treatments, and emerging biological approaches [20].

Traditional biofilm control methods using chemical disinfectants, antibiotics, and preservatives face significant limitations, including antimicrobial resistance development, toxic residue concerns, and limited penetration through biofilm matrices [21,22]. These challenges have driven research toward sustainable, biologically derived alternatives. Natural control methods show promise, including bacteriocins, bacteriophages, essential oils, plant extracts, and enzymatic treatments [23,24]. Emerging strategies encompass nanotechnology-based approaches, quorum-sensing (QS) inhibition, antimicrobial photodynamic therapy, and ultrasonic systems [25,26]. Microbe-derived biological agents offer eco-friendly solutions to combat mono- and mixed-bacterial biofilms while avoiding the negative environmental and health impacts of conventional chemicals [27]. Combinatory approaches integrating multiple anti-biofilm strategies are increasingly recognized as necessary to enhance effectiveness and overcome biofilm resistance [24,28].

Lactic acid bacteria (LAB) are Gram-positive, non-sporulating, generally recognized as safe (GRAS) microorganisms that serve as promising natural biocontrol agents against foodborne pathogens [29]. LAB produce diverse antimicrobial metabolites, including organic acids (lactic, acetic), hydrogen peroxide, diacetyl, carbon dioxide, bacteriocins, reuterin, and biosurfactants that effectively inhibit pathogenic microorganisms [30,31]. These compounds demonstrate significant antibiofilm activity against major foodborne pathogens such as *L. monocytogenes*, *S. enterica*, *E. coli*, and *S. aureus* on food contact surfaces [32,33].

LAB employ multiple antimicrobial mechanisms that make them effective biocontrol agents in food systems. The primary mechanism involves organic acid production, which lowers environmental pH and creates hostile conditions for pathogens [34]. LAB also produces hydrogen peroxide, contributing to oxidative stress that damages cellular components [35,36]. Bacteriocins, ribosomally synthesized antimicrobial peptides, specifically target closely related bacteria by disrupting cell membranes [31,32]. These compounds demonstrate particular effectiveness against foodborne pathogens, including *L. monocytogenes*, *S. aureus*, and *E. coli* [32]. Additionally, LAB compete with pathogens for nutrients and adhesion sites, limiting their colonization ability [36]. These multifaceted antimicrobial properties position LAB as promising natural alternatives to chemical preservatives in food preservation [37].

Recent research has significantly expanded LAB applications beyond traditional fermentation to include innovative delivery systems and sustainable packaging solutions. LAB-derived metabolites, particularly bacteriocins and organic acids, are being incorporated into edible films and active packaging materials to extend food shelf life through antimicrobial activity [38,39]. These biodegradable films offer the dual benefits of environmental sustainability and effective pathogen control [40,41]. LAB exopolysaccharides demonstrate excellent film-forming properties for edible packaging applications while providing bioactive functions, including antioxidant and antimicrobial activities [39].

https://doi.org/10.3390/antibiotics15030248

Advanced delivery systems utilize LAB as both passive encapsulation targets and active carriers through surface adsorption, intracellular loading, and co-encapsulation in hydrogels [42]. These bio-based approaches align with consumer demand for clean-label products and environmentally responsible technologies, supporting applications in functional foods, precision nutrition, and sustainable agriculture [43–45].

Furthermore, the LAB products have been extensively utilized to synthesize metal nanoparticles, including silver and gold, which exhibit potent antimicrobial and antibiofilm activities against pathogenic bacteria such as *P. aeruginosa* and *S. aureus* [46,47]. These biogenically synthesized nanoparticles effectively inhibit biofilm formation and eradicate established biofilms while reducing virulence factors [47]. LAB produce antimicrobial compounds like bacteriocins that demonstrate dose-dependent biofilm inhibition against foodborne pathogens, including *L. monocytogenes*, *S. aureus*, and *E. coli* [32]. LAB biofilms themselves possess antimicrobial properties against pathogenic microorganisms [48]. The combination of LAB metabolites with other antimicrobials creates synergistic effects, enhancing their antibiofilm activity [32,49]. These natural biopreservation strategies offer promising alternatives to conventional chemical preservatives in food safety applications [29,35].

The present review aims to provide a comprehensive discussion on the application of LAB and their secondary metabolites as potential antibiofilm and antivirulence agents against foodborne pathogens. Furthermore, the review highlights the use of nanotechnology-based approaches fabricated using LAB-derived products to control biofilm formation and virulence traits in these pathogens. Additionally, the synergistic effects of combining LAB and their secondary metabolites with conventional antibiotics for the management of foodborne pathogens are also discussed in detail.

2. Impact of Biofilms on Food and the Food Industry

2.1. Biofilms in Food Production and Storage

Biofilm causes many risks during food production and storage. Due to the complexity of food matrix components, food-borne pathogens are easy to attach and generate biofilms. Major foodborne pathogens generating biofilm related to food issues are *Bacillus cereus*, *E. coli*, *L. monocytogenes*, *S. enterica*, *S. aureus*, *Pseudomonas* spp., etc. Depending on the food group, the foods have different characteristics, and they have different pathogens of concern (Table 1).

Table 1. Biofilm-forming pathogens associated with different food groups.

Food Group	Characteristics	Pathogens of Concerns	Refs
Fruits	High in sugar and moisture	*L. monocytogenes*, *E. coli* *Salmonella* spp.,	[50–53]
Vegetables	Contaminated by contacting soil and irrigation water.	*L. monocytogenes*, *Salmonella* spp., *E. coli*	[53–55]
Grains	Although grains are dry and have low water activity, pathogens can persist during processing and storage.	*B. cereus*, *S. enterica*	[56]
Protein foods (Meat, poultry, seafoods, and legumes)	Protein-rich foods support biofilm formation, especially in processing environments.	*L. monocytogenes*, *Salmonella* spp., *Campylobacter jejuni*, *Pseudomonas* spp., *B. cereus*, *Vibrio parahaemolyticus*, *Aeromonas hydrophila*, *E. coli*	[19,57,58]

https://doi.org/10.3390/antibiotics15030248

Table 1. *Cont.*

Food Group	Characteristics	Pathogens of Concerns	Refs
Dairy	Milk and dairy processing environments support bacterial biofilm formation, leading to contamination.	*L. monocytogenes*, *S. aureus*, *Pseudomonas* spp., *B. cereus*	[59,60]

Fruits are typically high in sugar and moisture, which can support the growth of biofilm-forming pathogens. Moreover, the increase in the consumption of fresh-cut ready-to-eat fruits increases the chance of microbial spoilage and foodborne illness compared to the consumption of whole products [61,62]. *Salmonella* spp. are one of the foodborne pathogens that form biofilms on fruits. According to Annous et al. [50], *Salmonella* forms biofilms on cantaloupe melon, making them resistant to aqueous sanitizers. *L. monocytogenes* is another foodborne pathogen that can easily contaminate fresh produce, including fruits, because of its prevalence in soil, manure, and water [52]. There are several studies investigating the effects of biofilm of *L. monocytogenes* on their survival. Biofilm increases the persistence of *L. monocytogenes* and increases resistance to biocide [63,64]. Another foodborne pathogen of concern related to biofilm on fruits is *E. coli*. Amrutha et al. [53] examined the potential of biofilm formation of *E. coli* and *Salmonella* spp. from fresh fruits and vegetables [53]. According to their findings, both bacteria were revealed as potential biofilm formation.

Leafy greens and root vegetables are prone to contamination due to their contact with contaminated soil and irrigation water. Harvesting and processing are associated with plant tissue damage promoting the multiplication of foodborne pathogens. According to [62], damage in plant tissue increases the *E. coli* multiplication, suggesting harvesting and processing is considered a critical point of the *E. coli* contamination of fresh produce. Sun and their team investigated the biofilm formation of *E. coli* on cucumber [54]. According to their findings, *E. coli* O157:H7 favors 25 °C over 4 °C to form biofilm. Also, they found that biofilm formed more in vascular tissues than in other tissues. *Salmonella* spp. are another foodborne pathogen that forms biofilm on vegetables. According to Pastel et al., *S. enterica* serovars have the ability to attach and colonize intact and cut lettuce and cabbage [65]. They found that *Salmonella* spp. are prone to attach to the cut surface, but the attached population on cut surfaces and intact surfaces was similar. *L. monocytogenes* forms strong biofilms on leafy greens. The interaction between *L. monocytogenes* and lettuce was studied by Gorski et al. [66]. *L. monocytogenes* has interactions with the cut edge and veins of lettuce leaves. They also found that different products have different interacting factors.

Although grains like wheat, rice, and flour have low water activity, pathogens can persist based on treatment, processing, and storage, raising food safety risks. *B. cereus* [67–69] and *Salmonella* spp. [70,71] commonly form biofilms in grains. These bacteria can contaminate raw materials from soil or post-harvest environments and survive desiccation, leading to potential cross-contamination during milling, packaging, or further processing into products like flour and ready-to-eat cereals [60]. Sarrías et al. [69] reported that *B. cereus* populations are higher in unhusked rice compared to husked ones, highlighting the protective role of husk against environmental contamination. Processing steps such as drying, husking, and polishing progressively reduce *B. cereus* levels in the final products [69]. For *S. enterica* ser. Enteritidis, biofilm formation was unrelated to dryness, but biofilm quantity positively correlated with thermal resistance. This indicates that *Salmonella* biofilms on low-moisture foods resist elimination by heat processing [70].

Protein-rich foods support biofilm formation, especially in processing environments [72]. These contain meat, poultry, seafood, and legumes. In the case of meat products, biofilm

https://doi.org/10.3390/antibiotics15030248

remains a serious problem to be concerned about because it is hard to sanitize properly [73]. Therefore, the transfer efficiency of cells from biofilm and cell density has a great effect on the biofilm formation on meat by *E. coli*, and *L. monocytogenes*. This aspect also affects poultry, seafood, and even salami [62,74,75]. Additionally, according to Wang et al., there was a diverse group of *S. enterica* strains collected in various meat plants [76]. In the case of seafood, it contains high levels of proteins, lipids, and minerals that provide excellent substrate for bacterial attachment and biofilm development [77]. *Vibrio* spp., *A. hydrophile*, *Salmonella* spp., and *L. monocytogenes* are widely known bacteria generating biofilm on seafood [78–80].

Several pathogenic and spoilage bacteria such as *B. cereus* and *Bacillus substiles* form biofilms directly in or on dairy products, supported by a high-nutrient environment, neutral pH, and residual moisture that favor microbial adhesion and matrix production [81,82]. Typical biofilm-forming groups in dairy include members of the Enterobacteriaceae family, *S. aureus*, *Bacillus* spp., *L. monocytogenes*, and *Pseudomonas* spp., which are associated with both mastitis in dairy animals and with spoilage or foodborne disease in consumers [83,84]. Enterobacteriaceae significantly influence cheese safety and quality, often originating from raw milk based on hygiene and quality levels, and easily integrate into the cheese matrix early in processing and ripening under suboptimal salt and temperature conditions [85]. Cell populations typically decrease during later stages of ripening due to lactic acid bacteria activity, decreasing pH, and other stressors. However, strains like *E. coli*, *Klebsiella pneumoniae*, and *Salmonella* spp. can still create health hazards and degrade sensory attributes [86,87]. Therefore, managing Enterobacteriaceae across cheese production remains essential for safety and quality assurance [84]. *S. aureus* is a significant concern in dairy products because of its association with foodborne outbreaks [88]. This species can produce heat-stable enterotoxins in milk, meaning that toxins may persist even after pasteurization [89]. This strain has also been detected in infant powdered formula, highlighting the risk for vulnerable populations [90]. *L. monocytogenes* is another important dairy-associated biofilm-forming bacteria, frequently isolated from cheeses and other ready-to-eat dairy products. It has been reported to persist for extended periods, with some strains surviving for years in contaminated cheese and Scandinavian dairy products, emphasizing its ability to withstand storage conditions [91,92].

2.2. Biofilms in Food Processing Facilities

Biofilms in processing facilities pose a major challenge to both human health as they serve as persistent reservoirs for foodborne pathogens that can contaminate products and trigger outbreaks, and threaten economic stability in the food industry, due to costly product recalls. These microbial communities adhere to equipment surfaces like pipes, tanks, knives, and conveyors made by stainless steel, wood, glass, polyethylene, rubber, and polypropylene, releasing cells that contaminate processed foods, including pasteurized products such as milk, juices, and ready-to-eat products [2]. These environments have positive effects on biofilm formation by acting as artificial substrates [93]. Pathogens like *L. monocytogenes*, *Salmonella* spp., and *E. coli* persist in biofilms, leading to outbreaks even after thermal treatments.

Biofilm-forming species such as *Bacillus* spp. produce resilient endospores that withstand heat, desiccation, and cleaning agents, making them difficult to eliminate. These spores show hydrophobicity, facilitating attachment to processing surfaces, and surviving spores develop into vegetative cells that contaminate food products [60,94]. Because of the difficulties in sanitation, biofilms in food facilities increase operational costs through frequent deep cleaning and equipment downtime [71]. Therefore, rigorous cleaning-in-place

https://doi.org/10.3390/antibiotics15030248

(CIP) protocols, surface modifications, and monitoring are essential to mitigate biofilm contamination [95].

3. LAB Secondary Metabolites and Their Role in Biofilm Control

LAB are increasingly recognized by their ability to combat biofilm formation from pathogenic microorganisms through their diverse secondary metabolites. These include organic acids (such as lactic, acetic, and secondary bile acids), antimicrobial peptides (bacteriocins and related peptides), amino acid derivatives, EPS, and other bioactive compounds like hydrogen peroxide [96–101]. There is an increasing trend toward the application of LAB-derived secondary metabolites to control microbial pathogens known to form biofilms in the food industry (Figure 2).

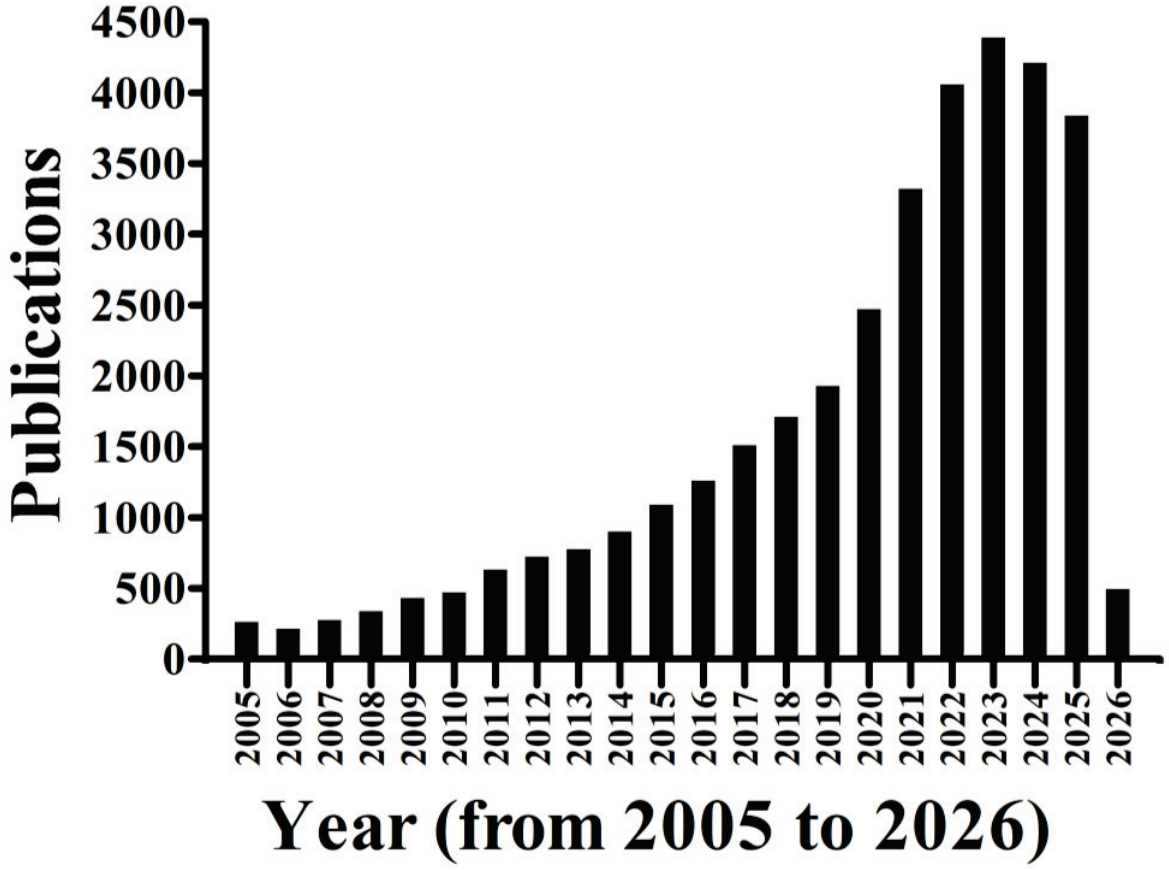

Figure 2. The list of publications on the application of LAB secondary metabolites as biofilm controlling agents in the food industry (from 2005 to 29 January 2026 searched in Google Scholar using the keyword "Lactic acid bacteria secondary metabolites as biofilm controlling agents in the food industry").

Their production is highly strain-dependent, so metabolite profiles differ significantly among different genera [101]. These metabolites inhibit the biofilm formation, disrupting established biofilm, and combating virulence pathogens. Organic acids primarily inhibit pathogens by lowering extracellular pH and intracellular homeostasis through weak-acid diffusion mechanisms, while bacteriocins are ribosomally synthesized antimicrobial peptides that typically exert their activity via membrane disruption or inhibition of cell wall biosynthesis, depending on the bacteriocin class [34,102–105]. EPS can modulate biofilm formation by influencing microbial adhesion and matrix structure, with effects that are highly dependent on the producing organism and environmental context [106,107]. Figure 3 summarizes the mechanisms by which LAB secondary metabolites control biofilms [108].

https://doi.org/10.3390/antibiotics15030248

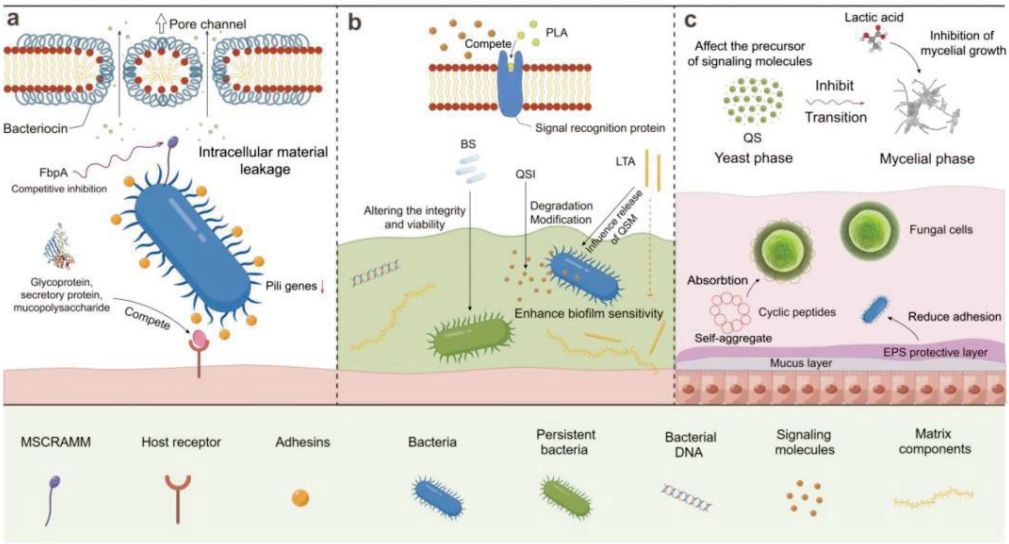

Figure 3. Modes of action of LAB secondary metabolites in biofilm control. Probiotics from LAB can (**a**) kill planktonic cells and prevent their initial attachment to host surfaces, (**b**) interfere with cell-to-cell signaling and biofilm stability, thereby inhibiting biofilm maturation, and (**c**) use organic acid and small antimicrobial peptides to limit pathogen colonization. Reprinted from [108], Copyright © 2024 by the authors. Licensee MDPI, Basel, Switzerland.

Classification and Types of LAB Secondary Metabolites

The main classes of LAB secondary metabolites include organic acids, bacteriocins, amino acid derivatives, EPS, surface-active molecules, and other bioactive compounds (Table 2) [101]. First, organic acids, such as lactic acid, acetic acid, propionic acid, formic acid, succinic acid and phenyllactic acid are generated by LAB [40,109]. These acids reduce pH, creating hostile environments for pathogens by affecting the relative electrical conductivity and interfering with biofilm formation [34,101,110]. These organic acids are thermostable, but sensitive to neutralization of pH. Nevertheless, heat-treated organic acids and pH-neutralized organic acids in CFS still limit the biofilm formation of the pathogen [111]. According to Shokori et al., three organic acids, lactic acid, formic acid, and acetic acid, produced by *Limosilactobacillus fermentum*, showed a significant antibacterial effect in the absence of bacteriocin [112]. This shows the organic acid's postbiotic potential on pathogenic biofilm prevention and degradation.

Bacteriocins are ribosomally synthesized antimicrobial peptides [113], classified in four groups depending on the size and modification. This includes nisin [114], plantaricin (*Lactiplantibacillus plantarum*) [115], leucocin (*Leuconostoc lactis*) [116], and KCA from *Carnobacterium maltaromaticum* [117]. Different bacteria generate their own bacteriocin with different molecular weights, biochemical properties, and modes of action. They disrupt cell membranes or walls of target bacteria [102–104], showing the possibility of their usage in targeting specific pathogens [118]. Since they are evaluated as GRAS in the food industry, they are widely used and incorporated into foods [101].

Many LAB strains secrete capsular or slime EPS, including homopolysaccharides and heteropolysaccharides with complex repeating units [119]. Depending on their structural composition, LAB-derived EPS can either promote self-biofilm formation for probiotic persistence or exert antagonistic effects on pathogens by impairing cell division, blocking surface receptors, reducing surface stress, chelating ions, or interfering with biofilm matrix assembly [120]. In food systems, LAB-derived EPS can further contribute to pathogen control by reducing microbial adhesion to food matrices and processing environments, thereby limiting initial biofilm establishment [121].

https://doi.org/10.3390/antibiotics15030248

Surface-active molecules such as phospholipids, glycolipids, lipoprotein-lipopeptides, and lipid-polysaccharide complexes are produced by diverse microorganisms [122,123]. These biosurfactants can lower surface tension and decrease cell-surface hydrophobicity, thereby preventing initial colonization of stainless steel, plastics, and epithelial cells by foodborne pathogens. Biosurfactants purified from LAB have also been shown to downregulate biofilm-associated genes in other pathogenic bacteria. For example, biosurfactants like lactic acid and acetic acid from *Lactobacillus rhamnosus* downregulate biofilm-associated genes in *Acinetobacter baumannii*, a pathogen relevant to food contamination, by disrupting DNA repair genes [124].

Reactive antimicrobial molecules such as hydrogen peroxide (H_2O_2), reuterin, and diacetyl are also LAB metabolites showing antimicrobial activity [125]. Hydrogen peroxide effectively inhibits pathogenic bacteria growth by altering the membrane permeability [101,126]. Reuterin exhibits broad-spectrum antimicrobial activity against Gram-positive and -negative bacteria, fungi, yeasts, and viruses. Although the precise mechanisms remain incompletely understood, its reactive aldehyde group is assumed to bind sulfhydryl groups in proteins and other molecules such as reduced glutathione, thereby disrupting redox balance, membrane integrity, and biofilm formation [127,128]. Diacetyl, generated by LAB, inhibits and eradicates pathogen growth and QS, contributing to inhibiting biofilm formation by decreasing bacterial metabolism, auto-aggregation, and down-regulation of related gene expression [129].

These LAB metabolites target multiple biofilm stages with multiple mechanisms. These contain destabilization of early adhesion and matrix via acidification and oxidative stress, cell penetration, hydrophobicity alteration, and QS disruption. In food processing, such postbiotic cocktails synergize to control biofilm from pathogenic bacteria, offering sustainable alternatives to chemical sanitizers while minimizing resistance development.

Table 2. Major LAB-derived secondary metabolites and their producing LAB strains.

Major LAB Secondary Metabolites	LAB Strain	Potential Application or Mechanism	References
Sakacin A	*L. sakei* Lb706	Inhibition of *L. monocytogenes* by cell membrane permeabilization	[130]
Bacteriocin (free-form)	*L. curvatus* CWBI-B28	Disrupts *L. monocytogenes* membranes	[131]
Sakacin G, P	*L. Sakei* CWBI-BI1365, *L. curvatus* CWBI-B28	Both Sakacin G and P inhibit *L. monocytogenes* through their activity	[132]
Divergicine M35	*Carnobacterium divergens* M35	Culture supernatant proves more effective than purified bacteriocin. Inhibit *L. monocytogenes*	[133]
Nisin	*L. lactis*	Inhibits Clostridium spores, widely used as a food bio preservative	[134]
Plantaricin	*L. plantarum* 2C12	Antimicrobial activity by cell membrane disruption	[135]
Lactocin 705, AL 705	*L. curvatus* CRL705	Bacteriocin was effective in controlling spoilage bacteria in refrigerated storage for 60 days	[136]

https://doi.org/10.3390/antibiotics15030248

Table 2. *Cont.*

Major LAB Secondary Metabolites	LAB Strain	Potential Application or Mechanism	References
Reuterin	*L. reuteri* INIA P572	Antimicrobial effects on *L. monocytogenes* and *E. coli*	[137]
Sakacin Q	*L. curvatus* ACU-1I	Inhibits *L. innocua* in the form of freeze-dried reconstituted supernatant	[138]
Sakacin P, X	*L. curvatus* MBSa2, MBSa3	Heat, pH, NaCl stable bacteriocins inhibiting *L. monocytogenes*	[139]
LD-phenyllactic acid (PLA)	*L. plantarum* CXG9	Inhibit *L. monocytogenes* by cell membrane integrity	[140]

4. LAB-Based Strategies for Biofilm Prevention and Removal

4.1. LAB in Food Products for Natural Preservation

LAB are well characterized for their strong antimicrobial activity against planktonic cells, whereas research specifically addressing their antibiofilm effects remains relatively limited. Therefore, in this section, we examine how LAB and their metabolites can prevent biofilm establishment by inhibiting microbial growth and surface colonization prior to biofilm maturation.

LAB have been utilized in a wide range of foods, including fermented dairy, meat, seafood, and vegetables, because of their natural preservation efficacy. For example, in dairy fermentations, LAB such as *Streptococcus thermophilus* and *Lactobacillus delbrueckii* subsp. *Bulgaricus*, together with other beneficial species such as *Lactobacillus acidophilus*, *L. rhamnosus*, *Lactobacillus casei*, and *Bifidobacterium* spp., contributes to the development of yogurt and cheese. These microorganisms help inhibit spoilage and pathogenic bacteria through acidification, production of bacteriocins, and competition for nutrients thereby enhancing both the safety and quality of the final products [141–144].

In the case of meat products, there are two ways of LAB application. One is a direct LAB application method, such as using it as a starter culture to make fermented meat sausage, and LAB attachment on meat surface to have an antagonistic effect. The other indirect method is applying purified biologically active LAB metabolites such as lactococcin, BZ and plantaricin (Figure 4) [145]. Direct application of LAB focused on eliminating pathogens such as *Salmonella* spp. or *E. coli* [49]. According to Sakaridis et al. *Ligilactobacillus salivarius* had an effective inhibition effect on *Salmonella* spp. and *L. monocytogenes* on chicken [146]. Other applications of LAB as a non-starter ingredient are the application of *Lactobacillus sakei* on fresh pork sausage for *S. enterica* serotype Choleraesuis control, *Latilactobacillus curvatus* for *Pseudomonas* spp. inhibition of vacuum-packed fresh beef steak, *L. plantarum* or *Limosilactobacillus reuteri* on ground beef, and sucuk sausage for *L. monocytogenes* prevention [136,147–149]. *L. plantarum* strains and *L. sakei* strain were also used as starter cultures for meat fermentation, such as dry-cured sausage [150]. The two bioprotective cultures, as bacteriocin producers, effectively controlled *L. monocytogenes* primarily through their bacteriocin production rather than pH modification. *Pediococcus acidilactici* showed the same effects when they were used as a starter culture in the beef product [151,152].

https://doi.org/10.3390/antibiotics15030248

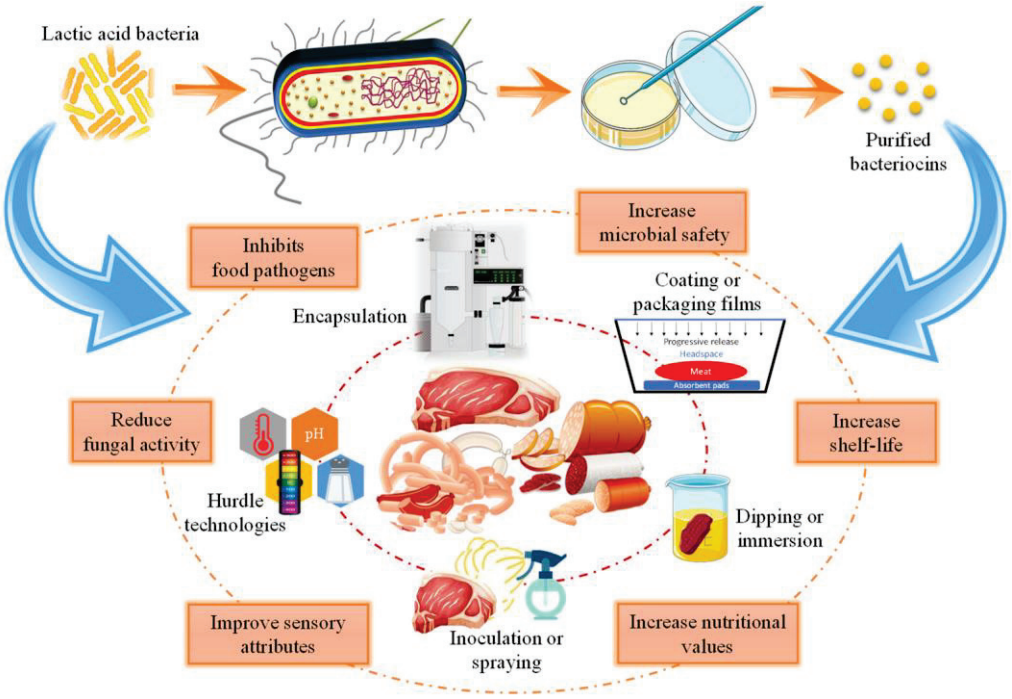

Figure 4. Application of LAB and bacteriocins in meat products. Direct use, such as starter cultures in fermentation and non-starter additives, indirect via semi-purified or purified bacteriocins incorporated as functional ingredients. Reprinted from [145], Copyright © 2022 by the authors. Licensee MDPI, Basel, Switzerland.

Indirect methods apply LAB metabolites such as lactococcin BZ, plantaricin, BacFL31, leucocin A, sakacin A, nisin, and CFS via dipping, spraying, or films [134,135,153–157]. Those bacteriocins or metabolites were combined with other treatments, such as chemical and physical methods that disrupt the bacterial cell wall, showing a synergistic effect on the inhibition of the pathogen [158]. This can be applied to hurdle technology and active packaging [49]. Sakacin A with pullulan biopolymer inhibits the growth of *L. monocytogenes* on meat products. In this case, the antimicrobials were protected from degradation, maintaining their antimicrobial activity, showing the bacteriocin ability of sakacin A and bacteriocin-delivering ability of pullulan [159]. Xie et al. [160] used a plantaricin solution to be absorbed in polyvinylidene chloride film and applied it to fresh pork to check their antimicrobial effect. They were successfully inhibiting *L. monocytogenes* [160]. Microencapsulation techniques showed effectiveness for slow biopreservative release and protection from degradation. Ghabraie et al. encapsulate antimicrobial agents such as nicin, nitrite, and organic acid salts into alginate-cellulose microbeads for a better delivery method [161].

In seafood, LAB strains including *Lactobacillus pentosus*, *Leuconostoc mensenteroids*, *L. casei*, *L. plantarum*, *Carnobacterium maltaromaticum* (formerly *C. piscicola*), *C. divergens*, *L. sakei* and *L. curvatus* are introduced during fermentation or as protective cultures to suppress *L. monocytogenes* growth and extend shelf life in fresh salmon, smoked salmon and trout [133,162–172]. These strains are applied by spraying or dipping filet surfaces or direct inoculation, effectively reducing *L. monocytogenes* growth and biofilm formation under refrigerated storage conditions without adverse sensory effects.

Many lactic acid bacteria isolated from plant materials and food products can be applied directly as protective cultures. LAB use on fresh produce and minimally processed vegetables is gaining interest as a biopreservation method to combat microbial growth driven by high moisture and nutrient content during storage and transport. Including LAB in dipping or washing solutions protects these products from pathogenic bacteria. For example, *Lactobacillus* spp. strains applied to apples and lettuce effectively control spoilage

https://doi.org/10.3390/antibiotics15030248

microorganisms without negatively affecting quality. This can serve as a chlorine alternative widely used on leafy greens and hexanal or 2-E-Hexenal for ready-to-eat fruits [173]. Microencapsulation enhances LAB viability by immobilizing cells in hydrocolloid matrices such as alginate, protecting them from environmental stresses [174]. Since cell viability and activity are critical for probiotic efficacy, microencapsulation improves post-harvest biopreservation on fresh produce by immobilization on produce surface and combat pathogenic microbial growth [175].

4.2. LAB in the Food Industry for Equipment and Facility Hygiene

LAB contribute to food industry equipment and facility hygiene through protective biofilms, bacteriocin-producing CFS, and postbiotics that compete with or disrupt pathogenic biofilms [33,176]. They form biofilms that occupy adhesion sites on processing equipment, counteracting pathogens such as *L. monocytogenes*, *Salmonella* Typhimurium, *B. cereus*, and *E. coli* O157:H7. In dairy facilities, LAB biofilms actively inhibit pathogenic bacteria colonization on stainless steel by generating lactic acid and antimicrobial compounds such as hydrogen peroxide, ammonia, acetic acid, and bacteriocins, reducing pathogen attachment [176,177]. LAB biofilms such as *Enterococcus faecium* and *Pediococcus pentosaceus* are used in food processing facilities to control foodborne pathogen biofilms [178,179].

LAB CFS, rich in bacteriocins, organic acids, and biosurfactants, are sprayed or incorporated into cleaning protocols to eradicate pre-formed biofilms without chemical sanitizers. It is shown that the usage of semi-purified bacteriocin from *L. sakei* showed more effective inhibition of pre-established *L. monocytogenes* biofilm than displacement, indicating that other metabolites did not play an important role in inhibition of *L. monocytogenes* biofilm [33]. Tan et al. [180] tested pathogenic bacteria biofilms such as *L. monocytogenes*, *S. aureus*, *E. coli*, and *Salmonella* spp. prevention or reduction by exclusion, competition, and displacement on different abiotic surfaces such as stainless steel, polyvinyl chloride (PVC), and glass. All tested methods reduced pathogenic biofilms on these surfaces, but pre-established LAB biofilms generally provided the greatest and most consistent reductions compared with competition or displacement strategies [180].

Masebe et al. [181] reported comparable results, demonstrating anti-biofilm potential of CFS from commercial probiotics, *L. acidophilus* LA14 150B and *L. plantarum* B411, *L. rhamnosus* against *L. monocytogenes* isolated from avocado, cucumber, and an avocado plant. All strains formed moderate to strong biofilms on PVC and stainless steel, mimicking food-contact equipment surfaces. CFS inhibited biofilm formation and dispersed pre-formed biofilms, significantly downregulating *prfA* virulence gene expression. These findings establish LAB CFS as promising food-grade sanitizers for fresh produce lines, targeting *L. monocytogenes* dislodgement from surfaces to fruits like avocados and cucumbers [181].

However, the implementation of LAB biofilms and postbiotic cleaners requires careful strain selection to avoid unintended contamination or resistance gene transfer [32,176]. Future work could focus on multi-strain protective effect, immobilization of LAB on reusable carrier materials, and integration of LAB-based agents with physical treatments to achieve robust and sustainable control of pathogenic biofilms on food contact surfaces [21,32].

5. Enhancing LAB Application: Derivatives and Nano-Formulations

5.1. LAB-Derived Antimicrobial Coating and Packaging

LAB produce a range of antimicrobial metabolites, including organic acids, hydrogen peroxide, and bacteriocins, which have been explored for use in active and biodegradable food packaging. Recent studies have shown that incorporating LAB metabolites into edible films can enhance the shelf life and microbial safety of perishable foods by inhibiting spoilage and pathogenic microorganisms (Figure 5) [182–184]. These films not only serve

https://doi.org/10.3390/antibiotics15030248

as protective barriers but also function as carriers for the slow and controlled release of antimicrobial agents [185]. Furthermore, biodegradable and antimicrobial packaging materials infused with bacteriocins represent sustainable alternatives to synthetic preservatives, aligning with the growing demand for eco-friendly and health-conscious food preservation methods [186].

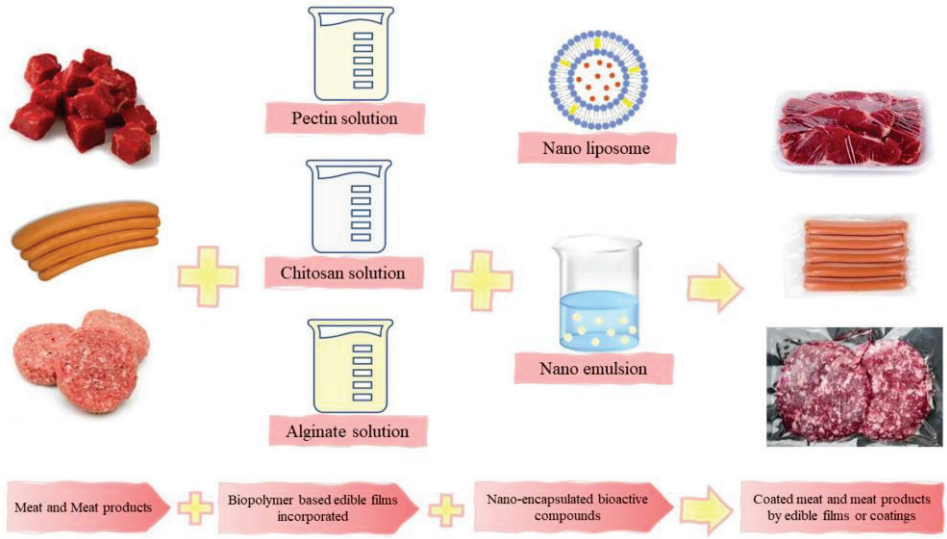

Figure 5. Schematic of encapsulated LAB metabolites incorporated into edible biopolymer films for coating meat products. Reprinted from [184], Copyright © 2023 by the authors. Licensee MDPI, Basel, Switzerland.

The metabolites of LAB have been incorporated with active packaging systems in different forms, such as sachet packages, coatings onto the packaging material surface, bulk incorporation into packaging polymer films or multilayer films, and covalent immobilization onto the film surface [187]. The incorporation can be done by several methods, such as surface coating, solvent casting, extrusion, electrospinning, layer-by-layer, and encapsulation [188]. Table 3 illustrates diverse LAB coating applications across food categories, consistently demonstrating microbial control and quality preservation.

Table 3. LAB-based edible coatings and films for diverse food products.

Application	LAB Strain	Components Used	Outcomes	Reference
'Tommy Atkins' mango coating	*L. casei*	Five nanolayers of pectin and chitosan	Better quality in weight loss, total soluble solids, and titrable acidity	[189]
Melon coating	*L. plantarum*	Alginate and chitosan	Enhances the physiological and microbial quality of fresh-cut melon	[190]
Akihime's strawberry	*L. casei*	CMC with chitosan	Inhibition of the loss of fruit firmness and aroma volatiles of strawberry	[191]
Cheese coating	*L. helveticus* M-LH13	Liquid acid whey protein concentrate, apple pectin, sunflower oil, glycerol	Improved appearance, slowed down discoloration of cheese	[192]

https://doi.org/10.3390/antibiotics15030248

Table 3. *Cont.*

Application	LAB Strain	Components Used	Outcomes	Reference
Beef slice coating	*L. sakei*	Sodium caseinate film	Reduce the growth of *L. monocytogenes*	[193]
Ham coating	*L. curvatus*	Whey protein-based film with bacteriocin producing strain	Reduce listeria contamination	[194]
Blueberry coating	*L. rhamnonsus*	Alginate, prebiotics, and probiotics	Reduce the level of *L. innocua*	[195]
Apple coating	*L. rhamnosus*, *B. lactis*	Alginate, prebiotics (fructooligosaccharides and insulin)	Preserve freshness and safety, shows antagonistic properties	[196]
Trout filet coating	*Lactobacillus* spp., *B. bifidum*	Carboxymethyle cellulose and sodium caseinate films	Improves quality and shelf-life	[197]
Artificially contaminated chicken filet	*Enterococcus caseiflavus*	Poluthylene terephthalate films (PET)	Produces anti-listeria substances, lowering *L. monocytogenes* contamination	[198]

While current studies primarily documented antimicrobial activity against planktonic cells, these coatings are expected to prevent biofilm formation by continuously suppressing microbial growth and surface colonization at food packaging interfaces.

5.2. Nanotechnology for LAB Metabolites Delivery

Nanotechnology provides versatile carriers to enhance the stability and bioavailability of LAB-derived antimicrobials, including bacteriocins, organic acids, and other bioactive metabolites. Nanoparticles enhance the stability and solubility of the encapsulated substances, promote their efficient transport and extend their circulation time, which ultimately increases both safety and therapeutic efficiency [199]. Some vitamins, essential oils, phenolic compounds, or carotenoids have beneficial properties for human health but are poorly soluble in water, and sometimes sensitive to temperature and oxidation, which limits their use in the food industry [200]. Encapsulation protects these bioactives using a protective wall. In food packaging, nanosized materials improve properties, extend shelf life, preserve flavor, color, aroma, and texture, and shield against pests and microbes [201].

LAB enables green biosynthesis of antimicrobial metal nanoparticles (MNPs) using CFS as bio-reductants and stabilizers at ambient temperature [202]. MNP synthesis is carried out at room temperature using metal salts with plant extract or microbial supernatants [203]. X-ray and transmission electron microscopy are used to confirm the formation of both metallic and oxide nanoparticles [204]. However, despite the similarities in these approaches, slight variations exist in the biosynthesis of different types of MNPs [205]. For instance, variations in the choice of precursors can lead to metal nanoparticles exhibiting distinct physicochemical characteristics [206]. Additionally, variations in the concentration of certain elements, such as molecular oxygen (O_2) or chloride ions (Cl^-), can influence the synthesis outcome, leading to the formation of metal oxide nanoparticles (e.g., Ag_2O NPs) or metal chloride nanoparticles (e.g., AgCl NPs) instead of pure metal nanoparticles (e.g., Ag NPs) [207]. Moreover, numerous reaction parameters, including temperature, oxygen availability, pH, precursor (metal salt) concentration, microbial growth phase at the time of supernatant collection, incubation duration, and irradiation, have

https://doi.org/10.3390/antibiotics15030248

been shown to significantly affect both the yield of the reaction and the physicochemical properties of the resulting MNPs [208,209].

5.3. Synergistic Approaches with LAB Metabolites

Synergistic combinations of LAB metabolites with essential oils, plant phenolics, organic acids, and polysaccharides address the narrow antimicrobial spectra, pH sensitivity, and stability limitations of natural preservatives. For example, cationic bacteriocins such as nisin and pediocin selectively disrupt Gram-positive *L. monocytogenes* cytoplasmic membranes while hydrophobic essential oil components, including thymol, carvacrol, and cinnamaldehyde, permeabilize Gram-negative *Salmonella* Typhimurium and *E. coli* [210–212]. Synergistic use of LAB metabolites with natural preservatives and established food safety systems offers a promising route toward sustainable, natural, and consumer-safe food preservation strategies. This multi-target mechanism expands pathogen coverage, reduces minimum inhibitory concentrations, minimizes resistance development, and achieves lower organoleptic impacts compared to higher doses of single agents that often impart off-flavors [213].

Essential oils combined with nisin achieve the highest reductions in *L. monocytogenes* in poultry compared to individual treatments without sensory deterioration [214]. Enterocin 416K1, produced by *Enterococcus casseliflavus*, incorporated into a coating on low-density polyethylene (LDPE) film, reduces *L. monocytogenes* counts by 5 log units and effectively inhibits its growth on sausage and fresh cheese for up to seven days [215]. Similarly, the CFS of *L. rhamnosus*, combined with whey protein isolate or calcium caseinate films, exhibited strong antimicrobial activity. These protein-based films effectively inhibited *L. monocytogenes*, *S. aureus*, *E. coli*, and *S. enterica* ser. Typhimurium [216]. Moreover, whey protein isolate films with *L. sakei* cell-free supernatant effectively reduced pathogens on fresh beef. *E. coli* was eliminated after 36 h of refrigeration, and *L. monocytogenes* declined by 4 log units after 120 h. This highlights strong antimicrobial potential during cold storage [217].

These examples illustrate the substantial promise of synergistic LAB metabolite applications in coating materials for food, which enhance food safety through broad-spectrum pathogen control and reduce reliance on synthetic preservatives facing regulatory restrictions. However, continued research remains essential to optimize formulation stability under commercial processing conditions, scale up coating application technologies, and validate long-term sensory performance required for widespread industry adoption.

6. Conclusions

LAB and their metabolites offer versatile, food-grade solutions for biofilm control across products and contact surfaces [48,218]. Direct applications include using LAB as starter cultures or surface sprays, as well as CFS or purified bacteriocins to inhibit pathogens via acidification, competitive exclusion, and interference with QS [219]. Indirect methods like bacteriocin-integrated active packaging and sanitizers extend shelf life and enhance safety with minimal adverse sensory effects under optimized conditions [220]. Protective biofilms and CFS have demonstrated strong potential for facility hygiene, outcompeting or eradicating persistent pathogens on stainless steel, polyvinyl alcohol, wood, and glass, thereby establishing LAB as a sustainable alternative to chemical sanitizers [48].

Despite their promise, hurdles include strain variability in metabolite yield and stability under industrial stress, regulatory approval for probiotics in hygiene applications, costs of CFS production and scaling, and potential overgrowth leading to off-odors or histamine formation in high protein foods [21,221]. Validating multi-surface efficacy and long-term persistence remains critical to prevent rebound contamination [222].

https://doi.org/10.3390/antibiotics15030248

Future efforts should include the antibacterial and antibiofilm effect of multi-strain LAB that can enhance the effect and synergistic effect. Immobilizing the LAB metabolites on reusable carriers such as beads and membranes, robust and sustainable pathogenic bacteria prevention or control on the food surface could be addressed. Using hurdle technologies such as ultrasound or cold plasma by sequential integration with LAB or LAB metabolites on food or food facilities may further enable synergy [223,224]. Also, emerging work on biogenic nanoparticles indicates that nanoscale materials can enhance antimicrobial potency via increased surface area and reactive oxygen species-mediated membrane disruption [225–228]. This suggests that LAB-derived or LAB-synthesized nanoparticles embedded in biodegradable films could become a new platform for active food packaging and biofilm control. Moreover, encapsulation strategies could provide controlled, pH triggered release of LAB-derived bacteriocins and improved probiotic survival, forming advanced LAB-based preservatives and biofilm control tools [229,230]. Pilot trials in diverse facilities, omics analyses of biofilm dynamics, and economic assessments will accelerate the revolution of food safety and control.

Overall, LAB are promising candidates as natural antimicrobials and antibiofilm agents that can be applied across diverse food categories and food facilities. Sourcing beneficial human probiotics or LAB isolated from natural foods will facilitate clean-label applications.

Author Contributions: Conceptualization, M.K.; writing—original draft preparation, M.K.; writing—review and editing, M.K., J.K., F.K. and Y.-M.K.; supervision, F.K. and Y.-M.K. All authors have read and agreed to the published version of the manuscript.

Funding: This research was supported by 2024 Postdoctoral Support Project of the Industry-University Cooperation Foundation at Pukyong National University. The Basic Science Research Program provided additional support through the National Research Foundation of Korea (NRF) funded by the Ministry of Education (RS-2021-NR060118).

Data Availability Statement: No new data were created or analyzed in this study.

Conflicts of Interest: The authors declare no conflicts of interest. The funding sponsors had no role in the design of the study; in the collection, analyses, or interpretation of data; in the writing of the manuscript, and in the decision to publish the results.

Abbreviations

The following abbreviations are used in this manuscript:

LAB	Lactic Acid Bacteria
QS	Quorum Sensing
EPS	Exopolysaccharides
GRAS	Generally Recognized as Safe
CFS	Cell Free Supernatant
PVC	Polyvinyl chloride
CIP	Cleaning-in-place
MNPs	Metal nanoparticles
LDPE	Low Density Polyethylene

References

1. Ban-Cucerzan, A.; Imre, K.; Morar, A.; Marcu, A.; Hotea, I.; Popa, S.-A.; Pătrînjan, R.-T.; Bucur, I.-M.; Gașpar, C.; Plotuna, A.-M.; et al. Persistent Threats: A Comprehensive Review of Biofilm Formation, Control, and Economic Implications in Food Processing Environments. *Microorganisms* **2025**, *13*, 1805. [CrossRef] [PubMed]
2. Carrascosa, C.; Raheem, D.; Ramos, F.; Saraiva, A.; Raposo, A. Microbial Biofilms in the Food Industry—A Comprehensive Review. *Int. J. Environ. Res. Public Health* **2021**, *18*, 2014. [CrossRef] [PubMed]

https://doi.org/10.3390/antibiotics15030248

3. Abebe, G.M. The Role of Bacterial Biofilm in Antibiotic Resistance and Food Contamination. *Int. J. Microbiol.* **2020**, *2020*, 1705814. [CrossRef] [PubMed]
4. Elafify, M.; Liao, X.; Feng, J.; Ahn, J.; Ding, T. Biofilm formation in food industries: Challenges and control strategies for food safety. *Food Res. Int.* **2024**, *190*, 114650. [CrossRef]
5. Chmielewski, R.A.N.; Frank, J.F. Biofilm Formation and Control in Food Processing Facilities. *Compr. Rev. Food Sci. Food Saf.* **2003**, *2*, 22–32. [CrossRef]
6. Alvarez-Ordóñez, A.; Coughlan, L.M.; Briandet, R.; Cotter, P.D. Biofilms in Food Processing Environments: Challenges and Opportunities. *Annu. Rev. Food Sci. Technol.* **2019**, *10*, 173–195. [CrossRef]
7. Flemming, H.-C.; Wingender, J. The biofilm matrix. *Nat. Rev. Microbiol.* **2010**, *8*, 623–633. [CrossRef]
8. Muhammad, M.H.; Idris, A.L.; Fan, X.; Guo, Y.; Yu, Y.; Jin, X.; Qiu, J.; Guan, X.; Huang, T. Beyond Risk: Bacterial Biofilms and Their Regulating Approaches. *Front. Microbiol.* **2020**, *11*, 928. [CrossRef]
9. Dunne, W.M. Bacterial Adhesion: Seen Any Good Biofilms Lately? *Clin. Microbiol. Rev.* **2002**, *15*, 155–166. [CrossRef]
10. Donlan, R.M. Biofilms: Microbial Life on Surfaces. *Emerg. Infect. Dis.* **2002**, *8*, 9. [CrossRef]
11. Yang, L.; Liu, Y.; Wu, H.; Song, Z.; Høiby, N.; Molin, S.; Givskov, M. Combating biofilms. *FEMS Immunol. Med. Microbiol.* **2012**, *65*, 146–157. [CrossRef] [PubMed]
12. Barraud, N.; Kjelleberg, S.; Rice Scott, A. Dispersal from Microbial Biofilms. *Microbiol. Spectr.* **2015**, *3*, 343–362. [CrossRef] [PubMed]
13. Zehra, A.; Ahmad, Z.; Rasheed, M.U.; Shahzadi, N.; Abid, F.; Emaan, R.; Sherwani, M.I.K. Lastest Perspetives In Bacterial Biofilm Eradication. *J. Med. Health Sci. Rev.* **2025**, *2*. [CrossRef]
14. Blackman, I.C.; Frank, J.F. Growth of *Listeria monocytogenes* as a Biofilm on Various Food-Processing Surfaces. *J. Food Prot.* **1996**, *59*, 827–831. [CrossRef]
15. Myszka, K.; Czaczyk, K. Bacterial Biofilms on Food Contact Surfaces—A Review. *Pol. J. Food Nutr. Sci.* **2011**, *61*, 173–180. [CrossRef]
16. Bai, X.; Nakatsu, C.H.; Bhunia, A.K. Bacterial Biofilms and Their Implications in Pathogenesis and Food Safety. *Foods* **2021**, *10*, 2117. [CrossRef]
17. Galié, S.; García-Gutiérrez, C.; Miguélez, E.M.; Villar, C.J.; Lombó, F. Biofilms in the Food Industry: Health Aspects and Control Methods. *Front. Microbiol.* **2018**, *9*, 315815. [CrossRef]
18. Møretrø, T.; Langsrud, S. *Listeria monocytogenes*: Biofilm formation and persistence in food-processing environments. *Biofilms* **2004**, *1*, 107–121. [CrossRef]
19. Liu, X.; Yao, H.; Zhao, X.; Ge, C. Biofilm Formation and Control of Foodborne Pathogenic Bacteria. *Molecules* **2023**, *28*, 2432. [CrossRef]
20. Hua, Z.; Zhu, M.-J. Comprehensive strategies for controlling *Listeria monocytogenes* biofilms on food-contact surfaces. *Compr. Rev. Food Sci. Food Saf.* **2024**, *23*, e13348. [CrossRef]
21. Dawan, J.; Zhang, S.; Ahn, J. Recent Advances in Biofilm Control Technologies for the Food Industry. *Antibiotics* **2025**, *14*, 254. [CrossRef]
22. Singh, B.P.; Ghosh, S.; Chauhan, A. Control of Bacterial Biofilms for Mitigating Antimicrobial Resistance. In *Sustainable Agriculture Reviews 46: Mitigation of Antimicrobial Resistance Vol 1 Tools and Targets*; Panwar, H., Sharma, C., Lichtfouse, E., Eds.; Springer International Publishing: Cham, Switzerland, 2020; pp. 147–176.
23. Esposito, M.M.; Turku, S. The Use of Natural Methods to Control Foodborne Biofilms. *Pathogens* **2023**, *12*, 45. [CrossRef]
24. Fernandes, S.; Gomes, I.B.; Simões, M.; Simões, L.C. Novel chemical-based approaches for biofilm cleaning and disinfection. *Curr. Opin. Food Sci.* **2024**, *55*, 101124. [CrossRef]
25. Javanmard, Z.; Pourhajibagher, M.; Bahador, A. Advancing Anti-Biofilm Strategies: Innovations to Combat Biofilm-Related Challenges and Enhance Efficacy. *J. Basic Microbiol.* **2024**, *64*, e2400271. [CrossRef] [PubMed]
26. Mevo, S.I.U.; Ashrafudoulla, M.; Furkanur Rahaman Mizan, M.; Park, S.H.; Ha, S.-D. Promising strategies to control persistent enemies: Some new technologies to combat biofilm in the food industry—A review. *Compr. Rev. Food Sci. Food Saf.* **2021**, *20*, 5938–5964. [CrossRef] [PubMed]
27. Toushik, S.H.; Mizan, M.F.R.; Hossain, M.I.; Ha, S.-D. Fighting with old foes: The pledge of microbe-derived biological agents to defeat mono- and mixed-bacterial biofilms concerning food industries. *Trends Food Sci. Technol.* **2020**, *99*, 413–425. [CrossRef]
28. Sadekuzzaman, M.; Yang, S.; Mizan, M.F.R.; Ha, S.D. Current and Recent Advanced Strategies for Combating Biofilms. *Compr. Rev. Food Sci. Food Saf.* **2015**, *14*, 491–509. [CrossRef]
29. Castellano, P.; Pérez Ibarreche, M.; Blanco Massani, M.; Fontana, C.; Vignolo, G.M. Strategies for Pathogen Biocontrol Using Lactic Acid Bacteria and Their Metabolites: A Focus on Meat Ecosystems and Industrial Environments. *Microorganisms* **2017**, *5*, 38. [CrossRef]

https://doi.org/10.3390/antibiotics15030248

30. Giaouris, E. Chapter 9—Application of lactic acid bacteria and their metabolites against foodborne pathogenic bacterial biofilms. In *Recent Trends in Biofilm Science and Technology*; Simoes, M., Borges, A., Chaves Simoes, L., Eds.; Academic Press: Cambridge, MA, USA, 2020; pp. 205–232.
31. Cirat, R.; Capozzi, V.; Benmechernene, Z.; Spano, G.; Grieco, F.; Fragasso, M. LAB Antagonistic Activities and Their Significance in Food Biotechnology: Molecular Mechanisms, Food Targets, and Other Related Traits of Interest. *Fermentation* **2024**, *10*, 222. [CrossRef]
32. Pang, X.; Song, X.; Chen, M.; Tian, S.; Lu, Z.; Sun, J.; Li, X.; Lu, Y.; Yuk, H.-G. Combating biofilms of foodborne pathogens with bacteriocins by lactic acid bacteria in the food industry. *Compr. Rev. Food Sci. Food Saf.* **2022**, *21*, 1657–1676. [CrossRef]
33. Camargo, A.C.; Todorov, S.D.; Chihib, N.E.; Drider, D.; Nero, L.A. Lactic Acid Bacteria (LAB) and Their Bacteriocins as Alternative Biotechnological Tools to Control Listeria monocytogenes Biofilms in Food Processing Facilities. *Mol. Biotechnol.* **2018**, *60*, 712–726. [CrossRef]
34. Saragoça, A.; Canha, H.; Varanda, C.M.R.; Materatski, P.; Cordeiro, A.I.; Gama, J. Lactic acid bacteria: A sustainable solution against phytopathogenic agents. *Environ. Microbiol. Rep.* **2024**, *16*, e70021. [CrossRef] [PubMed]
35. Ibrahim, S.A.; Ayivi, R.D.; Zimmerman, T.; Siddiqui, S.A.; Altemimi, A.B.; Fidan, H.; Esatbeyoglu, T.; Bakhshayesh, R.V. Lactic Acid Bacteria as Antimicrobial Agents: Food Safety and Microbial Food Spoilage Prevention. *Foods* **2021**, *10*, 3131. [CrossRef] [PubMed]
36. Daliri, F.; Aboagye, A.A.; Daliri, E.B.-M. Inactivation of Foodborne Pathogens by Lactic Acid Bacteria. *J. Food Hyg. Saf.* **2020**, *35*, 419–429. [CrossRef]
37. Siedler, S.; Balti, R.; Neves, A.R. Bioprotective mechanisms of lactic acid bacteria against fungal spoilage of food. *Curr. Opin. Biotechnol.* **2019**, *56*, 138–146. [CrossRef]
38. Silva, S.P.M.; Teixeira, J.A.; Silva, C.C.G. Recent advances in the use of edible films and coatings with probiotic and bacteriocin-producing lactic acid bacteria. *Food Biosci.* **2023**, *56*, 103196. [CrossRef]
39. Moradi, M.; Guimarães, J.T.; Sahin, S. Current applications of exopolysaccharides from lactic acid bacteria in the development of food active edible packaging. *Curr. Opin. Food Sci.* **2021**, *40*, 33–39. [CrossRef]
40. Punia Bangar, S.; Suri, S.; Trif, M.; Ozogul, F. Organic acids production from lactic acid bacteria: A preservation approach. *Food Biosci.* **2022**, *46*, 101615. [CrossRef]
41. Mokoena, M.P.; Omatola, C.A.; Olaniran, A.O. Applications of Lactic Acid Bacteria and Their Bacteriocins against Food Spoilage Microorganisms and Foodborne Pathogens. *Molecules* **2021**, *26*, 7055. [CrossRef]
42. Zang, J.; Kou, Y.; Shi, Y.; Xiao, L.; Ma, K.; Zhang, C.; Geng, S.; Rui, X.; Lin, T.; Li, W. Structural and functional roles of lactic acid bacteria in food delivery systems: A dual perspective of passive encapsulation and active carriers. *Adv. Colloid Interface Sci.* **2025**, *344*, 103599. [CrossRef]
43. Wang, Y.; Wu, J.; Lv, M.; Shao, Z.; Hungwe, M.; Wang, J.; Bai, X.; Xie, J.; Wang, Y.; Geng, W. Metabolism Characteristics of Lactic Acid Bacteria and the Expanding Applications in Food Industry. *Front. Bioeng. Biotechnol.* **2021**, *9*, 612285. [CrossRef]
44. Murata, R.; Shim, Y.Y.; Kim, Y.J.; Reaney, M.J.T.; Tse, T.J. Exploring lactic acid bacteria in food, human health, and agriculture. *Crit. Rev. Food Sci. Nutr.* **2025**, *65*, 8122–8148. [CrossRef]
45. Stabnikov, V.; Kovshar, I.; Stabnikova, O. Recent advances in the study of the properties and applications of lactic acid bacteria. *World J. Microbiol. Biotechnol.* **2025**, *41*, 287. [CrossRef] [PubMed]
46. Gregirchak, N.; Syniavska, D.; Khonkiv, M.; Stabnikov, V. Lactic acid bacteria for the synthesis of metals nanoparticles. *Ukr. Food J.* **2023**, *12*, 599–626. [CrossRef]
47. Kang, M.-G.; Khan, F.; Tabassum, N.; Cho, K.-J.; Jo, D.-M.; Kim, Y.-M. Inhibition of Biofilm and Virulence Properties of Pathogenic Bacteria by Silver and Gold Nanoparticles Synthesized from *Lactiplantibacillus* sp. Strain C1. *ACS Omega* **2023**, *8*, 9873–9888. [CrossRef] [PubMed]
48. Mgomi, F.C.; Yang, Y.-r.; Cheng, G.; Yang, Z.-q. Lactic acid bacteria biofilms and their antimicrobial potential against pathogenic microorganisms. *Biofilm* **2023**, *5*, 100118. [CrossRef]
49. Barcenilla, C.; Ducic, M.; López, M.; Prieto, M.; Álvarez-Ordóñez, A. Application of lactic acid bacteria for the biopreservation of meat products: A systematic review. *Meat Sci.* **2022**, *183*, 108661. [CrossRef]
50. Annous, B.A.; Solomon, E.B.; Cooke, P.H.; Burke, A. Biofilm formation by *Salmonella* spp. on cantaloupe melons. *J. Food Saf.* **2005**, *25*, 276–287. [CrossRef]
51. Rolon, M.L.; Voloshchuk, O.; Bartlett, K.V.; LaBorde, L.F.; Kovac, J. Multi-species biofilms of environmental microbiota isolated from fruit packing facilities promoted tolerance of *Listeria monocytogenes* to benzalkonium chloride. *Biofilm* **2024**, *7*, 100177. [CrossRef]
52. Zhu, Q.; Gooneratne, R.; Hussain, M.A. *Listeria monocytogenes* in Fresh Produce: Outbreaks, Prevalence and Contamination Levels. *Foods* **2017**, *6*, 21. [CrossRef]
53. Amrutha, B.; Sundar, K.; Shetty, P.H. Study on *E. coli* and *Salmonella* biofilms from fresh fruits and vegetables. *J. Food Sci. Technol.* **2017**, *54*, 1091–1097. [CrossRef] [PubMed]

https://doi.org/10.3390/antibiotics15030248

54. Sun, Y.; Ma, Y.; Guan, H.; Liang, H.; Zhao, X.; Wang, D. Adhesion mechanism and biofilm formation of *Escherichia coli* O157:H7 in infected cucumber (*Cucumis sativus* L.). *Food Microbiol.* **2022**, *105*, 103885. [CrossRef] [PubMed]
55. Schlechter Rudolf, O.; Marti, E.; Remus-Emsermann Mitja, N.P.; Drissner, D.; Gekenidis, M.-T. Correlation of in vitro biofilm formation capacity with persistence of antibiotic-resistant *Escherichia coli* on gnotobiotic lamb's lettuce. *Appl. Environ. Microbiol.* **2025**, *91*, e00299-25. [CrossRef] [PubMed]
56. Ghosh, B.; Dhar, J.; Mukhopadhyay, M.; Bhattacharya, D. *Bacillus cereus* biofilm: Implications for food and diseases. *Microbe* **2024**, *4*, 100129. [CrossRef]
57. Todd, E.C.D. Foodborne Diseases: Overview of Biological Hazards and Foodborne Diseases. In *Encyclopedia of Food Safety*; Motarjemi, Y., Ed.; Academic Press: Waltham, MA, USA, 2014; pp. 221–242.
58. Klančnik, A.; Šimunović, K.; Sterniša, M.; Ramić, D.; Smole Možina, S.; Bucar, F. Anti-adhesion activity of phytochemicals to prevent *Campylobacter jejuni* biofilm formation on abiotic surfaces. *Phytochem. Rev.* **2021**, *20*, 55–84. [CrossRef]
59. Stenfors Arnesen, L.P.; Fagerlund, A.; Granum, P.E. From soil to gut: *Bacillus cereus* and its food poisoning toxins. *FEMS Microbiol. Rev.* **2008**, *32*, 579–606. [CrossRef]
60. Yang, S.; Wang, Y.; Ren, F.; Wang, X.; Zhang, W.; Pei, X.; Dong, Q. The Sources of *Bacillus cereus* Contamination and their Association with Cereulide Production in Dairy and Cooked Rice Processing Lines. *Food Qual. Saf.* **2023**, *7*, fyad023. [CrossRef]
61. Annous, B.A.; Smith, J.L.; Fratamico, P.M.; Solomon, E.B. Biofilms in fresh fruit and vegetables. In *Biofilms in the Food and Beverage Industries*; Fratamico, P.M., Annous, B.A., Gunther, N.W., Eds.; Woodhead Publishing: Cambridge, UK, 2009; pp. 517–535.
62. Brandl, M.T. Plant Lesions Promote the Rapid Multiplication of *Escherichia coli* O157:H7 on Postharvest Lettuce. *Appl. Environ. Microbiol.* **2008**, *74*, 5285–5289. [CrossRef]
63. Robbins, J.B.; Fisher, C.W.; Moltz, A.G.; Martin, S.E. Elimination of *Listeria monocytogenes* Biofilms by Ozone, Chlorine, and Hydrogen Peroxide. *J. Food Prot.* **2005**, *68*, 494–498. [CrossRef]
64. Høiby, N.; Bjarnsholt, T.; Givskov, M.; Molin, S.; Ciofu, O. Antibiotic resistance of bacterial biofilms. *Int. J. Antimicrob. Agents* **2010**, *35*, 322–332. [CrossRef]
65. Patel, J.; Sharma, M. Differences in attachment of *Salmonella enterica* serovars to cabbage and lettuce leaves. *Int. J. Food Microbiol.* **2010**, *139*, 41–47. [CrossRef] [PubMed]
66. Gorski, L.; Walker, S.; Romanolo, K.F.; Kathariou, S. Growth and Survival of Attached *Listeria* on Lettuce and Stainless Steel Varies by Strain and Surface Type. *J. Food Prot.* **2021**, *84*, 903–911. [CrossRef]
67. Pagedar, A.; Singh, J. Influence of physiological cell stages on biofilm formation by *Bacillus cereus* of dairy origin. *Int. Dairy J.* **2012**, *23*, 30–35. [CrossRef]
68. Tewari, A.; Abdullah, S. *Bacillus cereus* food poisoning: International and Indian perspective. *J. Food Sci. Technol.* **2015**, *52*, 2500–2511. [CrossRef] [PubMed]
69. Sarrías, J.A.; Valero, M.; Salmerón, M.C. Enumeration, isolation and characterization of *Bacillus cereus* strains from Spanish raw rice. *Food Microbiol.* **2002**, *19*, 589–595. [CrossRef]
70. Villa-Rojas, R.; Zhu, M.-J.; Paul, N.C.; Gray, P.; Xu, J.; Shah, D.H.; Tang, J. Biofilm forming *Salmonella* strains exhibit enhanced thermal resistance in wheat flour. *Food Control* **2017**, *73*, 689–695. [CrossRef]
71. Pang, X.; Hu, X.; Du, X.; Lv, C.; Yuk, H.-G. Biofilm formation in food processing plants and novel control strategies to combat resistant biofilms: The case of *Salmonella* spp. *Food Sci. Biotechnol.* **2023**, *32*, 1703–1718. [CrossRef]
72. Zhao, X.; Zhao, F.; Wang, J.; Zhong, N. Biofilm formation and control strategies of foodborne pathogens: Food safety perspectives. *RSC Adv.* **2017**, *7*, 36670–36683. [CrossRef]
73. Wang, R. Biofilms and Meat Safety: A Mini-Review. *J. Food Prot.* **2019**, *82*, 120–127. [CrossRef]
74. Truelstrup Hansen, L.; Vogel, B.F. Desiccation of adhering and biofilm *Listeria monocytogenes* on stainless steel: Survival and transfer to salmon products. *Int. J. Food Microbiol.* **2011**, *146*, 88–93. [CrossRef]
75. Keskinen, L.A.; Todd, E.C.D.; Ryser, E.T. Impact of bacterial stress and biofilm-forming ability on transfer of surface-dried *Listeria monocytogenes* during slicing of delicatessen meats. *Int. J. Food Microbiol.* **2008**, *127*, 298–304. [CrossRef]
76. Wang, R.; Schmidt, J.W.; Harhay, D.M.; Bosilevac, J.M.; King, D.A.; Arthur, T.M. Biofilm Formation, Antimicrobial Resistance, and Sanitizer Tolerance of *Salmonella enterica* Strains Isolated from Beef Trim. *Foodborne Pathog. Dis.* **2017**, *14*, 687–695. [CrossRef] [PubMed]
77. Mizan, M.F.R.; Jahid, I.K.; Ha, S.-D. Microbial biofilms in seafood: A food-hygiene challenge. *Food Microbiol.* **2015**, *49*, 41–55. [CrossRef] [PubMed]
78. Aagesen, A.M.; Phuvasate, S.; Su, Y.-C.; Häse, C.C. Persistence of *Vibrio parahaemolyticus* in the Pacific Oyster, Crassostrea gigas, Is a Multifactorial Process Involving Pili and Flagella but Not Type III Secretion Systems or Phase Variation. *Appl. Environ. Microbiol.* **2013**, *79*, 3303–3305. [CrossRef] [PubMed]
79. Jahid, I.K.; Lee, N.-Y.; Kim, A.; Ha, S.-D. Influence of Glucose Concentrations on Biofilm Formation, Motility, Exoprotease Production, and Quorum Sensing in Aeromonas hydrophila. *J. Food Prot.* **2013**, *76*, 239–247. [CrossRef]

https://doi.org/10.3390/antibiotics15030248

80. Vestby, L.K.; Møretrø, T.; Langsrud, S.; Heir, E.; Nesse, L.L. Biofilm forming abilities of *Salmonella* are correlated with persistence in fish meal- and feed factories. *BMC Vet. Res.* **2009**, *5*, 20. [CrossRef]
81. Catania, A.M.; Di Ciccio, P.; Ferrocino, I.; Civera, T.; Cannizzo, F.T.; Dalmasso, A. Evaluation of the biofilm-forming ability and molecular characterization of dairy *Bacillus* spp. isolates. *Front. Cell. Infect. Microbiol.* **2023**, *13*, 1229460. [CrossRef]
82. Fysun, O.; Kern, H.; Wilke, B.; Langowski, H.-C. Evaluation of factors influencing dairy biofilm formation in filling hoses of food-processing equipment. *Food Bioprod. Process.* **2019**, *113*, 39–48. [CrossRef]
83. Goetz, C.; Sanschagrin, L.; Jubinville, E.; Jacques, M.; Jean, J. Biofilm Formation in Dairy: A Food Safety Concern—Recent progress in antibiofilm strategies in the dairy industry. *J. Dairy Sci.* **2025**, *108*, 8157–8175. [CrossRef]
84. Marković, K.G.; Grujović, M.Ž.; Stefanović, O.D. Biofilms in dairy products: Safety hazard or beneficial asset? *Int. Dairy J.* **2025**, *171*, 106381. [CrossRef]
85. Mladenović, K.G.; Muruzović, M.Ž.; Čomić, L.R. The effects of environmental factors on planktonic growth and biofilm formation of *Serratia odorifera* and *Serratia marcescens* isolated from traditionally made cheese. *Acta Aliment.* **2018**, *47*, 370–378. [CrossRef]
86. Mladenović, K.G.; Grujović, M.Ž.; Kiš, M.; Furmeg, S.; Tkalec, V.J.; Stefanović, O.D.; Kocić-Tanackov, S.D. Enterobacteriaceae in food safety with an emphasis on raw milk and meat. *Appl. Microbiol. Biotechnol.* **2021**, *105*, 8615–8627. [CrossRef] [PubMed]
87. Grujović, M.Ž.; Mladenović, K.G.; Semedo-Lemsaddek, T.; Laranjo, M.; Stefanović, O.D.; Kocić-Tanackov, S.D. Advantages and disadvantages of non-starter lactic acid bacteria from traditional fermented foods: Potential use as starters or probiotics. *Compr. Rev. Food Sci. Food Saf.* **2022**, *21*, 1537–1567. [CrossRef] [PubMed]
88. McMillan, K.; Moore, S.C.; McAuley, C.M.; Fegan, N.; Fox, E.M. Characterization of *Staphylococcus aureus* isolates from raw milk sources in Victoria, Australia. *BMC Microbiol.* **2016**, *16*, 169. [CrossRef]
89. Rall, V.L.M.; Vieira, F.P.; Rall, R.; Vieitis, R.L.; Fernandes, A.; Candeias, J.M.G.; Cardoso, K.F.G.; Araújo, J.P. PCR detection of staphylococcal enterotoxin genes in *Staphylococcus aureus* strains isolated from raw and pasteurized milk. *Vet. Microbiol.* **2008**, *132*, 408–413. [CrossRef]
90. Wang, X.; Meng, J.; Zhang, J.; Zhou, T.; Zhang, Y.; Yang, B.; Xi, M.; Xia, X. Characterization of *Staphylococcus aureus* isolated from powdered infant formula milk and infant rice cereal in China. *Int. J. Food Microbiol.* **2012**, *153*, 142–147. [CrossRef]
91. Unnerstad, H.; Bannerman, E.; Bille, J.; Danielsson-Tham, M.; Waak, E.; Tham, W. Prolonged contamination of a dairy with Listeria monocytogenes. *Neth. Milk Dairy J.* **1996**, *50*, 493–499.
92. Simões, M.; Simões, L.C.; Vieira, M.J. A review of current and emergent biofilm control strategies. *LWT—Food Sci. Technol.* **2010**, *43*, 573–583. [CrossRef]
93. Abdallah, M.; Khelissa, O.; Ibrahim, A.; Benoliel, C.; Heliot, L.; Dhulster, P.; Chihib, N.-E. Impact of growth temperature and surface type on the resistance of *Pseudomonas aeruginosa* and *Staphylococcus aureus* biofilms to disinfectants. *Int. J. Food Microbiol.* **2015**, *214*, 38–47. [CrossRef]
94. Lindsay, D.; Brözel, V.S.; Von Holy, A. Biofilm-Spore Response in *Bacillus cereus* and *Bacillus subtilis* during Nutrient Limitation. *J. Food Prot.* **2006**, *69*, 1168–1172. [CrossRef]
95. Pant, K.J.; Cotter, P.D.; Wilkinson, M.G.; Sheehan, J.J. Towards sustainable Cleaning-in-Place (CIP) in dairy processing: Exploring enzyme-based approaches to cleaning in the Cheese industry. *Compr. Rev. Food Sci. Food Saf.* **2023**, *22*, 3602–3619. [CrossRef] [PubMed]
96. Abdel-Rahman, M.A.; Tashiro, Y.; Sonomoto, K. Recent advances in lactic acid production by microbial fermentation processes. *Biotechnol. Adv.* **2013**, *31*, 877–902. [CrossRef] [PubMed]
97. Kwak, M.-K.; Liu, R.; Kwon, J.-O.; Kim, M.-K.; Kim, A.H.; Kang, S.-O. Cyclic dipeptides from lactic acid bacteria inhibit proliferation of the influenza a virus. *J. Microbiol.* **2013**, *51*, 836–843. [CrossRef] [PubMed]
98. Juturu, V.; Wu, J.C. Microbial production of lactic acid: The latest development. *Crit. Rev. Biotechnol.* **2016**, *36*, 967–977. [CrossRef]
99. Shanker, E.; Federle, M.J. Quorum Sensing Regulation of Competence and Bacteriocins in *Streptococcus pneumoniae* and mutans. *Genes* **2017**, *8*, 15. [CrossRef]
100. Lim, S.-M.; Lee, N.-K.; Paik, H.-D. Antibacterial and anticavity activity of probiotic Lactobacillus plantarum 200661 isolated from fermented foods against Streptococcus mutans. *LWT* **2020**, *118*, 108840. [CrossRef]
101. Tang, H.; Huang, W.; Yao, Y.-F. The metabolites of lactic acid bacteria: Classification, biosynthesis and modulation of gut microbiota. *Microb. Cell* **2023**, *10*, 49–62. [CrossRef]
102. Ahmad, V.; Khan, M.S.; Jamal, Q.M.S.; Alzohairy, M.A.; Al Karaawi, M.A.; Siddiqui, M.U. Antimicrobial potential of bacteriocins: In therapy, agriculture and food preservation. *Int. J. Antimicrob. Agents* **2017**, *49*, 1–11. [CrossRef]
103. Demirgül, F.; Kaya, H.İ.; Ucar, R.A.; Mitaf, N.A.; Şimşek, Ö. Expanding Layers of Bacteriocin Applications: From Food Preservation to Human Health Interventions. *Fermentation* **2025**, *11*, 142. [CrossRef]
104. Zhao, C.; Shen, J.; Cai, X.; Zhao, Y.; Meng, X.; Liu, Z.; Qian, Y. A novel bacteriostatic system for seafood preservation: Impact of plantaricin Bac-329 on bacterial cell wall integrity driven by lactic acid levels. *Food Control* **2025**, *176*, 111331. [CrossRef]
105. Solis-Balandra, M.A.; Sanchez-Salas, J.L. Classification and Multi-Functional Use of Bacteriocins in Health, Biotechnology, and Food Industry. *Antibiotics* **2024**, *13*, 666. [CrossRef] [PubMed]

https://doi.org/10.3390/antibiotics15030248

106. Tarifa, M.C.; Agustín, M.d.R.; Brugnoni, L.I. Biological control of foodborne pathogens by lactic acid bacteria: A focus on juice processing industries. *Rev. Argent. De Microbiol.* **2023**, *55*, 378–386. [CrossRef] [PubMed]
107. Jiang, P.; Li, J.; Han, F.; Duan, G.; Lu, X.; Gu, Y.; Yu, W. Antibiofilm Activity of an Exopolysaccharide from Marine Bacterium *Vibrio* sp. QY101. *PLoS ONE* **2011**, *6*, e18514. [CrossRef] [PubMed]
108. Che, J.; Shi, J.; Fang, C.; Zeng, X.; Wu, Z.; Du, Q.; Tu, M.; Pan, D. Elimination of Pathogen Biofilms via Postbiotics from Lactic Acid Bacteria: A Promising Method in Food and Biomedicine. *Microorganisms* **2024**, *12*, 704. [CrossRef]
109. Jung, S.; Hwang, H.; Lee, J.-H. Effect of lactic acid bacteria on phenyllactic acid production in kimchi. *Food Control* **2019**, *106*, 106701. [CrossRef]
110. Aguirre-Garcia, Y.L.; Cerda-Alvarez, N.C.; Santiago-Santiago, R.M.; Chantre-López, A.R.; Rangel-Ortega, S.D.C.; Rodríguez-Herrera, R. The Metabolites Produced by Lactic Acid Bacteria and Their Role in the Microbiota–Gut–Brain Axis. *Fermentation* **2025**, *11*, 378. [CrossRef]
111. Singh, N.; Sharma, C.; Gulhane, R.D.; Rokana, N.; Singh, B.P.; Puniya, A.K.; Attri, S.; Goel, G.; Panwar, H. Inhibitory effects of lactobacilli of goat's milk origin against growth and biofilm formation by pathogens: An in vitro study. *Food Biosci.* **2018**, *22*, 129–138. [CrossRef]
112. Shokri, D.; Khorasgani, M.R.; Mohkam, M.; Fatemi, S.M.; Ghasemi, Y.; Taheri-Kafrani, A. The Inhibition Effect of Lactobacilli Against Growth and Biofilm Formation of *Pseudomonas aeruginosa*. *Probiotics Antimicrob. Proteins* **2018**, *10*, 34–42. [CrossRef]
113. Perez, R.H.; Zendo, T.; Sonomoto, K. Novel bacteriocins from lactic acid bacteria (LAB): Various structures and applications. *Microb. Cell Factories* **2014**, *13*, S3. [CrossRef]
114. Cleveland, J.; Montville, T.J.; Nes, I.F.; Chikindas, M.L. Bacteriocins: Safe, natural antimicrobials for food preservation. *Int. J. Food Microbiol.* **2001**, *71*, 1–20. [CrossRef]
115. Ismael, M.; Wang, T.; Yue, F.; Cui, Y.; Yantin, Q.; Qayyum, N.; Lü, X. A comparison of mining methods to extract novel bacteriocins from *Lactiplantibacillus plantarum* NWAFU-BIO-BS29. *Anal. Biochem.* **2023**, *661*, 114938. [CrossRef] [PubMed]
116. Sacks, D.; Baxter, B.; Campbell, B.C.V.; Carpenter, J.S.; Cognard, C.; Dippel, D.; Eesa, M.; Fischer, U.; Hausegger, K.; Hirsch, J.A.; et al. Multisociety Consensus Quality Improvement Revised Consensus Statement for Endovascular Therapy of Acute Ischemic Stroke. *Int. J. Stroke* **2018**, *13*, 612–632. [CrossRef] [PubMed]
117. Kim, J.; Ahn, J.; Ahn, C. Characterization of novel bacteriocin produced by bacteriocinogenic *Carnobacterium maltaromaticum* isolated from raw milk. *Microb. Pathog.* **2022**, *173*, 105872. [CrossRef] [PubMed]
118. Gontijo, M.T.P.; Silva, J.d.S.; Vidigal, P.M.P.; Martin, J.G.P. Phylogenetic distribution of the bacteriocin repertoire of lactic acid bacteria species associated with artisanal cheese. *Food Res. Int.* **2020**, *128*, 108783. [CrossRef]
119. Angelin, J.; Kavitha, M. Exopolysaccharides from probiotic bacteria and their health potential. *Int. J. Biol. Macromol.* **2020**, *162*, 853–865. [CrossRef]
120. Riaz Rajoka, M.S.; Jin, M.; Haobin, Z.; Li, Q.; Shao, D.; Jiang, C.; Huang, Q.; Yang, H.; Shi, J.; Hussain, N. Functional characterization and biotechnological potential of exopolysaccharide produced by *Lactobacillus rhamnosus* strains isolated from human breast milk. *LWT* **2018**, *89*, 638–647. [CrossRef]
121. Liang, S.; Wang, X.; Li, C.; Liu, L. Biological Activity of Lactic Acid Bacteria Exopolysaccharides and Their Applications in the Food and Pharmaceutical Industries. *Foods* **2024**, *13*, 1621. [CrossRef]
122. Nataraj, B.H.; Ramesh, C.; Mallappa, R.H. Functional group characterization of lactic bacterial biosurfactants and evaluation of antagonistic actions against clinical isolates of methicillin-resistant *Staphylococcus aureus*. *Lett. Appl. Microbiol.* **2021**, *73*, 372–382. [CrossRef]
123. Koohestani, M.; Moradi, M.; Tajik, H.; Badali, A. Effects of cell-free supernatant of Lactobacillus acidophilus LA5 and *Lactobacillus casei* 431 against planktonic form and biofilm of *Staphylococcus aureus*. *Vet. Res. Forum* **2018**, *9*, 301–306. [CrossRef]
124. Al-Shamiri Mona, M.; Wang, J.; Zhang, S.; Li, P.; Odhiambo Woodvine, O.; Chen, Y.; Han, B.; Yang, E.; Xun, M.; Han, L.; et al. Probiotic Lactobacillus Species and Their Biosurfactants Eliminate *Acinetobacter baumannii* Biofilm in Various Manners. *Microbiol. Spectr.* **2023**, *11*, e04614–e04622. [CrossRef]
125. Aman, M.; Aneeqha, N.; Bristi, K.; Deeksha, J.; Afza, N.; Sindhuja, V.; Shastry, R.P. Lactic acid bacteria inhibits quorum sensing and biofilm formation of *Pseudomonas aeruginosa* strain JUPG01 isolated from rancid butter. *Biocatal. Agric. Biotechnol.* **2021**, *36*, 102115. [CrossRef]
126. Zhang, C.; Zhang, S.; Liu, W.; Guo, T.; Gu, R.; Kong, J. Potential Application and Bactericidal Mechanism of Lactic Acid–Hydrogen Peroxide Consortium. *Appl. Biochem. Biotechnol.* **2019**, *189*, 822–833. [CrossRef]
127. Vollenweider, S.; Evers, S.; Zurbriggen, K.; Lacroix, C. Unraveling the Hydroxypropionaldehyde (HPA) System: An Active Antimicrobial Agent against Human Pathogens. *J. Agric. Food Chem.* **2010**, *58*, 10315–10322. [CrossRef] [PubMed]
128. Sun, M.-C.; Hu, Z.-Y.; Li, D.-D.; Chen, Y.-X.; Xi, J.-H.; Zhao, C.-H. Application of the Reuterin System as Food Preservative or Health-Promoting Agent: A Critical Review. *Foods* **2022**, *11*, 4000. [CrossRef] [PubMed]

https://doi.org/10.3390/antibiotics15030248

129. Shi, C.; Jia, L.; Chen, Y.; Aziz, T.; Shami, A.; Al-Asmari, F.; Al-Joufi, F.A.; Cui, H.; Lin, L. Exploration of the inhibitory and eradicative effects of diacetyl on *Listeria monocytogenes* biofilms and its potential application on cantaloupe preservation. *Food Control* **2026**, *179*, 111584. [CrossRef]
130. Aras Şükriye Hİ, S.A.R.; Güzin, K.; Olcay Hİ, S.A.R.; Telat, Y.; Mükerrem, K. Effect of *Lactobacillus sakei* Lb706 on behavior of *Listeria monocytogenes* in vacuum-packed rainbow trout fillets. *Turk. J. Vet. Anim. Sci.* **2005**, *29*, 1039–1044.
131. Ghalfi, H.; Allaoui, A.; Destain, J.; Benkerroum, N.; Thonart, P. Bacteriocin Activity by *Lactobacillus curvatus* CWBI-B28 To Inactivate *Listeria monocytogenes* in Cold-Smoked Salmon during 4 °C Storage. *J. Food Prot.* **2006**, *69*, 1066–1071. [CrossRef]
132. Dortu, C.; Huch, M.; Holzapfel, W.H.; Franz, C.M.A.P.; Thonart, P. Anti-listerial activity of bacteriocin-producing Lactobacillus curvatus CWBI-B28 and *Lactobacillus sakei* CWBI-B1365 on raw beef and poultry meat. *Lett. Appl. Microbiol.* **2008**, *47*, 581–586. [CrossRef]
133. Tahiri, I.; Desbiens, M.; Kheadr, E.; Lacroix, C.; Fliss, I. Comparison of different application strategies of divergicin M35 for inactivation of *Listeria monocytogenes* in cold-smoked wild salmon. *Food Microbiol.* **2009**, *26*, 783–793. [CrossRef]
134. Wijnker, J.J.; Weerts, E.A.W.S.; Breukink, E.J.; Houben, J.H.; Lipman, L.J.A. Reduction of *Clostridium sporogenes* spore outgrowth in natural sausage casings using nisin. *Food Microbiol.* **2011**, *28*, 974–979. [CrossRef]
135. Arief, I.I.; Jenie, B.S.L.; Suryati, T.; Ayuningtyas, G.; Fuziawan, A. Antimicrobial activity of bacteriocin from indigenous *Lactobacillus plantarum* 2c12 and its application on beef meatball as biopreservative. *J. Indones. Trop. Anim. Agric.* **2012**, *37*, 7. [CrossRef]
136. Castellano, P.; González, C.; Carduza, F.; Vignolo, G. Protective action of *Lactobacillus curvatus* CRL705 on vacuum-packaged raw beef. Effect on sensory and structural characteristics. *Meat Sci.* **2010**, *85*, 394–401. [CrossRef] [PubMed]
137. Langa, S.; Martín-Cabrejas, I.; Montiel, R.; Peirotén, Á.; Arqués, J.L.; Medina, M. Protective effect of reuterin-producing *Lactobacillus reuteri* against *Listeria monocytogenes* and *Escherichia coli* O157:H7 in semi-hard cheese. *Food Control* **2018**, *84*, 284–289. [CrossRef]
138. Rivas, F.P.; Castro, M.P.; Vallejo, M.; Marguet, E.; Campos, C.A. Sakacin Q produced by *Lactobacillus curvatus* ACU-1: Functionality characterization and antilisterial activity on cooked meat surface. *Meat Sci.* **2014**, *97*, 475–479. [CrossRef]
139. de Souza Barbosa, M.; Todorov, S.D.; Ivanova, I.; Chobert, J.-M.; Haertlé, T.; de Melo Franco, B.D.G. Improving safety of salami by application of bacteriocins produced by an autochthonous *Lactobacillus curvatus* isolate. *Food Microbiol.* **2015**, *46*, 254–262. [CrossRef]
140. Zhang, J.; Zhang, C.; Lei, P.; Xin, X.; Liu, D.; Yi, H. Isolation, purification, identification, and discovery of the antibacterial mechanism of ld-phenyllactic acid produced by *Lactiplantibacillus plantarum* CXG9 isolated from a traditional Chinese fermented vegetable. *Food Control* **2022**, *132*, 108490. [CrossRef]
141. García-Burgos, M.; Moreno-Fernández, J.; Alférez, M.J.M.; Díaz-Castro, J.; López-Aliaga, I. New perspectives in fermented dairy products and their health relevance. *J. Funct. Foods* **2020**, *72*, 104059. [CrossRef]
142. Hill, D.; Sugrue, I.; Arendt, E.; Hill, C.; Stanton, C.; Ross, R. Recent advances in microbial fermentation for dairy and health [version 1; peer review: 3 approved]. *F1000Research* **2017**, *6*, 751. [CrossRef]
143. Granier, A.; Goulet, O.; Hoarau, C. Fermentation products: Immunological effects on human and animal models. *Pediatr. Res.* **2013**, *74*, 238–244. [CrossRef]
144. Savaiano, D.A.; Hutkins, R.W. Yogurt, cultured fermented milk, and health: A systematic review. *Nutr. Rev.* **2020**, *79*, 599–614. [CrossRef]
145. Bhattacharya, D.; Nanda, P.K.; Pateiro, M.; Lorenzo, J.M.; Dhar, P.; Das, A.K. Lactic Acid Bacteria and Bacteriocins: Novel Biotechnological Approach for Biopreservation of Meat and Meat Products. *Microorganisms* **2022**, *10*, 2058. [CrossRef] [PubMed]
146. Sakaridis, I.; Soultos, N.; Batzios, C.; Ambrosiadis, I.; Koidis, P. Lactic acid bacteria isolated from chicken carcasses with inhibitory activity against *Salmonella* spp. and *Listeria monocytogenes*. *Czech J. Food Sci.* **2014**, *32*, 61–68. [CrossRef]
147. Kamiloğlu, A.; Kaban, G.; Kaya, M. Effects of autochthonous Lactobacillus plantarum strains on *Listeria monocytogenes* in sucuk during ripening. *J. Food Saf.* **2019**, *39*, e12618. [CrossRef]
148. Khalili Sadaghiani, S.; Aliakbarlu, J.; Tajik, H.; Mahmoudian, A. Anti-listeria activity and shelf life extension effects of *Lactobacillus* along with garlic extract in ground beef. *J. Food Saf.* **2019**, *39*, e12709. [CrossRef]
149. Gelinski, J.M.L.N.; Baratto, C.M.; Casagrande, M.; Oliveira, T.P.d.; Megiolaro, F.; Soares, F.A.S.d.M.; Souza, E.M.B.d.; Vicente, V.A.; Fonseca, G.G. Control of pathogens in fresh pork sausage by inclusion of *Lactobacillus sakei* BAS0117. *Can. J. Microbiol.* **2019**, *65*, 831–841. [CrossRef]
150. Ortiz, S.; López, V.; Garriga, M.; Martínez-Suárez, J.V. Antilisterial effect of two bioprotective cultures in a model system of Iberian chorizo fermentation. *Int. J. Food Sci. Technol.* **2014**, *49*, 753–758. [CrossRef]
151. Olaoye, O.A.; Onilude, A.A. Investigation on the potential application of biological agents in the extension of shelf life of fresh beef in Nigeria. *World J. Microbiol. Biotechnol.* **2010**, *26*, 1445–1454. [CrossRef]

https://doi.org/10.3390/antibiotics15030248

152. Ben Slima, S.; Ktari, N.; Triki, M.; Trabelsi, I.; Abdeslam, A.; Moussa, H.; Makni, I.; Herrero, A.M.; Jiménez-Colmenero, F.; Ruiz-Capillas, C.; et al. Effects of probiotic strains, *Lactobacillus plantarum* TN8 and *Pediococcus acidilactici*, on microbiological and physico-chemical characteristics of beef sausages. *LWT* **2018**, *92*, 195–203. [CrossRef]
153. Yıldırım, Z.; Yerlikaya, S.; Öncül, N.; Sakin, T. Inhibitory Effect of *Lactococcin* BZ Against Listeria innocua and Indigenous Microbiota of Fresh Beef. *Food Technol. Biotechnol.* **2016**, *54*, 317–323. [CrossRef]
154. Chakchouk-Mtibaa, A.; Smaoui, S.; Ktari, N.; Sellem, I.; Najah, S.; Karray-Rebai, I.; Mellouli, L. Biopreservative Efficacy of Bacteriocin BacFL31 in Raw Ground Turkey Meat in terms of Microbiological, Physicochemical, and Sensory Qualities. *Biocontrol Sci.* **2017**, *22*, 67–77. [CrossRef]
155. Balay, D.R.; Dangeti, R.V.; Kaur, K.; McMullen, L.M. Purification of leucocin A for use on wieners to inhibit Listeria monocytogenes in the presence of spoilage organisms. *Int. J. Food Microbiol.* **2017**, *255*, 25–31. [CrossRef]
156. Ruiz, A.; Williams, S.K.; Djeri, N.; Hinton, A.; Rodrick, G.E. Nisin affects the growth of *Listeria monocytogenes* on ready-to-eat turkey ham stored at four degrees Celsius for sixty-three days. *Poult. Sci.* **2010**, *89*, 353–358. [CrossRef]
157. Kęska, P.; Zielińska, D.; Karbowiak, M.; Kruk, M.; Lisiecka, U.; Stadnik, J. The potential of cell-free supernatants from *Lacticaseibacillus paracasei* B1 and *Lactiplantibacillus plantarum* O24 as antioxidant and antimicrobial agents. *Food Chem.* **2025**, *492*, 145408. [CrossRef] [PubMed]
158. Acuña, L.; Picariello, G.; Sesma, F.; Morero, R.D.; Bellomio, A. A new hybrid bacteriocin, Ent35–MccV, displays antimicrobial activity against pathogenic Gram-positive and Gram-negative bacteria. *FEBS Open Bio* **2012**, *2*, 12–19. [CrossRef] [PubMed]
159. Trinetta, V.; Floros, J.D.; Cutter, C.N. Sakacin A-containing pullulan film: An active packaging system to control epidemic clones of *Listeria monocytogenes* in ready-to-eat foods. *J. Food Saf.* **2010**, *30*, 366–381. [CrossRef]
160. Xie, Y.; Zhang, M.; Gao, X.; Shao, Y.; Liu, H.; Jin, J.; Yang, W.; Zhang, H. Development and antimicrobial application of plantaricin BM-1 incorporating a PVDC film on fresh pork meat during cold storage. *J. Appl. Microbiol.* **2018**, *125*, 1108–1116. [CrossRef]
161. Ghabraie, M.; Vu, K.D.; Huq, T.; Khan, A.; Lacroix, M. Antilisterial effects of antibacterial formulations containing essential oils, nisin, nitrite and organic acid salts in a sausage model. *J. Food Sci. Technol.* **2016**, *53*, 2625–2633. [CrossRef]
162. Anacarso, I.; Messi, P.; Condò, C.; Iseppi, R.; Bondi, M.; Sabia, C.; de Niederhäusern, S. A bacteriocin-like substance produced from *Lactobacillus pentosus* 39 is a natural antagonist for the control of *Aeromonas hydrophila* and *Listeria monocytogenes* in fresh salmon fillets. *LWT—Food Sci. Technol.* **2014**, *55*, 604–611. [CrossRef]
163. Jakobsen, A.; Stupar, J.; Lerfall, J.; Sunniva, H.; Turid, R. Biopreservation of Ready-to-Eat Atlantic Salmon (*Salmo salar*) by Lactic Acid Bacteria: Effect on Safety and Quality Parameters. 2025. Available online: https://ssrn.com/abstract=5332555 (accessed on 30 January 2026).
164. Stupar, J.; Hoel, S.; Strømseth, S.; Lerfall, J.; Rustad, T.; Jakobsen, A.N. Selection of lactic acid bacteria for biopreservation of salmon products applying processing-dependent growth kinetic parameters and antimicrobial mechanisms. *Heliyon* **2023**, *9*, e19887. [CrossRef]
165. Brillet, A.; Pilet, M.-F.; Prevost, H.; Cardinal, M.; Leroi, F. Effect of inoculation of *Carnobacterium divergens* V41, a biopreservative strain against *Listeria monocytogenes* risk, on the microbiological, chemical and sensory quality of cold-smoked salmon. *Int. J. Food Microbiol.* **2005**, *104*, 309–324. [CrossRef]
166. Brillet, A.; Pilet, M.F.; Prevost, H.; Bouttefroy, A.; Leroi, F. Biodiversity of *Listeria monocytogenes* sensitivity to bacteriocin-producing *Carnobacterium* strains and application in sterile cold-smoked salmon. *J. Appl. Microbiol.* **2004**, *97*, 1029–1037. [CrossRef]
167. Nilsson, L.; Gram, L.; Huss, H.H. Growth Control of *Listeria monocytogenes* on Cold-Smoked Salmon Using a Competitive Lactic Acid Bacteria Flora. *J. Food Prot.* **1999**, *62*, 336–342. [CrossRef]
168. Katla, T.; Møretrø, T.; Aasen, I.M.; Holck, A.; Axelsson, L.; Naterstad, K. Inhibition of *Listeria monocytogenes* in cold smoked salmon by addition of sakacin P and/or live *Lactobacillus sakei* cultures. *Food Microbiol.* **2001**, *18*, 431–439. [CrossRef]
169. Tomé, E.; Gibbs, P.A.; Teixeira, P.C. Growth control of *Listeria innocua* 2030c on vacuum-packaged cold-smoked salmon by lactic acid bacteria. *Int. J. Food Microbiol.* **2008**, *121*, 285–294. [CrossRef] [PubMed]
170. Aymerich, T.; Rodríguez, M.; Garriga, M.; Bover-Cid, S. Assessment of the bioprotective potential of lactic acid bacteria against *Listeria monocytogenes* on vacuum-packed cold-smoked salmon stored at 8 °C. *Food Microbiol.* **2019**, *83*, 64–70. [CrossRef] [PubMed]
171. Jakobsen, A.N.; Hoel, S. Controlling *Listeria monocytogenes* in ready-to-eat salmon products using bioprotective cultures of lactic acid bacteria: What hinders the transition from research to industrial application? *Int. J. Food Microbiol.* **2025**, *443*, 111400. [CrossRef]
172. Sánchez-Martín, J.; Serrano-Heredia, S.M.; Possas, A.; Valero, A.; Carrasco, E. Evaluation of the Antimicrobial Effect of Bioprotective Lactic Acid Bacteria Cultures Against *Listeria monocytogenes* in Vacuum-Packaged Cold-Smoked Rainbow Trout (*Oncorhynchus mykiss*) at Different Temperatures. *Foods* **2025**, *14*, 1951. [CrossRef]
173. Siroli, L.; Patrignani, F.; Serrazanetti, D.I.; Tabanelli, G.; Montanari, C.; Gardini, F.; Lanciotti, R. Lactic acid bacteria and natural antimicrobials to improve the safety and shelf-life of minimally processed sliced apples and lamb's lettuce. *Food Microbiol.* **2015**, *47*, 74–84. [CrossRef]

https://doi.org/10.3390/antibiotics15030248

174. Chun, H.; Kim, C.-h.; Cho, Y.-h. Microencapsulation of Lactobacillus plantarum DKL 109 using External Ionic Gelation Method. *Korean J. Food Sci. Anim. Resour.* **2014**, *34*, 692–699. [CrossRef]
175. Linares-Morales, J.R.; Gutiérrez-Méndez, N.; Rivera-Chavira, B.E.; Pérez-Vega, S.B.; Nevárez-Moorillón, G.V. Biocontrol Processes in Fruits and Fresh Produce, the Use of Lactic Acid Bacteria as a Sustainable Option. *Front. Sustain. Food Syst.* **2018**, *2*, 50. [CrossRef]
176. Zanzan, M.; Ezzaky, Y.; Achemchem, F.; Hamadi, F. Leveraging lactic acid bacteria biofilms and bioactive substances to counteract pathogenic biofilms in the dairy processing. *Food Humanit.* **2024**, *3*, 100448. [CrossRef]
177. Speranza, B.; Sinigaglia, M.; Corbo, M.R. Non starter lactic acid bacteria biofilms: A means to control the growth of *Listeria monocytogenes* in soft cheese. *Food Control* **2009**, *20*, 1063–1067. [CrossRef]
178. Zhao, T.; Podtburg, T.C.; Zhao, P.; Chen, D.; Baker, D.A.; Cords, B.; Doyle, M.P. Reduction by Competitive Bacteria of Listeria monocytogenes in Biofilms and Listeria Bacteria in Floor Drains in a Ready-to-Eat Poultry Processing Plant. *J. Food Prot.* **2013**, *76*, 601–607. [CrossRef] [PubMed]
179. Tatsaporn, T.; Kornkanok, K. Using Potential Lactic Acid Bacteria Biofilms and their Compounds to Control Biofilms of Foodborne Pathogens. *Biotechnol. Rep.* **2020**, *26*, e00477. [CrossRef]
180. Tan, X.; Han, Y.; Xiao, H.; Zhou, Z. Pediococcus Acidilactici Inhibit Biofilm Formation of Food-Borne Pathogens on Abiotic Surfaces. *Trans. Tianjin Univ.* **2017**, *23*, 70–77. [CrossRef]
181. Masebe, R.D.; Thantsha, M.S. Anti-Biofilm Activity of Cell Free Supernatants of Selected Lactic Acid Bacteria against *Listeria monocytogenes* Isolated from Avocado and Cucumber Fruits, and from an Avocado Processing Plant. *Foods* **2022**, *11*, 2872. [CrossRef]
182. Obafemi, Y.D.; Obiukwu, A.C.; Oranusi, S.U. Revisiting the application, current trends, and prospect of bacteriocins in food preservation. *Discov. Food* **2025**, *5*, 165. [CrossRef]
183. Boelter, J.F.; Brandelli, A. Innovative bionanocomposite films of edible proteins containing liposome-encapsulated nisin and halloysite nanoclay. *Colloids Surf. B Biointerfaces* **2016**, *145*, 740–747. [CrossRef]
184. Hashemi, S.M.; Kaveh, S.; Abedi, E.; Phimolsiripol, Y. Polysaccharide-Based Edible Films/Coatings for the Preservation of Meat and Fish Products: Emphasis on Incorporation of Lipid-Based Nanosystems Loaded with Bioactive Compounds. *Foods* **2023**, *12*, 3268. [CrossRef]
185. Hou, T.; Ma, S.; Wang, F.; Wang, L. A comprehensive review of intelligent controlled release antimicrobial packaging in food preservation. *Food Sci. Biotechnol.* **2023**, *32*, 1459–1478. [CrossRef]
186. Lisboa, H.M.; Pasquali, M.B.; dos Anjos, A.I.; Sarinho, A.M.; de Melo, E.D.; Andrade, R.; Batista, L.; Lima, J.; Diniz, Y.; Barros, A. Innovative and Sustainable Food Preservation Techniques: Enhancing Food Quality, Safety, and Environmental Sustainability. *Sustainability* **2024**, *16*, 8223. [CrossRef]
187. Benbettaïeb, N.; Debeaufort, F.; Karbowiak, T. Bioactive edible films for food applications: Mechanisms of antimicrobial and antioxidant activity. *Crit. Rev. Food Sci. Nutr.* **2019**, *59*, 3431–3455. [CrossRef]
188. Nor, A.H.A.; Jalil, M.T.M.; Seow, E.-K.; Idris, M.H.M.; Yahya, M.F.Z.R. Antimicrobial packaging: Mechanisms, materials, incorporation methods, strategies, biodegradability, and smart innovations—A comprehensive review. *Food Mater. Res.* **2025**, *5*, e009. [CrossRef]
189. Medeiros, B.G.S.; Pinheiro, A.C.; Carneiro-da-Cunha, M.G.; Vicente, A.A. Development and characterization of a nanomultilayer coating of pectin and chitosan—Evaluation of its gas barrier properties and application on 'Tommy Atkins' mangoes. *J. Food Eng.* **2012**, *110*, 457–464. [CrossRef]
190. Poverenov, E.; Danino, S.; Horev, B.; Granit, R.; Vinokur, Y.; Rodov, V. Layer-by-Layer Electrostatic Deposition of Edible Coating on Fresh Cut Melon Model: Anticipated and Unexpected Effects of Alginate–Chitosan Combination. *Food Bioprocess Technol.* **2014**, *7*, 1424–1432. [CrossRef]
191. Yan, J.; Luo, Z.; Ban, Z.; Lu, H.; Li, D.; Yang, D.; Aghdam, M.S.; Li, L. The effect of the layer-by-layer (LBL) edible coating on strawberry quality and metabolites during storage. *Postharvest Biol. Technol.* **2019**, *147*, 29–38. [CrossRef]
192. Vasiliauskaite, A.; Mileriene, J.; Songisepp, E.; Rud, I.; Muizniece-Brasava, S.; Ciprovica, I.; Axelsson, L.; Lutter, L.; Aleksandrovas, E.; Tammsaar, E.; et al. Application of Edible Coating Based on Liquid Acid Whey Protein Concentrate with Indigenous Lactobacillus helveticus for Acid-Curd Cheese Quality Improvement. *Foods* **2022**, *11*, 3353. [CrossRef]
193. Gialamas, H.; Zinoviadou, K.G.; Biliaderis, C.G.; Koutsoumanis, K.P. Development of a novel bioactive packaging based on the incorporation of Lactobacillus sakei into sodium-caseinate films for controlling *Listeria monocytogenes* in foods. *Food Res. Int.* **2010**, *43*, 2402–2408. [CrossRef]
194. La Storia, A.; Di Giuseppe, F.A.; Volpe, S.; Oliviero, V.; Villani, F.; Torrieri, E. Physical properties and antimicrobial activity of bioactive film based on whey protein and *Lactobacillus curvatus* 54M16 producer of bacteriocins. *Food Hydrocoll.* **2020**, *108*, 105959. [CrossRef]
195. Bambace, M.F.; Alvarez, M.V.; Moreira, M.d.R. Novel functional blueberries: Fructo-oligosaccharides and probiotic lactobacilli incorporated into alginate edible coatings. *Food Res. Int.* **2019**, *122*, 653–660. [CrossRef]

https://doi.org/10.3390/antibiotics15030248

196. Alvarez, M.V.; Bambace, M.F.; Quintana, G.; Gomez-Zavaglia, A.; Moreira, M.d.R. Prebiotic-alginate edible coating on fresh-cut apple as a new carrier for probiotic lactobacilli and bifidobacteria. *LWT* **2021**, *137*, 110483. [CrossRef]
197. Mozaffarzogh, M.; Misaghi, A.; Shahbazi, Y.; Kamkar, A. Evaluation of probiotic carboxymethyl cellulose-sodium caseinate films and their application in extending shelf life quality of fresh trout fillets. *LWT* **2020**, *126*, 109305. [CrossRef]
198. Degli Esposti, M.; Toselli, M.; Sabia, C.; Messi, P.; de Niederhäusern, S.; Bondi, M.; Iseppi, R. Effectiveness of polymeric coated films containing bacteriocin-producer living bacteria for *Listeria monocytogenes* control under simulated cold chain break. *Food Microbiol.* **2018**, *76*, 173–179. [CrossRef] [PubMed]
199. Cheng, X.; Xie, Q.; Sun, Y. Advances in nanomaterial-based targeted drug delivery systems. *Front. Bioeng. Biotechnol.* **2023**, *11*, 1177151. [CrossRef] [PubMed]
200. Gressler, S.; Hipfinger, C.; Part, F.; Pavlicek, A.; Zafiu, C.; Giese, B. A systematic review of nanocarriers used in medicine and beyond—Definition and categorization framework. *J. Nanobiotechnology* **2025**, *23*, 90. [CrossRef]
201. Anandharamakrishnan, C.; Moses, J.A.; Leena, M.M. *Nanotechnology for Sustainable Food Packaging*; John Wiley & Sons: Hoboken, NJ, USA, 2025.
202. Fadel, N.; Abu-Elghait, M.; Gebreel, H.; Zendo, T.; Youssef, H. Lactic Acid Bacteria-Mediated Synthesis of Selenium Nanoparticles: A Smart Strategy Against Multidrug-Resistant Pathogens. *Appl. Microbiol.* **2025**, *5*, 121. [CrossRef]
203. Kumar, P.; Gautam, S.; Bansal, D.; Kaur, R. Starch-based antibacterial food packaging with ZnO nanoparticle. *J. Food Sci. Technol.* **2024**, *61*, 178–191. [CrossRef]
204. Jha, A.K.; Prasad, K. Biosynthesis of metal and oxide nanoparticles using Lactobacilli from yoghurt and probiotic spore tablets. *Biotechnol. J.* **2010**, *5*, 285–291. [CrossRef]
205. Carrapiço, A.; Martins, M.R.; Caldeira, A.T.; Mirão, J.; Dias, L. Biosynthesis of Metal and Metal Oxide Nanoparticles Using Microbial Cultures: Mechanisms, Antimicrobial Activity and Applications to Cultural Heritage. *Microorganisms* **2023**, *11*, 378. [CrossRef]
206. Chang, H.; Kim, B.H.; Lim, S.G.; Baek, H.; Park, J.; Hyeon, T. Role of the Precursor Composition in the Synthesis of Metal Ferrite Nanoparticles. *Inorg. Chem.* **2021**, *60*, 4261–4268. [CrossRef]
207. Jeevanandam, J.; Chan, Y.S.; Danquah, M.K. Biosynthesis of Metal and Metal Oxide Nanoparticles. *ChemBioEng Rev.* **2016**, *3*, 55–67. [CrossRef]
208. Zikalala, N.; Matshetshe, K.; Parani, S.; Oluwafemi, O.S. Biosynthesis protocols for colloidal metal oxide nanoparticles. *Nano-Struct. Nano-Objects* **2018**, *16*, 288–299. [CrossRef]
209. Huq, M.A.; Ashrafudoulla, M.; Rahman, M.M.; Balusamy, S.R.; Akter, S. Green Synthesis and Potential Antibacterial Applications of Bioactive Silver Nanoparticles: A Review. *Polymers* **2022**, *14*, 742. [CrossRef] [PubMed]
210. Alves, F.C.B.; Barbosa, L.N.; Andrade, B.F.M.T.; Albano, M.; Furtado, F.B.; Marques Pereira, A.F.; Rall, V.L.M.; Júnior, A.F. Short communication: Inhibitory activities of the lantibiotic nisin combined with phenolic compounds against *Staphylococcus aureus* and Listeria monocytogenes in cow milk. *J. Dairy Sci.* **2016**, *99*, 1831–1836. [CrossRef] [PubMed]
211. Campion, A.; Morrissey, R.; Field, D.; Cotter, P.D.; Hill, C.; Ross, R.P. Use of enhanced nisin derivatives in combination with food-grade oils or citric acid to control *Cronobacter sakazakii* and *Escherichia coli* O157:H7. *Food Microbiol.* **2017**, *65*, 254–263. [CrossRef]
212. Kumar, N.; Kumar, V.; Waheed, S.M.; Pradhan, D. Efficacy of reuterin and bacteriocins nisin and pediocin in the preservation of raw milk from dairy farms. *Food Technol. Biotechnol.* **2020**, *58*, 359–369. [CrossRef] [PubMed]
213. Zhang, L.; Ben Said, L.; Diarra, M.S.; Fliss, I. Inhibitory Activity of Natural Synergetic Antimicrobial Consortia Against *Salmonella enterica* on Broiler Chicken Carcasses. *Front. Microbiol.* **2021**, *12*, 656956. [CrossRef]
214. Raeisi, M.; Tabaraei, A.; Hashemi, M.; Behnampour, N. Effect of sodium alginate coating incorporated with nisin, Cinnamomum zeylanicum, and rosemary essential oils on microbial quality of chicken meat and fate of *Listeria monocytogenes* during refrigeration. *Int. J. Food Microbiol.* **2016**, *238*, 139–145. [CrossRef]
215. Iseppi, R.; Pilati, F.; Marini, M.; Toselli, M.; de Niederhäusern, S.; Guerrieri, E.; Messi, P.; Sabia, C.; Manicardi, G.; Anacarso, I.; et al. Anti-listerial activity of a polymeric film coated with hybrid coatings doped with Enterocin 416K1 for use as bioactive food packaging. *Int. J. Food Microbiol.* **2008**, *123*, 281–287. [CrossRef]
216. Beristain-Bauza, S.C.; Mani-López, E.; Palou, E.; López-Malo, A. Antimicrobial activity and physical properties of protein films added with cell-free supernatant of *Lactobacillus rhamnosus*. *Food Control* **2016**, *62*, 44–51. [CrossRef]
217. Beristain-Bauza, S.d.C.; Mani-López, E.; Palou, E.; López-Malo, A. Antimicrobial activity of whey protein films supplemented with *Lactobacillus sakei* cell-free supernatant on fresh beef. *Food Microbiol.* **2017**, *62*, 207–211. [CrossRef]
218. Toushik, S.H.; Kim, K.; Ashrafudoulla, M.; Mizan, M.F.R.; Roy, P.K.; Nahar, S.; Kim, Y.; Ha, S.-D. Korean kimchi-derived lactic acid bacteria inhibit foodborne pathogenic biofilm growth on seafood and food processing surface materials. *Food Control* **2021**, *129*, 108276. [CrossRef]
219. Yahya, M.F.Z.R.; Aazmi, M.S.; Ismail, M.F. Antibiofilm potential of lactic acid bacteria: Mechanism of cell-free supernatant, metabolite insights, and prospects for edible coating applications in food quality control. *Food Mater. Res.* **2025**, *5*, e006. [CrossRef]

https://doi.org/10.3390/antibiotics15030248

220. Negash, A.W.; Tsehai, B.A. Current Applications of Bacteriocin. *Int. J. Microbiol.* **2020**, *2020*, 4374891. [CrossRef] [PubMed]
221. Moniente, M.; García-Gonzalo, D.; Ontañón, I.; Pagán, R.; Botello-Morte, L. Histamine accumulation in dairy products: Microbial causes, techniques for the detection of histamine-producing microbiota, and potential solutions. *Compr. Rev. Food Sci. Food Saf.* **2021**, *20*, 1481–1523. [CrossRef] [PubMed]
222. Sun, L.; Xu, B.; Tao, Y.; Liang, Y.; Chen, X. Exploring Intervention Strategies for Microbial Biofilms in the Food Industry Based on a Biomolecular Mechanism Perspective: Recent Advances and Emerging Trends. *Foods* **2025**, *14*, 4192. [CrossRef]
223. Gilmore, B.F.; Flynn, P.B.; O'Brien, S.; Hickok, N.; Freeman, T.; Bourke, P. Cold Plasmas for Biofilm Control: Opportunities and Challenges. *Trends Biotechnol.* **2018**, *36*, 627–638. [CrossRef]
224. Oliulla, H.; Mizan, M.F.R.; Ashrafudoulla, M.; Meghla, N.S.; Ha, A.J.-w.; Park, S.H.; Ha, S.-D. The challenges and prospects of using cold plasma to prevent bacterial contamination and biofilm formation in the meat industry. *Meat Sci.* **2024**, *217*, 109596. [CrossRef]
225. Sirelkhatim, A.; Mahmud, S.; Seeni, A.; Kaus, N.H.M.; Ann, L.C.; Bakhori, S.K.M.; Hasan, H.; Mohamad, D. Review on Zinc Oxide Nanoparticles: Antibacterial Activity and Toxicity Mechanism. *Nano-Micro Lett.* **2015**, *7*, 219–242. [CrossRef]
226. Yang, D.; Liu, Q.; Gao, Y.; Wan, S.; Meng, F.; Weng, W.; Zhang, Y. Characterization of silver nanoparticles loaded chitosan/polyvinyl alcohol antibacterial films for food packaging. *Food Hydrocoll.* **2023**, *136*, 108305. [CrossRef]
227. Vasiljevic, Z.Z.; Vunduk, J.; Dojcinovic, M.P.; Miskovic, G.; Tadic, N.B.; Vidic, J.; Nikolic, M.V. ZnO and Fe2TiO5 nanoparticles obtained by green synthesis as active components of alginate food packaging films. *Food Packag. Shelf Life* **2024**, *43*, 101280. [CrossRef]
228. Sharma, D.; Sharma, A.; Gautam, H.R. Green synthesized nanoparticles for disease management in vegetable crops: A review. *Plant Nano Biol.* **2025**, *13*, 100179. [CrossRef]
229. Afzaal, M.; Saeed, F.; Hussain, S.; Mohamed, A.A.; Alamri, M.S.; Ahmad, A.; Ateeq, H.; Tufail, T.; Hussain, M. Survival and storage stability of encapsulated probiotic under simulated digestion conditions and on dried apple snacks. *Food Sci. Nutr.* **2020**, *8*, 5392–5401. [CrossRef]
230. Sbehat, M.; Mauriello, G.; Altamimi, M. Microencapsulation of Probiotics for Food Functionalization: An Update on Literature Reviews. *Microorganisms* **2022**, *10*, 1948. [CrossRef]

Disclaimer/Publisher's Note: The statements, opinions and data contained in all publications are solely those of the individual author(s) and contributor(s) and not of MDPI and/or the editor(s). MDPI and/or the editor(s) disclaim responsibility for any injury to people or property resulting from any ideas, methods, instructions or products referred to in the content.

https://doi.org/10.3390/antibiotics15030248

antibiotics

MDPI

Article

Evaluation of the Antifungal Activity of the Polyphenol Formulation *Viroelixir* Against *Candida albicans*

Manal Dahdah [1], Yasmine Ettouil [1], Hawraa Issa [2], Latifa Koussih [3], Mikhlid H. Almutairi [4], Mahmoud Rouabhia [1] and Abdelhabib Semlali [1,*]

[1] GREB Research Group, Faculty of Dentistry, Laval University, Québec, QC G1V 0A6, Canada; manal.dahdah.1@ulaval.ca (M.D.); yasmine.et-touil.1@ulaval.ca (Y.E.); mahmoud.rouabhia@fmd.ulaval.ca (M.R.)
[2] DREAM-CV Lab, Centre for Outcomes Research and Evaluation, Research Institute of the McGill University Health Centre, Montreal, QC H4A 3J1, Canada; hawraa.issa.1@ulaval.ca
[3] Département des Sciences Expérimentales, Université de Saint-Boniface, Winnipeg, MB R2H 3B8, Canada; lkoussih@ustboniface.ca
[4] Zoology Department, College of Science, King Saud University, P.O. Box 2455, Riyadh 11451, Saudi Arabia; malmutairi@ksu.edu.sa
* Correspondence: abdelhabib.semlali@greb.ulaval.ca

Abstract

Candida albicans (*C. albicans*) is an opportunistic fungal pathogen capable of causing a wide range of infections, including mucosal and systemic candidiasis. In the oral cavity, fungi represent a minor component of the microbiome but can significantly contribute to morbidity, particularly under conditions of dysbiosis or immunosuppression. Treatment remains challenging due to increasing multidrug resistance. This study investigates the in vitro antifungal potential of *Viroelixir*, a standardized polyphenol blend derived from green tea and pomegranate and enriched in catechins (including epigallocatechin gallate, EGCG), ellagitannins (notably punicalagin), ellagic acid, and flavonoids, with particular focus on its potential anti-virulence mechanisms. Methods: The effect of *Viroelixir* on *C. albicans* growth was assessed using MTT assay, optical density measurements, colony formation, carbohydrate quantification, and pH variation analysis. Biofilm formation, morphological transition, ROS production, necrosis, virulence gene expression, adhesion, and host immune responses were also evaluated. Results: *Viroelixir* significantly inhibited *C. albicans* growth and reduced colony formation compared with untreated controls. The formulation also inhibited biofilm formation and markedly reduced pseudohyphal development, reaching up to 94% reduction under specific treatment conditions. Flow cytometry analysis showed an increase in dead fungal cells, reaching approximately 88% following exposure to *Viroelixir* at the highest tested concentration. In addition, *Viroelixir* reduced the transcript levels of several virulence-associated genes, including SAP1–SAP9 and EAP1. In epithelial cell co-culture models, pre-treatment of *C. albicans* with *Viroelixir* reduced fungal adhesion and attenuated epithelial inflammatory responses, including IL-6, IL-8, and hBD-2 production, and was associated with reduced activation of the TLR4-NF-κB signaling pathway. Conclusions: These findings suggest that the antifungal and anti-virulence effects observed may be associated with the polyphenolic compounds present in the *Viroelixir* formulation, highlighting its potential as a promising in vitro antifungal candidate against *C. albicans*.

Keywords: *Candida albicans*; *Viroelixir*; antifungal activity; virulence; adhesion; SAPs expression; cytokines; TLR4-NF-κB pathway

1. Introduction

A diverse microflora, consisting of over 700 species of bacteria, viruses, fungi, and protozoa, inhabits the human oral cavity [1]. Although fungi represent a relatively small proportion of the human microbiome, opportunistic fungal pathogens can cause a wide range of mucosal and systemic infections, particularly in immunocompromised individuals [2,3]. *Candida* species are responsible for the majority of human fungal infections, with *C. albicans* being the most frequently isolated species in cases of oral candidiasis [4,5]. While *C. albicans* commonly exists as a commensal organism in the oral, gastrointestinal, and genital tracts of many healthy individuals, under certain conditions it can cause superficial infections such as oral candidiasis or progress to invasive systemic infections [6,7]. Chronic infections and inflammation have also been implicated in carcinogenesis [8,9], and emerging evidence suggests that *C. albicans* may contribute to oral carcinogenesis through mechanisms including chronic inflammation, toxin production, and induction of pro-inflammatory cytokines [10–14].

The ability of *C. albicans* to undergo morphological transition from yeast to hyphae holds significant importance for establishing invasive disease by traversing mucosal barriers and entering deep tissues [6]. Another important factor influencing the virulence of *C. albicans* and ensuring resistance to antifungal agents is its ability to form biofilm on abiotic or biotic surfaces [7,15]. The transition from individual growth to growth within a biofilm, accompanied by a complex modification of phenotypic characteristics, is facilitated by changes in virulence gene expression [16]. Notably, hydrolytic enzymes and adhesins play essential roles in *C. albicans* pathogenicity. For example, epithelial adhesin protein 1 (EAP1) is involved in adhesion to human epithelial cells [17]. While secreted aspartyl proteases (SAPs) family members facilitate cellular digestion to support nutrient acquisition, tissue invasion, and immune evasion [18]. *C. albicans* initially interacts with epithelial cells, which play a key role in defending the body against various pathogens and serve as a barrier against oral candidiasis. This fungus is recognized by the Toll-like receptors (TLRs), such as TLR2 and TLR4, which trigger the production of pro-inflammatory cytokines and antimicrobial peptides in diverse cell types, including epithelial cells [19–21]. Specifically, β-defensins 2 and 3 demonstrate antifungal efficacy against *C. albicans* [22,23]. In response to infection, TLRs effects are mainly mediated by PKC, p38 MAPK, and NF-κB signaling pathways [24].

Current guidelines for the management of fungal infections are based on polyenes such as *Amphotericin B* (*Ampho-B*) (5 μg/mL), azoles, and echinocandins [25]. These antifungals function by targeting distinct fungal components: polyenes destroy the fungal cell membrane, azoles hinder ergosterol production, and echinocandins obstruct cell wall synthesis [26]. Despite their tendency to cause hepatotoxicity, ranging from asymptomatic liver abnormalities to very severe hepatocellular injury, causing fulminant liver failure [27], the polyenes class of antifungals are also costly. Another growing concern, associated with reduced treatment efficacy and the increasing prevalence of opportunistic and systemic fungal infections, is microbial resistance, which primarily affects immunocompromised individuals. As a result, there is a rising interest in novel antifungal agents, including a variety of synthetic and natural antimicrobial compounds [28]. Since the beginning of the 20th century, therapeutic choices have relied on synthesizing new drugs based on identified molecular pathways. Although the western medicine approach was declared effective in some situations, the reported lack of efficacy and serious adverse effects [29], have directed attention towards the medicinal capabilities of plant-derived products [15]. In this respect, the World Health Organization has proclaimed the importance of phytotherapy in primary health care, thereby encouraging further research to explore the potential of plants and their detailed mechanisms of action [30].

https://doi.org/10.3390/antibiotics15040420

Pomegranate, a fruit of the *Punica granatum* L. (Lythraceae) tree, is native to the geographic area covering modern Iran and Iraq. Notably, the characteristics of this fruit, such as its color, flavor, and antioxidant properties, appear to be influenced by environmental factors [31]. Importantly, pomegranate, including its seeds, has been shown to possess significant antioxidant and anti-inflammatory properties [32,33], which are likely attributed to its high polyphenol content [34], particularly anthocyanins, 3-glucosides, delphinidin, cyanidin, pelargonidin [35], ellagitannins, ellagic acid, and other flavonoids [36]. The antimicrobial properties of pomegranate have recently garnered considerable attention due to their effect on multiple microbial species. In this regard, punicalagin, found in pomegranate peel, has been reported to exhibit potent antifungal activity against *C. albicans* and *Candida parasitosis* [37]. On the other hand, green tea has gained widespread attention due to its beneficial effects across multiple disease models [38]. More specifically, the *Camellia sinensis* (L.) Kuntze (Theaceae) species has demonstrated anti-cancer and anti-inflammatory properties [39]. Furthermore, tea polyphenols have shown antimicrobial potential against several human pathogens [40]. Given its potential antifungal activity, we investigated a standardized polyphenol-rich formulation derived from green tea and pomegranate. This product, commercially known as *Viroelixir*, is a blend of plant-derived polyphenols that may represent a promising in vitro antifungal candidate. In this study, our primary objective was to evaluate the antifungal potential of *Viroelixir* in vitro against the *C. albicans* model. Overall, we investigated its effect on fungal growth and mortality, sugar content, environmental pH, biofilm formation, pathogen phenotype, ROS production, and the expression of virulence determinants, including hydrolytic enzymes and adhesins. Additionally, we assessed its impact on fungal adhesion and host epithelial cells immunity and defense system.

2. Results

2.1. Viroelixir Inhibits C. albicans Growth and Interferes with Cell Viability

Based on component analysis previously reported [41], *Viroelixir* contains a defined mixture of bioactive polyphenols, including catechins such as EGCG from green tea and ellagitannins such as punicalagin and ellagic acid from pomegranate. These compounds are known to exert antimicrobial and anti-virulence effects and have been associated with antimicrobial activity in this study.

The effect of *Viroelixir* on *C. albicans* growth was evaluated by measuring the optical density (OD) variation at 660 nm every 2 h over a period of 24 h (Figure 1A) and confirmed by MTT assay at 6 h and 24 h (Figure 1B) and by colony formation on solid agar plates (Figure 1C,D). Exposure of *C. albicans* to *Viroelixir* resulted in concentration-dependent growth inhibition, with a minimum inhibitory concentration (MIC) corresponding to *Viroelixir* diluted at 1/50 of *v*/*v* of the stock solution. At 1/50, the effect of *Viroelixir* was comparable to that of the antifungal drug *Ampho-B* (5 µg/mL). The untreated *C. albicans* (0) increased from 100% to nearly 1000% after 14 h while *C. albicans* treated with the IC50 concentration (around of dilution 1/200) showed a 350% growth increase, reflecting a 70% suppression of proliferation. At a 1/50 (*v*/*v* of the stock solution) dilution of *Viroelixir*, a growth inhibition based on OD measurements. was observed, with untreated *C. albicans* (0) proliferating to 1000% after 24 h, while the treated *C. albicans* barely reached 100%, indicating significant inhibition (Figure 1A). These data were confirmed by the MTT assay (metabolic activity associated with viability, not direct viability) after 24 h of *Viroelixir* treatment, showing a significant decrease in viability, from 100% to 43% at the IC50 (1/200). The same pattern was observed after 6 h of treatment and *Ampho-B* (5 µg/mL) showed parallel efficacy to *Viroelixir* (Figure 1B). The extract fungicidal activity towards *C. albicans*

https://doi.org/10.3390/antibiotics15040420

was further confirmed by monitoring colony formation on solid agar plates. At this level, *Viroelixir* strongly prevented colony formation starting 1/1000 dilution (Figure 1C,D).

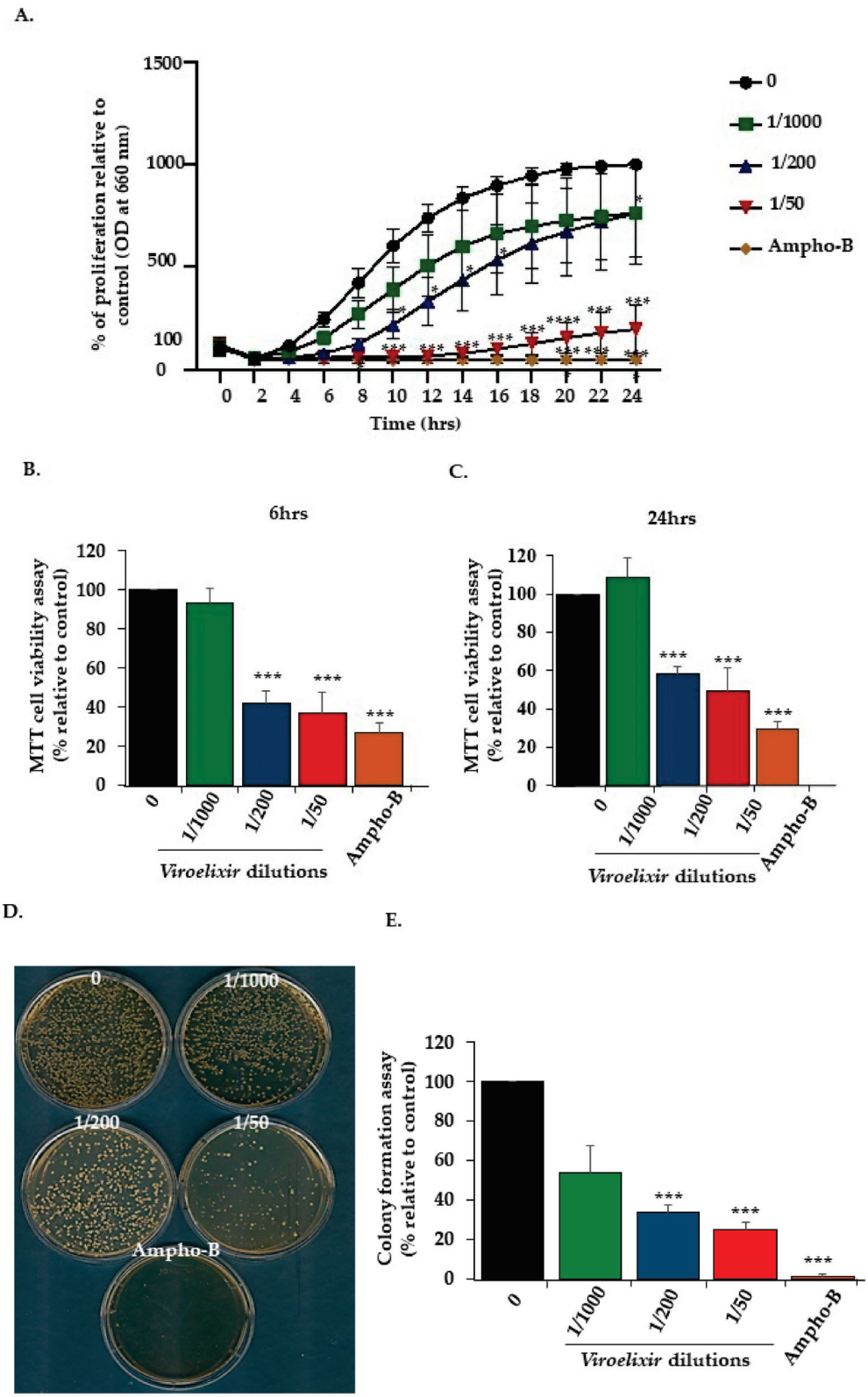

Figure 1. *Effect of Viroelixir on C. albicans growth and viability.* (**A**) Optical density recorded at 660 nm (n = 4 and quadruplet per experiment) over 24 h to reflect *C. albicans* growth. Comparison was performed relative to untreated *C. albicans* at the same time point. (**B**) MTT cell viability and proliferation assay (n = 4, quadruplicates per experiment) performed after 6 h of treatment with

https://doi.org/10.3390/antibiotics15040420

different *Viroelixir* dilutions (1/1000, 1/200, and 1/50). (**C**). MTT cell viability and proliferation assay (n = 4, quadruplicates per experiment) performed after 24 h of treatment with different *Viroelixir* dilutions (1/1000, 1/200, and 1/50). (**D**) Colony formation potential (n = 5) under *Viroelixir* effect. (**E**) Quantitative data corresponding to the number. The results are presented as a percentage, with 100% representing the number of colonies in untreated controls (n = 4). Antifungal drug *Ampho-B* (5 μg/mL) was used as the positive control. The Student's t-test is a statistical test used to determine whether the difference between the control group and the *Viroelixir*-treated group is statistically significant. * $p < 0.05$, *** $p < 0.001$ and **** $p < 0.0001$ were considered statistically significant.

2.2. Effect of Viroelixir on Media pH and Carbohydrate Content

Carbohydrate content in culture supernatants was measured using a colorimetric method to quantify sugars, as described in Section 4. As shown in Figure 2A, the higher residual glucose concentration in the media following *Viroelixir* and *Ampho-B* (5 μg/mL) treatment indicates reduced nutrient consumption due to fungal growth inhibition. Under our experimental conditions, glucose was initially provided at a final concentration of 1 mg/mL. The effect of *Viroelixir* on acid production by *C. albicans* was evaluated by monitoring changes in medium pH. Briefly, a decrease in pH was observed after 24 h of incubation with *C. albicans*, confirming acid production by the fungus. In contrast, a more neutral pH was recorded in cultures supplemented with *Viroelixir* and *Ampho-B* (5 μg/mL) compared to untreated controls. Although this shift may partly reflect reduced fungal viability, the increase in Sabouraud medium pH from 5.6 to approximately 6–7 in the presence of *Viroelixir* (1/50) and *Ampho-B* (5 μg/mL) may also suggest the production of basic metabolites. These findings indicate that antifungal treatments may alter *C. albicans* metabolic activity, particularly pathways involved in acid production (Figure 2B).

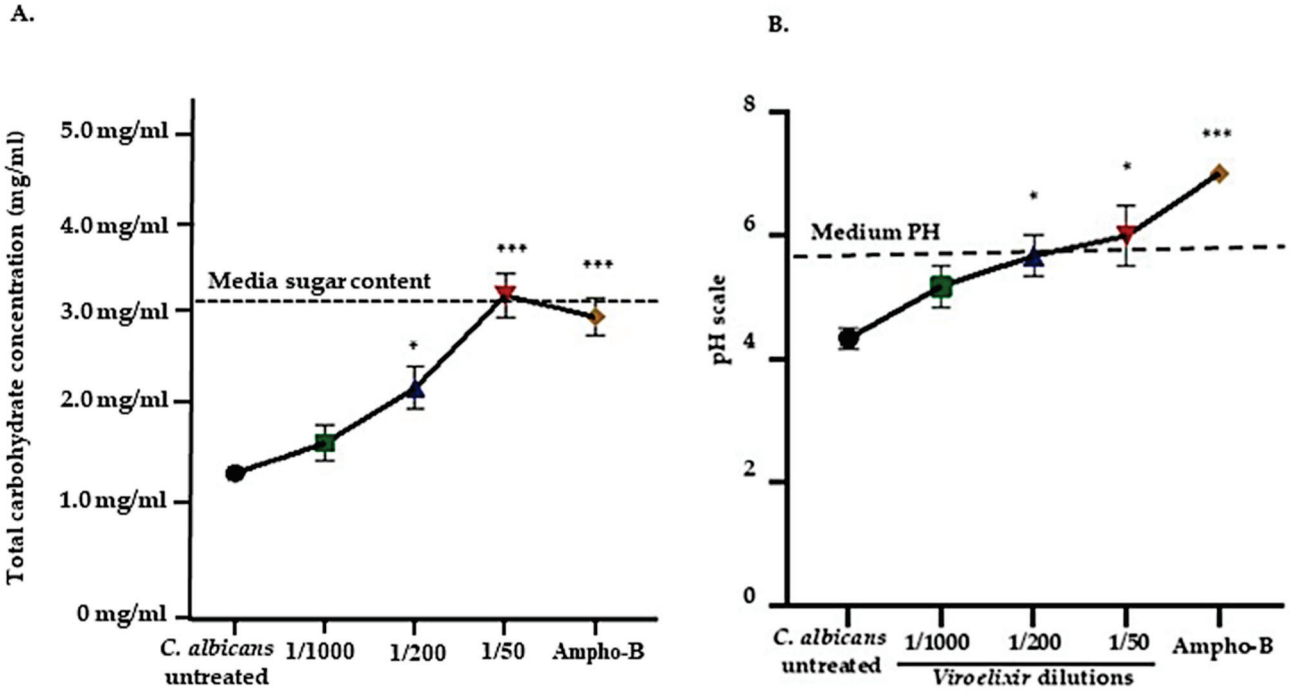

Figure 2. *Effect of Viroelixir on carbohydrate content and media pH.* (**A**) Total carbohydrate content (n = 3). (**B**) Evaluation of medium pH variation (n = 3) in culture media. The antifungal agent *Ampho-B* (5 μg/mL) served as the positive control, and comparisons are presented against untreated *C. albicans* cultures. Different colors represent the experimental conditions: untreated *C. albicans* (black), *Viroelixir* at 1/1000 (green), 1/200 (blue), 1/50 (red), and *Ampho-B* (orange) All data are expressed as mean values ± SEM. Student's t-test is a statistical test used to test whether the difference between the control group and *Viroelixir* treated group is statistically significant or not. * $p < 0.05$, and *** $p < 0.001$ are considered as statistically significant.

https://doi.org/10.3390/antibiotics15040420

2.3. Viroelixir Counteracts Biofilm Formation

Early biofilm formation, assessed at 6 and 24 h using the crystal violet assay, revealed that *Viroelixir*, reduced the biofilm formation after 6 h of *Viroelixir* exposure compared to untreated controls. Similar results were observed with crystal violet after 24 h of *Viroelixir* treatment (Figure 3A). As indicated in the Section 4, the biofilm formation assay was performed on a CollaTape membrane over 6 days, and the results were visualized by scanning electron microscopy (SEM) (Figure 3B). Overall, *Viroelixir* clearly inhibited biofilm formation starting at a 1/200 dilution. Interestingly, the images obtained with *Viroelixir* at 1/50 were comparable to those of the positive control, *Ampho-B* (5 µg/mL). Another important observation is that the non-virulent yeast phenotype was predominant following exposure to the natural product extract.

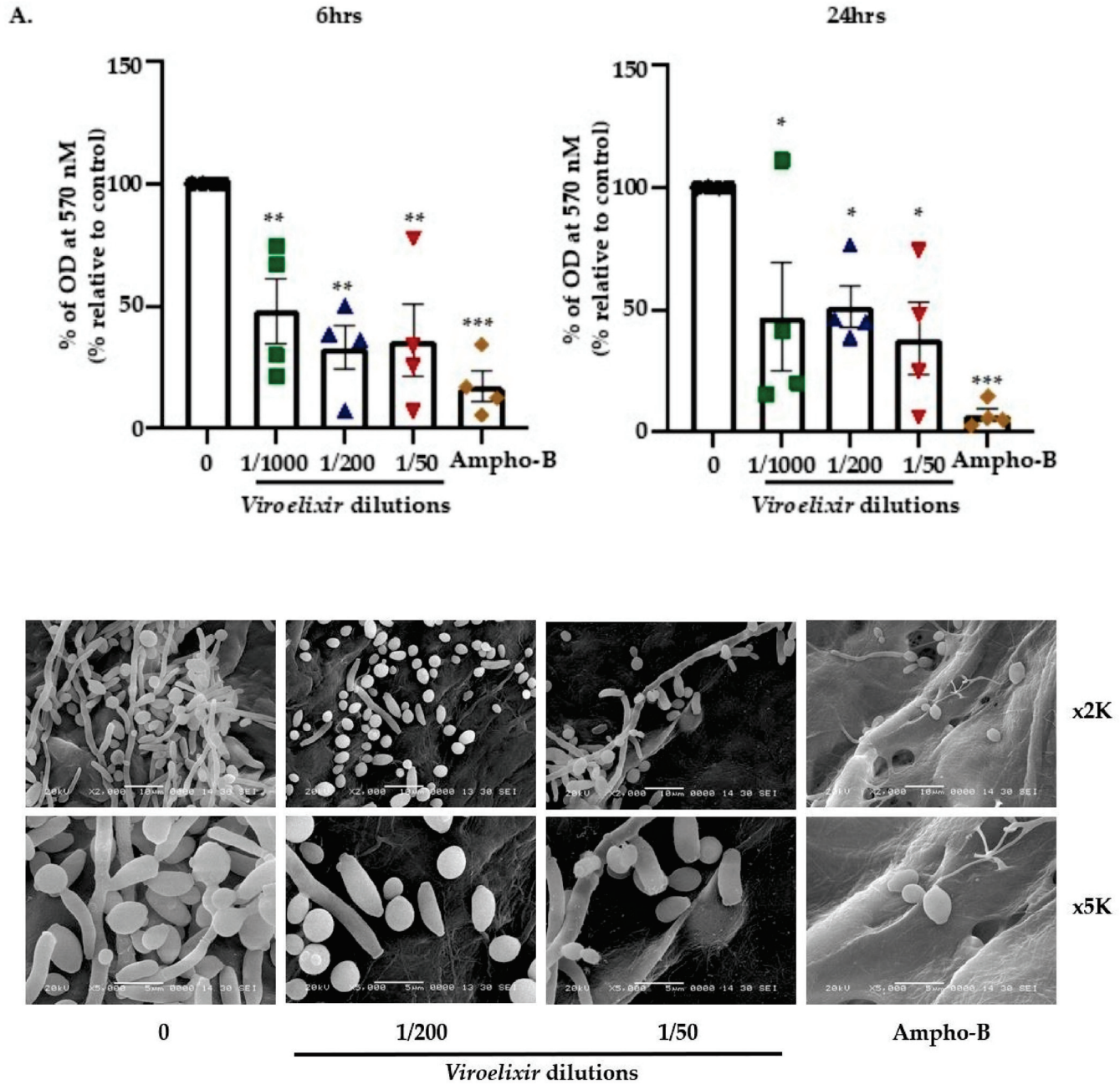

Figure 3. Effect of *Viroelixir* on biofilm formation. (**A**) Crystal Violet staining (n = 4) performed after treatment of fungal cells with different dilutions of *Viroelixir* (0, 1/1000, 1/200, 1/50 of v/v of

https://doi.org/10.3390/antibiotics15040420

the stock solution) for a total duration of 6 and 24 h. Antifungal agent *Ampho-B* (5 μg/mL) served as a positive control, and comparisons are presented against untreated controls. Different colors represent the experimental conditions: untreated control (black), *Viroelixir* at 1/1000 (green), 1/200 (blue), 1/50 (red), and *Ampho-B* (orange). All data are expressed as mean values ± SEM. Student's *t*-test is a statistical test used to test whether the difference between the control group and *Viroelixir* treated group is statistically significant or not. * $p < 0.05$, ** $p < 0.005$, and *** $p < 0.0005$ are considered statistically significant. (**B**) Scanning electron microscopy images ($n = 3$) corresponding to 6 days of *C. albicans* biofilm evolution on porous membrane scaffolds following exposure to either *Viroelixir* or the positive control *Ampho-B* (5 μg/mL). Comparisons were performed relative to the untreated control.

2.4. Viroelixir Favors the Elimination of C. albicans Virulent Forms

Due to its association with invasion and biofilm formation, *C. albicans* morphology was examined at 3 and 6 h of culture under hyphae-inducing conditions (10% FBS at 37 °C). Our data showed no effect on phenotypic switching. However, a decrease in hyphal formation was observed at a dilution of 1/1000 at both time points. A similar trend was observed for pseudohyphae, with a marked reduction at a dilution of 1/200. At this dilution, pseudohyphal formation was strongly reduced at 3 h. Although no significant difference was observed in yeast form numbers, this less virulent form gradually became dominant as the *Viroelixir* dilution increased from 1/1000 to 1/50. Interestingly, at the highest concentration tested (1/50), *Viroelixir* was almost as effective as the *Ampho-B* (5 μg/mL) positive control (Figure 4A,B).

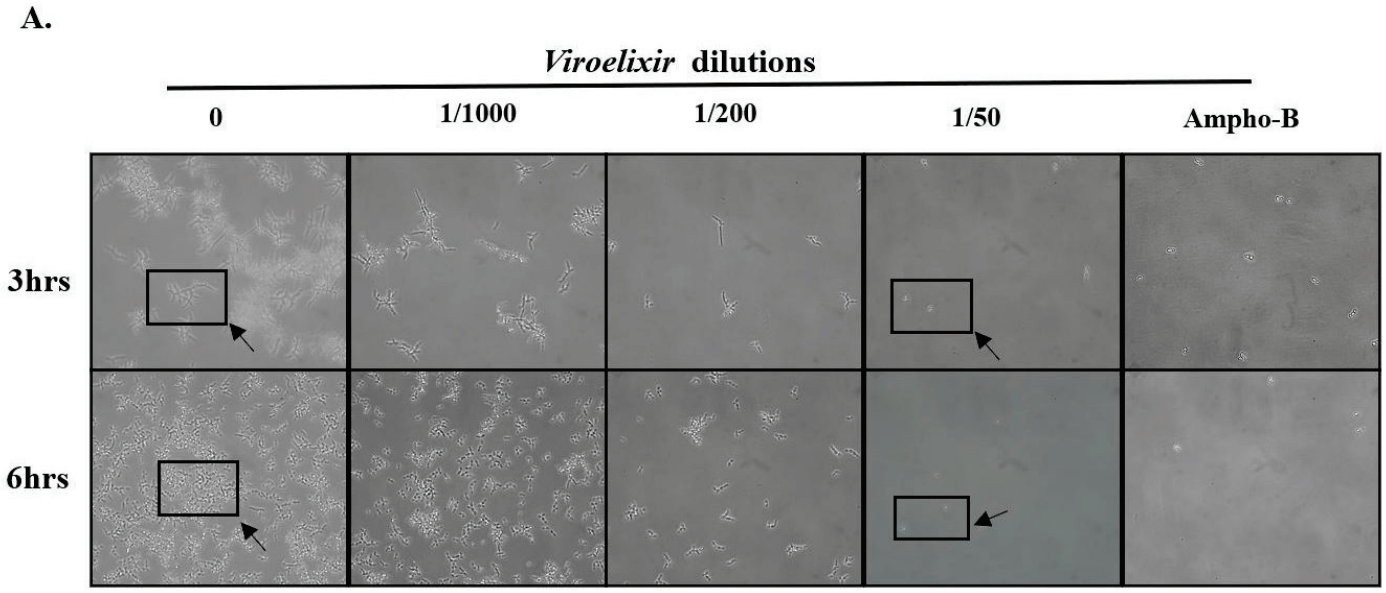

Figure 4. *Cont.*

https://doi.org/10.3390/antibiotics15040420

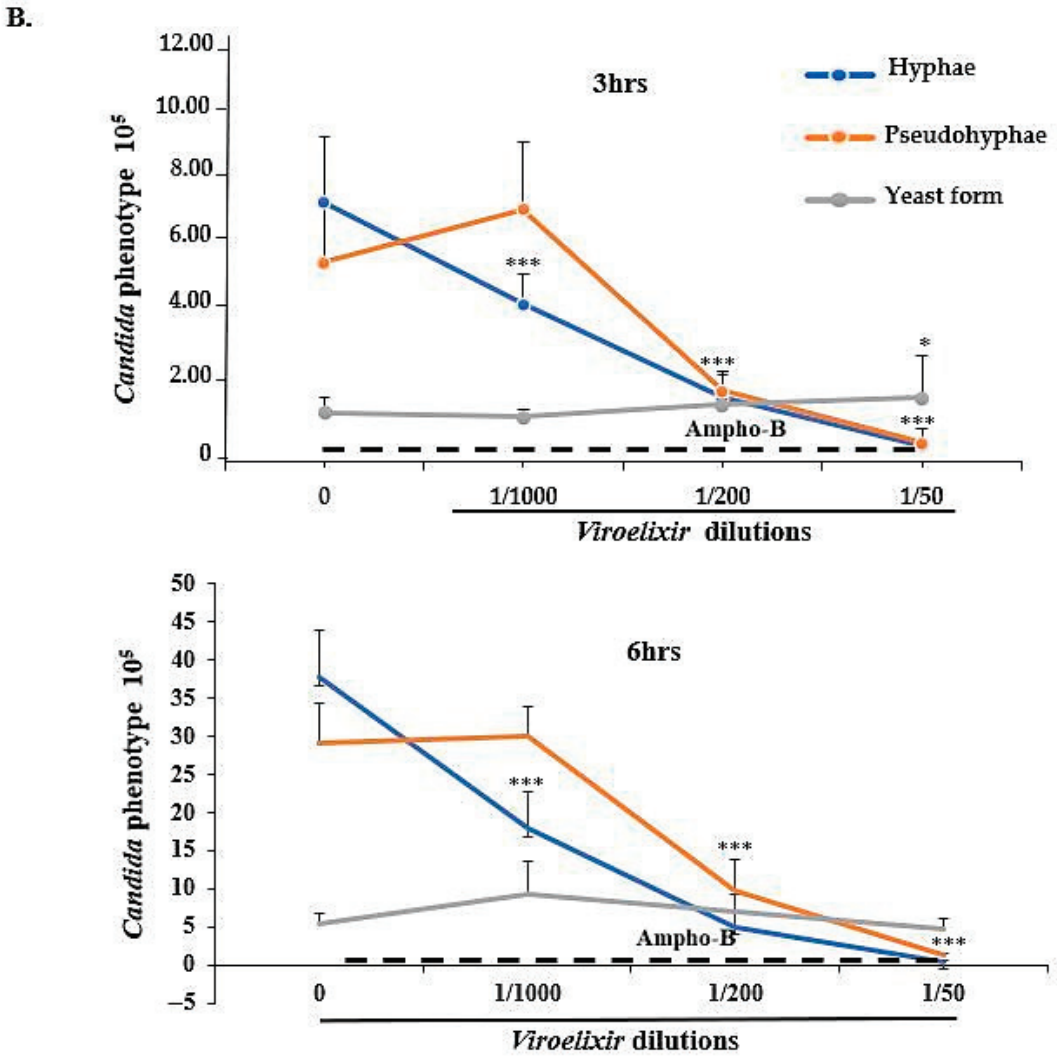

Figure 4. *Effect of Viroelixir on C. albicans morphology.* (**A**) *C. albicans* forms corresponding to yeast forms, pseudohyphae, and hyphal phenotypes were detected microscopically (n = 3). (**B**) These forms were counted (n = 3) after 3 and 6 h exposure to *Viroelixir* at 1/1000, 1/200, and 1/50 under hyphal growth conditions. *Ampho-B* (5 μg/mL) served as the positive control, and comparisons are presented against untreated controls. The dashed horizontal line represents the *Amphotericin B* (*Ampho-B*) treatment used as a reference control. All data are expressed as mean values ± SEM. * $p < 0.05$ and *** $p < 0.001$ were considered as statistically significant.

2.5. Viroelixir Induces C. albicans Dead Cells "(PI-Positive)", Possibly Through a ROS-Dependent Mechanism

Following 24 h *Viroelixir* (1/200, and 1/50 of *v*/*v* of the stock solution) and *Ampho-B* treatment, we investigated *C. albicans* dead cells and oxidative stress. Flow cytometry analysis showed a significant shift towards *C. albicans* dead cells. More specifically, the percentage of dead cells increased from 1.95 ± 0.45% in untreated *C. albicans* cultures to 88.0 ± 2.96% and 90.7 ± 5.16% in the presence of 1/50 *Viroelixir* and the positive control *Ampho-B* (5 μg/mL), respectively (Figure 5A,B). Of note, a significant change in total ROS levels was observed only following exposure to *Viroelixir* 1/50. In particular, the percentage of ROS positive cells increased more than threefold under this condition, suggesting that additional or alternative mechanisms may contribute (Figure 5C,D).

https://doi.org/10.3390/antibiotics15040420

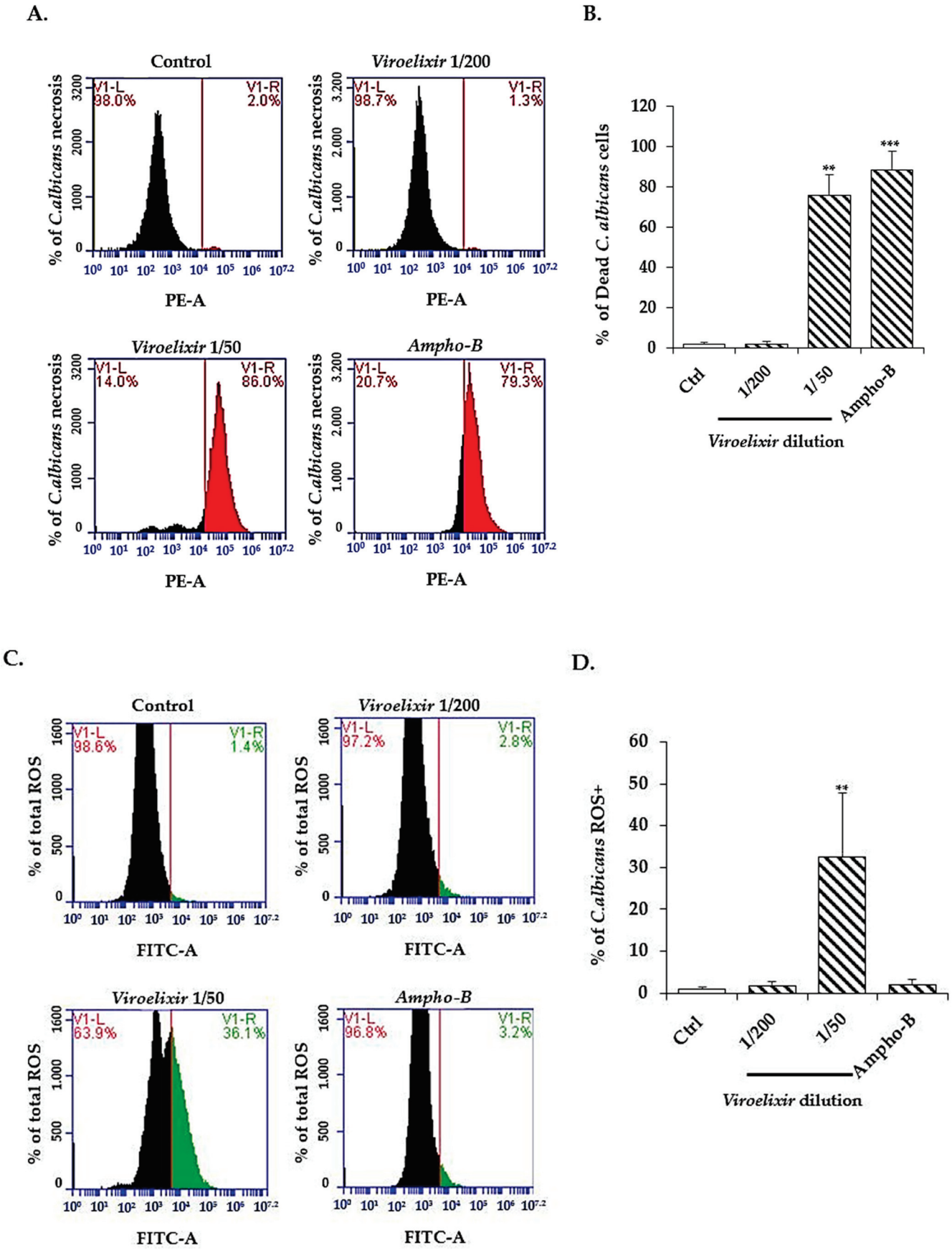

Figure 5. *Viroelixir controls C. albicans growth via necrosis/ROS pathways.* (**A**) Flow cytometry analysis of necrotic *C. albicans* using propidium iodide (PI) stain. The panels show positively marked *C. albicans*

https://doi.org/10.3390/antibiotics15040420

cells, under various treatment conditions (0, *Viroelixir* 1/200, *Viroelixir* 1/50 and *Ampho-B*) (5 µg/mL) In flow cytometry histograms, black peaks represent the total cell population, while colored regions indicate gated PI-positive cells. (**B**) Representative data presented as mean values ± SEM. (**C**) Flow cytometry panels showing total ROS production in *C. albicans* under the same conditions. Black histograms represent the total population, whereas colored regions indicate ROS-positive gated cells. (**D**) Summary of 4 independent experiments following statistical analysis. The Student's *t*-test is a statistical test used to determine whether the difference between the control group and the *Viroelixir*-treated group is statistically significant. Significance is indicated as ** $p < 0.01$, and *** $p < 0.001$.

2.6. Viroelixir Treatment Reduces the Transcript Levels of Virulence-Associated Genes

To understand the anti-virulence mechanisms of action, we evaluated *Viroelixir* impact on EAP1 adhesion protein and SAPs hydrolytic enzymes expression. To ensure that differences in mRNA levels were not due to variations in cell number, samples were normalized prior to RNA extraction using an equivalent number of cells (based on CFU/OD measurements). These enzymes are known to play a key role in adhesion, tissue invasion, and immune evasion. Our results showed that treatment with *Viroelixir* at 1/50 dilution significantly reduced the mRNA levels of EAP1 and aspartyl proteinases family (SAP1 to SAP9) by more than 2.5-fold. *Viroelixir* treatment (1/50) significantly reduced the mRNA expression levels of EAP1 and the aspartyl proteinase family (SAP1–SAP9), with expression levels ranging from 0.36 ± 0.14 (SAP1), 0.28 ± 0.11 (SAP2), 0.15 ± 0.012 (SAP3), 0.25 ± 0.089 (SAP4), 0.32 ± 0.11 (SAP5), 0.11 ± 0.05 (SAP6), 0.23 ± 0.06 (SAP7), 0.21 ± 0.10 (SAP8), and 0.065 ± 0.02 (SAP9), as well as 0.18 ± 0.07 for EAP1, compared to untreated controls (set to 1) (Figure 6).

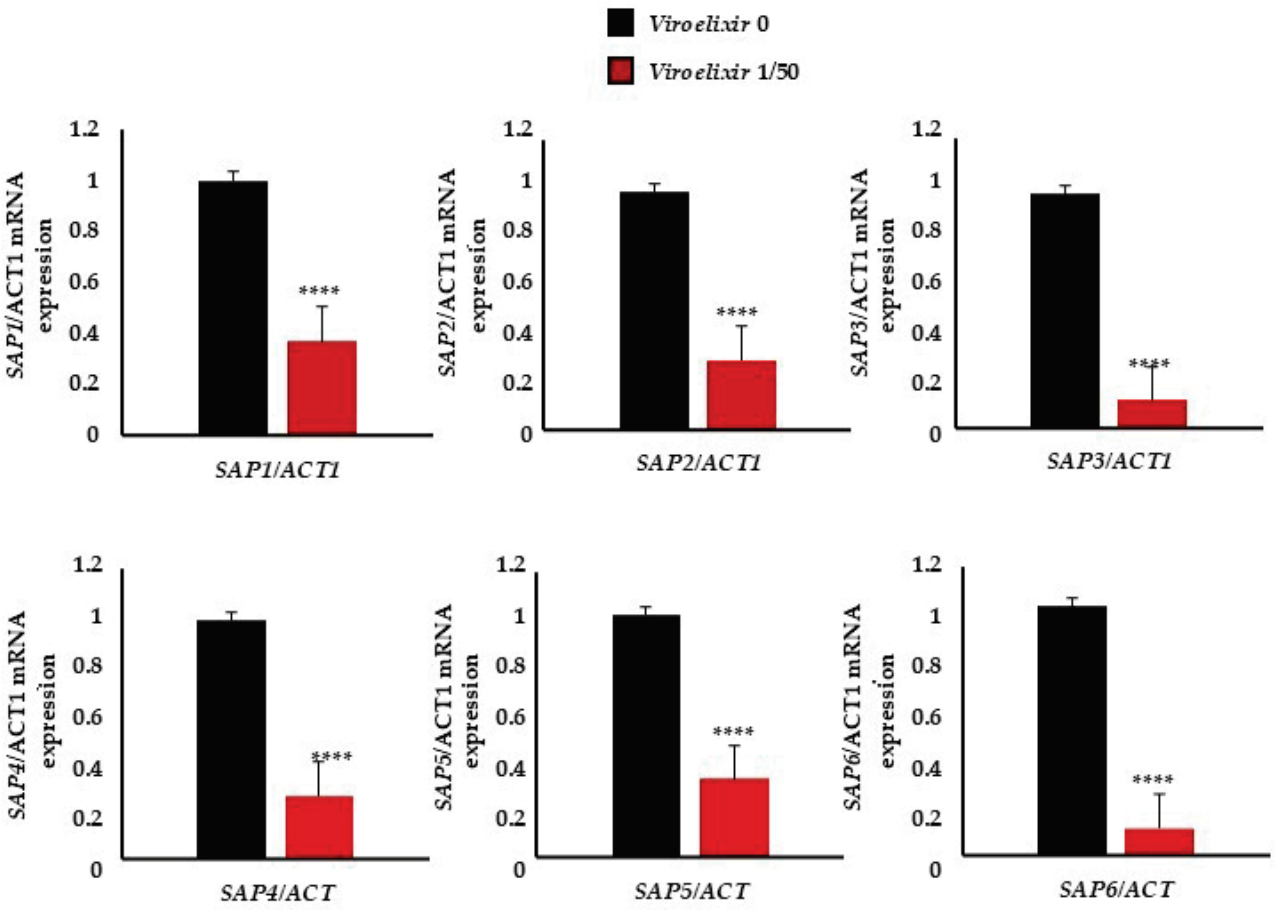

Figure 6. *Cont.*

https://doi.org/10.3390/antibiotics15040420

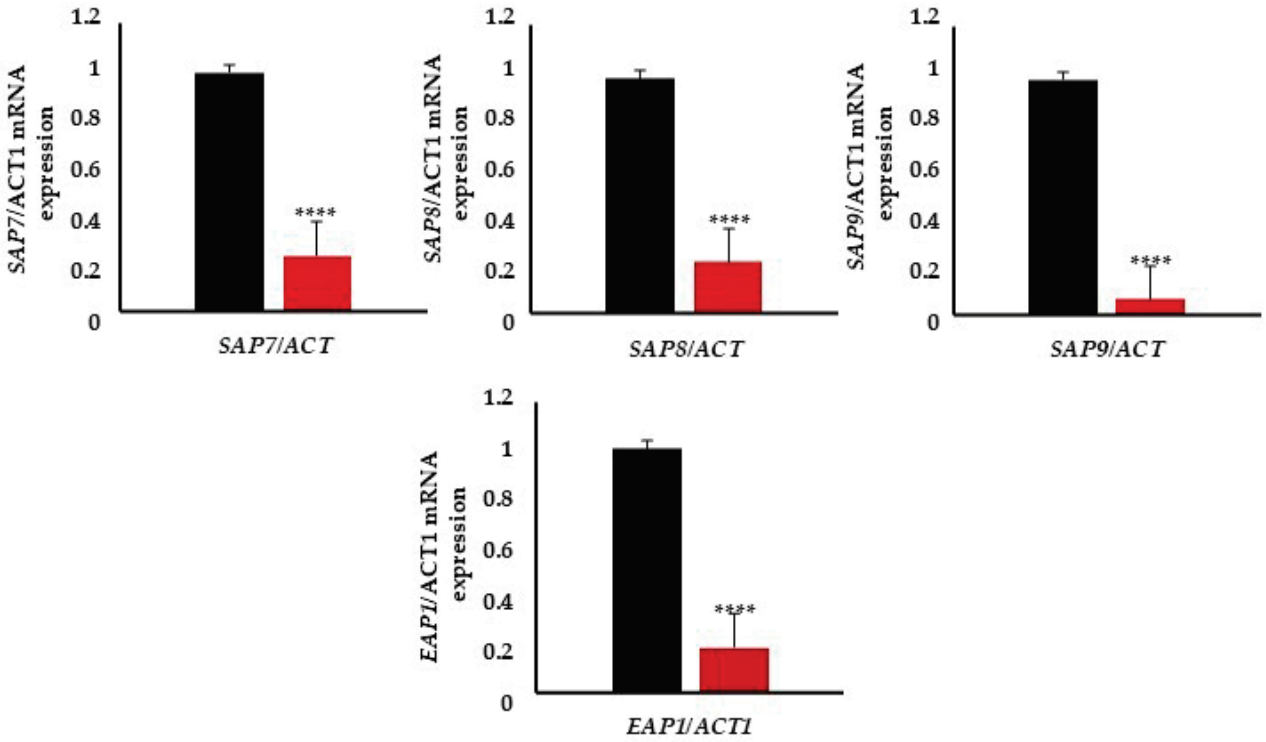

Figure 6. *Relative mRNA expression of SAP1–SAP9 and EAP1 normalized to ACT1.* Data are presented as mean ± SEM of independent experiments ($n = 3$). Statistical significance was determined using one-way ANOVA. **** $p < 0.0001$ compared to untreated control. Control (untreated) and *Viroelixir* (1/50 dilution).

2.7. Viroelixir Causes an Irreversible Damage to C. albicans Adhesion Potential

C. albicans-gingival epithelial cells co-cultures were performed to confirm the irreversible antimycotic potential of *Viroelixir*, primarily at the level of adhesion. Briefly, when *C. albicans* were pretreated with the highest concentration tested of *Viroelixir* at 1/50 for 24 h. Following the 24 h pre-treatment with *Viroelixir*, *C. albicans* cells were collected, quantified, and re-adjusted to the same cell density prior to co-culture with epithelial cells. This normalization step ensured that an equivalent number of fungal cells was used across all conditions, thereby allowing a direct evaluation of adhesion capacity independent of cell viability the adhesion capacity of the fungal cells was significantly reduced. This is evident after 24 h co-culture period where pre-treated *C. albicans* cells were not capable of adhering to the cell monolayer in a similar manner to untreated *C. albicans*. Consequently, the cytotoxicity and morphological changes in gingival epithelial cells caused by the virulent *C. albicans* form were almost completely absent, leaving the epithelial cells in a state comparable to uninfected cells. The few *C. albicans* cells that did adhere to gingival cells after *Viroelixir* pre-treatment exhibited a less virulent phenotype, primarily known as yeast forms (Figure 7). The results are presented as qualitative observations only. Importantly, under our experimental conditions, a clear and reproducible reduction in adherent *C. albicans* cells was consistently observed in the *Viroelixir*-treated group compared to untreated controls, supporting the reported trend.

https://doi.org/10.3390/antibiotics15040420

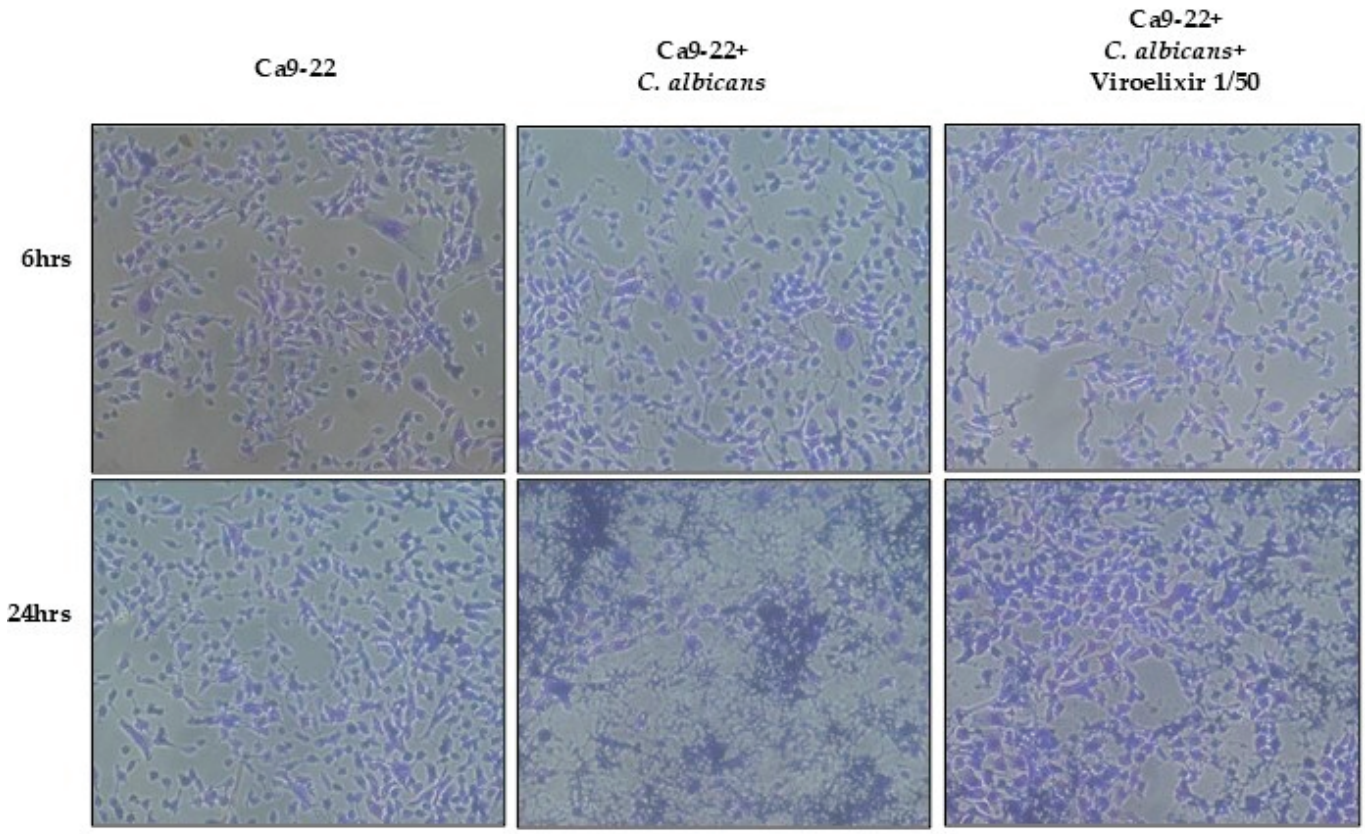

Figure 7. *Effect of Viroelixir on C. albicans adhesion potential. C. albicans* adhesion to gingival epithelial cells was assessed microscopically (n = 3) using the crystal violet staining assay. Overall, gingival epithelial cell monolayers were exposed for 6 and 24 h to *C. albicans* whether pre-treated or not with *Viroelixir* at 1/50.

2.8. Viroelixir Attenuates Epithelial Cytokine and Antimicrobial Responses

In this section, we examined the effect of *Viroelixir* pretreatment, i.e., *C. albicans* virulence attenuation, on epithelial cell defense mechanisms. To this end, *C. albicans* cells (pretreated or not with *Viroelixir*) were co-cultured with non-oncogenic human epithelial cell lines (GMSMK). To ensure that differences in mRNA levels were not due to variations in cell number, samples were normalized prior to RNA extraction using an equivalent number of cells (based on CFU/OD measurements). The ability of epithelial cells to express and secrete pro-inflammatory cytokines (such as IL-6 and IL-8), as well as antimicrobial peptides (e.g., hBD-2), was assessed by real-time PCR and ELISA. As shown in Figure 8, virulent *C. albicans* significantly induced IL-6, IL-8, and hBD-2 mRNA expression and protein secretion in GMSMK cells. In contrast, *Viroelixir* pretreatment reduced *C. albicans* virulence and adhesion potential, thereby attenuating the activation of epithelial cell defense responses. This was reflected by overall lower mRNA expression and secretion levels of pro-inflammatory cytokines (IL-6 and IL-8) and the antimicrobial peptide hBD-2 (Figure 8). Similar trends were observed for IL-1β, hBD-1, hBD-3, and hBD-4 (Figures S1–S4).

https://doi.org/10.3390/antibiotics15040420

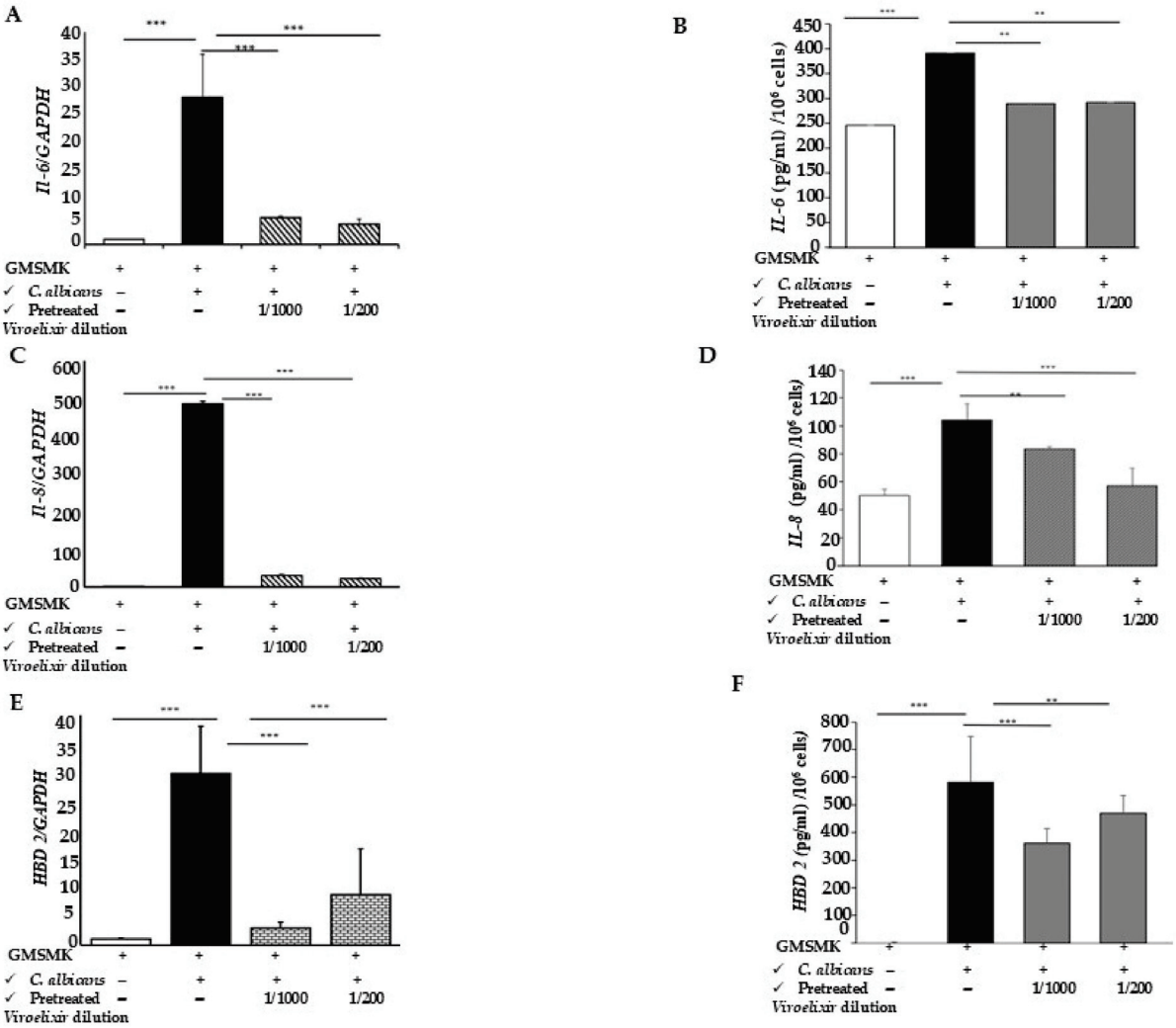

Figure 8. *Viroelixir attenuates C. albicans virulence and relieves GMSMK defense mechanisms.* (**A**) IL-6, (**C**) IL-8, and (**E**) hBD-2 mRNA expression levels in GMSMK cells following co-culture with *C. albicans*, whether pre-exposed or not to *Viroelixir* at 1/1000 and 1/200. mRNA expression was analyzed by qRT-PCR and normalized to GAPDH. (**B**) IL-6, (**D**). IL-8, and (**F**). hBD-2 protein levels in culture supernatants quantified by ELISA, in the bar charts, white bars represent GMSMK cells alone, black bars represent GMSMK cells in contact with untreated *C. albicans*, and gray bars represent GMSMK cells in contact with *Viroelixir*-treated *C. albicans* at the indicated dilutions. Data are presented as mean ± SEM. ** $p < 0.01$, and *** $p < 0.001$ are considered as statistically significant.

2.9. Pretreatment by Viroelixir Inhibits Signaling Pathways Induced by C. albicans Infection in the Oral Cavity

As shown in Figure 9A,B, TLR4 expression tended to decrease in GMSMK cells infected with *C. albicans*, regardless of whether the fungus was treated with *Viroelixir* or not, compared to non-infected cells. To ensure that differences in mRNA levels were not due to variations in cell number, samples were normalized prior to RNA extraction using an equivalent number of cells (based on CFU/OD measurements). NF-κB activation was significantly increased in GMSMK cells following infection with untreated *C. albicans* (57.83 ± 1.85%) compared to non-infected cells (34.8 ± 0.16%) (Figure 9C,D). Pre-treatment of *C. albicans* with *Viroelixir* reduced NF-κB activation in a dose-dependent manner. Specifically, infection with *C. albicans* pre-treated at 1/1000 resulted in an activation level of 53.4 ± 2.44%, while pre-treatment at 1/200 further reduced activation to 43.46 ± 2.90%.

https://doi.org/10.3390/antibiotics15040420

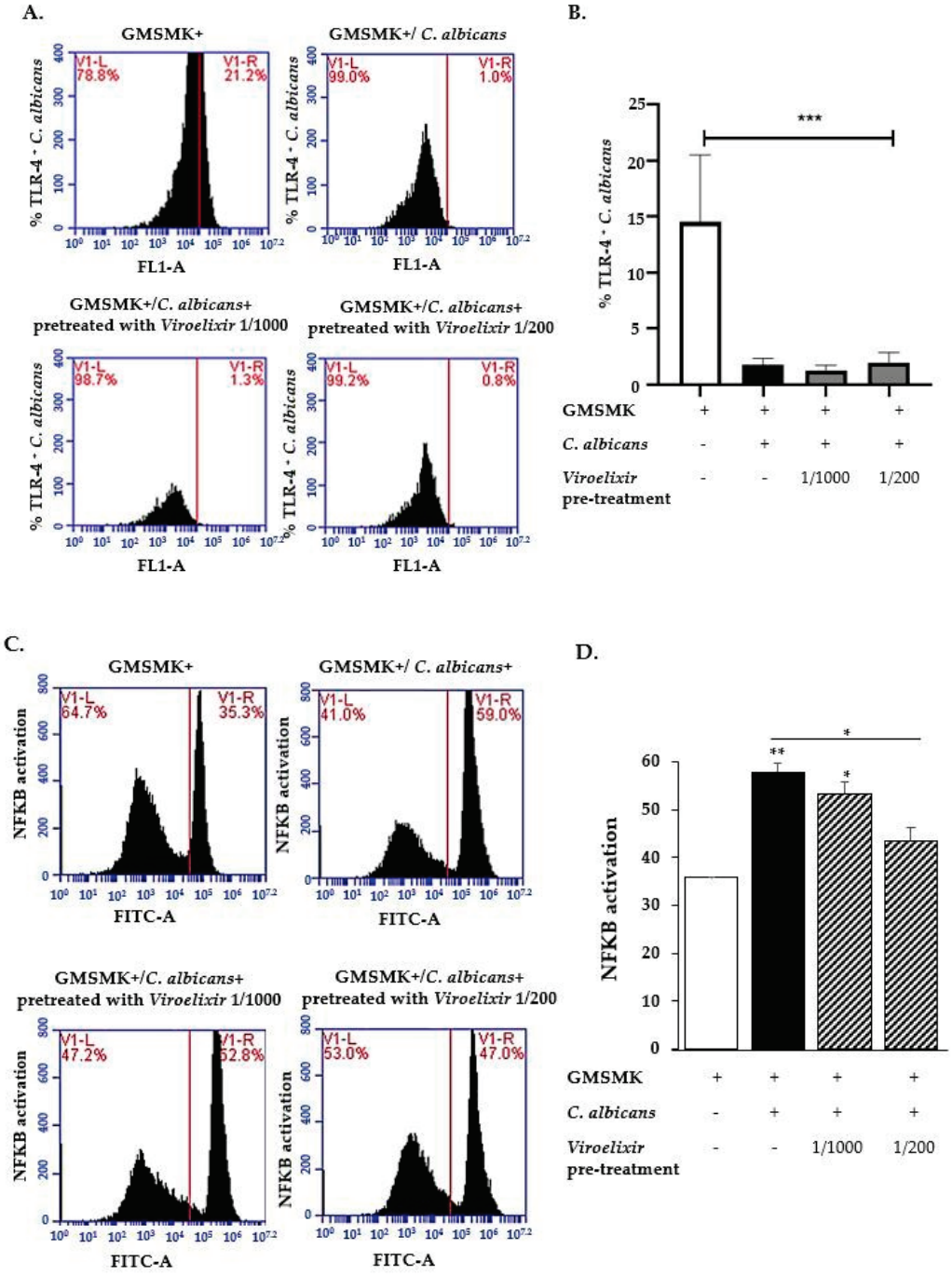

Figure 9. *Viroelixir* modulates *C. albicans* infection via the TLR4-NF-κB signaling pathway. (**A**) Flow cytometry analysis of TLR4 expression in *C. albicans*-infected GMSMK cells and *C. albicans* pretreated with different dilutions of *Viroelixir* (1/1000 and 1/200) before infection of GMSMK cells. The panels show GMSMK cells, marked for TLR4 positivity, following infection with untreated *C. albicans* and *C. albicans* pretreated with various dilutions of *Viroelixir* (1/1000 and 1/200). In the bar charts, white bars represent GMSMK cells alone, black bars represent GMSMK cells in contact with untreated *C. albicans*, and gray bars represent GMSMK cells in contact with *Viroelixir*-treated *C. albicans* at the indicated dilutions (**B**) Summary of three independent experiments. (**C**) Flow cytometry analysis of NF-κB activation in *C. albicans*-infected GMSMK cells and *C. albicans* pretreated with different dilutions of *Viroelixir* (1/1000 and 1/200) before infection of GMSMK cells. The panels show GMSMK cells, marked for p65 positivity, following infection with untreated *C. albicans* and *C. albicans* pre-treated with various dilutions of *Viroelixir* (1/1000 and 1/200). (**D**) Summary of three independent experiments. The analysis data are presented as mean values ± SEM. Statistical significance is indicated as * $p < 0.05$, ** $p < 0.05$, and *** $p < 0.005$ are considered as statistically significant.

https://doi.org/10.3390/antibiotics15040420

These reductions were statistically significant compared to cells infected with untreated *C. albicans* ($p < 0.05$), with a more pronounced decrease observed at the 1/200 dilution. Data represent the mean ± SEM of three independent experiments.

3. Discussion

The antifungal effects observed in this study are consistent with the known antimicrobial activity of catechins and ellagitannins identified in the *Viroelixir* formulation, including EGCG and punicalagin, as confirmed in our previous component analysis study.

Natural antifungal compounds derived from plant sources have been increasingly investigated as potential alternatives or complements to conventional antifungal therapies. These compounds are generally characterized by multi-target activity, relatively low toxicity, and the ability to modulate microbial virulence [42]. The present study illustrates the impact of *Viroelixir*, a novel pomegranate and green tea extract, on the growth and virulence determinants of *C. albicans*. Although both plants exhibit antimycotic potential, the introduction of the *Viroelixir* mixture is expected to provide greater benefits due to the presence of multiple active ingredients targeting diverse molecular pathways. This multi-targeted approach not only helps limit or delay the development of resistance but also exerts anti-inflammatory effects, enhancing its overall efficacy [42]. According to the literature, green tea has been demonstrated to be effective against several microbial species and tea catechins have been shown to act synergistically with *Ampho-B* and *fluconazole* against both susceptible and resistant *C. albicans* strains [43]. Overall, the protective effect of green tea polyphenols includes *C. albicans* biofilm formation and exopolysaccharide secretion. The active ingredients in tea are also known to influence the expression of surface proteins implicated in adhesion, such as hyphal wall protein 1 (HWP1) and agglutinin-like sequence 3 (ALS3) [44]. On the other hand, the antimicrobial potential of pomegranate products has been validated against a wide range of pathogenic bacterial species [45–47] as well as certain fungi [48]. take. In this regard, one study demonstrated that both crude pomegranate extract and its pure compound, punicalagin, exhibit antifungal effects against *C. albicans*, with their activity further enhanced by the supplementation of *fluconazole*, a well-known drug for the treatment of candidiasis [37], which is consistent with our findings.

After conducting the first series of experiments, we were able to confirm that *Viroelixir* was associated with reduced fungal growth and increased ROS levels. Based on previous studies with flavonoid-rich compounds, this increase in oxidative stress may contribute to fungal cell damage [49]. However, the precise mechanisms underlying this effect remain to be fully elucidated.

This mechanism could play a key role in the antifungal effects of *Viroelixir*, further corroborating its potential as an effective treatment against *C. albicans* infections. Although sugar sensing and carbon source utilization are generally considered key factors for more virulent behavior such as increased adhesion, transition to hyphae, biofilm formation, matrix polysaccharide secretion, hydrolytic enzyme activity, cell wall structural organization, oxidative stress resistance, invasion, and antifungal drug tolerance [50,51], the increase in carbohydrate levels observed after administering *Viroelixir* does not seem to potentiate virulence. This is most likely a direct result of fungal elimination, leading to reduced consumption of carbon sources. It is important to note that fungal species can adapt and proliferate under both nutrient-rich and nutrient-poor conditions, reflecting real-life situations where different glucose concentrations are available at various sites of *C. albicans* infection [51].

Having demonstrated *Viroelixir*'s impact on growth inhibition, we aimed to investigate its effect on biofilm formation, given its strong association with pathogenicity. It is important to highlight that fungal biofilm do not only protect *C. albicans* from host immune

https://doi.org/10.3390/antibiotics15040420

defenses but are also closely linked to the development of drug resistance. The increase in resistance and the need for higher drug dosages may be attributed to several factors, including a lack of effect on adhesion, enhanced drug metabolism, and drug sequestration and diffusion prevention by exopolysaccharides. In this context, *Viroelixir*'s anti-biofilm properties were evident even at higher dilutions. Based on evidence showing that biofilm initiation and *C. albicans* virulence is promoted by its morphological transition from yeast formto hyphal form; yeast morphological changes were also investigated. It is not surprising that hyphal assembly marks biofilm formation. At this level, the ability of hyphae to act as a supporting scaffold by adhering to one another and to other cell morphologies in polymicrobial biofilms is critical for maintaining architectural stability [52,53]. Hyphae also facilitate host tissue invasion through penetration and induce endocytosis. Among its various properties, this pathogenic phenotype expresses morphology-dependent adhesins, invasins, proteases, and secretes specific toxins, such as candidalysin, which is crucial for damaging host cells and contributes to the development of systemic candidiasis and mortality. The morphological switch is essential for virulence, as different *C. albicans* forms affect immune recognition differently. Hyphae stimulate lower cytokine responses and alter the availability of surface immunostimulatory ligands [54–56]. The observed reduction in hyphal formation may be associated with decreased biofilm development and invasive potential, although this relationship requires further validation in more complex biological models.

Considering these findings, investigating the impact on the adhesion step was of utmost importance, as co-culture data confirmed the inhibition of *C. albicans* attachment to epithelial cells. In this respect, *Viroelixir* treatment was associated with the downregulation of several virulence-related genes, including EAP1 and members of the SAP family, suggesting a potential impact on adhesion and pathogenicity mechanisms [57]. Although SAPs are recognized as key virulence determinants due to their role in tissue degradation and phenotypic switching, their specific involvement in the attachment process remains not fully understood. Researchers suggest that surface SAPs might function as non-enzymatic adhesins, while secreted SAPs could alter host cell surface proteins to expose proper binding ligands [58]. Importantly, SAP1 to SAP7 genes were found to be present in 31 susceptible or resistant *C. albicans* isolates [58,59], highlighting the potential advantage offered by *Viroelixir* in managing fungal infections. It seems that the effect of our extract on SAPs can be further enhanced by favoring a more neutral pH. Although *C. albicans* can adapt to a broad range of pH fluctuations [60], it has been shown that proteolytic activity in *C. albicans* isolates from 20 clinical cases across five different infection sites, including the oral cavity, was detected at a more acidic pH [61]. In another study, the optimal pH for SAP activity was found to be 2.5–4 for SAP2, 3, and 8, while the remaining SAPs were most active at pH 5–6.5 [62]. Another important observation is that SAPs are linked to severe early childhood caries [63]. This is likely due to *C. albicans*'s ability to secrete organic acids [64], which aligns with our finding that *C. albicans* cells can acidify the culture media. Despite reports indicating a complete adverse effect on environmental pH due to amino acid metabolism contributing to ammonia release, the possible role of *Viroelixir* in the management of caries cannot be neglected as *C. albicans* behavior is susceptible to change based on carbon source availability (amino acids/glucose) [65].

In the current study, *Viroelixir* influenced *C. albicans* interaction with gingival epithelial cells, supporting its role in pathogen adhesion and host-mediated defense mechanisms. During oral infections, hyphae invade by penetrating epithelial cells, which responds by producing pro-inflammatory cytokines and triggering antimicrobial peptides, particularly those of the β-defensin family (hBDs) [66]. Notably, antimicrobial peptides such as hBD-2 and hBD-3 have been shown to reduce the invasive capacity of *C. albicans* and to modulate

https://doi.org/10.3390/antibiotics15040420

host defense pathways [67]. hBDs are also essential for controlling early mucosal infections and play a critical role in the induction of innate inflammatory mediators [68–71]. Persistent infection disrupts this balance, playing a key role in the pathogenesis of various inflammatory diseases [72]. Therefore, the pro-inflammatory cytokines (IL-1β, IL-6, and IL-8) and hBDs were analyzed in oral epithelial cells following infection with *C. albicans*. While *C. albicans* infection induced increased expression of pro-inflammatory cytokines and hBDs, less virulent forms, pretreated with *Viroelixir*, were shown to alleviate this defense response. This finding is similar to the effects observed in *C. albicans* under monolaurin treatment [73]. However, conflicting evidence exists regarding the extent to which modulation of fungal virulence directly translates into reduced host inflammatory responses, suggesting that additional host-dependent factors may be involved.

Evidence highlights the critical role of TLR4-mediated signaling, primarily through NF-κB, in protecting epithelial cells from *C. albicans* infection [74,75]. Receptor activation may also induce AP-1, while virulent *C. albicans* (hyphal forms) can activate the MAPK1 and FOS pathways, facilitating tissue invasion [76]. Hyphae invade by penetrating epithelial cells, which produce cytokines via the MAPK1 pathway, and trigger β-defensins with anti-*C. albicans* activity. Compared to virulent *C. albicans*, inflammatory cytokines and antimicrobial peptides were reduced to baseline levels. Interestingly, TLR4 recognizes both virulent and non-virulent strains, with varying immune responses depending on pathogen recognition. It also recognizes heat-killed *C. albicans* due to conserved mannans [77]. In our study, we observed a decrease in surface expression of TLR4 in epithelial cells infected with *C. albicans*, whether treated with *Viroelixir* or not, compared to non-infected cells. This apparent reduction may be explained by TLR4 internalization, a well-documented mechanism that occurs upon immune stimulation [78]. After recognizing fungal components, TLR4 is internalized from the plasma membrane into intracellular compartments such as $Rab5^+$ early endosomes and $Rab7^+$ late endosomes, where it continues to activate signaling pathways, including the TRIF-dependent cascade leading to NF-κB activation [79,80]. Upon recognition of pathogen-associated molecular patterns (PAMPs), TLR4 is internalized into Rab5-positive early endosomes, where it interacts with the adaptor protein TRAM and activates the TRIF-dependent signaling cascade. This pathway leads to the production of type I interferons and the expression of IFN-induced genes, as well as sustained activation of NF-κB [81]. Our findings are consistent with this mechanism since NF-κB activation remained significant despite the observed reduction in membrane-associated TLR4. These observations are consistent with previously described mechanisms of TLR4 internalization and intracellular signaling. The maintained NF-κB activation despite reduced surface TLR4 expression may reflect ongoing signaling from internalized receptors; however, additional investigations are required to confirm this hypothesis. In addition, differences in experimental conditions, including fungal strains and in vitro models, may influence the observed effects and should be considered when interpreting these results.

This study has several limitations that should be acknowledged. In addition, pH measurements were performed using indicator strips, which provide semi-quantitative estimates and may lack precision compared to electronic pH meters. This limitation may affect the accuracy of pH-related interpretations. First, the experiments were conducted using in vitro models, which do not fully recapitulate the complexity of the oral mucosal environment. Second, although significant associations were observed between *Viroelixir* treatment and modulation of fungal virulence and host responses, the underlying molecular mechanisms were not directly investigated. Third, the use of specific cell lines may limit the generalizability of the findings to other epithelial models. Additionally, only selected signaling pathways were evaluated, and other relevant pathways may also be involved.

https://doi.org/10.3390/antibiotics15040420

Finally, further studies using advanced models, such as engineered human oral mucosa or in vivo systems, will be necessary to confirm the translational relevance of these findings.

4. Materials and Methods

4.1. C. albicans Strain and Epithelial Cell Culture

C. albicans, a major opportunistic pathogen associated with candidiasis, was used in this study (reference strain ATCC MYA-2876; ATCC, Manassas, VA, USA). *C. albicans* was grown in Sabouraud dextrose broth (Becton Dickinson, Hong Kong, China; cat. #238230) containing 5 g/L peptone, 5 g/L peptic digest of animal tissue, 2 g/L pancreatic digest, and 20 g/L dextrose. The Sabouraud liquid medium was supplemented with glucose to a final concentration of 1 mg/mL and adjusted to pH 5.6. Glucose was used as the primary carbon source to support fungal growth and metabolic activity, which are essential for biofilm formation and virulence-related processes. The human oral squamous cell carcinoma cell line Ca9-22 (RIKEN BioResource Research Center, CVCL_1102, Ibaraki, Japan) and gingival epithelial cells GMSMK (provided by Dr. Daniel Grenier, Faculty of Dentistry, Laval University, Québec City, QC, Canada) were used in this study. Ca9-22 cells were cultured in RPMI 1640 medium (Gibco, Burlington, ON, Canada; cat. #10-040-CV) supplemented with 5% fetal bovine serum (FBS) (Thermo Fisher Scientific, Burlington, ON, Canada; cat. #10099-141), 0.2% *Amphotericin B* (*Ampho-B*) (Sigma-Aldrich, Oakville, ON, Canada; cat. #A2942), and 0.2% penicillin–streptomycin (P/S) (Sigma-Aldrich, St. Louis, MO, USA; cat. #P4333). GMSMK cells were maintained in DMEM medium (Gibco, Burlington, ON, Canada; cat. #11320033) supplemented with 10% FBS, 0.2% *Ampho-B*, and 0.2% P/S. Epithelial cells were cultured at 37 °C in a humidified atmosphere containing 5% CO_2, whereas *C. albicans* cultures were incubated under standard aerobic conditions.

4.2. Viroelixir Agent Preparation

The *Viroelixir* agent, a standardized polyphenol blend derived from green tea (*Camellia sinensis* (L.) Kuntze, Theaceae) and pomegranate (*Punica granatum* L., Lythraceae), was provided by Dr. Gin Wu (Comcast, Taiwan, China). The extract was prepared by mixing green tea leaves and pomegranate peel powder (5 g each) in 100 mL of sterile water, followed by centrifugation and sterile filtration, as previously described. The preparation consisted of an aqueous extract obtained from a 1:1 mixture of green tea leaves and pomegranate peel powder. *Viroelixir* was supplied by the collaborator as a filtered liquid preparation (1 L batch). Upon receipt, the solution was aliquoted into sterile 5 mL tubes and stored at 4 °C until use. No specific batch number was assigned to this preparation. Component analysis performed in our previous study identified major bioactive constituents, including catechins (epigallocatechin gallate [EGCG] and epicatechin gallate), ellagitannins (punicalagin), ellagic acid, as well as other flavonoids and phenolic acids. The composition of the extract was previously characterized to confirm the presence of these major polyphenolic compounds, which are known for their antimicrobial, antioxidant, and anti-virulence properties. The stock solution (5% *m*/*v*) was stored at 4 °C until use.

4.3. Antifungal Agent Preparation

Amphotericin B (*Ampho-B*; Sigma-Aldrich, Oakville, ON, Canada; cat. #A2942) was used as a positive control at a final concentration of 5 μg/mL. The stock solution was prepared at a concentration of 250 μg/mL and sterile-filtered through a 0.22 μm pore-size membrane prior to use [82]. For all experiments, a working concentration of 5 μg/mL was used.

https://doi.org/10.3390/antibiotics15040420

4.4. C. albicans Growth Assay

As detailed in our previous findings [83], *C. albicans* were seeded at 2×10^4 cells per well of a 96-well plate and exposed to different dilutions of *Viroelixir* (1/1000, 1/200, and 1/50 of v/v of the stock solution). *Ampho-B* (5 μg/mL) was used as a positive control. *C. albicans* growth was assessed by reading the optical density at 660 nm over a total period of 24 h. Optical density values were automatically recorded every 2 h using an Agilent BioTek Synergy H1 microplate reader (Agilent BioTek Instruments, Winooski, VT, USA). This method ensures a quantitative and reproducible assessment of the effect of *Viroelixir* on *C. albicans* growth [84].

4.5. MTT Viability and Proliferation Assay

Cultures of *C. albicans*, initially at a density of 10^5 cells/mL, were incubated for 6 and 24 h in the presence of *Viroelixir* (1/1000, 1/200, and 1/50 of v/v of the stock solution). Cell viability and proliferation were then assessed by measuring mitochondrial activity using the 3-(4,5-dimethylthiazol-2-yl)-2,5-diphenyltetrazolium bromide (MTT) assay. For further details, MTT (Millipore, Burlington, MA, USA; Cat# C501/CT02) was added to the Sabouraud medium containing the cells at a concentration of 0.5 mg/mL and incubated for 3 at 37 °C in the dark. Subsequently, the formazan crystals formed were dissolved in isopropanol containing 0.04% hydrochloric acid, and absorbance was measured at 550 nm using a Bio-Rad reader, as previously reported [82,85]. The results are represented as percentages using the following formula: % of proliferation = (treated cells OD/untreated cells OD) × 100. Four technical replicates and four to five biological replicates were carried out.

4.6. Effect of Viroelixir on Colony Formation

C. albicans cultures containing 10^3 cells/mL were prepared in Sabouraud liquid medium. 20 μL of each condition were plated onto 60 mm diameter agar plates. Colonies were incubated at 37 °C for 24 h before being photographed and counted. The results are represented as percentages, with 100% corresponding to the number of colonies in untreated conditions [68]. Five biological replicates were carried out.

4.7. Effect of Viroelixir on Carbohydrate Content

Carbohydrate content was measured using the colorimetric method described by Dubois et al. [86]. Total sugar was quantified in the culture supernatants collected from *C. albicans* cultures after incubation under the experimental conditions. Briefly, 200 μL of supernatant was mixed with 100 μL of 5% phenol and 500 μL of H_2SO_4. The tubes were then incubated for 20 min at 30 °C, then cooled with water at 20 °C. Under the action of concentrated sulfuric acid, the hexoses and pentoses in the medium undergo dehydration to form furfural and 5-hydroxymethylfurfural derivatives, which react with phenol to form a yellowish complex. Optical density was measured at 485 nm using the Bio-Rad xMark microplate spectrophotometer (xMark™ Microplate Absorbance Spectrophotometer (Bio-Rad Laboratories, Hercules, CA, USA). Carbohydrate concentrations were determined using a glucose standard curve and expressed as glucose equivalents (mg/mL). Three technical replicates and three biological replicates were carried out.

4.8. Measurement of Environmental pH

To evaluate the effect of *Viroelixir* on environmental pH, *C. albicans* biofilms were formed in the presence of various dilutions of this natural product (1/1000, 1/200, and 1/50 of v/v of the stock solution). Given that the pH of *Viroelixir* is 2.45, while that of *Ampho-B* (5 μg/mL) is 5.43, the overall change in the pH of Sabouraud culture medium

https://doi.org/10.3390/antibiotics15040420

(pH = 5.6) was recorded after 24 h. The pH was measured using pH indicator strips (MColorpHast^{TM} pH-indicator strips, universal indicator (pH 0–14), Millipore, Burlington, MA, USA; Cat# 1.09535.0001). Three technical replicates and three biological replicates were performed.

4.9. Crystal Violet Assay

It should be noted that biomass quantification reflects total attached biomass and does not directly correspond to viable cell counts (CFU). In addition, *C. albicans* at a concentration of 10^6 cells/mL were exposed to different dilutions of *Viroelixir* for 6 and 24 h. The staining procedure involved discarding the culture medium, fixing the cells with 200 µL of cold methanol for 10 min, rinsing with PBS, and staining with a 1% crystal violet solution (Sigma-Aldrich, 548-62-9). The stained cells were then washed thoroughly with PBS to remove any excess dye. Afterward, the samples were left to air dry for 24 h before adding 400 µL of pure glacial acetic acid to dissolve the stain. Absorbance readings were recorded at 570 nm using a Bio-Rad xMark microplate spectrophotometer (Bio-Rad Laboratories, Hercules, CA, USA). All experiments were performed in at least three independents technical replicates and four biological replicates were carried out.

4.10. Biofilm Formation and Scanning Electron Microscopy

As per our previous study [85], *C. albicans* cells were seeded on a porous collagen scaffold to promote biofilm formation while maintaining structural integrity. Briefly, 5 mm × 5 mm samples of porous collagen scaffold (CollaTape®, Zimmer Dental Inc., Carlsbad, CA, USA) were placed in 24-well plates. The scaffolds were rinsed twice with culture medium and inoculated with *C. albicans* (10^5 cells), followed by incubation for 60 min at 30 °C without shaking to allow initial adhesion.

Fresh Sabouraud medium was then added in the presence or absence of different dilutions of *Viroelixir* (0, 1/200, and 1/50). Two control conditions were included: untreated *C. albicans* as a negative control and cells treated with *Ampho-B* (5 µg/mL) as a positive control.

The *C. albicans*-seeded scaffolds were incubated at 30 °C for 6 days to allow biofilm development. Incubation at 30 °C was selected to promote optimal biofilm formation and maturation, as commonly described in in vitro models. The culture medium containing *Viroelixir,* or *Ampho-B* was renewed every 48 h to maintain consistent treatment conditions.

After the 6-day incubation period, biofilms were fixed with 4% (*v*/*v*) paraformaldehyde overnight at room temperature. Samples were then washed with phosphate-buffered saline (PBS) and processed for scanning electron microscopy (SEM) analysis by a specialized imaging facility using standard preparation procedures, including dehydration, drying, and sputter-coating before imaging.

All experiments were performed in at least three independent experiments, each conducted in triplicate.

4.11. Effect of Viroelixir on C. albicans Transition

C. albicans were grown in 6-well plates at 10^6 cells per mL and exposed to varying dilutions of *Viroelixir*. Negative controls consisted of *C. albicans* cultures without Viroelixir, while positive controls corresponded to *Ampho-B* (5 µg/mL) supplementation. 10% FBS (Thermo Fisher, Burlington, ON, Canada, cat #10 099-141) was added, and the cells were incubated at 37 °C for 3 and 6 "h" to induce phenotypic transition from yeast to hyphal form. At the end of each incubation period, images were captured using a Nikon Eclipse TS100 microscope at 20× magnification. Trypan blue was used to facilitate the counting of *C. albicans* phenotypes (hyphae, pseudohyphae, and yeast forms). All experiments were performed in at least three independent experiments, each conducted in triplicate.

https://doi.org/10.3390/antibiotics15040420

4.12. Cell Viability Analysis by Propidium Iodide (PI) Staining

Cell death was evaluated using Propidium Iodide (PI) stainingKit (BioLegend, San Diego, CA, USA). Briefly, after 24 h of treatment with Viroelixir (1/200 and 1/50 dilutions) or *Ampho-B* (5 µg/mL) (positive control), *C. albicans* cells (10^7 cells/mL) were centrifuged at 500× *g* for 5 min and washed with sterile PBS. The cell pellets were then stained with 10 µL PI after being resuspended in 100 µL PBS. Following 15 min incubation at room temperature in the dark, 400 µL of assay buffer was added to each tube, and flow cytometry analysis was performed using the BD Accuri C6 Plus Flow Cytometer (BD Biosciences, San Jose, CA, USA). A total of 50,000 events per sample were collected and classified as necrotic cells (PI+). All experiments were performed in at least three independent experiments, each conducted in triplicate.

4.13. Reactive Oxygen Species (ROS) Analysis by Flow Cytometry

Oxidative stress in *C. albicans* was assessed by flow cytometry using a total ROS detection kit (ImmunoChemistry Technologies, Burlington, ON, Canada), according to the manufacturer's instructions. Briefly, after 24 h of treatment with *Viroelixir* (1/200 and 1/50 dilutions of *v*/*v* of the stock solution) or *Ampho-B* (5 µg/mL) (positive control), *C. albicans* cells (10^7 cells/mL) were centrifuged at 500× *g* for 5 min and washed with sterile PBS. The cells were then labeled with 10 µL ROS detection reagent (previously reconstituted in DMSO and diluted in assay buffer) after being resuspended in a total volume of 490 µL assay buffer. After incubation in the dark at 30 °C for 1 h, ROS levels were measured using a green fluorescent ROS-sensitive probe (excitation/emission ~488 nm) and analyzed using a BD Accuri™ C6 Plus Flow Cytometer (BD Biosciences, San Jose, CA, USA). All experiments were performed in at least three independent experiments, each conducted in triplicate.

4.14. Reverse Transcription and Polymerase Chain Reaction

C. albicans (10^7 cells) were either stimulated or not with 1/50 of *v*/*v* of the stock solution of *Viroelixir* for 24 h. Briefly, the samples were centrifuged for 10 min at 15,000 RPM. After centrifugation, 350 µL of Qiagen lysis buffer (Qiagen, Hilden, Germany, cat # 160035113) supplemented with 7 µL of ß-mercaptoethanol (Sigma-Aldrich, St. Louis, MO, USA, cat # 1003664856) was added to the pellets, along with 200 µL of magnetic beads. To promote membrane lysis, the samples were vigorously vortexed and exposed to a Biospec Products mini bead beater machine (Biospec Products, Bartlesville, OK, USA). Total RNA was extracted using the RNeasy Plus Mini Kit (Qiagen, Hilden, Germany, cat # 74104) according to the manufacturer's instructions. The RNA quantity and quality were evaluated using the Nanodrop 8000 spectrophotometer (Thermo Fisher Scientific, Waltham, MA, USA). Subsequently, 2 µg of total RNA were reverse transcribed into cDNA using the iScript™ cDNA Synthesis Kit (Bio-Rad, Hercules, CA, USA, cat # 1708841) and the Bio-Rad MyCycler thermal cycler (Bio-Rad, Hercules, CA, USA). Gene expression profiles of SAP family members, the EAP1 adhesion gene, pro-inflammatory cytokines, and human β-defensins (hBD-1 to hBD-4) were evaluated by real-time PCR using gene-specific primers (Tables 1 and 2) with the iTaq™ Universal SYBR® Green Supermix (Bio-Rad Laboratories, Hercules, CA, USA; cat. #1725124). ACT1 and GAPDH were used as housekeeping genes for fungal and human cells, respectively. Relative gene expression levels were calculated using the $2^{-\Delta\Delta Ct}$ method. Three technical replicates and four biological replicates were performed.

https://doi.org/10.3390/antibiotics15040420

Table 1. Primers sequences corresponding to the SAPs family, EAP1 and ACT1 fungal genes.

C. albicans Genes	Primer Sequence	Amp Size (bp)
EAP1	5′-CTGCTCACTCAACTTCAATTGTCG-3′ 3′-GAACACATCCACCTTCGGGA-5′	51
SAP1	5′-TTTCATCGCTCTTGCTATTGCTT-3′ 3′TGACATCAAAGTCTAAAGTGACAAAACC-5′	86
SAP2	5′-TCCTGATGTTAATGTTGATTGTCAAG-3′ 3′-TGGATCATATGTCCCCTTTTGTT-5′	82
SAP3	5′GGACCAGTAACATTTTTATGAGTTTTGAT-3′ 3′-TGCTACTCCAACAACTTTCAACAAT-5′	87
SAP4	5′-AGATATTGAGCCCACAGAAATTCC-3′ 3′-CAATTTAACTGCAACAGGTCCTCTT-5′	81
SAP5	5′-CATTGTGCAAAGTAACTGCAACAG-3′ 3′-CAGAATTTCCCGTCGATGAGA-5′	77
SAP6	5′-CCTTTATGAGCACTAGTAGACCAAACG-3′ 3′-TTACGCAAAAGGTAACTTGTATCAAGA-5′	101
SAP7	5′-GAAATGCAAAGAGTATTAGAGTTATTAC 3′GAATGATTTGGTTTACATCATCTTCAACTG-5′	196
SAP8	5′-TCCCTGAAGACATTGATAAAAGAGC-3′ 3′-AGAATCAACCACCCATAAATCAGAA-5′	278
SAP9	5′-ATTTACTCCACAGTTTATCACTGAAGGT-3′ 3′-CCACAAGAACCACCCTCAGTT-5′	86
ACT1	5′-GCTGGTAGAGACTTGACCAACCA-3′ 3′-GACAATTTCTCTTTCAGCACTAGTAGTGA-5′	87

Table 2. Primers sequences used for qRT-PCR to evaluate the expression of pro- inflammatory cytokines and β-defensin genes in human gingival epithelial cells.

Human Genes	Primer Sequence	Amp Size (bp)
IL-1β	5′-CTGTCCTGCGTGTTGAAAGA-3′ 3′-TTGGGTAATTTTTGGGATCTACA-5′	69
IL-6	5′-TCTCCACAAGCGCCTTCG-3′ 3′-CTCAGGGCTGAGATGCCG-5′	203
IL-8	5′-TTGGCAGCCTTCCTGATT-3′ 3′-AACTTCTCCACAACCCTCTG-5′	248
hBD-1	5′-GCCTCTCCCCAGTTCCTGAA-3′ 3′-GCAGAGAGTAAACAGCAGAAGGTA-5′	82
hBD-2	5′-TGTGGTCTCCCTGGAACAAAAT-3′ 3′-GTCGCACGTCTCTGATGAGG-5′	105
hBD-3	5′-CTTCTGTTTGCTTTGCTCTTCCT-3′ 3′-CTGTTCCTCCTTTGGAAGGCA-5′	138
hBD-4	5′-CACTCTACCAACACGCACCTAG-3′ 3′-CGCAACTGGAACCACACACT-5′	133
GAPDH	5′-GGTATCGTCGAAGGACTCATGAC-3′ 3′-ATGCCAGTGAGCTTCCCGTTCAGC-5′	180

https://doi.org/10.3390/antibiotics15040420

4.15. Adhesion of C. albicans to Gingival Epithelial Cells

C. albicans cells were either pretreated or not with *Viroelixir* at a dilution of 1/50 for 24 h prior to co-culture. Subsequently, 2×10^6 fungal cells were added to 6-well plates containing 5×10^5 Ca9-22 epithelial cells per well. Ca9-22 cells were seeded 24 h prior to infection in antibiotic- and antifungal-free medium. After 6 and 24 h of co-culture, cells were washed three times with phosphate-buffered saline (PBS) to remove non-adherent *C. albicans*, and adherent cells were stained with crystal violet as previously described. Images were acquired using a Nikon Eclipse TS100 optical microscope at 20× magnification. A higher *Viroelixir* concentration (1/50) was selected for this assay to ensure a measurable effect on fungal adhesion to epithelial cells. All experiments were performed in at least four independent biological replicates, each conducted in triplicate.

4.16. ELISA Assay

A total of 3×10^5 GMSMK cells were seeded in 6-well plates and co-cultured with 2×10^5 *C. albicans* cells, pretreated or not with *Viroelixir* at dilutions of 1/1000 and 1/200 (*v*/*v* of the stock solution), for 24 h. Lower *Viroelixir* concentrations (1/1000 and 1/200) were selected in this assay to allow detection of subtle changes in host inflammatory responses without excessive perturbation of epithelial cells. Following co-culture, supernatants were collected, and pro-inflammatory cytokines and antimicrobial peptides were quantified using Thermo Fisher ELISA kits according to the manufacturer's instructions: IL-6 (Cat# 88-7068-88), IL-8 (Cat# 88-8086-88), and hBD-2 (Cat# EK-072-37). Protein levels were normalized to 10^6 cells. All experiments were performed in at least five independent biological replicates, each conducted in triplicate.

4.17. Signaling Pathways Study by Flow Cytometry

GMSMK cells (3×10^5) were seeded in a 6-well plate with DMEM medium (Gibco, Thermo Fisher Scientific, Waltham, MA, USA; Cat# 11320033) supplemented with 10% FBS. After 24 h of adhesion, cells were serum-starved for 12 h. GMSMK cells were then incubated with 2×10^5 *C. albicans* cells, pretreated for 24 h with varying dilutions of *Viroelixir* (1/1000 and 1/200 of *v*/*v* of the stock solution) or untreated *C. albicans*, at 37 °C in a 5% CO_2 incubator for 60 min. After incubation, GMSMK cells were washed three times with PBS (1×) to remove *C. albicans* and were examined using a phase contrast microscope. Photographs were acquired using an epifluorescence light microscope (Axiophot, Zeiss, Oberkochen, Germany). Flow cytometric analysis was performed using an Accuri™ C6 flow cytometer (Becton Dickinson, Franklin Lakes, NJ, USA). A minimum of 10,000 cells per sample were collected and analyzed. After washing with PBS containing 2% FBS, GMSMK cells were labeled with 5 µL of CD284 (TLR4) monoclonal antibody (HTA125), Alexa Fluor™ 488 (eBioscience™, San Diego, CA, USA, Cat# 53-9917-42) and incubated at room temperature in the dark for 60 min in PBS with 2% FBS. For NF-κB measurement, cells were fixed with 10% formaldehyde at room temperature for 20 min, centrifuged at 500× *g* for 5 min, and washed twice with PBS containing 2% FBS. Fixed cells were resuspended in 90% methanol and incubated at 4 °C for 20 min. Cells were then incubated with NF-κB p65 (F-6) monoclonal antibody (1:200) (Santa Cruz Biotechnology, Dallas, TX, USA, Cat# sc-8008) for 60 min at room temperature. After washing, cells were incubated in the dark with the secondary antibody Anti-Mouse IgG (H + L), $F(ab')_2$ Fragment (Alexa Fluor® 488 Conjugate) (eBioscience™, San Diego, CA, USA, Cat# 53-9890-42) (1:200) for 30 min in PBS + 2% FBS. Following the immunoreaction, cells were resuspended in PBS + 2% FBS, and fluorescence intensities of FITC were measured by flow cytometry. All experiments were performed in at least three independent experiments, each conducted in triplicate.

https://doi.org/10.3390/antibiotics15040420

4.18. Statistical Analysis

All experiments were repeated at least three times, with experimental values presented as mean ± SEM. Differences between the controls and treatment conditions were determined using the one-way ANOVA or the two-way ANOVA tests. GraphPad PRISM 9.4.0 software was used for this purpose. PCR data were analyzed using the $2^{-\Delta\Delta Ct}$ relative expression method (Livak). Values * $p < 0.05$, ** $p < 0.01$, and *** $p < 0.001$ were considered statistically significant.

5. Conclusions

This study highlights that *Viroelixir* is associated with reduced *C. albicans* growth and modulation of several virulence-related traits, including biofilm formation, hyphal transition, and adhesion capacity. These changes were accompanied by alterations in host inflammatory responses, particularly in NF-κB activation and cytokine production in gingival epithelial cells.

The findings suggest that *Viroelixir* may influence host–pathogen interactions by modulating fungal behavior and the epithelial immune response. However, the underlying molecular mechanisms remain to be fully elucidated.

Overall, these results support the potential of natural antifungal compounds as complementary approaches for managing fungal infections. Further investigations using advanced models, including engineered oral mucosa or vivo systems, are required to confirm the translational relevance of these observations.

Supplementary Materials: The following supporting information can be downloaded at: https://www.mdpi.com/article/10.3390/antibiotics15040420/s1, Figures S1–S4. (A) IL-1 expression at mRNA level after stimulation with *Viroelixir*, (B) hBD-1 expression. (C) hBD-3 and (D) hBD-4 *mRNA* expression levels in GMSMK cells following co-culture with *C. albicans* whether pre-exposed or not to Viroelixir at 1/1000 and 1/200. mRNA expression was analyzed by qRT-PCR and normalized to GAPDH. Data are presented as mean ± SEM. ** $p < 0.001$, and *** $p < 0.0001$ are considered as statistically significant.

Author Contributions: M.D. conducted all core experiments and wrote the first draft of the manuscript. Y.E. assisted in experimental work. H.I. followed up on students' progress and took the responsibility of editing the manuscript. L.K. provided *Viroelixir* and edited the final version of the manuscript, M.H.A. performed data analysis, and M.R. revised the manuscript and supervised the project. A.S. was responsible for paper conceptualization and students' supervision. All authors have read and agreed to the published version of the manuscript.

Funding: This research received no external funding.

Institutional Review Board Statement: Not applicable.

Informed Consent Statement: Not applicable.

Data Availability Statement: All data generated or analyzed during this study are included in this published article.

Acknowledgments: The authors extend their appreciation to the Ongoing Research Funding Program (ORF-2026-191), King Saud University, Riyadh, Saudi Arabia.

Conflicts of Interest: The authors declare no conflicts of interest.

Abbreviations

C. albicans	*Candida albicans*
Ampho-B	*Amphotericin B*
OD	Optical Density

https://doi.org/10.3390/antibiotics15040420

ELISA	Enzyme-Linked Immunosorbent Assay
EAP1	Epithelial Adhesin Protein 1
GMSMK	Gingival Stromal Mesenchymal Cells
hBD	Human Beta-Defensin
IC50	Half Maximal Inhibitory Concentration
MIC	Minimum inhibitory concentration
MTT	3-(4,5-Dimethylthiazol-2-yl)-2,5-Diphenyltetrazolium Bromide
NF-κB	Nuclear Factor Kappa-Light-Chain-Enhancer of Activated B Cells
PKC	Protein Kinase C
ROS	Reactive Oxygen Species
RT-PCR	Reverse Transcription Polymerase Chain Reaction
SAP	Secreted Aspartyl Protease
TLR	Toll-Like Receptor
TNF-α	Tumor Necrosis Factor Alpha
HWP1	Hyphal Wall Protein 1
p38 MAPK	p38 Mitogen-Activated Protein Kinases
JNK	c-Jun N-terminal Kinase
IL-6, IL-8, IL-1β	Interleukin-6, Interleukin-8, Interleukin-1 Beta
RPMI	Roswell Park Memorial Institute Medium
DMSO	Dimethyl Sulfoxide
FBS	Fetal Bovine Serum
SEM	Scanning Electron Microscopy
PBS	Phosphate-Buffered Saline
DMEM	Dulbecco's Modified Eagle Medium
FITC	Fluorescein Isothiocyanate
RNA	Ribonucleic Acid
DNA	Deoxyribonucleic Acid
cDNA	Complementary DNA
PCR	Polymerase Chain Reaction
Ct	Cycle Threshold
bp	Base Pair
PI	Propidium Iodide
MEC	Minimal effective concentration

References

1. Pathak, J.L.; Yan, Y.; Zhang, Q.; Wang, L.; Ge, L. The Role of Oral Microbiome in Respiratory Health and Diseases. *Respir. Med.* **2021**, *185*, 106475. [CrossRef]
2. Brown, G.D.; Denning, D.W.; Gow, N.A.R.; Levitz, S.M.; Netea, M.G.; White, T.C. Hidden Killers: Human Fungal Infections. *Sci. Transl. Med.* **2012**, *4*, 165rv13. [CrossRef]
3. Bongomin, F.; Gago, S.; Oladele, R.O.; Denning, D.W. Global and Multi-National Prevalence of Fungal Diseases-Estimate Precision. *J. Fungi* **2017**, *3*, 57. [CrossRef] [PubMed]
4. Brandt, M.E. Candida and Candidiasis. *Emerg. Infect. Dis.* **2002**, *8*, 876. [CrossRef]
5. Williams, D.; Lewis, M. Pathogenesis and Treatment of Oral Candidosis. *J. Oral Microbiol.* **2011**, *3*, 5771. [CrossRef] [PubMed]
6. Lopes, J.P.; Lionakis, M.S. Pathogenesis and Virulence of *Candida albicans*. *Virulence* **2022**, *13*, 89–121. [CrossRef]
7. Mayer, F.L.; Wilson, D.; Hube, B. *Candida albicans* Pathogenicity Mechanisms. *Virulence* **2013**, *4*, 119–128. [CrossRef]
8. Ramirez-Garcia, A.; Rementeria, A.; Aguirre-Urizar, J.M.; Moragues, M.D.; Antoran, A.; Pellon, A.; Abad-Diaz-de-Cerio, A.; Hernando, F.L. *Candida albicans* and Cancer: Can This Yeast Induce Cancer Development or Progression? *Crit. Rev. Microbiol.* **2016**, *42*, 181–193. [CrossRef]
9. Allavena, P.; Garlanda, C.; Borrello, M.G.; Sica, A.; Mantovani, A. Pathways Connecting Inflammation and Cancer. *Curr. Opin. Genet. Dev.* **2008**, *18*, 3–10. [CrossRef]
10. Tuominen, H.; Rautava, J. Oral Microbiota and Cancer Development. *Pathobiology* **2020**, *88*, 116–126. [CrossRef]

https://doi.org/10.3390/antibiotics15040420

11. Hsia, C.C.; Sun, T.T.; Wang, Y.Y.; Anderson, L.M.; Armstrong, D.; Good, R.A. Enhancement of Formation of the Esophageal Carcinogen Benzylmethylnitrosamine from Its Precursors by *Candida albicans*. *Proc. Natl. Acad. Sci. USA* **1981**, *78*, 1878–1881. [CrossRef] [PubMed]
12. Tasso, C.O.; Ferrisse, T.M.; de Oliveira, A.B.; Ribas, B.R.; Jorge, J.H. Candida Species as Potential Risk Factors for Oral Squamous Cell Carcinoma: Systematic Review and Meta-Analysis. *Cancer Epidemiol.* **2023**, *86*, 102451. [CrossRef] [PubMed]
13. Bakri, M.M.; Rich, A.M.; Cannon, R.D.; Holmes, A.R. In Vitro Expression of *Candida albicans* Alcohol Dehydrogenase Genes Involved in Acetaldehyde Metabolism. *Mol. Oral Microbiol.* **2015**, *30*, 27–38. [CrossRef]
14. Reddy, M.G.S.; Kakodkar, P.; Nayanar, G. Capacity of Candida Species to Produce Acetaldehyde at Various Concentrations of Alcohol. *J. Oral Maxillofac. Pathol.* **2022**, *26*, 161–165. [CrossRef]
15. Martins, N.; Ferreira, I.C.F.R.; Barros, L.; Silva, S.; Henriques, M. Candidiasis: Predisposing Factors, Prevention, Diagnosis and Alternative Treatment. *Mycopathologia* **2014**, *177*, 223–240. [CrossRef]
16. Ponde, N.O.; Lortal, L.; Ramage, G.; Naglik, J.R.; Richardson, J.P. *Candida albicans* Biofilms and Polymicrobial Interactions. *Crit. Rev. Microbiol.* **2021**, *47*, 91–111. [CrossRef]
17. Li, F.; Palecek, S.P. EAP1, a *Candida albicans* Gene Involved in Binding Human Epithelial Cells. *Eukaryot. Cell* **2003**, *2*, 1266–1273. [CrossRef]
18. Naglik, J.R.; Challacombe, S.J.; Hube, B. *Candida albicans* Secreted Aspartyl Proteinases in Virulence and Pathogenesis. *Microbiol. Mol. Biol. Rev.* **2003**, *67*, 400–428. [CrossRef]
19. Kiyoura, Y.; Tamai, R. Innate Immunity to *Candida albicans*. *Jpn. Dent. Sci. Rev.* **2015**, *51*, 59–64. [CrossRef]
20. Willment, J.A.; Brown, G.D. C-Type Lectin Receptors in Antifungal Immunity. *Trends Microbiol.* **2008**, *16*, 27–32. [CrossRef] [PubMed]
21. Weindl, G.; Wagener, J.; Schaller, M. Epithelial Cells and Innate Antifungal Defense. *J. Dent. Res.* **2010**, *89*, 666–675. [CrossRef]
22. Joly, S.; Maze, C.; McCray, P.B.; Guthmiller, J.M. Human Beta-Defensins 2 and 3 Demonstrate Strain-Selective Activity against Oral Microorganisms. *J. Clin. Microbiol.* **2004**, *42*, 1024–1029. [CrossRef]
23. Vylkova, S.; Nayyar, N.; Li, W.; Edgerton, M. Human Beta-Defensins Kill *Candida albicans* in an Energy-Dependent and Salt-Sensitive Manner without Causing Membrane Disruption. *Antimicrob. Agents Chemother.* **2007**, *51*, 154–161. [CrossRef]
24. Deva, R.; Shankaranarayanan, P.; Ciccoli, R.; Nigam, S. *Candida albicans* Induces Selectively Transcriptional Activation of Cyclooxygenase-2 in HeLa Cells: Pivotal Roles of Toll-like Receptors, P38 Mitogen-Activated Protein Kinase, and NF-Kappa B. *J. Immunol.* **2003**, *171*, 3047–3055. [CrossRef] [PubMed]
25. Lanternier, F.; Lortholary, O. Liposomal Amphotericin B: What Is Its Role in 2008? *Clin. Microbiol. Infect.* **2008**, *14*, 71–83. [CrossRef] [PubMed]
26. Gonzalez-Jimenez, I.; Perlin, D.S.; Shor, E. Reactive Oxidant Species Induced by Antifungal Drugs: Identity, Origins, Functions, and Connection to Stress-Induced Cell Death. *Front. Cell. Infect. Microbiol.* **2023**, *13*, 1276406. [CrossRef] [PubMed]
27. Kyriakidis, I.; Tragiannidis, A.; Munchen, S.; Groll, A.H. Clinical Hepatotoxicity Associated with Antifungal Agents. *Expert Opin. Drug Saf.* **2017**, *16*, 149–165. [CrossRef]
28. Semlali, A.; Leung, K.P.; Curt, S.; Rouabhia, M. Antimicrobial Decapeptide KSL-W Attenuates *Candida albicans* Virulence by Modulating Its Effects on Toll-like Receptor, Human β-Defensin, and Cytokine Expression by Engineered Human Oral Mucosa. *Peptides* **2011**, *32*, 859–867. [CrossRef]
29. Minghetti, P.; Franzè, S.; Zaccara, V.; Raso, F.; Morazzoni, P. Innovation in Phytotherapy: Is a New Regulation the Feasible Perspective in Europe? *Planta Med.* **2016**, *82*, 591–595. [CrossRef]
30. Lopes, C.M.C.; Lazzarini, J.R.; Soares Júnior, J.M.; Baracat, E.C. Phytotherapy: Yesterday, Today, and Forever? *Rev. Assoc. Medica Bras.* **2018**, *64*, 765–768. [CrossRef]
31. Schwartz, E.; Tzulker, R.; Glazer, I.; Bar-Ya'akov, I.; Wiesman, Z.; Tripler, E.; Bar-Ilan, I.; Fromm, H.; Borochov-Neori, H.; Holland, D.; et al. Environmental Conditions Affect the Color, Taste, and Antioxidant Capacity of 11 Pomegranate Accessions' Fruits. *J. Agric. Food Chem.* **2009**, *57*, 9197–9209. [CrossRef]
32. Sharma, P.; McClees, S.F.; Afaq, F. Pomegranate for Prevention and Treatment of Cancer: An Update. *Molecules* **2017**, *22*, 177. [CrossRef]
33. Syed, D.N.; Chamcheu, J.-C.; Adhami, V.M.; Mukhtar, H. Pomegranate Extracts and Cancer Prevention: Molecular and Cellular Activities. *Anticancer Agents Med. Chem.* **2013**, *13*, 1149–1161. [CrossRef]
34. Aviram, M.; Kaplan, M.; Rosenblat, M.; Fuhrman, B. Dietary Antioxidants and Paraoxonases Against LDL Oxidation and Atherosclerosis Development. In *Atherosclerosis: Diet and Drugs*; von Eckardstein, A., Ed.; Handbook of Experimental Pharmacology; Springer: Berlin/Heidelberg, Germany, 2005; pp. 263–300.
35. Turrini, E.; Ferruzzi, L.; Fimognari, C. Potential Effects of Pomegranate Polyphenols in Cancer Prevention and Therapy. *Oxid. Med. Cell. Longev.* **2015**, *2015*, 938475. [CrossRef]

https://doi.org/10.3390/antibiotics15040420

36. Seeram, N.P.; Adams, L.S.; Henning, S.M.; Niu, Y.; Zhang, Y.; Nair, M.G.; Heber, D. In Vitro Antiproliferative, Apoptotic and Antioxidant Activities of Punicalagin, Ellagic Acid and a Total Pomegranate Tannin Extract Are Enhanced in Combination with Other Polyphenols as Found in Pomegranate Juice. *J. Nutr. Biochem.* **2005**, *16*, 360–367. [CrossRef] [PubMed]
37. Endo, E.H.; Garcia Cortez, D.A.; Ueda-Nakamura, T.; Nakamura, C.V.; Dias Filho, B.P. Potent Antifungal Activity of Extracts and Pure Compound Isolated from Pomegranate Peels and Synergism with Fluconazole against *Candida albicans*. *Res. Microbiol.* **2010**, *161*, 534–540. [CrossRef] [PubMed]
38. Ohishi, T.; Goto, S.; Monira, P.; Isemura, M.; Nakamura, Y. Anti-Inflammatory Action of Green Tea. *Anti-Inflamm. Anti-Allergy Agents Med. Chem.* **2016**, *15*, 74–90. [CrossRef]
39. Musial, C.; Kuban-Jankowska, A.; Gorska-Ponikowska, M. Beneficial Properties of Green Tea Catechins. *Int. J. Mol. Sci.* **2020**, *21*, 1744. [CrossRef]
40. Yang, Y.; Zhang, T. Antimicrobial Activities of Tea Polyphenol on Phytopathogens: A Review. *Molecules* **2019**, *24*, 816. [CrossRef]
41. Dahdah, M.; Nimbarte, V.D.; Rouabhia, M.; Ettouil, Y.; Issa, H.; Koussih, L.; Almutairi, M.H.; Semlali, A. Mechanistic Insights into the Anti-Virulence Effects of Viroelixir, a Phenolic Blend from Green Tea and Pomegranate, on Streptococcus Mutans. *Antibiotics* **2026**, *15*, 406. [CrossRef]
42. Deresa, E.M.; Diriba, T.F. Phytochemicals as Alternative Fungicides for Controlling Plant Diseases: A Comprehensive Review of Their Efficacy, Commercial Representatives, Advantages, Challenges for Adoption, and Possible Solutions. *Heliyon* **2023**, *9*, e13810. [CrossRef]
43. Hirasawa, M.; Takada, K. Multiple Effects of Green Tea Catechin on the Antifungal Activity of Antimycotics against *Candida albicans*. *J. Antimicrob. Chemother.* **2004**, *53*, 225–229. [CrossRef]
44. Farkash, Y.; Feldman, M.; Ginsburg, I.; Steinberg, D.; Shalish, M. Green Tea Polyphenols and Padma Hepaten Inhibit *Candida albicans* Biofilm Formation. *Evid. Based Complement. Altern. Med.* **2018**, *2018*, e1690747. [CrossRef]
45. Al-Zoreky, N.S. Antimicrobial Activity of Pomegranate (*Punica granatum* L.) Fruit Peels. *Int. J. Food Microbiol.* **2009**, *134*, 244–248. [CrossRef]
46. Dell'Agli, M.; Galli, G.V.; Corbett, Y.; Taramelli, D.; Lucantoni, L.; Habluetzel, A.; Maschi, O.; Caruso, D.; Giavarini, F.; Romeo, S.; et al. Antiplasmodial Activity of *Punica granatum* L. Fruit Rind. *J. Ethnopharmacol.* **2009**, *125*, 279–285. [CrossRef]
47. Meléndez, P.A.; Capriles, V.A. Antibacterial Properties of Tropical Plants from Puerto Rico. *Phytomedicine* **2006**, *13*, 272–276. [CrossRef]
48. Foss, S.R.; Nakamura, C.V.; Ueda-Nakamura, T.; Cortez, D.A.; Endo, E.H.; Dias Filho, B.P. Antifungal Activity of Pomegranate Peel Extract and Isolated Compound Punicalagin against Dermatophytes. *Ann. Clin. Microbiol. Antimicrob.* **2014**, *13*, 32. [CrossRef] [PubMed]
49. Kim, H.; Lee, D.G. Naringin-Generated ROS Promotes Mitochondria-Mediated Apoptosis in *Candida albicans*. *IUBMB Life* **2021**, *73*, 953–967. [CrossRef] [PubMed]
50. Pemmaraju, S.C.; Pruthi, P.A.; Prasad, R.; Pruthi, V. Modulation of *Candida albicans* Biofilm by Different Carbon Sources. *Mycopathologia* **2016**, *181*, 341–352. [CrossRef]
51. Van Ende, M.; Wijnants, S.; Van Dijck, P. Sugar Sensing and Signaling in *Candida albicans* and Candida Glabrata. *Front. Microbiol.* **2019**, *10*, 99. [CrossRef] [PubMed]
52. Atriwal, T.; Azeem, K.; Husain, F.M.; Hussain, A.; Khan, M.N.; Alajmi, M.F.; Abid, M. Mechanistic Understanding of *Candida albicans* Biofilm Formation and Approaches for Its Inhibition. *Front. Microbiol.* **2021**, *12*, 638609. [CrossRef]
53. Gulati, M.; Nobile, C.J. *Candida albicans* Biofilms: Development, Regulation, and Molecular Mechanisms. *Microbes Infect.* **2016**, *18*, 310–321. [CrossRef] [PubMed]
54. Mukaremera, L.; Lee, K.K.; Mora-Montes, H.M.; Gow, N.A.R. *Candida albicans* Yeast, Pseudohyphal, and Hyphal Morphogenesis Differentially Affects Immune Recognition. *Front. Immunol.* **2017**, *8*, 629. [CrossRef]
55. Talapko, J.; Juzbašić, M.; Matijević, T.; Pustijanac, E.; Bekić, S.; Kotris, I.; Škrlec, I. *Candida albicans*—The Virulence Factors and Clinical Manifestations of Infection. *J. Fungi* **2021**, *7*, 79. [CrossRef]
56. Tazi, N.; Pigeon, X.; Mbuyi-Boisvert, J.M.; Giret, S.; Béland, F.; Rouabhia, M. Effect of Cannabis Smoke Condensate on *C. albicans* Growth and Biofilm Formation. *Microorganisms* **2021**, *9*, 2348. [CrossRef]
57. Samot, J.; Rouabhia, M. Effect of Dermaseptin S4 on *C. albicans* Growth and EAP1 and HWP1 Gene Expression. *Probiotics Antimicrob. Proteins* **2021**, *13*, 287–298. [CrossRef]
58. Kumar, R.; Saraswat, D.; Tati, S.; Edgerton, M. Novel Aggregation Properties of *Candida albicans* Secreted Aspartyl Proteinase Sap6 Mediate Virulence in Oral Candidiasis. *Infect. Immun.* **2015**, *83*, 2614–2626. [CrossRef]
59. Costa, C.R.; Jesuíno, R.S.A.; de Aquino Lemos, J.; de Fátima Lisboa Fernandes, O.; Hasimoto e Souza, L.K.; Passos, X.S.; do Rosário Rodrigues Silva, M. Effects of Antifungal Agents in Sap Activity of *Candida albicans* Isolates. *Mycopathologia* **2010**, *169*, 91–98. [CrossRef]

https://doi.org/10.3390/antibiotics15040420

60. Alves, R.; Barata-Antunes, C.; Casal, M.; Brown, A.J.P.; Van Dijck, P.; Paiva, S. Adapting to Survive: How *Candida* Overcomes Host-Imposed Constraints during Human Colonization. *PLoS Pathog.* **2020**, *16*, e1008478. [CrossRef] [PubMed]
61. Ramos-Pardo, A.; Castro-Álvarez, R.; Quindós, G.; Eraso, E.; Sevillano, E.; Kaberdin, V.R. Assessing pH-Dependent Activities of Virulence Factors Secreted by *Candida albicans*. *MicrobiologyOpen* **2023**, *12*, e1342. [CrossRef] [PubMed]
62. Aoki, W.; Kitahara, N.; Miura, N.; Morisaka, H.; Yamamoto, Y.; Kuroda, K.; Ueda, M. Comprehensive Characterization of Secreted Aspartic Proteases Encoded by a Virulence Gene Family in *Candida albicans*. *J. Biochem.* **2011**, *150*, 431–438. [CrossRef]
63. Li, W.; Yu, D.; Gao, S.; Lin, J.; Chen, Z.; Zhao, W. Role of *Candida albicans*-Secreted Aspartyl Proteinases (Saps) in Severe Early Childhood Caries. *Int. J. Mol. Sci.* **2014**, *15*, 10766–10779. [CrossRef]
64. Klinke, T.; Kneist, S.; De Soet, J.J.; Kuhlisch, E.; Mauersberger, S.; Förster, A.; Klimm, W. Acid Production by Oral Strains of *Candida albicans* and *Lactobacilli*. *Caries Res.* **2009**, *43*, 83–91. [CrossRef] [PubMed]
65. Vylkova, S.; Carman, A.J.; Danhof, H.A.; Collette, J.R.; Zhou, H.; Lorenz, M.C. The Fungal Pathogen *Candida albicans* Autoinduces Hyphal Morphogenesis by Raising Extracellular pH. *mBio* **2011**, *2*, e00055-11. [CrossRef]
66. Dale, B.A.; Fredericks, L.P. Antimicrobial Peptides in the Oral Environment: Expression and Function in Health and Disease. *Curr. Issues Mol. Biol.* **2005**, *7*, 119–133. [CrossRef]
67. Fusco, A.; Savio, V.; Donniacuo, M.; Perfetto, B.; Donnarumma, G. Antimicrobial Peptides Human Beta-Defensin-2 and -3 Protect the Gut During *Candida albicans* Infections Enhancing the Intestinal Barrier Integrity: In Vitro Study. *Front. Cell. Infect. Microbiol.* **2021**, *11*, 666900. [CrossRef]
68. Alanazi, H.; Semlali, A.; Perraud, L.; Chmielewski, W.; Zakrzewski, A.; Rouabhia, M. Cigarette Smoke-Exposed *Candida albicans* Increased Chitin Production and Modulated Human Fibroblast Cell Responses. *BioMed Res. Int.* **2014**, *2014*, 963156. [CrossRef]
69. Lermann, U.; Morschhäuser, J. Secreted Aspartic Proteases Are Not Required for Invasion of Reconstituted Human Epithelia by *Candida albicans*. *Microbiology* **2008**, *154*, 3281–3295. [CrossRef] [PubMed]
70. Ramage, G.; Vandewalle, K.; Wickes, B.L.; López-Ribot, J.L. Characteristics of Biofilm Formation by *Candida albicans*. *Rev. Iberoam. Micol.* **2001**, *18*, 163–170. [PubMed]
71. Tomalka, J.; Azodi, E.; Narra, H.P.; Patel, K.; O'Neill, S.; Cardwell, C.; Hall, B.A.; Wilson, J.M.; Hise, A.G. β-Defensin 1 Plays a Role in Acute Mucosal Defense against *Candida albicans*. *J. Immunol.* **2015**, *194*, 1788–1795. [CrossRef]
72. Zhang, N.; Li, H.; Jia, J.; He, M. Anti-Inflammatory Effect of Curcumin on Mast Cell-Mediated Allergic Responses in Ovalbumin-Induced Allergic Rhinitis Mouse. *Cell. Immunol.* **2015**, *298*, 88–95. [CrossRef]
73. Seleem, D.; Chen, E.; Benso, B.; Pardi, V.; Murata, R.M. In Vitro Evaluation of Antifungal Activity of Monolaurin against *Candida albicans* Biofilms. *PeerJ* **2016**, *4*, e2148. [CrossRef]
74. Li, W.; Yin, Y.; Li, T.; Wang, Y.; Shi, W. Licochalcone A Protects Vaginal Epithelial Cells Against *Candida albicans* Infection Via the TLR4/NF-κB Signaling Pathway. *J. Microbiol.* **2024**, *62*, 525–533. [CrossRef]
75. Weindl, G.; Naglik, J.R.; Kaesler, S.; Biedermann, T.; Hube, B.; Korting, H.C.; Schaller, M. Human Epithelial Cells Establish Direct Antifungal Defense through TLR4-Mediated Signaling. *J. Clin. Investig.* **2007**, *117*, 3664–3672. [CrossRef] [PubMed]
76. Moyes, D.L.; Runglall, M.; Murciano, C.; Shen, C.; Nayar, D.; Thavaraj, S.; Kohli, A.; Islam, A.; Mora-Montes, H.; Challacombe, S.J.; et al. A Biphasic Innate Immune MAPK Response Discriminates between the Yeast and Hyphal Forms of *Candida albicans* in Epithelial Cells. *Cell Host Microbe* **2010**, *8*, 225–235. [CrossRef] [PubMed]
77. Netea, M.G.; Gow, N.A.R.; Joosten, L.A.B.; Verschueren, I.; van der Meer, J.W.M.; Kullberg, B.J. Variable Recognition of *Candida albicans* Strains by TLR4 and Lectin Recognition Receptors. *Med. Mycol.* **2010**, *48*, 897–903. [CrossRef] [PubMed]
78. Ciesielska, A.; Matyjek, M.; Kwiatkowska, K. TLR4 and CD14 Trafficking and Its Influence on LPS-Induced pro-Inflammatory Signaling. *Cell. Mol. Life Sci.* **2021**, *78*, 1233–1261. [CrossRef]
79. Tan, Y.; Zanoni, I.; Cullen, T.W.; Goodman, A.L.; Kagan, J.C. Mechanisms of Toll-like Receptor 4 Endocytosis Reveal a Common Immune-Evasion Strategy Used by Pathogenic and Commensal Bacteria. *Immunity* **2015**, *43*, 909–922. [CrossRef]
80. Kagan, J.C.; Su, T.; Horng, T.; Chow, A.; Akira, S.; Medzhitov, R. TRAM Couples Endocytosis of Toll-like Receptor 4 to the Induction of Interferon-β. *Nat. Immunol.* **2008**, *9*, 361–368. [CrossRef]
81. Akbar, M.A.; Mandraju, R.; Tracy, C.; Hu, W.; Pasare, C.; Krämer, H. ARC Syndrome-Linked Vps33B Protein Is Required for Inflammatory Endosomal Maturation and Signal Termination. *Immunity* **2016**, *45*, 267–279. [CrossRef]
82. Belmadani, A.; Semlali, A.; Rouabhia, M. Dermaseptin-S1 Decreases *Candida albicans* Growth, Biofilm Formation and the Expression of Hyphal Wall Protein 1 and Aspartic Protease Genes. *J. Appl. Microbiol.* **2018**, *125*, 72–83. [CrossRef]
83. Mezni, G.; Issa, H.; Dahdah, M.; Poulin, A.; Daïch, A.; Alamri, A.; Rouabhia, M.; Semlali, A. New Curcumin Analogue (PAC) Inhibits *Candida albicans* Virulence, Restricts Its Adhesion Potential, and Relieves Oral Epithelial Cell Inflammation and Defense Mechanisms. *Antibiotics* **2025**, *14*, 495. [CrossRef]
84. Dumitru, R.; Hornby, J.M.; Nickerson, K.W. Defined Anaerobic Growth Medium for Studying *Candida albicans* Basic Biology and Resistance to Eight Antifungal Drugs. *Antimicrob. Agents Chemother.* **2004**, *48*, 2350–2354. [CrossRef] [PubMed]

https://doi.org/10.3390/antibiotics15040420

85. Theberge, S.; Semlali, A.; Alamri, A.; Leung, K.P.; Rouabhia, M.C. *albicans* Growth, Transition, Biofilm Formation, and Gene Expression Modulation by Antimicrobial Decapeptide KSL-W. *BMC Microbiol.* **2013**, *13*, 246. [CrossRef] [PubMed]
86. DuBois, M.; Gilles, K.A.; Hamilton, J.K.; Rebers, P.A.; Smith, F. Colorimetric Method for Determination of Sugars and Related Substances. *Anal. Chem.* **1956**, *28*, 350–356. [CrossRef]

Disclaimer/Publisher's Note: The statements, opinions and data contained in all publications are solely those of the individual author(s) and contributor(s) and not of MDPI and/or the editor(s). MDPI and/or the editor(s) disclaim responsibility for any injury to people or property resulting from any ideas, methods, instructions or products referred to in the content.

https://doi.org/10.3390/antibiotics15040420

MDPI AG
Grosspeteranlage 5
4052 Basel
Switzerland
Tel.: +41 61 683 77 34

Antibiotics Editorial Office
E-mail: antibiotics@mdpi.com
www.mdpi.com/journal/antibiotics



Disclaimer/Publisher's Note: The title and front matter of this reprint are at the discretion of the Guest Editors. The publisher is not responsible for their content or any associated concerns. The statements, opinions and data contained in all individual articles are solely those of the individual Editors and contributors and not of MDPI. MDPI disclaims responsibility for any injury to people or property resulting from any ideas, methods, instructions or products referred to in the content.





Academic Open
Access Publishing

mdpi.com

ISBN 978-3-7258-8904-4